

Fugro - Earth Mechanics
A JOINT VENTURE

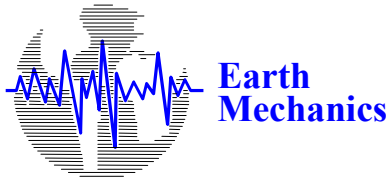
**REVISED FINAL
OAKLAND SHORE APPROACH
GEOTECHNICAL SITE CHARACTERIZATION REPORT
SAN FRANCISCO-OAKLAND BAY BRIDGE
EAST SPAN SEISMIC SAFETY PROJECT**

VOLUME 1 - MAIN TEXT



**Prepared for
CALIFORNIA DEPARTMENT OF TRANSPORTATION**

March 2001



Fugro - Earth Mechanics
A JOINT VENTURE

March 5, 2001
Project No. 98-42-0058/EMI Project No. 98-145

7700 Edgewater Drive, Suite 848
Oakland, California 94621
Tel: (510) 633-5100
Fax: (510) 633-5101

California Department of Transportation
Engineering Service Center
Office of Structural Foundations
5900 Folsom Boulevard
Sacramento, California 95819-0128

Attention: Mr. Mark Willian
Contract Manager

**Final Oakland Shore Approach Geotechnical Site Characterization
SFOBB East Span Seismic Safety Project**

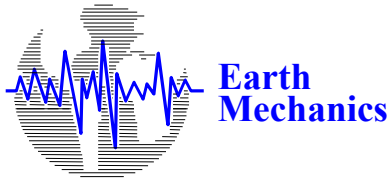
Dear Mr. Willian:

The geologic and geotechnical studies for the San Francisco-Oakland Bay Bridge (SFOBB) East Span Seismic Safety Project are being conducted by Fugro-Earth Mechanics (a joint venture of Fugro West, Inc., and Earth Mechanics, Inc.) under California Department of Transportation (Caltrans) Contract 59A0053. The majority of the Oakland Mole exploration was conducted as part of the Phase 2, Task 5 (final site characterization phase) studies of the referenced contract, although three cone penetration test (CPT) soundings were conducted as part of the earlier Phase 1, Task 3 work scope (preliminary site characterization) of the referenced contract.

The field exploration conducted on the Oakland Mole in the Spring and Fall of 1998 as part of the referenced contract included 25 soil borings (designated in the subsurface database created for the project as 98-51 through 98-75) and 9 CPT soundings (designated as 98-16 through 98-18 and 98-101 through 98-110 [several planned locations were abandoned due to electrical interference]). A total of 53 offshore tethered Seascout CPT soundings were conducted in December 1998 during seasonal high tides on the tidal flat to the north of the Oakland Mole. Fifteen all-terrain CPT soundings were conducted on the Tidal Flat to the north of the Mole in March 1999 during low tide conditions. Two trench and two pit excavations were conducted in April 1999. In Fall 2000, 11 marine Seacalf CPT soundings were performed in the vicinity of the Oakland Shore Approach to the west and northwest of the western tip of the Mole. The Seacalf CPTs were conducted as part of the Phase 3 field investigation program.

This Oakland Shore Approach Geotechnical Site Characterization report summarizes the field exploration for the Oakland Shore Approach and describes our interpretation of the geotechnical conditions based on the information collected from the exploration. Our present interpretations are based on the field data from the borings, the results of laboratory tests completed in the onshore laboratories, and the CPT soundings.

This report is provided in four volumes. Volume 1 provides the interpretational text and illustrations. Volume 2 contains 27 appendices that provide boring logs and test data from 25 land borings on the Oakland Mole and 2 marine borings offshore from the northwest tip of the Oakland Mole. Volume 3 contains the



Fugro - Earth Mechanics
A JOINT VENTURE

California Department of Transportation
March 5, 2001 (Fugro 98-42-0058/EMI 98-145)


results of the CPT soundings conducted on land, on the northern shore of the tidal flat, and offshore to the north and west of the Oakland Mole. Volume 4 contains four documents that include a preliminary study of approach fills at the Oakland Mole, studies on lateral spreading of fills at the Oakland Mole, findings from trench and pit excavations, and the advanced geotechnical laboratory studies conducted at the University of California at Berkeley.

On behalf of the project team, we appreciate the opportunity to contribute to Caltrans' design of the new bridge to replace the existing SFOBB East Span. Please call if we can answer any questions relative to the information presented in the enclosed report.


Sincerely,

FUGRO-EARTH MECHANICS, A Joint Venture

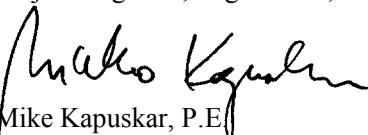



Roger Howard, Jr., P.E.
Project Engineer, Fugro West, Inc.

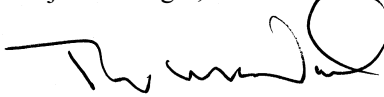



Jacob Chacko, P.E.
Project Engineer, Fugro West, Inc.




Mike Kapuskar, P.E.
Project Manager, Earth Mechanics, Inc.




Thomas W. McNeilan, C.E., G.E.
Vice President, Fugro West, Inc.

Attachment

Copies submitted:

- Mr. Mark Willian, Caltrans
- Mr. Saba Mohan, Caltrans
- Mr. Robert Price, Caltrans
- Dr. Brian Maroney, Caltrans
- Ms. Sharon Naramore, Caltrans
- Mr. Gerry Houlahan, TY Lin/M&N
- Mr. Sajid Abbas, TY Lin/M&N
- Mr. Al Ely, TY Lin/M&N

**SAN FRANCISCO-OAKLAND BAY BRIDGE
EAST SPAN SEISMIC SAFETY PROJECT
CALTRANS CONTRACT 59A0053**

**REVISED FINAL
OAKLAND SHORE APPROACH
GEOTECHNICAL SITE CHARACTERIZATION REPORT**

VOLUME 1 - MAIN TEXT

MARCH 2001

Prepared For:

CALIFORNIA DEPARTMENT OF TRANSPORTATION
Engineering Service Center
Office of Structural Foundations
5900 Folsom Boulevard
Sacramento, California 95819-0128

Prepared By:

FUGRO-EARTH MECHANICS
A Joint Venture
7700 Edgewater Drive, Suite 848
Oakland, California 94621



CONTENTS

VOLUME 1 - MAIN TEXT

	Page
EXECUTIVE SUMMARY	ES-1
1.0 INTRODUCTION.....	1-1
1.1 Background	1-1
1.1.1 Bridge and Route Description	1-1
1.1.2 Earthquake Damage and Retrofit Evaluation	1-2
1.1.3 Replacement Bridge	1-2
1.2 N6 Alignment	1-3
1.2.1 Area of Interest.....	1-3
1.2.2 N6 Alignment Description	1-3
1.2.3 Oakland Shore Approach Structure	1-4
1.3 Caltrans Contract for Geotechnical and Geological Investigations for the Project	1-5
1.4 Site Investigation	1-6
1.4.1 Project Datum.....	1-6
1.4.2 Site Investigation Scope of Work	1-6
1.5 Final Oakland Shore Approach Site Characterization Report	1-7
1.5.1 Basis of Characterization	1-7
1.5.2 Integrated Approach and GIS Database.....	1-7
1.5.3 Report Organization	1-8
1.6 Related Reports Prepared by Fugro-Earth Mechanics	1-9
2.0 FIELD EXPLORATION	2-1
2.1 General Overview	2-1
2.1.1 Purpose	2-1
2.1.2 Previous Investigations	2-1
2.1.3 Current Investigation	2-1
2.1.4 Organizational Roles	2-3
2.2 Land-Based Borings	2-4
2.2.1 Overview	2-4
2.2.2 Drilling and Field Methods	2-5
2.2.3 Sampling Methods and Intervals	2-5
2.2.4 Soil Sample Preparation and Field Testing	2-7
2.2.5 In Situ Testing (Remote Vane)	2-7





VOLUME 1 CONTENTS -- CONTINUED

	Page
2.2.6 Elevation and Position	2-8
2.2.7 Borehole Abandonment and Soil Disposal	2-8
2.3 Land-Based Cone Penetration Testing/Seismic Cone Testing	2-8
2.3.1 On Land, Truck-Mounted CPT	2-9
2.3.2 Tidal Flat, ATV-Mounted CPT	2-9
2.3.3 CPT System Equipment and Procedure	2-10
2.3.4 Elevation and Position	2-11
2.4 Tidal Flat Tethered Seascout CPT Testing	2-11
2.4.1 Introduction	2-11
2.4.2 In Situ CPT Sounding Methods and Equipment	2-12
2.4.3 Data Processing and Presentation of Results	2-14
2.4.4 Standardization	2-14
2.4.5 Data Interpretation	2-15
2.5 Excavations and Trenches	2-16
2.5.1 Trench Excavations	2-16
2.5.2 Pit Excavations	2-16
2.6 Adjacent Offshore Borings	2-17
2.7 Phase 3 Marine Cone Penetration Testing Program	2-17
2.7.1 Overview	2-17
2.7.2 Sounding Results	2-17
2.7.3 Vessel	2-18
2.7.4 Survey and Water Depth Measurements	2-18
2.7.5 Marine CPT Equipment and Procedure	2-18
3.0 LABORATORY TESTING	3-1
3.1 Introduction	3-1
3.2 Classification Tests	3-1
3.3 Soil Shear Strength Tests	3-2
3.3.1 Undrained Shear Strength	3-2
3.3.2 Drained Strength Tests	3-4
3.4 Consolidation Tests	3-5
3.4.1 Incremental Consolidation Tests	3-5
3.4.2 Controlled-Rate-of-Strain (CRS) Consolidation Test	3-6
3.5 Additional Laboratory Testing	3-7
3.5.1 R-Value Testing	3-7
3.5.2 Corrosion Testing	3-7



VOLUME 1 CONTENTS -- CONTINUED

	Page
3.6 University of California at Berkeley Testing	3-7
3.6.1 Simple Shear Testing	3-8
3.6.2 Consolidation Testing	3-8
4.0 SITE CHARACTERIZATION	4-1
4.1 Site History	4-1
4.1.1 Mole Key	4-1
4.1.2 Northern Mole Extension	4-1
4.2 Topography	4-3
4.3 Bathymetry	4-3
4.4 General Subsurface Soil Conditions	4-4
4.4.1 Stratigraphic Sequence Under Mole	4-4
4.4.2 Stratigraphic Relationships	4-4
4.4.3 Tidal Flat Sediments	4-6
4.5 Geologic and Cultural Features	4-7
4.5.1 Mole Fills	4-7
4.5.2 Buried Rock Dikes	4-7
4.5.3 Tidal Flat to the North of the Mole	4-7
4.5.4 Paleochannels	4-8
4.5.5 Description of Stratigraphic Units	4-8
5.0 ENGINEERING SOIL PROPERTIES	5-1
5.1 Classification Properties and Unit Weight of Sediments	5-1
5.1.1 Classification Properties of Fine-Grained Sediments	5-1
5.1.2 Classification Properties of Granular Sediments	5-2
5.1.3 Water Content and Unit Weights	5-3
5.2 Consistency and Shear Strength of Fine-Grained Sediments	5-5
5.2.1 Undrained Shear Strengths from Laboratory and Remote Vane Testing	5-5
5.2.2 Undrained Shear Strengths Interpreted from CPT Testing	5-5
5.2.3 Isotropically Consolidated-Undrained Triaxial Compression (CIUC) Results	5-6
5.2.4 Variability of Undrained Shear Strength Measurements	5-6
5.2.5 Spatial Variability of Undrained Strength	5-8
5.2.6 Summary of Undrained Strength	5-9
5.2.7 Effect of Cyclic Loading on Undrained Shear Strength of Young Bay Mud	5-9





VOLUME 1 CONTENTS -- CONTINUED

	Page
5.2.8 Strain Rate Effects	5-10
5.2.9 Sensitivity and ϵ_{50}	5-10
5.3 Density and Condition of Granular Sediments	5-11
5.3.1 Relative Density	5-11
5.3.2 Drained Strength	5-14
5.4 Consolidation and Compressibility Properties of Sediments	5-16
5.4.1 State of Consolidation	5-16
5.4.2 Compressibility	5-18
5.4.3 Coefficient of Consolidation	5-19
5.5 Shear Wave Velocity of Sediments	5-20
5.6 Cyclic Properties of Young Bay Mud	5-21
5.6.1 Test on Mole Boring Samples	5-21
5.6.2 Tests on Phase 1 Marine Boring Samples	5-22
6.0 OAKLAND MOLE STABILITY ISSUES	6-1
6.1 Introduction	6-1
6.1.1 Description of Anticipated New Approach Fills	6-1
6.1.2 Overview of Subsurface Conditions	6-1
6.1.3 Implications of Subsurface Conditions	6-2
6.2 Settlement Considerations	6-2
6.2.1 Sources and Implications	6-2
6.2.2 Historical Settlement of 1930s Northern Mole Extension	6-3
6.2.3 Predicted Total Settlement Due to New Fill	6-3
6.2.4 Time Rate of Settlement Considerations	6-4
6.3 Soil Liquefaction	6-4
6.3.1 Definition	6-4
6.3.2 Method of Evaluation	6-5
6.3.3 Earthquake Ground Motion Assumed for Analyses	6-6
6.3.4 Presentation of Results	6-6
6.3.5 Conclusions	6-7
6.4 Ground Settlement Due to Earthquake Shaking	6-7
6.4.1 Liquefaction-Induced Settlement	6-8
6.4.2 Seismically-Induced Settlement of Dry Fill	6-8
6.5 Seismically-Induced Strength Degradation of Young Bay Mud	6-9
6.6 Lateral Spreading	6-9
7.0 REFERENCES	7-1





VOLUME 1 CONTENTS -- CONTINUED

TABLES

	Table
On-Land Soil Boring Locations and Depths	2.1
On-Land CPT Locations and Depths	2.2
Marine-Based Seacalf CPT Locations and Depths	2.3
Summary of Laboratory Testing Program	3.1
Summary Results of Consolidated-Undrained Triaxial Compression Testing	5.1
Summary of Cyclic Shear Testing Program on Young Bay Mud.....	5.2
Summary of Consolidated-Drained Triaxial Test Results, Boring 98-59	5.3
Summary of Consolidation Test Results	5.4a-h

PLATES

	Plate
Site Vicinity Map	1.1
Site Location Map	1.2
Final Fugro-EM Reports	1.3
Delineation of Areas Addressed by Fugro-EM Reports	1.4
Exploration Location Map	2.1a
Exploration Location Map	2.1b
The Dolphin Downhole Remote Vane	2.2
Truck-Mounted CPT Operations	2.3
Truck-Mounted CPT Operations	2.4
Tethered Seascout Deployment	2.5a
Tethered Seascout Retrieval	2.5b
Comparison Between Land, Dolphin and Seascout CPTs	2.6
Seacalf CPT Operations	2.7a
Seacalf CPT Operations	2.7b
Morphology of Oakland Mole	4.1
Northern Extension of Key System Mole	4.2
Oakland Mole Historic Settlement Profile	4.3
Bathymetry	4.4
Cross Section Location Map	4.5
Key to Cross Sections	4.6





VOLUME 1 CONTENTS -- CONTINUED

PLATES -- CONTINUED

	Plate
Subsurface Cross Sections,	
With Undrained Shear Strength,	
M1-M1'	4.7a
M2-M2'	4.7b
A-A'	4.7c
B-B'	4.7d
With Undrained Shear Strength and CPT Tip Resistance,	
A1-A1'	4.7e
B1-B1'	4.7f
With Undrained Shear Strength,	
C-C'	4.8
D-D'	4.9
E-E'	4.10
F-F'	4.11
With Shear Wave Velocity,	
A-A'	4.12
Approximate Beach Sand Thickness	4.13
Approximate Buried Sand Thickness	4.14
Simplified Cross-Section Through Northern Tidal Flat and Oakland Shore Approach	4.15
Base of Young Bay Mud Contours	4.16
Plasticity Chart	5.1
Liquid Limit Profile	5.2
Plasticity Index Profile	5.3
Typical Grain Size Distribution Curves	5.4
Fines Content Profile	5.5
D50 Profile	5.6
Water Content Profile	5.7
Unit Weight Profile	5.8
Undrained Shear Strength Profile	5.9
Undrained Shear Strength Profile,	
Western Portion of the Mole	5.10
Central Portion of the Mole	5.11
Eastern Portion of the Mole	5.12
From CPT Tip Resistance ($N_k = 12$)	5.13





VOLUME 1 CONTENTS -- CONTINUED

PLATES -- CONTINUED

	Plate
Cumulative Frequency of Undrained Shear Strength	
Young Bay Mud	5.14
Old Bay Mud	5.15
Undrained Shear Strength from CPT Data on the Mole and Tidal Flat	5.16a
Undrained Shear Strength Profile	5.16b
Sensitivity Profile	5.17
E50 Profile	5.18
Relative Density Interpreted from CPT Data	5.19
Normalized Blow Count Profile	5.20
Relative Density Profile Interpreted From Blow Counts	5.21
Effective Angle of Friction Interpreted from CPT Data	5.22
Preconsolidation Stress Interpreted from CPT and Laboratory Data	5.23
Preconsolidation Pressure Interpreted from CPT Data	5.24
Preconsolidation Stress from CPT and Laboratory Data	5.25
Overconsolidation Ratio Interpreted from Laboratory Data	5.26
Compression and Recompression Ratio Profile	5.27
Remolded Consolidation Test Results	5.28
Coefficient of Consolidation Profile	5.29
Shear Wave Velocity Profile	5.30
Subsurface Cross Section With Liquefaction Evaluation,	
A-A'	6.1a
B-B'	6.1b
C-C'	6.2
E-E'	6.3

VOLUMES 2A AND 2B - APPENDICES (Land and Marine Borings)

VOLUME 2A Land Borings 98-51 Through 98-60

VOLUME 2B Land Borings 98-61 Through 98-75, Marine Borings 98-39 and 98-44

For a guide to boring-specific appendix plate numbers in Volumes 2A and 2B, please refer to the chart on the following page.







VOLUMES 2A & 2B CONTENTS -- CONTINUED

BORING-SPECIFIC APPENDIX PLATE NUMBERING GUIDE

Contents	VOLUME 2A										VOLUME 2B																			
	Land										Land																		Marine	
	98-51	98-52	98-53	98-54	98-55	98-56	98-57	98-58	98-59	98-60	98-61	98-62	98-63	98-64	98-65	98-66	98-67	98-68	98-69	98-70	98-71	98-72	98-73	98-74	98-75	98-39	98-44			
Summary of Field Operations																											1	1a-b		
Boring Depth and Location Reference Map																											2	2		
Boring Logs:																														
Single page boring logs w/soil and rock test results	1	1	1	1	1	1	1	1	1	1	1	1	1	1	1	1	1	1	1	1	1	1	1	1	1	1	3	3		
Single page boring logs w/CPT data																											4	4		
Single page boring logs w/suspension logging data																											5	5		
Multi-page boring logs w/soil and rock test results																											6a-c	6a-c		
Multi-page boring logs w/CPT data																											7a-c	7a-c		
Log of near-surface materials																											8	8		
Field Test Results:																														
Remote vane test data	2a-k	2a-h	2a-e	2a-h	2a-l	2a-f	2a-k	2a-l	2a-h	2a-h	2	2	2	2	2	2	2	2	2	2	2	2	2	2	2	2	2	9a-d	9	
Laboratory Test Results:																														
Summary of laboratory test results	3a-f	3a-c	3a-c	3a-c	3a-e	3a-d	3a-d	3a-d	3a-c	3a-d	3a-b	3a-b	3a-b	3a-b	3a-b	3	3a-b	3	3	3a-b	3a-b	3	3a-b	3	3a-b	3	3a-b	10a-g	10a-g	
Grain size distribution curves	4	4	4	4	4	4	4	4	4	4	4a-c	4a-b	4	4	4	4	4	4	4	4	4	4	4	4	4a-b	11a-c	11a-b			
Plasticity chart	5	5	5	5	5	5	5	5	5	5	5	5	5	5	5	5	5	5	5	5	5	5	5	5	5	12	12			
Stress-strain curves	6a-c	6	6	6	6a-b	6a-b	6a-b	6a-b	6	6a-b	6a-b	6	6	6	6	6	6	6	6	6	6	6	6	6	6	13a-c	13a-d			
CRS/Incremental consolidation	7a-g	7	7a-b	7a-d	7a-e	7a-c	7a-d	7a-d	7a-b	7a-b	7a-f	7a-c	7a-d	7a-c	7a-g	7	7	7	7	7a-c	7a-b	7	7a-d	7	7a-d	14a-h	14a-l			
Consolidated-undrained triaxial compression	8	8	8	8	8	8	8a-b	8	8	8	8	8	8	8a-b	8	8	8a-b	8	8	8	8	8	8	8	8	15a.1-a.2 15b.1-b.2	15			
Consolidated-drained triaxial compression	9	9	9	9	9	9	9	9	9	9	9	9	9	9	9	9	9	9	9	9	9	9	9	9	9	16	16			
R-value laboratory testing	10	10	10	10	10	10	10	10	10	10	10	10	10	10	10	10	10	10	10	10	10	10	10	10	10					
Corrosion testing	11	11	11	11	11	11	11	11	11	11	11	11	11	11	11	11	11	11	11	11	11	11	11	11	11					
Soil Property Profiles:																														
Plasticity index	12	12	12	12	12	12	12	12	12	12	12	12	12	12	12	12	12	12	12	12	12	12	12	12	12	17	17			
Liquidity index	13	13	13	13	13	13	13	13	13	13	13	13	13	13	13	13	13	13	13	13	13	13	13	13	13	18	18			
Soil sensitivity	14	14	14	14	14	14	14	14	14	14	14	14	14	14	14	14	14	14	14	14	14	14	14	14	14	19	19			
ε ₅₀	15	15	15	15	15	15	15	15	15	15	15	15	15	15	15	15	15	15	15	15	15	15	15	15	15	20	20			
Preconsolidation stress	16	16	16	16	16	16	16	16	16	16	16	16	16	16	16	16	16	16	16	16	16	16	16	16	16	21	21			
Direct shear test													17																	
Relative density																										22	22			

 Testing performed

 No testing performed



CONTENTS -- CONTINUED

VOLUME 3 - APPENDICES (CPT Soundings)

- VOLUME 3 Appendix 3A - Land-Based CPT Data
 Appendix 3B - Tethered Seascout CPT Data
 Appendix 3C - Marine-Based Seacalf CPT Data

VOLUME 4 - ADDITIONAL REPORTS

FUGRO-EM PROJECT MEMORANDA

- Preliminary Study of Approach Fills at Oakland Mole
- Studies on Lateral Spreading of Fills at Oakland Mole
- Findings From Trench and Pit Excavations on Oakland Mole (Updated)

UNIVERSITY OF CALIFORNIA AT BERKELEY

- Geotechnical Testing for the East Bay Crossing of the San Francisco-Oakland Bay Bridge





EXECUTIVE SUMMARY

Project Background and Study Description

The geologic and geotechnical studies for the San Francisco-Oakland Bay Bridge (SFOBB) East Span Seismic Safety Project are being conducted by Fugro-Earth Mechanics (a joint venture between Fugro West, Inc., and Earth Mechanics, Inc.) under California Department of Transportation (Caltrans) Contract No. 59A0053.

Report Description and Intent

The purpose of this Oakland Shore Approach Site Characterization report is to provide a reference document and basis for future geotechnical reports addressing detailed foundation design and stability for the proposed approach and structures. Specifically, it: 1) documents the Phase 1 through 3 exploration activities and results, 2) presents the laboratory test results completed to date, 3) provides our interpretations of subsurface geotechnical conditions, 4) describes the analyses of anticipated pertinent site conditions, and 5) provides comments regarding ground stability issues pertinent to geotechnical design and construction of the Oakland Shore Approach.

The report is physically bound in four volumes. Volume 1 provides the interpretational text and illustrations. Volumes 2A and 2B contain 25 appendices that provide boring logs and boring-specific test data from each land boring as well as two marine borings drilled on the tidal flat to the north and northwest of the western tip of the Mole. Volume 3 contains three appendices that provide logs of cone penetration test (CPT) soundings, including: 1) land (truck-mounted and all-terrain-vehicle- [ATV-] mounted equipment) CPT soundings; 2) marine tethered Seascout CPT soundings on the tidal flat; and 3) marine Seacalf CPT soundings in the vicinity of the Oakland Mole. Volume 4 contains three additional documents including a summary of lateral spreading analyses, a memorandum discussing observations and findings from trench and pit excavations on the Mole, and a subcontract report from the University of California at Berkeley.

Area of Interest

This report addresses the subsurface conditions underlying the Oakland Shore Approach at the Oakland Mole. The Oakland Mole is a former shallow water/tidal flat area that was filled prior to the construction of the existing SFOBB in the 1930s. Two small northern extensions ("jughandles") were created in the 1950s and 1960s. The area included in this description is limited to the northern two-thirds of the Mole (from its western tip to a point approximately 800 meters to the east) and the adjacent tidal flat to the north. This portion of the Mole represents the





site of the proposed N6 alignment of the new bridge and approach, and includes portions of the existing Interstate 80 alignment.

Anticipated Mole Structures

The marine area of the Oakland Shore Approach structures extends about 300 meters from about Pier E17 through Pier E22. Farther to the east, alternative slab-on-pile-supported and fill-supported roadways were initially considered. The slab-on-pile structure was designed by TY Lin/M&N (and was carried through 65-percent design). Subsequent to the submittal of the 65-percent submittals, Caltrans selected the fill-supported roadway option for final design. Two alternative structures (designated "Long Structure Alternative" and "Short Structure Alternative") were also considered with differing abutment locations. Separate 85-percent design submittals were presented for each of those structures. Subsequently Caltrans decided that the 100-percent design will be for the Short Structure Alternative with a fill-supported roadway linking the structure to existing roads on the Oakland Mole. TY Lin/M&N is designing the Short Structure Alternative of the Oakland Shore Approach, and Caltrans is designing the fill-supported roadway.

The 85-percent drawings for the Short Structure Alternative show the following:

- Twin bridge and approach structures carrying separate east- and westbound traffic. Eastbound alignment is to the south of the westbound alignment. The westernmost tip of the Oakland Mole is south of about Station 84+00 of the new structures.
- The elevated pile-supported superstructures are shown to extend eastward, terminating at abutments at approximately Station 86+11 on the eastbound route and Station 86+42 on the westbound route.

Geotechnical Site Exploration

The site investigation program for the Oakland Shore Approach included:

- a. 25 Land-Based Borings (Fall 1998)
 - 10 foundation borings
 - 14 pavement borings
 - 1 boring for proposed electrical substation location
- b. 24 Land-Based CPT Soundings
 - Oakland Mole (truck-mounted equipment)
 - 2 seismic and 1 piezocone CPTs during Phase 1 (Spring 1998)
 - 3 seismic and 3 piezocone CPTs during Phase 2 (Fall 1998)





- Tidal flat along northern toe of Mole slope (ATV-mounted equipment; Winter 1999)
 - 2 seismic and 13 piezocone CPTs during Phase 2
 - Soil sample collection at 2 CPT locations
- c. 2 Marine Borings Offshore From the Mole (Fall 1998)
- d. 53 Tethered Seascout CPT Soundings on Tidal Flat (December 1998)
- e. 2 Trench and 2 Pit Excavations (April 1999)
- f. 11 Seacalf CPT soundings in the vicinity of the Oakland Shore Approach Structure (September 2000).

As described in the report, an extensive laboratory testing program was conducted as part of the site investigation.

General Subsurface Conditions

The subsurface conditions underlying the Oakland Mole and adjacent tidal flat include the following geologic features and strata:

- The existing Mole is composed primarily of poorly graded sands with variable amounts of rubble, cobbles, and rock. The fill is typically about 4.5 to 9 meters thick, but locally is as thick as 12.5 meters. The thickest fill section occurs over the location of a buried Young Bay Mud-filled paleochannel. The fill is generally dense above about elevation (El.) 0 mean sea level (MSL). In contrast, the fill is typically medium dense with loose layers below about El. 0 MSL. Standard penetration test (SPT) N-values in the submerged fill typically are between about 9 and 23.
- The Mole is underlain by about 5 to 15 meters of firm to stiff Young Bay Mud. The Young Bay Mud is normally consolidated (relative to the overburden pressure imposed by the Mole fill) beneath the 1930s' northern Mole extension, but slightly underconsolidated beneath the two more recent jughandle additions to the Mole.
- On the tidal flat to the north of the Mole where the Young Bay Mud has not been consolidated by the weight of the Mole fill, the top of the Young Bay Mud is about 0.5 to 2 meters higher than the surface of the Young Bay Mud beneath the Mole fill. That elevation difference is consistent with reported settlement of the Mole fill.
- The Young Bay Mud is overlain on the tidal flat by about 3 to 5 meters of sediments deposited during and since the construction of the northern extension of the Mole. Those tidal flat sediments locally include some or all of the following:
 - A locally continuous layer of sand that was probably deposited during the hydraulic placement of the lower submerged Mole fill.



- A layer of very soft clay, subsequently referred to as "historical bay mud".
- A layered deposit of sands and historical bay mud.
- A surface "beach sand" layer in the western portion of the tidal flat.
- A distinct north-south-trending Young Bay Mud paleochannel crosses beneath the proposed new bridge alignment between the two jughandle additions to the Mole. The width of the paleochannel increases significantly and the paleochannel thalweg deepens to the north of the Mole. Between the jughandles, the base of the Young Bay Mud infill is at about El. -22 meters.
- The Young Bay Mud is underlain by layered sands and clays of the Merritt-Posey-San Antonio (MPSA) Formations except where removed by channeling. That sequence typically includes a distinct 3- to 5-meter-thick very dense sand (Merritt) layer. The MPSA Formations are generally present between about El. -8 and El. -20 meters. Locally, on the eastern flank of the Young Bay Mud-filled paleochannel, the very dense sand layer (or a separate sand layer with similar characteristics) within the sequence appears to be displaced about 5 meters downward.
- The layered MPSA Formations are underlain by Old Bay Mud (a thick sequence of very stiff to hard marine clays). Old Bay Mud includes a distinct crust at its surface as well as other deeper crust layers. The crusts are typically flat-lying and relatively continuous, although the crusts will be discontinuous where channels locally have eroded through the crust layers.

Geotechnical Stability Issues

The Oakland Mole is a hydraulic fill of variable density that is adjacent to a tidal flat and underlain by geologically Recent clay. The subsurface conditions have a number of implications regarding the stability of the Oakland Mole and new fill that might be placed to either raise or extend the Mole. The settlement and seismic stability of approach structures will be key elements in determining the types of approach structures and locating the transitions between different structures. Those settlement and seismic stability issues also will have a profound effect on the design and performance of any of the possible structure types.

Static stability issues include considerations of:

- Compression and settlement due to the weight of additional fill,
- Variations of total settlement due to variable thicknesses of the historical and Young Bay Muds, and the variations in the existing state of consolidation of the Young Bay Mud, and
- The time rate of settlement.



Seismic shaking may cause several potential problems:

- Liquefaction of the saturated fill,
- Ground surface settlement due to seismic shaking,
- Differential settlement and gapping between proposed bridge abutment or slab deck and adjacent ground,
- Cyclic degradation and loss of strength in the Young Bay Mud, and
- Lateral spreading or large lateral soil displacements if liquefaction or other strength degradation occurs behind the present slopes.

Preliminary discussions of those considerations are included in Section 6.0 of this report.



SECTION 1.0 INTRODUCTION



1.0 INTRODUCTION

This report is being provided to assist the California Department of Transportation (Caltrans) and its design team during the final design of the San Francisco-Oakland Bay Bridge (SFOBB) East Span Seismic Safety Project.

The study area is the site of the proposed northern alignment alternatives for the new bridge shore approach that extends from the western tip of the Oakland Mole to a point approximately 800 meters to the east. The site area is shown in Plates 1.1 and 1.2 and includes the existing I-80 alignment and the adjacent tidal flat to the north of the Mole.

The purpose of this report is to: 1) document the Phase 1 through Phase 3 exploration activities and results; 2) present the laboratory test results; 3) provide our interpretations of subsurface geotechnical conditions; 4) describe the analyses of anticipated pertinent site conditions; and 5) provide comments regarding ground stability and foundation considerations to aid geotechnical design and construction of the Oakland Mole Shore Approach.

The report is physically bound in four volumes. Volume 1 provides the interpretational text and illustrations. Volumes 2A and 2B contain 25 appendices that provide boring logs and boring-specific test data from each land boring as well as two marine borings drilled on the tidal flat to the north and northwest of the western tip of the Mole. Volume 3 contains three appendices that provide logs of cone penetration test (CPT) soundings including: a) land (truck-mounted and all-terrain-vehicle- [ATV-] mounted equipment) CPT soundings; b) marine tethered Seascout CPT soundings on the tidal flatland; and c) marine Seacalf CPT soundings in the vicinity of the Oakland Mole. Volume 4 contains three additional documents including a summary of lateral spreading analyses, a memorandum discussing observations and findings from trench and pit excavations on the Mole, and a subcontract report from the University of California at Berkeley.

1.1 BACKGROUND

1.1.1 Bridge and Route Description

The SFOBB carries 10 lanes of Interstate 80 traffic, five eastbound and five westbound, across San Francisco Bay. The bridge is bisected longitudinally by Yerba Buena Island, with the West Span(s) extending from San Francisco to Yerba Buena Island and the East Span(s) extending from Yerba Buena Island to Oakland. The existing bridge is a double-decked structure that was constructed in the 1930s.





1.1.2 Earthquake Damage and Retrofit Evaluation

During the 1989 Loma Prieta earthquake, the East Span(s) of the bridge suffered considerable damage, including the collapse of one span. Recognizing the vulnerability of the structure to future earthquake shaking, Caltrans embarked on a seismic retrofit program to upgrade the bridge. In the summer of 1995, Caltrans presented their retrofit strategy for the SFOBB East Span to the Seismic Advisory Board, who suggested replacement in lieu of retrofit.

Subsequently, Caltrans developed a 30-percent design of a continuous viaduct replacement structure. In 1996, that 30-percent design was presented to the Bay Bridge Design Task Force, who had been appointed by the Metropolitan Transportation Commission (MTC) to select a bridge type for the East Span replacement structure. The MTC and their task force then formed an Engineering and Design Advisory Panel (EDAP), who advised against Caltrans' proposed replacement bridge type.

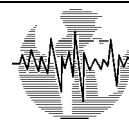
1.1.3 Replacement Bridge

Following EDAP's recommendations, Caltrans contracted with a joint venture between TY Lin International and Moffatt & Nichol Engineers (TY Lin/M&N) to develop 30-percent designs for two alternative bridge types (Phase 1 design). The two bridge-type alternatives included a cable-supported Main Span offshore from Yerba Buena Island and a Skyway structure farther to the east, as well as the associated Yerba Buena Island transition structure(s) and Oakland Shore Approach structure(s). The locations of the various components of the chosen N6 alignment are shown on Plate 1.1. Alternative cable-supported main structures that were considered included single-tower or dual-tower, cable-stayed and self-anchored suspension bridge structures. The timing for the design project required that Caltrans and TY Lin/M&N submit 30-percent design-level schedule and cost estimates to EDAP and MTC by May 29, 1998.

In June 1998, EDAP and MTC selected the single-tower, self-anchored suspension bridge structures and haunched, concrete Skyway structures for final design. Final design of the chosen structure types and alignment was begun by the TY Lin/M&N team in late Fall 1998. The following table summarizes the submission dates for the various design submittals that have since been prepared. The last of the submittals for each component of the replacement bridge provides the basis for the structure descriptions presented in this report.

Design Submittal	Main Span	Skyway	Oakland Shore Approach
45%	January 1999	January 1999	January 1999
65%	August 1999	July 1999	August 1999
85%	In Preparation	February 2000	August 2000 (Long Structure) September 2000 (Short Structure)
100%		November 2000 (Draft)	In Preparation





1.2 N6 ALIGNMENT

1.2.1 Area of Interest

This report addresses the subsurface conditions underlying the Oakland Shore Approach at the Oakland Mole. The Oakland Mole is a former shallow water/tidal flat area that was filled prior to the construction of the existing SFOBB in the 1930s. The original Mole served as a roadway and railroad trackbed for a ferry terminal that extended into the bay to the west of the western end of the Mole. The Mole was then subsequently extended to the north during the construction of the SFOBB.

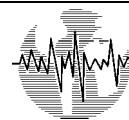
The area characterized in this report is primarily the northern two-thirds of the Mole, from its western tip to a point approximately 800 meters to the east, which includes the alignment of the existing SFOBB. The focus of the site exploration phase of the project was to develop the site characterization for the area being considered for the N6 alignment of the replacement bridge and its easternmost or Oakland Shore Approach (Plate 1.1). This alignment generally parallels the northern edge of the Oakland Mole, and includes areas on the existing Mole as well as overlying the tidal flat to the north of the Mole.

1.2.2 N6 Alignment Description

The N6 alignment, as received from TY Lin/M&N (2001) is shown on Plate 1.1. The proposed N6 alignment lies to the north of the existing alignment generally as follows:

- The proposed N6 alignment transitions from a double-decked structure at the tunnel portal on Yerba Buena Island to two, parallel, side-by-side structures north of the existing bridge.
- The maximum deviation between the alignments is to the east of existing Bridge Pier E4. At that point, the centerline of the N6 alignment is about 220 meters to the north of the centerline of the existing bridge alignment.
- From its point of curvature, the new alignment extends easterly to the Oakland Mole. The proposed alignment centerline is about 80 meters north of the existing bridge centerline at the point of curvature of the existing bridge at Pier E10.
- At the western end of the Oakland Mole, the proposed new alignment centerline is about 55 meters to the north of the existing bridge centerline.
- At its easternmost end, the N6 alignment is coincident with the existing at-grade SFOBB approach to the west of the toll plaza.





The N6 alignment structure is understood to include the following features:

- Twin bridge structures carrying separate east- and westbound traffic.
- A 70-meter-wide corridor for the new structures. The replacement bridge provides for five lanes of traffic in either direction and for a bike path along the eastbound structure.
- A total width of the corridor for the new structures of about 70 meters. The replacement bridge provides for 5 lanes of traffic in either direction, and a bike path along the eastbound structure.
- A transition structure extending 460 meters from the Yerba Buena Island Tunnel to the eastern tip of Yerba Buena Island.
- A self-anchored suspension cable, main-span signature structure extending 620 meters offshore the northeast tip of Yerba Buena Island.
- A four-frame Skyway structure extending approximately 2100 meters from the signature structure, eastward to the Oakland Shore Approach.
- An Oakland Shore Approach Structure extending about 700 meters from the Skyway structure to the north side of the Oakland Mole.
- An earthen fill transition from the Oakland Shore Approach Structure to the roadways leading to and from the existing bridge.

1.2.3 Oakland Shore Approach Structure

The marine area of the Oakland Shore Approach structure extends about 300 meters from about Pier E17 through Pier E22. Farther to the east, alternative slab-on-pile-supported and fill-supported roadways were initially considered. The slab-on-pile structure was designed by TY Lin/M&N (and was carried through 65-percent design). Subsequent to the submittal of the 65-percent submittals, Caltrans selected the fill-supported roadway option for final design. Two alternative structures (designated "Long Structure Alternative" and "Short Structure Alternative") were also considered with differing abutment locations. Separate 85-percent design submittals were presented for each of those structures. Subsequently, Caltrans decided that the 100-percent design will be for the "Short Structure" alternative with a fill-supported roadway linking the structure to existing roads on the Oakland Mole. The "short" Oakland Shore Approach structure is being designed by TY Lin/M&N while the fill-supported roadway is being designed by Caltrans.





As shown on the 85-percent design plans for the Short Structure Alternative, the proposed N6 alignment compares to the existing alignment as follows:

- At the westernmost tip of the Oakland Mole, the proposed new alignment centerline is about 50 meters to the north of the existing bridge centerline.
- At the easternmost end of the Short Structure Alternative, the eastbound structure of the N6 alignment essentially overlaps the existing SFOBB approach at just past existing Bent E32.

The 85-percent drawings for the Short Structure Alternative show the following:

- Twin bridge and approach structures carrying separate east- and westbound traffic. Eastbound alignment is to the south of the westbound alignment. The westernmost tip of the Oakland Mole is south of about Station 84+00 of the new structures.
- A total corridor width of about 70 meters for the new structures.
- The elevated pile-supported superstructures are shown to extend eastward, terminating at abutments at approximately Station 86+11 on the eastbound route and Station 86+42 on the westbound route.
- As the height of the bridge decreases, the pier spacing for the westbound alignment decreases from 64 meters between Piers E17 and E18 to 42 meters between Pier E22 and Abutment E23.
- Likewise, the pier spacing for the eastbound alignment decreases from 63.5 meters between Piers E17 and E18 to 41.7 meters between Pier E22 and Abutment E23.
- Piers E17 through E22 are supported by vertical 1.8-meter-diameter steel pipe piles.
- Abutment E23 is supported by vertical 0.61-meter-diameter, precast, prestressed octagonal concrete piles.
- The westbound Pier E18 footprint is rotated approximately 45 degrees relative to adjacent piers to avoid existing utility lines.

1.3 CALTRANS CONTRACT FOR GEOTECHNICAL AND GEOLOGICAL INVESTIGATIONS FOR THE PROJECT

To support their design efforts, Caltrans also has contracted with Fugro-Earth Mechanics (a joint venture between Fugro West, Inc., and Earth Mechanics, Inc.) to conduct geotechnical and geological investigations and studies for the replacement bridge. Caltrans Contract 59A0053, dated August 27, 1997, authorized those studies.





To date, six task orders have been issued under contract 59A0053. The six task orders include:

- Task Order No. 1 - Initial Site Characterization-Geophysical Surveys Phase with a Notice to Proceed issued January 6, 1998.
- Task Order No. 2 - Project Management and Coordination with a Notice to Proceed issued January 26, 1998.
- Task Order No. 3 - Preliminary Site Exploration and Testing with a Notice to Proceed issued January 26, 1998.
- Task Order No. 4 - Probabilistic Seismic Hazard Analysis Update and Preliminary Site Response Analysis with a Notice to Proceed issued May 19, 1998.
- Task Order No. 5 - Phase 2 Site Exploration and Characterization with a Notice to Proceed issued July 23, 1998.
- Task Order No. 6 - Pile Installation Demonstration Project Engineering/Monitoring with a Notice to Proceed issued December 23, 1998.

The Task Order No. 5 work scope included provisions for the final design phase of site exploration, testing, and characterization for the chosen bridge alignment and structures. The task order authorized the extensive marine exploration and land exploration programs on Yerba Buena Island and the Oakland Mole.

1.4 SITE INVESTIGATION

1.4.1 Project Datum

The horizontal and vertical datum specified by Caltrans (1997) for use on this project were as follows:

- Horizontal Datum: California Coordinate System Zone 3, NAD 1983 (meters)
- Vertical Datum: MSL Datum of 1929

Locations and elevations presented in this report are in reference to this project datum. The NGVD 29 datum is generally equivalent to mean sea level (MSL) datum, and is 0.942 meter above mean lower low water (MLLW) datum (e.g., to convert MLLW elevations to MSL elevations, *subtract* 0.942 meter from the MLLW elevation values).

1.4.2 Site Investigation Scope of Work

The site investigation programs conducted for the Oakland Shore Approach, as part of Caltrans Contract 59A0053, have included the following exploration and investigation activities:





- a. 25 Land-Based Borings (Fall 1998)
 - 10 foundation borings
 - 14 pavement borings
 - 1 boring for proposed electrical substation location
- b. 24 Land-Based CPT Soundings
 - Oakland Mole (truck-mounted equipment)
 - 2 seismic and 1 piezocone CPTs during Phase 1 (Spring 1998)
 - 3 seismic and 3 piezocone CPTs during Phase 2 (Fall 1998)
 - Tidal flat along northern toe of Mole slope (ATV-mounted equipment; Winter 1998)
 - 2 seismic and 13 piezocone CPTs during Phase 2
 - Soil sample collection at 2 CPT locations
- c. 2 Marine Borings Offshore From the Mole (Fall 1998)
- d. 53 Tethered Seascout CPT Soundings on Tidal Flat (December 1998)
- e. 2 Trench and 2 Pit Excavations (April 1999)
- f. 11 Seacalf CPT Soundings in the vicinity of the Oakland Shore Approach Structure (September 2000).

The locations of and designated numbers for those explorations are shown on Plate 2.1.

1.5 FINAL OAKLAND SHORE APPROACH SITE CHARACTERIZATION REPORT

1.5.1 Basis of Characterization

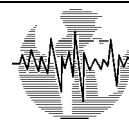
The interpretation of the subsurface conditions presented in this report is based primarily on the Fugro-EM site investigation activities conducted from January through April 1998 (Phase 1), September through November 1998 (Phase 2), and September and October 2000 (Phase 3). In addition to the above site investigation data, the following were also considered:

- Various previous borings completed from 1994 through 1996 for the Caltrans' retrofit studies
- Other historic drilling information

1.5.2 Integrated Approach and GIS Database

For the interpretations presented in this report, primary emphasis was placed on the site-specific conditions encountered in the 1998 borings and the 1999-2000 CPTs. The 1998 borings include extensive in situ and laboratory test data (on relatively undisturbed push samples), whereas the older borings include variable (and often limited) quantities of test data (on





comparatively disturbed driven samples). Testing on samples recovered from the 1998 borings together with the 1998 and 2000 in situ test data are the principal basis for the interpretations described herein. Other older data have generally been used to supplement the stratigraphic information provided in that new data.

The stratigraphy in the borings and CPTs has been compared and integrated with the interpreted stratigraphic relationships imaged by the adjacent marine-based explorations (borings, CPTs, and geophysical seismic reflection) performed for the marine portions of the project and presented in the Final Marine Geotechnical Site Characterization report (Fugro-EM, 2001d).

All of the new and past drilling data have been input into a Geographic Information System (GIS) to allow synthesis, comparison, analysis, and output of the data.

1.5.3 Report Organization

Main Text - Volume 1. The main text of the Revised Final Oakland Shore Approach Geotechnical Site Characterization report is composed of the following sections:

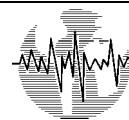
- Section 1.0 - Introduction
- Section 2.0 - Field Exploration
- Section 3.0 - Laboratory Testing
- Section 4.0 - Site Characterization
- Section 5.0 - Engineering Soil Properties
- Section 6.0 - Oakland Mole Stability Issues
- Section 7.0 - References

Various information is provided on illustrations that follow the main text.

Boring-Specific Appendices - Volumes 2A and 2B. The data and interpretations from each individual land boring are provided in Appendices 98-51 through 98-75. The boring-specific appendices for Borings 98-51 through 98-60 are contained in Volume 2A, while the remainder of the boring-specific appendices for Borings 98-61 through 98-75 are contained in Volume 2B. In addition, boring-specific appendices for two marine borings (98-39 and 98-44) are included at the end of Volume 2B. The appendices for the land borings generally include:

- Boring logs with soil test results
- In situ remote vane test data (Borings 98-51 through 98-60 only)
- Laboratory test results, including: summaries of test results, grain size curves, plasticity chart, stress-strain curves, consolidation test results, consolidated drained and undrained triaxial test results, R-value test results, and corrosion test results, as applicable





- Soil properties versus depth, including: plasticity index, liquidity index, soil sensitivity, ϵ_{50} , and preconsolidation pressure

The same information is included for the two marine borings, as are additional copies of the boring logs that include downhole CPT results and suspension wave logs.

CPT Data Appendices - Volume 3. The CPT sounding data are provided in Volume 3. Appendix A includes the data for the land (truck-mounted CPTs on the Mole and ATV-mounted CPTs at the toe of the Mole slope). Appendix B includes the data for the marine tethered Seascout CPTs on the tidal flat to the north of the Mole. Appendix C includes the data from the marine-based Seacalf CPT soundings performed in the vicinity of the Oakland Shore Approach structure. The CPT logs include cone tip resistance, friction sleeve resistance, pore pressure, computed friction ratio versus depth, and, for the seismic cone soundings, the data also includes the calculated shear wave velocity profile. In addition to the CPT data, correlations with undrained shear strength, preconsolidation stress, and relative density are included for the truck-mounted and ATV-mounted CPTs. Laboratory test results have been included where sampling was performed at two ATV-mounted CPT locations (99C-12 and 99C-14). The laboratory test results include: summaries of test results, grain size curves, plasticity charts, and plasticity index and liquidity index profiles. The Seacalf CPT sounding logs include estimates of undrained shear strength interpreted from CPT tip resistance for fine-grained layers.

Additional Reports - Volume 4. The Volume 4 appendices contain four additional documents including a memorandum presenting preliminary studies of approach fills at the Oakland Mole, a memorandum presenting studies on lateral spreading of fills at the Oakland Mole, a memorandum presenting observations and findings from trench and pit excavations on the Mole, and a subcontractor report from the University of California at Berkeley. The lateral spreading memorandum consists of a summary description of the methods and assumptions used in the analyses as well as results. The trench and pit excavation includes descriptions and findings from the excavation, trench logs, and photographs of the excavations. The subcontractor report from the University of California at Berkeley documents specialized cyclic simple shear and radial consolidation tests performed at the University of California at Berkeley laboratories.

1.6 RELATED REPORTS PREPARED BY FUGRO-EARTH MECHANICS

The flowchart presented on Plate 1.3 has been prepared to clarify and delineate the areas and issues addressed (or to be addressed) by the primary reports prepared (or to be prepared) for the project by Fugro-Earth Mechanics (2001a-h). As shown on Plate 1.3, the project submittals have generally been divided into: a) geotechnical site characterization reports, and b) foundation design reports.



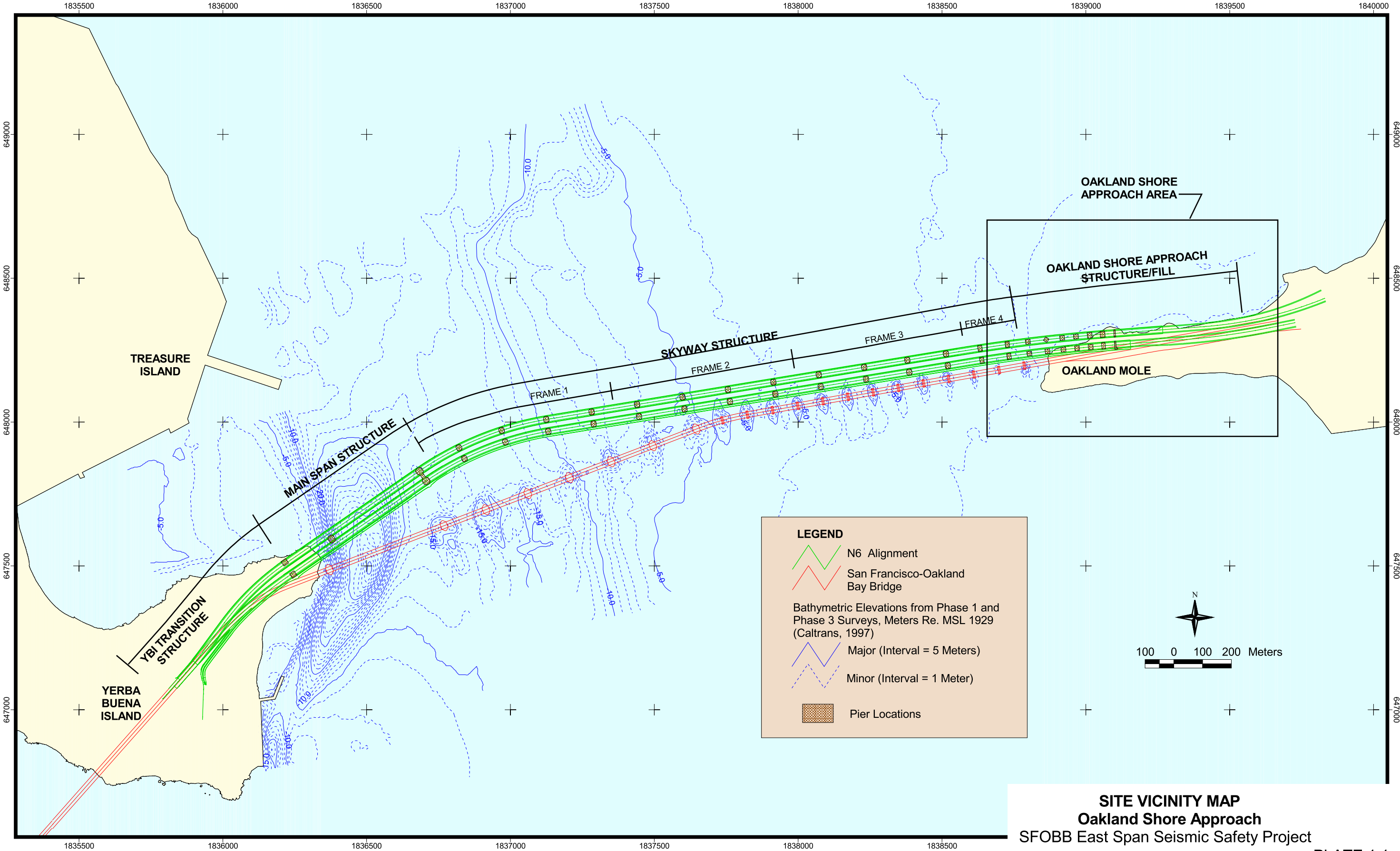


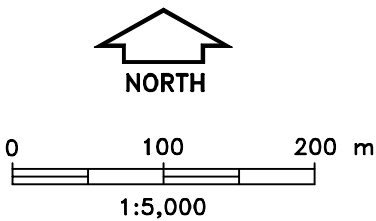
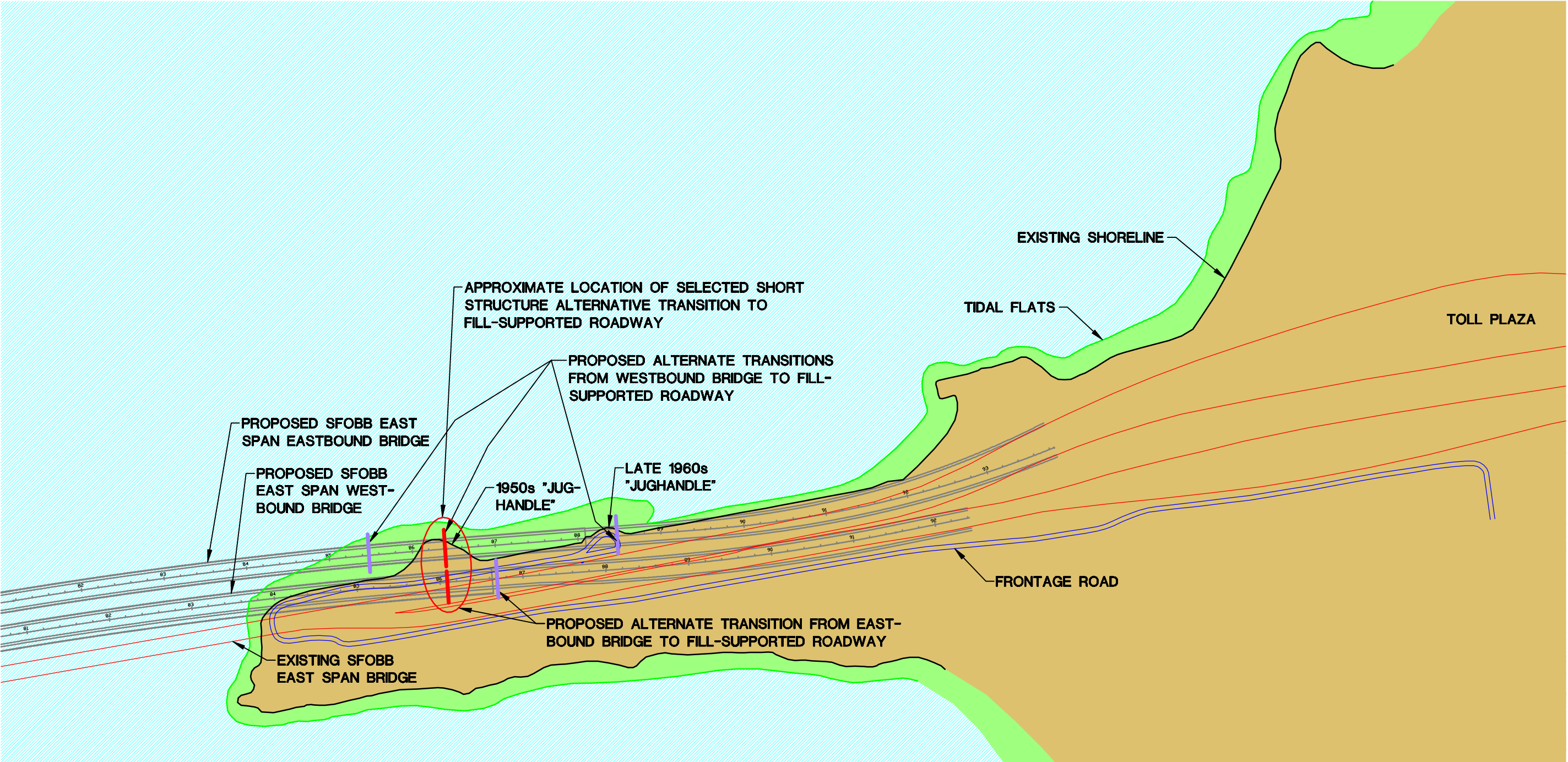
The site characterization submittals consist of: a) marine, b) Oakland Shore Approach, and c) Yerba Buena Island reports. Final foundation reports will be prepared to address: a) the Yerba Buena Island transition structures and Main Span-Pylon, b) the Main Span-East Pier and Skyway Piers (E3 through E16), and c) the Oakland Shore Approach structures to the east of Pier E16. In general, foundation design recommendations and results are developed interactively and iteratively with the structural engineers. Since the design loads and foundation layouts are still being modified, the foundation reports for the Oakland Shore Approach and Yerba Buena Island transition structures and Main Span-Pylon are still in preparation. Design recommendations are typically being provided to the design team via memoranda and will be included in the final foundation reports.

The areas addressed by the various site characterization and foundation reports are shown on Plate 1.4. As shown on Plate 1.4, the delineation of areas addressed by the site characterization reports is generally based on the site investigation techniques used. In contrast, the areas addressed by the final foundation reports are based on: a) the subsurface conditions (as defined in the geotechnical site characterization reports), and b) the requirements of the various bridge and structural engineering teams. Consequently, the break-up of areas addressed in each of the foundation reports is somewhat different from the break-up of areas addressed in each of the site characterization reports.

Reports that represent the final submittal for a particular area or structure type are shaded gray on Plate 1.3. The interpretations and design recommendations presented in those reports generally supercede those presented in the preceding reports. Those reports also include all relevant data from the preceding reports.



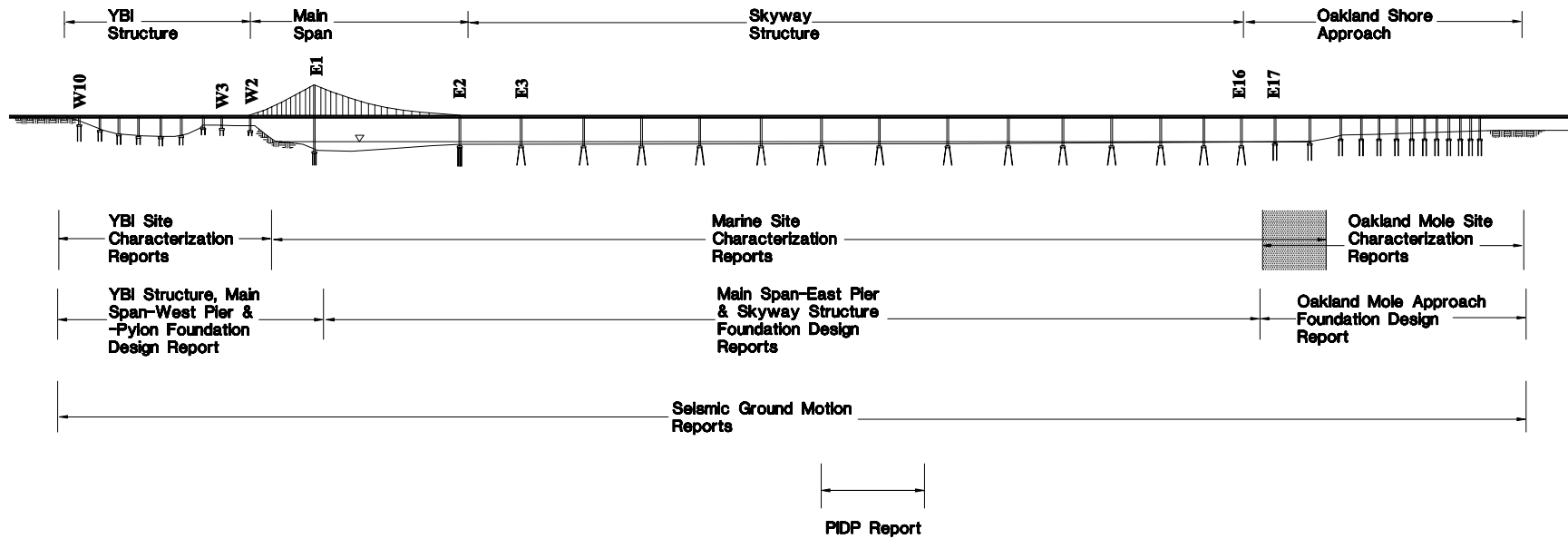




SITE LOCATION MAP
Oakland Shore Approach
SFOBB East Span Seismic Safety Project



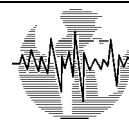




DELINEATION OF AREAS ADDRESSED BY FUGRO-EM REPORTS
SFOBB East Span Seismic Safety Project

SECTION 2.0 FIELD EXPLORATION

SECTION 2.0



2.0 FIELD EXPLORATION

2.1 GENERAL OVERVIEW

2.1.1 Purpose

The soil investigation program was performed to gather geotechnical data for design and construction of the Oakland Shore Approach for the new SFOBB East Span. The Oakland Shore Approach portion of the project generally includes a bridge structure, fill-supported roadway approaches to the new bridge, temporary detour roadways, and an electrical substation. As described in Section 1.0, the limits of the structural and fill-supported components of the Oakland Shore Approach have varied during design. However, it is understood from Caltrans that the 100-percent design will be for the "Short Structure" alternative with a fill-supported roadway linking the structure to existing roads on the Oakland Mole. Borings and CPT soundings were advanced to varying depths (depending on the geotechnical design issues in a given area) to characterize the soil stratigraphy and provide samples for classification and laboratory testing.

2.1.2 Previous Investigations

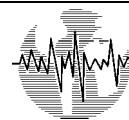
A series of borings were performed in the western 300 meters of the project site for the original construction of the Oakland Mole in the 1930s. In 1994, a series of borings and CPTs were conducted by Caltrans as part of the Oakland Bay Bridge Seismic Retrofit Program. This investigation included shear wave measurements, gamma ray, resistivity, and electric well logs. A permanent, deep, strong motion sensor was installed in Caltrans Boring B-4.

2.1.3 Current Investigation

Phase 1 - Scope. The Phase 1 investigation for the subject project included three land-based CPTs (designated as 98C-16 through 98C-18) conducted by Fugro Geosciences during Spring 1998. The CPT testing was performed to supplement the existing data and to provide preliminary site characterization of the Oakland Mole.

Phase 2 - Land Exploration. The Phase 2 investigation conducted on the Oakland Mole included 25 soil borings (designated as 98-51 through 98-75) and 6 CPT soundings (designated as 98C-101, 98C-102, 98C-104, 98C-105, 98C-109, 98C-110 [four planned locations, designated as 98C-103, 98C-106 through 98C-108, were abandoned due to electrical interference]). Phase 2 on-land Oakland Mole subsurface investigations were primarily conducted in Fall 1998. Trenches and test pits were excavated in April 1999. The locations of those explorations are shown on Plates 2.1a and 2.1b. A summary of the land-based exploration for the Oakland Mole approach is discussed below.





- **Foundation Borings** - Ten (10) relatively deep borings (98-51 through 98-60) were drilled to define subsurface conditions for foundation design. (Those borings were originally designated as B-1 through B-10.) The foundation borings were drilled to depths ranging from 36 to 71 meters.
- **Pavement and Electrical Substation Borings** - Fourteen (14) borings (98-61 through 98-74) were drilled for pavement design at locations selected by Parsons Brinckerhoff. (Those borings were originally designated as P-1 through P-14.) The pavement series borings were drilled to depths ranging from 7.5 to 25 meters. One additional boring (98-75) was added to the drilling program to investigate the subsurface conditions at the proposed electrical substation location. That boring was drilled to a depth of 31.1 meters.
- **CPT and Seismic CPT Soundings** - Six (6) CPT soundings were performed by Fugro Geosciences as part of the Phase 2 field exploration program, three of which included seismic velocity measurements. A total of 10 CPTs were attempted, but four could not be completed due to electrical interference and were abandoned.
- **Trench and Pit Excavations** - An investigation consisting of two exploratory trenches was conducted on the Oakland Mole for the purpose of visual inspection of subsurface ground conditions and buried rock dike materials for the design and construction of the new SFOBB East Approach. In addition, two pits were excavated in the beach areas at the north slopes to determine maximum excavation depths for the proposed fill construction.
- **Adjacent Phase 2 Marine Borings** - As part of the marine investigation (Fugro-EM, 2001d), Fugro also drilled two soil borings (98-39 and 98-44) on the tidal flat (see Plate 2.1a) off the present northwestern shore of the Oakland Mole.

Phase 2 - Tidal Flat Exploration. The new bridge and roadway alignments will overlie the existing tidal flat to the north of the Mole. Exploration of that shallow water and periodically exposed tidal flat required special equipment and techniques, which included:

- **Tethered Seascout CPTs** - Fifty-three (53) miniature cone Seascout CPTs were conducted in December 1998 during high tides to the north of the Mole. The soundings were conducted between about 15 and 110 meters to the north of the Mole. These CPT soundings typically extended to a penetration of 5 meters.
- **All-Terrain CPTs** - Fifteen (15) CPTs were conducted with an ATV-mounted CPT rig during low tide periods in March 1999 on the exposed tidal flat immediately to the north of the Mole. The CPT soundings were numbered 99C-1 through 99C-15. The ATV-mounted CPT soundings typically extended to a penetration of about 12 to 30 meters. Downhole seismic measurements were obtained in two of the ATV-mounted





CPT soundings (99C-13 and 99C-15). Samples also were obtained at two ATV-mounted CPT locations (99C-12 and 99C-14).

Phase 3 - Marine Seacalf CPT Program. The Phase 3 CPT operations consisted of a total of 77 CPT soundings performed along the N6 alignment, in the area north of Yerba Buena Island, and in the vicinity of the Oakland Shore Approach. The Phase 3 CPT operations were conducted between September 23 and October 6, 2000. The CPTs conducted in the vicinity of the Oakland Shore Approach included:

- Two (2) CPT soundings between Skyway Pier E16 and the Oakland Shore Approach Pier E17 where a temporary tower is planned to support the western-most section of the Skyway bridge deck prior to connecting the Skyway to the Oakland Shore Approach.
- Nine (9) CPT soundings along the alignment of the Oakland Shore Approach to refine the definition of the shallow stratigraphy in planned pier and anticipated falsework areas.

These CPT soundings were numbered 00C-64 to 00C-74 and their locations are shown on Plate 2.1a. The soundings in the vicinity of the Mole extended to penetrations ranging from 11 to 53 meters.

2.1.4 Organizational Roles

The following organizations have contributed to the execution of the Oakland Mole investigations:

- Fugro-EM provided definition of the onshore explorations program (with input relative to the pavement borings received from Parsons Brinckerhoff).
- CH2M Hill was tasked with logistical coordination of the land exploration, provided professional staff to log the land borings, and surveyed the locations of the land exploration.
- Pitcher Drilling Company drilled the borings.
- Spectrum Drilling predrilled and installed temporary casings.
- Fugro Geosciences conducted the CPT soundings.
- Fugro-EM personnel assisted in the field logistics, processed (tested and relogged) the samples on the offshore drilling barge, and conducted the in situ vane shear tests in 10 of the land borings.
- Integrated Wastestream Management performed soils disposal and Chromalab Environmental Services conducted environmental soils testing.





- CS Marine Constructors, Inc., supplied the barge from which the Seacalf CPT system was deployed.

2.2 LAND-BASED BORINGS

2.2.1 Overview

Boring Dates and Locations. The Phase 2 land borings included 25 borings drilled between September and November of 1998. Ten foundation borings (98-51 to 98-60) were located on the north side of the Oakland Mole, along the proposed N6 alignment. The 14 pavement borings (98-61 through 98-74) for roadway design were located on Interstate 80 with seven boreholes on or near the eastbound lanes and seven boreholes on the westbound lanes. Three boreholes (98-67 to 98-69) were moved from the inside eastbound shoulder to the inside westbound shoulder to accommodate traffic control considerations. Boring 98-75, for the proposed electrical substation, was located south of where the current eastbound lanes touch down on the Mole. The boring locations are shown on Plate 2.1.

Traffic Control Considerations. Many of the explorations required traffic control to close two lanes of the Interstate 80. The highway lane closures required encroachment permits from Caltrans and scheduling of the lane closures. The highway drilling operation was performed at night to minimize effects on daytime traffic. The allotted drilling time on westbound Interstate 80 was generally from 11:00 p.m. to 5:30 a.m. Borings in eastbound lanes also were drilled at night, but could remain closed until noon the following day. Borings that required consecutive days to drill were covered with a steel plate under the supervision of a Caltrans inspector.

Foundation Borings. The soil borings for the foundation design (Borings 98-51 through 98-60) consisted of a total of 10 deep boreholes that extended to depths of 35 to 70 meters. The purpose of these boreholes was to delineate the extent of the Mole fill, Young Bay Mud (YBM) and Merritt-Posey-San Antonio (MPSA) Formations, and to develop engineering properties for the fill, MPSA, YBM, and Old Bay Mud (OBM). Table 2.1 lists the boring locations and as-drilled penetration depths. Graphical boring logs are attached in Volume 2A.

Pavement and Electrical Substation Borings. Fourteen (14) shallow borings were drilled to shallower depths ranging from 8 to 23 meters for roadway pavement design (Borings 98-61 through 98-74). The borings were drilled to: 1) delineate the thickness of the fill and the top and, in some cases, the bottom of the Young Bay Mud layer; and 2) develop engineering properties of the fill and Young Bay Mud. Boring 98-75 was added at the end of this program and drilled to 31.1 meters for the design of the electrical substation.

Table 2.1 lists the boring locations and as-drilled penetration depths for the pavement and electrical substation boring locations. Graphical boring logs are attached in Volume 2B.





2.2.2 Drilling and Field Methods

The Phase 2 Oakland Shore Approach borings were drilled by Pitcher Drilling Company of Palo Alto, California, and were advanced by the rotary wash method using Failing 1500 drill-rigs with 124-mm (millimeter) drill bits.

The sampling process consisted of a combination of driven standard penetration test (SPT) and California liner sampling and pushed 76-mm tube samples. About two-thirds of the pushed tube samples were extruded in the field, while the remaining one-third were sealed in the tube (designated on the boring logs as "SAVE" tube samples).

In situ remote vane shear tests were conducted in the Young and Old Bay Mud deposits in the foundation borings (98-51 through 98-60). The in situ tests were conducted using Fugro's downhole Dolphin system. In situ vane shear tests were interspersed with the sampling, and the sampling interval was adjusted as required.

The samples collected from the land borings were classified and field tested, then transported to the marine drilling barge for further laboratory testing.

2.2.3 Sampling Methods and Intervals

Sampling Methods. SPTs as described in ASTM D1586 were performed through the fill material and in the Merritt Sand. At the top of the Young Bay Mud, a modified California sampler was used to collect clayey sand/sandy clay samples. The driven samplers were advanced using a standard SPT rope and cathead procedure. During the initial stages of the field exploration, driven California liner samples were occasionally taken in the Young and Old Bay Mud deposits. Due to the reduction in sample quality relative to the thin wall sampling procedures, the California liner sampling of the clay deposits was reduced or eliminated in the latter stages of the investigation.

Relatively undisturbed samples of the Young Bay Mud were collected using a 76-mm-OD (outside diameter), 72-mm-ID (inside diameter) Shelby tube sampler in accordance with procedures for Thin-Walled Tube Sampling of Soils (ASTM D1587). Shelby tube samples also were collected in the Old Bay Mud. About two-thirds of the pushed tube samples were extruded on the drill rig, while the remaining one-third were sealed in "SAVE" tubes.

In situ remote vane tests also were performed on the Young and Old Bay Mud deposits in the 10 foundation borings (98-51 through 98-60) using Fugro's downhole Dolphin remote vane system. The in situ vane shear tests were interspersed with the sampling.

Sampling Intervals. The sampling schedule used for the pavement borings (98-61 to 98-75) was as follows:



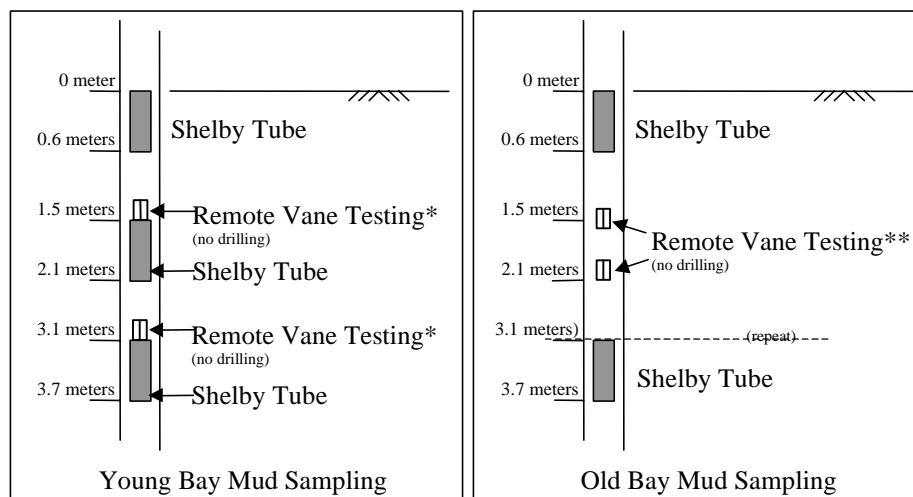


- One bulk sample and two SPT samples within the upper 1.5 meters of the fill
- Pavement cores
- SPT samples at 1.5-meter intervals within the fill material
- Pushed Shelby tube sampler every 1.5 meters in the Young Bay Mud
- No in situ field tests
- At least one SAVE Shelby tube collected in the Young Bay Mud layer
- SPT samples at 1.5-meter intervals within the Merritt Sand
- Shelby tube samples every 1.5 meters in the Old Bay Mud

The sampling schedule for the foundation borings (98-51 through 98-60) was similar to that of the pavement borings, with the following differences:

- One SPT sample within the upper 1.5 meters
- No pavement core
- Every third Shelby tube sample saved in "SAVE" tubes
- Remote vane shear testing in both the Young and Old Bay Muds

The remote vane testing interval in the Young Bay Mud was to follow a Shelby tube sample by pushing the remote vane to the next 1.5-meter interval. In the Old Bay Mud, Shelby tube samples were followed by two remote vane tests pushed 1.5 to 2.1 meters below the previous tube sample. In each case, the remote vane was pushed to the test depth. The remote vane testing intervals are shown in the figure below.



* B-Borings (98-51 through 98-60) only

** In P-Borings (98-61 through 98-74), a Shelby tube sample was collected instead of the remote vane.





2.2.4 Soil Sample Preparation and Field Testing

The Shelby tube samples were extruded for immediate testing or sealed in "SAVE" tubes for later testing. The extruded Shelby tubes were cut into sections approximately 150 mm in length. The soil samples were visually classified in general accordance with ASTM D2487. Pocket penetrometer tests and Torvane tests were conducted on the samples to estimate shear strengths. The sections were wrapped in plastic film and aluminum foil, then placed in 150-mm-tall plastic tubes (quarts), capped, and labeled. The quarts were transferred to a laboratory located on the Fugro barge used for the marine drilling operation. The "SAVE" tubes were visually classified, and a bag sample was taken from the bottom 80 mm of the tube. The tubes then were sealed with O-ring seals, capped, labeled, and stored for subsequent laboratory testing.

The modified California sampler contained three 61-mm-diameter by 150-mm-long liners. Liners with intact soil samples were capped and stored for later testing. Liners that were not completely full and SPT samples from the split-spoon sampler were stored and labeled in plastic bags.

The samples collected from the land borings were transported to the laboratory on the marine drilling barge daily. The samples were relogged, and water content and unit weight measurements were conducted on each sample. Undrained shear strength measurements including miniature vane, Swedish fall cone, and unconsolidated-undrained (UU) triaxial shear tests were conducted on the clay samples. Approximately one-third of the clay samples were remolded (at their in situ water content) and undrained shear strength tests were conducted on the remolded specimen.

After the onboard testing was completed, the samples were transferred to the refrigerated trailer sample storage facility at the Fugro-EM field office. The samples were dispersed to the onshore laboratories, as appropriate. The "SAVE" tubes were transferred to Fugro's laboratory at Houston and the laboratory at the University of California at Berkeley for more detailed (consolidation and dynamic strength) laboratory testing.

2.2.5 In Situ Testing (Remote Vane)

The Dolphin remote vane was used to measure the in situ shear strengths of the Young and Old Bay Muds. Vane testing was generally not performed in hard clay strata where the in situ shear strength of the soils exceeds the measuring capacity of the vane. The vane testing also was not performed on highly stratified (interlayered clay and sand) soil profiles.

A schematic drawing showing the downhole Dolphin remote vane is presented on Plate 2.2. The downhole vane tests were performed immediately after the push sampling operation. The operational sequence for performing a downhole vane test involved attaching the remote vane to the drill rod, lowering the remote vane downhole, pushing the four-bladed vane to the desired test depth, and running the test.





The tests were run for approximately 3 minutes. At the end of the test, the drill string could be lowered to push the tool an additional 0.6 meter to perform the second test. At the end of the second test, the tool was pulled out of the soil formation. Once the tool was out of the borehole, the remote memory unit (RMU) was connected to a computer for the data retrieval procedure and to generate a "quickplot" of the torques developed. The undrained shear strength was then computed from the maximum vane blade torques and transducer/vane blade calibration factors. The maximum shear strength that can be measured by the Dolphin remote vane device is approximately 263 kilopascals (kPa). After the data retrieval procedure was completed, the RMU was reinitialized and prepared for the next test.

2.2.6 Elevation and Position

Ground elevations and coordinates of each boring location were determined by conventional land survey methods using a United States Geological Survey (USGS) control location on the Mole.

2.2.7 Borehole Abandonment and Soil Disposal

The borings were abandoned by backfilling the holes with cement grout. The pavement was patched with asphalt concrete at locations where existing pavement had been cored.

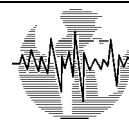
Environmental sampling (soil or water) was not required per instruction by the Caltrans Office of Structural Foundations, Sacramento, due to lack of environmental or hazardous waste reports for the Oakland Mole (Caltrans District IV, Environmental Planning - South).

Drilling cuttings, drill mud, and water from the borings were placed in a total of 59 Caltrans-approved, 208-liter (55-gallon) steel drums and stored in a secured Caltrans storage yard until disposal. All drums were opened and inspected by Integrated Wastestream Management, Inc. (IDM) of Milpitas. According to IDM, the mud had sedimented in the drums and water had risen to the top. The water and mud appeared uncontaminated by visual inspection. In October 1998, four (4) brass samples were extracted randomly from the mud in a total of 28 drums and composited in the certified laboratory of Chromalab Environmental Services, Inc. The Environmental Protection Agency (EPA) test results from a CAM 17 metals analysis indicated no major concentrations of contaminants. A total of 4,500 liters of water was removed from the muds and disposed of by Seaport Water Disposal Facility using a carbon-activated filtration/centrifuge system.

2.3 LAND-BASED CONE PENETRATION TESTING/SEISMIC CONE TESTING

CPT soundings were conducted by Fugro Geosciences on the Oakland Mole and in front of the toe of the Mole slope using truck-mounted and ATV-mounted CPT rigs, respectively. The CPT soundings were performed to: 1) help delineate the subsurface stratigraphy, 2) measure the in situ shear strengths of cohesive soils, and 3) estimate the relative density and frictional





characteristics of granular soils. Table 2.2 summarizes the CPT locations. The CPT sounding logs are provided in Volume 3.

2.3.1 On Land, Truck-Mounted CPT

Introduction. The Oakland Mole CPT soundings were conducted in two phases. The Phase 1 investigation (conducted in Spring 1998) consisted of two seismic CPT soundings (98-17 and 98-17) and one conventional piezocone sounding (98-16).

The Phase 2 program (conducted in Fall 1998) included six CPT soundings. The six Phase 2 soundings included three soundings with seismic velocity measurements and two piezocone CPTs. In addition to the six CPT soundings successfully conducted, four planned sounding locations (98C-103 and 98C-106 through 98C-108) were attempted, but then abandoned due to electrical interference. The CPT sounding locations are shown on Plate 2.1. Table 2.2 summarizes the CPT locations and penetration depths achieved. Logs of the CPT soundings are provided in Volume 3, Appendix A.

Field Operations. During Phase 1, CPT sounding 98C-16 was terminated at 17.4-meter depth after four attempts due to excessive deviation from vertical, which was believed to have been caused by the presence of boulders and cobbles in the upper zone of fill. The other two Phase 1 soundings were extended to between 48 and 53 meters.

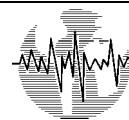
Due to the expected difficulty of advancing the cone through the fill at the Phase 2 CPT locations, Spectrum Drilling predrilled through the fill material and lined the hole with steel casing. The casing then had an internal steel sleeve inside, and the annulus between the casing and steel pipe was filled with a neat cement mixture. The conventional CPT portion of each of the nine soundings was continuous below a depth of approximately 3 to 4.5 meters. Data acquired within the cased interval have been deleted from the CPT sounding logs.

Difficulties in advancing the cone through the steel pipe occurred when saturated sand, under a hydraulic gradient, flowed into the pipe thereby seizing the cone. To remedy this, Fugro Geosciences either washed the inside of the pipe to clean out the blockage or Spectrum Drilling returned to redrill the hole. Four of the CPT holes could not be advanced past the bottom of the fill due to an electrical charge interfering with the CPT instrumentation. Several attempts were made to mitigate the interference, including replacing the steel sleeve with a PVC sleeve and grounding the CPT rig, but the problem was not resolved. A photograph of the land-based CPT operation is shown on Plate 2.3.

2.3.2 Tidal Flat, ATV-Mounted CPT

Introduction. To further characterize the conditions on the shallow tidal flat sediments adjacent to the north toe of the Oakland Mole, an ATV-mounted CPT rig was mobilized. The all-terrain CPT soundings were conducted (in March 1999) to supplement the existing land data





and offshore tethered Seascout CPT soundings. The all-terrain CPT vehicle has low ground pressure tracks that allow it to be mobilized onto soft sediment terrain.

Two of the 15 ATV-mounted CPT soundings (99C-1 through 99C-15) included seismic CPT (shear wave velocity) measurements while the other 13 soundings were conventional piezocone CPTs. In addition, small-diameter sleeve samples were collected from two sounding locations (99C-12 and 99C-14). Plate 2.1 indicates the location of the CPT soundings conducted as part of Phase 2 of the referenced contract.

Field Operations. To access the tidal flat area to the north of the Oakland Mole, the CPT soundings were conducted during periods of low tides. CPT soundings 99C-3 through 99C-10 were conducted during seasonal low tides during the week of March 1 to March 5, 1999, which allowed access onto the exposed mudflats for several hours a day. The CPT work continued during the next period of low tides, the week of March 15 to March 19, 1999. Plate 2.4 shows a photograph of the all-terrain CPT vehicle on the beach just north of the Oakland Mole.

2.3.3 CPT System Equipment and Procedure

CPT System Equipment. The CPT system consists of a seismic wave source, a seismic cone penetrometer (which is a conventional electric piezocone with an additional section that contains a geophone array), and a recording unit (seismograph). Soundings were performed using a standard three-channel piezocone penetrometer that measures cone tip resistance, sleeve resistance, and pore water pressure.

A 66.75-kilonewton (kN) piezocone with an apex angle of 60 degrees, a base area of 15 square centimeters (cm²), and a cylindrical sleeve area of 200 cm² was used. The pore water pressure measurements were taken immediately above the base of the piezocone (the filter is located 5 mm above the apex of the piezocone tip).

The CPT equipment was deployed from either a self-contained, 178-kN Fugro Geosciences truck on land or a Fugro Geosciences ATV-mounted rig on the tidal flat area. The vehicles contained a thrust mechanism to push the cone, a CPT recording unit, the seismograph, and other support equipment. The test equipment and procedures meet ASTM D5778-95 (ASTM, 1998) specifications. The truck was leveled and jacked up on four stabilizer pads to provide a stable reaction for the thrust of the cone.

The seismic wave source for generating shear waves consisted of a wooden beam anchored to the soil surface by the weight of one of the truck stabilizer pads and a swinging hammer that strikes the beam. The surface seismograph and downhole geophone array recorded the generated waves during interruptions in the CPT advancement.





Field Procedures. The penetration rate of the piezocone penetrometer was approximately 2 centimeters per second (cm/sec). During the test, measurements of piezocone tip resistance, sleeve friction, and pore water pressure were recorded simultaneously at about 1-second intervals.

The CPT system computer generated an instant "quickplot" of the data in the field that provided generalized information on the cone tip resistance, sleeve resistance, pore pressure, and rate of penetration. The CPT data were then processed and are presented in Volume 3. (For clarity, the plate number is the same as the designated sounding number [e.g., 98C-16].) The presentation of results from the CPTs consists of graphs showing tip resistance, sleeve friction, pore pressure, and friction ratio versus depth below the ground surface.

In tests with shear wave measurements, the CPT penetration was interrupted approximately every 1.5 meters in order to collect shear wave velocity data. The data are processed to calculate the average seismic wave velocities between individual test depths to produce a profile of average seismic wave velocities for contiguous depth intervals. Proprietary software assisted with digital filtering, amplitude scaling, event picking, velocity calculations, and data presentation.

At the completion of each boring, the CPT hole was grouted with a mixture of neat cement grout consisting of seven sacks of cement and one sack of gel per 26 liters of water. The mixture was pumped down the hole using a tremie pipe.

2.3.4 Elevation and Position

Ground elevations at and coordinates of each CPT sounding location were determined by conventional land survey methods using a USGS control location on the Mole.

2.4 TIDAL FLAT TETHERED SEASCOUT CPT TESTING

2.4.1 Introduction

Purpose of Soundings. Tethered Seascout CPT soundings were conducted to supplement existing land data and adjacent offshore boring data to further characterize the conditions of the shallow tidal flat sediments north of the Oakland Shore Approach. The Seascout was considered an ideal tool as it can be deployed from smaller vessels (e.g., geophysical survey vessels). Alternatives to using a CPT rig (e.g., drop coring, vibracoring, or jet probing) were considered unsatisfactory.

Seasonal high tides during the week of December 14 to 19, 1998, allowed access into otherwise unnavigable shallow water depths. Almost 100 Seascout CPT soundings were conducted along the N6 northern alignment. About half of the soundings were performed on the tidal flat north of the Oakland Mole. Fifty three (53) of those soundings were numbered





98C-446 to 98C-560, but are not sequential as some of the soundings were deferred. The remaining soundings (designated 98C-401 to 98C-445), were conducted along the proposed N6 alignment. Plate 2.1 shows the extent of the soundings included in this report. The interpreted conditions in the area are discussed in Section 4.0.

Description of Seascout CPT. Fugro's Seascout is a lightweight seafloor CPT system designed for tethered deployment from a modest-sized vessel. The Seascout CPT includes: a 2.4-meter-high triangular reaction frame with a 2-meter base dimension, a patented hydraulic thrust mechanism, a coiled CPT rod with spooling/straightening device, a miniature piezocone, and an associated data storage/processing computer. The weight of the Seascout frame in water is about 1,360 kilograms (kg).

As deployed at the tidal flat north of the Oakland Mole, the system has a maximum penetration of 5.2 meters. The lightweight design is based on a miniature cone penetrometer with a 100-square-millimeter (mm^2) cone base area rather than the conventional $1,000 \text{ mm}^2$. This results in a substantial reduction of thrust and reaction equipment requirements.

CPTs involve the in situ measurement of soil resistance to continuous penetration by cone-based push rods. The measurements comprise penetration depth, cone resistance, sleeve friction, pore pressure, and inclination from vertical. Use of the coiled CPT tube provides a continuous penetration push as opposed to a stroke-based penetration when using the more common 0.9-meter CPT rod segments.

2.4.2 In Situ CPT Sounding Methods and Equipment

Seascout Apparatus. Seascout apparatus consists of the following elements:

- **Thrust Machine** - Apparatus providing thrust to the coiled push rod system so that the required constant rate of penetration is controlled (underwater hydraulic power pack and patented wheeldrive thrust).
- **Reaction Equipment** - Reaction for the thrust machine (e.g., ballasted seabed frame, remotely operated vehicle, sled).
- **Coiled Push Rod System** - Thick-walled cylindrical tube used for advancing the penetrometer to the required test depth that is straightened upon penetration and coiled upon extraction.
- **Push Rod Casing** - Guide for the part of the push rod protruding above the soil and/or the push rod length exposed in water or soil so as to prevent buckling when the required penetration pressure increases beyond the safe limit for the exposed upstanding length of the push rod.
- **Piezocone Penetrometer** - Cylindrical terminal body mounted on the lower end of the push rods, including a cone, a friction sleeve, a filter, and internal sensing devices





for the measurement of cone resistance, sleeve friction, pressure, and (optionally) inclination.

- **Measuring System** - Apparatus and software, including sensors, data transmission apparatus, recording apparatus, and data processing apparatus.

Photographs taken during the deployment and subsequent retrieval of the Seascout are shown on Plates 2.5a and 2.5b.

Vessel. The SFOBB East Span Seismic Safety Project CPT soundings were conducted from the M/V *White Lightning*, a 15-meter workboat owned and operated by West Coast Sea Works. The Seascout was deployed off both the port and starboard sides of the vessel using a deck-mounted, hydraulically-operated crane. Station keeping was accomplished by "live-boating" over the location using vessel power. Soundings at the innermost locations closest to the Oakland Mole shoreline were conducted during flood tides when the maximum water depths allowed for safe boat-operating conditions.

Navigation. CPT locations were determined using Fugro's Differential Global Positioning System (DGPS), referenced to known base stations in the San Francisco Bay area. Coordinates calculated from the DGPS system are considered accurate to within about 1 meter. Coordinates for the CPT locations are reported relative to the California State Plane, Zone 3, NAD83 meters datum.

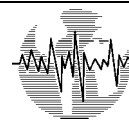
Procedure. The test procedure at each location included the following steps:

1. Positioning of vessel and Seascout at test location.
2. Lowering of Seascout frame to the mudline.
3. Advancement of the cone into the harbor bottom to the maximum 5.2-meter penetration or refusal.
4. Retraction of the cone rods and penetrometer.
5. Retrieval of the frame to the aft deck of the vessel, and moving to the next test location.
6. Data processing onboard the vessel.

All data were acquired digitally for subsequent computer-based processing (both on the vessel and later in the office) and presentation.

Due to the shallow water conditions, the soundings closest to the shoreline were conducted during peak high tides. Locally, those soundings were conducted within about 30 meters of the Oakland Mole dike in water depths of less than elevation (El.) -0.8 meter (MSL). During periods of flood tides, the Seascout was deployed so that the vessel drifted





towards the shoreline and away from the sounding area. During periods of slack tides, CPT soundings were conducted west of the Mole in deeper water.

Water Depth Measurement. Water depths at each CPT location were measured with a sounding tape and from marks fixed to the Seascout unit. These two methods enabled a check of the penetration of the Seascout unit itself into the seafloor. Where possible, the vessel's echo sounder was used as a cross-check. The measured water depths were corrected to MSL datum using the published tide charts for the nearby Matson Wharf.

2.4.3 Data Processing and Presentation of Results

The raw CPT sounding data were processed using proprietary processing algorithms (UNIPLLOT) developed for offshore CPT data processing. For each sounding, logs of cone point resistance, sleeve friction, friction ratio, and pore pressure are presented in Volume 3. The friction ratio is defined as the ratio of the friction sleeve value to the cone point resistance. Logs of the Seascout CPT data are provided in Volume 3, Appendix B.

2.4.4 Standardization

CPTs provide correlation parameters (such as cone resistance) rather than properties (such as compressive strength). A high degree of CPT standardization is therefore important to allow the correlation and interpretation of the results. The standardization includes cone penetrometer geometry and rate of penetration. Layering and soil structure also contribute to significant differences between various cone sizes.

Cone Size. An important standardization item of the cone penetrometer geometry is the area of the cone base. Conventionally, this area is 1,000 mm². The International Reference Test Procedure for Cone Penetration Test prepared by ISSMFE (1989) permits deviations from the Reference Test (1,000 mm²) under the following conditions:

- Explicit description, including a note on the graphs with the test results
- Tolerances for the cone base area to be adapted in direct proportion to the diameter
- Surface area of the sleeve to be adjusted proportionally with respect to the cross-sectional area of the cone

Although the 100 mm² Seascout cone penetrometer is not a conventional cone size, it meets the above-stated requirements of ISSMFE.

Rate of Penetration. The conventional rate of penetration for standard-sized CPTs is 20 ±5 millimeters per second (mm/sec). The Seascout rate of penetration is approximately 40 mm/sec. The selected higher penetration rate represents an estimated adjustment for cone penetrometer size. This adjustment relates to permeability (in particular, the transition zone between drained and undrained ground behavior during cone penetration). The higher





penetration rate possibly affects the tip resistance, sleeve friction, and pore pressure measurements, but with a limit of a few percent.

Significance of Layering and Soil Structure. Geotechnically, the results of a smaller cone penetrometer may differ from the 1,000-mm² cone penetrometer. Recognized factors that may contribute to differences include:

- Particle size of soil
- Soil layering
- Soil structure
- Density of loose granular sediments

The signature of a cone penetrometer may be affected where the D_{50} of a soil exceeds the equivalent of about six times the diameter of the cone penetrometer.

The loading response of a smaller cone penetrometer to soil layering is more rapid than that of a larger penetrometer. This relates to soil failure mechanisms in layered soils. Depending on ground conditions, the smaller cone penetrometer may show higher peak corrected cone tip resistance q_c values (see Section 5.2.2) and lower base values. In addition, the smaller cone is more sensitive to the presence of thin layers, whose resistance is averaged beneath a larger standard cone.

Soil structure may cause failure mechanisms to occur along zones of weakness. The larger penetrometer affects a larger mass of soil and thus a greater potential for soil structure effects. Therefore, the larger cone penetrometer may exhibit a lower cone resistance in structured soils.

Recent investigations of newly-placed granular hydraulic fill have shown that the cone resistances measured with the miniature cone are different than those measured with a standardized cone in loose to medium dense granular soils. The data show that the magnitude of those differences increases as the void ratio of the sediment increases.

2.4.5 Data Interpretation

Because of the factors discussed above, caution should be taken when interpreting the small-diameter Seascout CPT data. The Seascout uses a 100-mm² cone as compared to the 1,000-mm² "standard" cone. Cone type, cone size, scale, and rate effects can affect the measured tip and friction sleeve resistances and generated pore pressures. Plate 2.6 shows the difference in size and rate of penetration between the types of piezocones discussed.

Thus, the sounding results should be used as a qualitative indicator of subsurface conditions and quantitative empirical relationships should be used with caution. Only those





individuals experienced with the miniature cone should make the interpretation of soil parameters from the data.

2.5 EXCAVATIONS AND TRENCHES

On April 8 and 9, 1999, Earth Mechanics, Inc. (EMI) performed two trench and two pit excavations on the Oakland Mole. The trenches were performed for the purpose of visual inspection and verification of the location, extent, and composition of the pre-1950 rock dike presently buried beneath the existing northern edge of the Mole. The existence, location, and condition of the rock dike affects the design and construction of the proposed new SFOBB East Approach structures or fills. Per Caltrans' request, the two pits were excavated in the beach areas at the northern edge of the Mole. The purpose of these pits was to verify maximum unshored excavation depths and to determine whether removal of the (potentially liquefiable) beach sands was a feasible option. A memorandum documenting the trench and pit excavation program is included in Volume 4. The memorandum includes descriptions and findings from the excavations, trench logs, and photographs of the excavations.

2.5.1 Trench Excavations

The locations of the trenches are shown on Plates 2.1a and 2.1b. The locations were approximately in line with the visible northern edge of the Mole to the west and the east of the jughandles, reflecting the presumed location of a buried rock dike placed during the construction of part of the fill during the 1930s.

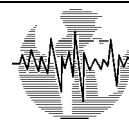
Trench 99T-1 was excavated on the western jughandle at the north edge of the existing Caltrans maintenance road pavement. Trench 99T-2 was cut inside the area circumscribed by the Caltrans road (the eastern jughandle), at approximately "W" Station 87+35. Both trenches were oriented in a north-south trend and were cut using a track-mounted excavator (Hyundai 290LC) with a 14.2-meter reach and a 0.6-meter-wide bucket. This rig was selected to cut pits in the adjacent beach areas between the jughandles. The materials excavated were temporarily stockpiled on plastic sheeting to prevent cross-contamination of underlying soils.

The trenches were backfilled with onsite soil and rock materials in lifts and compacted by tapping with the excavator bucket. Compaction led to some loss in total volume due to the loose consistency of original onsite soils, which was compensated for using soil borrowed from areas adjacent to the trench. At completion of the work, the original ground conditions were restored as well as possible.

2.5.2 Pit Excavations

Per Caltrans request, two pits were excavated in the tidal flat beach area between the two jughandles. The purpose of the pits was to verify how deep the cut would stay open unshored, and whether removal of the (potentially liquefiable) beach sands was a feasible option. The





locations are shown on the attached plan. The excavations were made by the long-reach excavator from onshore per National Environmental Policy Act Categorical Exclusion permit requirements.

2.6 ADJACENT OFFSHORE BORINGS

As part of the marine investigation (Fugro-EM, 2001d), two deep soil borings were drilled in the area (see Plate 2.1a) off the present north shore of the Oakland Mole. The two marine borings (98-39 and 98-44) were drilled in Fall 1998, immediately northwest and north of the western end of the Mole. The borings were respectively drilled to about 100- and 104-meter depths below the existing mudline.

To access those locations, the drilling barge was floated in at high tide and beached during low tide. The drilling methods, sampling procedures, and in situ and downhole geophysical testing methods and sequence are described in detail in Fugro-EM (2001d). By-boring appendices with lithographic logs with test data, CPT logs, and downhole geophysical logs for the two marine borings (98-39 and 98-44) are reproduced in Volume 2B of this report.

2.7 PHASE 3 MARINE CONE PENETRATION TESTING PROGRAM

2.7.1 Overview

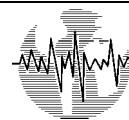
The marine CPT operations were conducted using Fugro's Seacalf CPT system. The Seacalf unit was deployed over the bow of a barge supplied and operated by CS Marine Constructors, Inc., of Vallejo, California.

The locations of the marine CPT soundings are shown on Plate 2.2a. A summary of the dates of exploration, coordinates for each sounding, and depths of penetration achieved is provided in Table 2.3. The marine CPT program was conducted by Fugro between September 23 and October 6, 2000. Operations were conducted 24 hours per day. Photographs of the operations, barge, and Seacalf equipment are included on Plate 2.7.

2.7.2 Sounding Results

The results of the 9 marine CPT soundings performed in the vicinity of the Oakland Shore Approach are presented in Volume 3 of this report. All 77 of the Seacalf CPTs performed during the Phase 3 field operations are presented in Volume 2H of the Final Marine Site Characterization Report (Fugro-EM, 2000d). The CPT logs provide graphical plots versus depth showing: a) tip resistance in megapascals (MPa), b) sleeve friction in MPa, c) friction ratio in percent, and d) pore pressure readings in MPa. In addition, the sounding logs show the range of undrained shear strengths that are calculated from CPT cone tip resistances (corrected for unequal end area effects) based on cone bearing capacity factors (N_k) of 12 and 15.





2.7.3 Vessel

The marine CPTs were conducted from *Barge 32*, an approximately 33-meter by 9-meter barge that was supplied and crewed by CS Marine. The barge included a four-point anchor system and two spuds.

Fugro equipment was mobilized onboard Barge 32 at CS Marine's dock in Vallejo. The CPT barge was and pushed and positioned over the proposed sounding locations by the shallow draft tugboat *Mudcat*, which also served as an anchor assist boat. The tugboat was owned and operated by Westar, Inc.

Except where water depth prohibited the use of spuds, the barge was held on position using two spuds. Where water depth exceeded the capacity of the spuds or if the spuds were considered likely to impact existing underwater utility lines, the barges were held on position using a four-point anchor spread only. At several locations where anchors were used, it was possible to winch over to more than one test location using the same anchor spread.

2.7.4 Survey and Water Depth Measurements

Position and Navigation. A DGPS and integrated navigation software, owned and operated by Fugro, were used to position vessels at the specified drilling locations and to determine final X-Y coordinates of the vessels at those locations. Coordinates calculated from Fugro's DGPS system are considered accurate to within about 1 meter (3 feet). The actual locations of the Seacalf unit were calculated from: 1) the measured offsets of the unit from the DGPS receiver onboard the tugboat; and 2) the final heading of the barge. The DGPS also was used to position the barge's anchors.

Water Depth Measurements. Prior to deploying the Seacalf CPT unit, preliminary water depth measurements were made using a lead line and echo sounder. Those preliminary water depth measurements were required to make several field decisions (e.g., determining the length of cone rod to deploy during lowering of the Seacalf unit). However, due to relatively strong water currents, those measurements were considered somewhat approximate and the final mudline elevations reported were calculated from the 2000 multi-beam and tidal flat bathymetric survey data for the project.

2.7.5 Marine CPT Equipment and Procedure

Seacalf CPT System. The marine CPT soundings were performed using Fugro's 10-ton, wheel-drive tethered Seacalf CPT system. Deployed from a cantilevered frame off the bow of the barge, the Seacalf unit was lowered to and raised from the bay floor with a winch mounted to the barge deck.





With the Seacalf, the cone rod was advanced through the unit and into the soil by a system of four wheels that gripped the rod and pushed it into the soil at a controlled rate of 2 cm/sec. As the cone penetrated the seabed, the variations in cone tip resistance, sleeve friction, and dynamic pore pressure were continuously recorded. The results were displayed graphically and simultaneously recorded as the test progressed.

Cone Assembly. The basic construction of the cone assembly used in the marine CPT soundings is similar to that of the 15-cm² cone used for the conventional land CPT. Cone tip resistance, sleeve friction, and dynamic pore pressure were measured in all of the soundings. The pore pressure element was located at the base of the cone tip.

CPT Sounding Termination. CPT soundings were generally advanced until practical refusal to penetration was encountered. Practical refusal was typically due to either excessive deflection within the CPT cone rods or due to very high tip resistance. As the test progressed, the CPT operator monitored the cone resistance and its deviation from vertical. A test at a given location continued until a refusal criterion was met. For most soundings, the cone rod was first advanced through the relatively soft Young Bay Mud (YBM) strata until stiff clay layers or dense sand layers of the underlying units were encountered. To reduce the potential for rod buckling, casing was then advanced around the cone rods to provide lateral support in the relatively soft YBM layers. After setting the casing, the cone rod was again pushed until practical refusal was encountered.

Several of the CPT soundings performed in the Oakland Shore Approach area and to the north of Yerba Buena Island were located in extremely shallow water depths. To reduce the potential for grounding the barge and tug, CPT soundings at those locations were typically performed at high tide. In a few instances, this precluded the use of casing to increase test depth since it was necessary to move the barge before it was grounded during a falling tide. In those instances, testing was continued until practical refusal was encountered typically slightly below the base of the YBM.

Data Entry. Data collected from each sounding were processed immediately and entered into a database. The electronic databases were used to generate preliminary CPT sounding logs and to interpret soil properties using published and site-specific correlations with CPT data in the field. In addition to providing preliminary information in a timely manner to Caltrans and the design team, the data processing allowed for onboard data evaluation. For example, faulty data were easily identifiable, which allowed for replacement of equipment and retesting prior to demobilization of the barge.





Boring	Easting	Northing	Station Along "W-Line"	Offset from "W-Line" (m)	Ground Surface Elevation (m MSL)	Exploration Depth (m)
Foundation Design						
98-51 (B-1)	1838901	648233	84+35	56 RT	+1.2	70.7
98-52 (B-2)	1838962	648256	84+99	40 RT	+1.7	35.7
98-53 (B-3)	1839052	648267	85+90	37 RT	+3.6	35.7
98-54 (B-4)	1839080	648270	86+18	37 RT	+3.4	35.7
98-55 (B-5)	1839073	648301	86+14	5 RT	+2.0	61.6
98-56 (B-6)	1839212	648294	87+52	23 RT	+3.1	44.8
98-57 (B-7)	1839266	648307	88+07	14 RT	+3.5	46.3
98-58 (B-8)	1839287	648327	88+29	5 LT	+3.9	60.0
98-59 (B-9)	1839435	648325	89+77	9 RT	+3.5	38.7
98-60 (B-10)	1839546	648349	90+89	0	+3.4	46.3
Roadway and Substation Design						
98-61 (P-1)	1839130	648280	86+69	30 RT	+2.9	23.5
98-62 (P-2)	1839320	648302	88+60	23 RT	+3.6	23.0
98-63 (P-3)	1839479	648334	90+21	5 RT	+3.5	23.5
98-64 (P-4)	1839605	648362	91+50	2 LT	+3.5	23.5
98-65 (P-5)	1839704	648395	92+54	9 LT	+3.4	23.5
98-66 (P-6)	1839317	648260	88+54	65 RT	+3.1	8.1
98-67 (P-7)	1839462	648313	90+02	23 RT	+3.7	15.8
98-68 (P-8)	1839597	648340	91+38	18 RT	+3.7	9.6
98-69 (P-9)	1839677	648359	92+19	18 RT	+3.8	13.0
98-70 (P-10)	1839259	648242	87+95	78 RT	+3.0	25.0
98-71 (P-11)	1839449	648283	89+86	52 RT	+3.2	12.8
98-72 (P-12)	1839568	648300	91+02	52 RT	+3.1	8.1
98-73 (P-13)	1839666	648322	91+99	51 RT	+2.8	12.8
98-74 (P-14)	1839832	648345	93+57	80 RT	+2.9	7.2
98-75 (P-15)	1838987	648200	85+18	98 RT	+2.4	31.1

ON-LAND SOIL BORING LOCATIONS AND DEPTHS
Oakland Shore Approach
SFOBB East Span Seismic Safety Project

TABLE 2.1





Designation	Easting	Northing	Station Along "W-Line"	Offset from "W-Line" (m)	Ground Surface Elevation (m MSL)	Depth (m)	Velocity Logging with Seismic Cone	Soil Sampling
Phase 1, Spring 1998								
98-16	1838906	648241	84+12	9RT	1.5	17.3	No	No
98-17	1839051	648271	85+59	6LT	3.5	53.1	Yes	No
98-18	1839237	648298	87+47	20LT	3.2	50.0	Yes	No
Phase 2, Fall 1998								
98-101 (CPT-1)	1839011	648267	85+19	6LT	3.1	49.8	Yes	No
98-102 (CPT-2)	1839111	648300	86+52	9RT	2.1	50.2	Yes	No
98-104 (CPT-4)	1839304	648323	88+46	1RT	3.7	21.9	No	No
98-105 (CPT-5)	1839372	648313	89+13	16RT	3.6	39.1	No	No
98-110 (CPT-10)	1839489	648287	89+96	15RT	3.1	46.8	No	No
98-109 (CPT-9)	1839339	648260	88+45	26RT	3.0	48.9	Yes	No
Phase 2, All-Terrain (Spring 1998)								
99C-1	1838969	648274	85+08	23RT	-0.2	29.3	No	No
99C-2	1839037	648290	85+77	13RT	-0.6	12.1	No	No
99C-3	1839150	648311	86+91	1RT	0.1	15.5	No	No
99C-4	1839208	648316	87+50	1RT	-0.1	15.4	No	No
99C-5	1839262	648328	88+04	7RT	-0.1	15.5	No	No
99C-6	1839329	648333	88+72	7RT	-0.4	16.6	No	No
99C-7	1839384	648343	89+27	13RT	-0.6	19.8	No	No
99C-8	1839431	648353	89+75	19RT	-0.6	15.6	No	No
99C-9	1839496	648364	90+42	23LT	-0.7	15.0	No	No
99C-10	1839558	648374	91+06	23LT	-0.6	15.4	No	No
99C-11	1839139	648320	86+81	10LT	-0.4	24.4	No	No
99C-12	1839174	648323	87+16	10LT	-0.4	29.5	No	Yes
99C-13	1839205	648325	87+47	9LT	-0.4	22.6	Yes	No
99C-14	1839250	648329	87+92	9LT	-0.3	16.6	No	Yes
99C-15	1839014	648299	85+55	2LT	-0.4	11.7	Yes	No

NOTE: Electrical interference prevented data acquisition at planned CPT locations 98C-103 (CPT-3), 98C-106 (CPT-6), 98C-107 (CPT-7), and 98C-108 (CPT-8).

ON-LAND CPT LOCATIONS AND DEPTHS
Oakland Shore Approach
SFOBB East Span Seismic Safety Project

TABLE 2.2



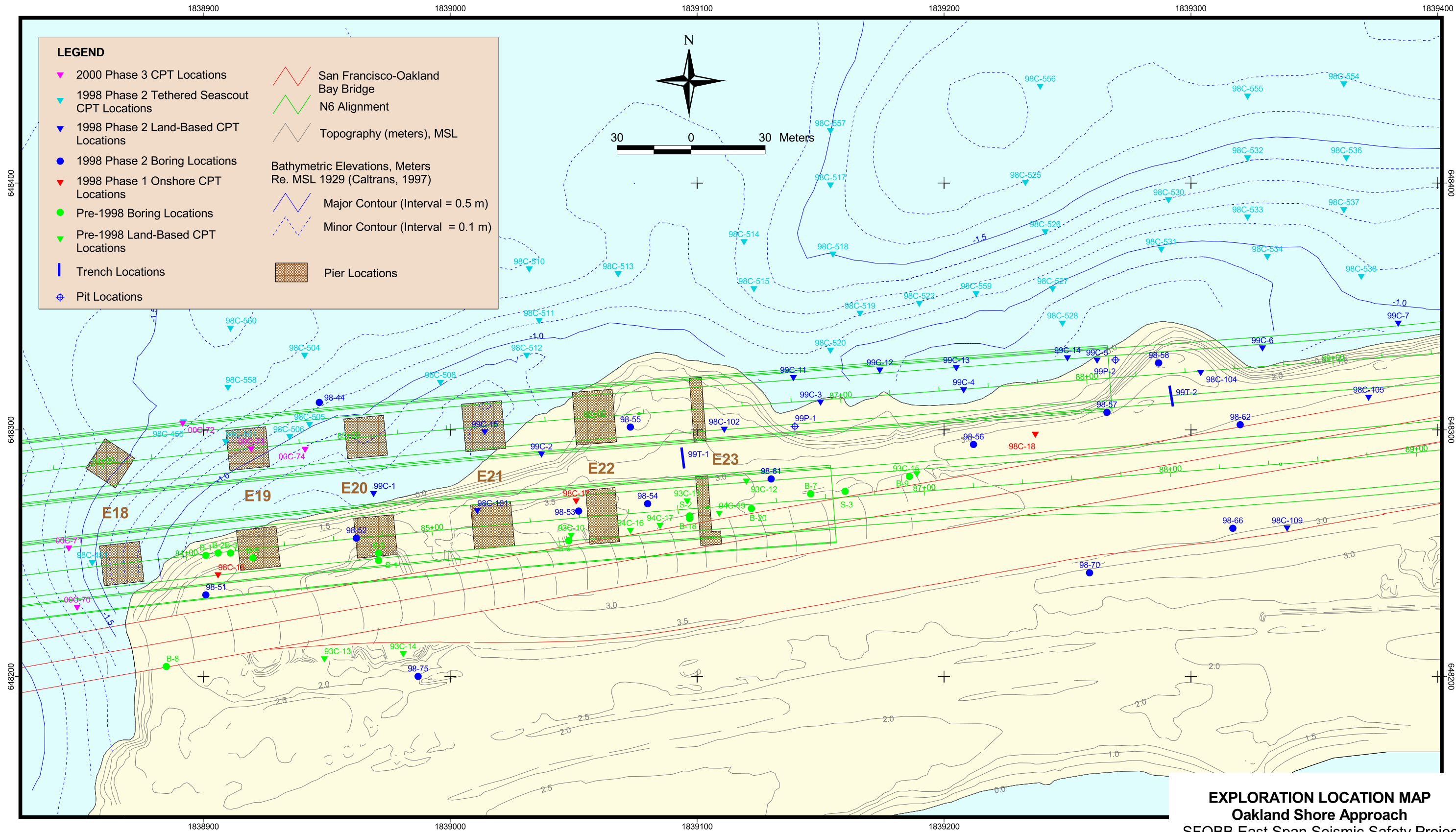


Designation	Easting	Northing	Station	Offset (m)	Ground Surface Elevation (m MSL)	Depth (m)	Velocity Logging with Seismic Cone	Soil Sampling
September - October, 2000								
00C-64	1838758	648273	"W" Sta. 83+00	1 m Left	-2.9	50.0	No	No
00C-65	1838765	648233	"E" Sta. 82+79	1 m Right	-2.9	29.7	No	No
00C-66	1838780	648262	"W" Sta. 83+20	13 m Right	-2.6	25.1	No	No
00C-67	1838786	648232	"E" Sta. 83+0	4 m Right	-2.6	39.9	No	No
00C-68	1838806	648225	"E" Sta. 83+20	14 m Right	-2.4	42.2	No	No
00C-69	1838823	648249	"E" Sta. 83+40	8 m Left	-0.9	40.0	No	No
00C-70	1838848	648227	"E" Sta. 83+59	16 m Right	-1.6	11.9	No	No
00C-71	1838845	648251	"E" Sta. 83+59	8 m Left	-1.6	11.1	No	No
00C-72	1838891	648302	"W" Sta. 84+40	14 m Left	-1.4	51.4	No	No
00C-73	1838919	648292	"W" Sta. 84+59	No offset	-1.1	17.9	No	No
00C-74	1838941	648291	"W" Sta. 85+0	2 m Right	-0.9	12.7	No	No

MARINE-BASED SEACALF CPT LOCATIONS AND DEPTHS
Oakland Shore Approach
SFOBB East Span Seismic Safety Project

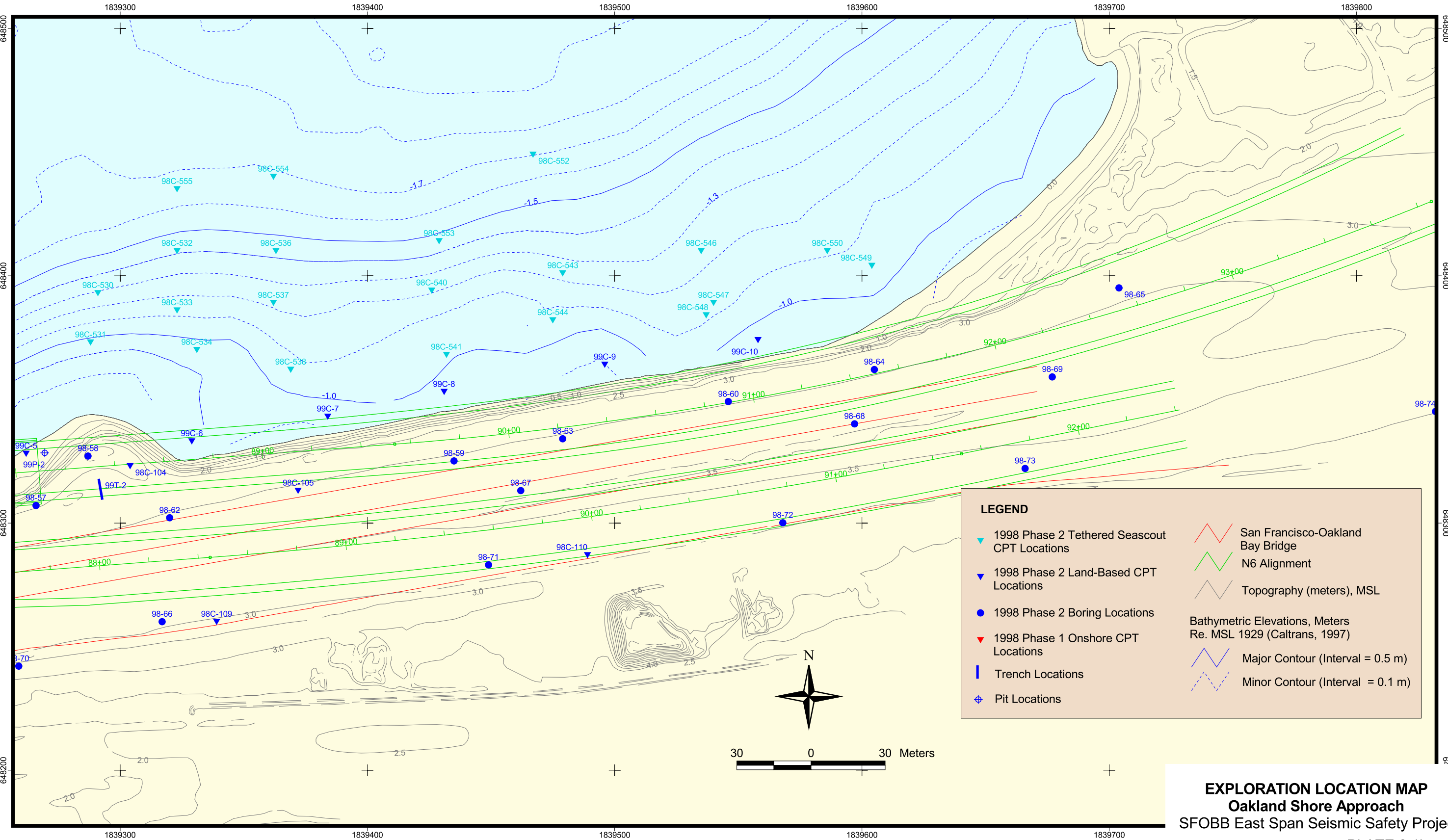
TABLE 2.3

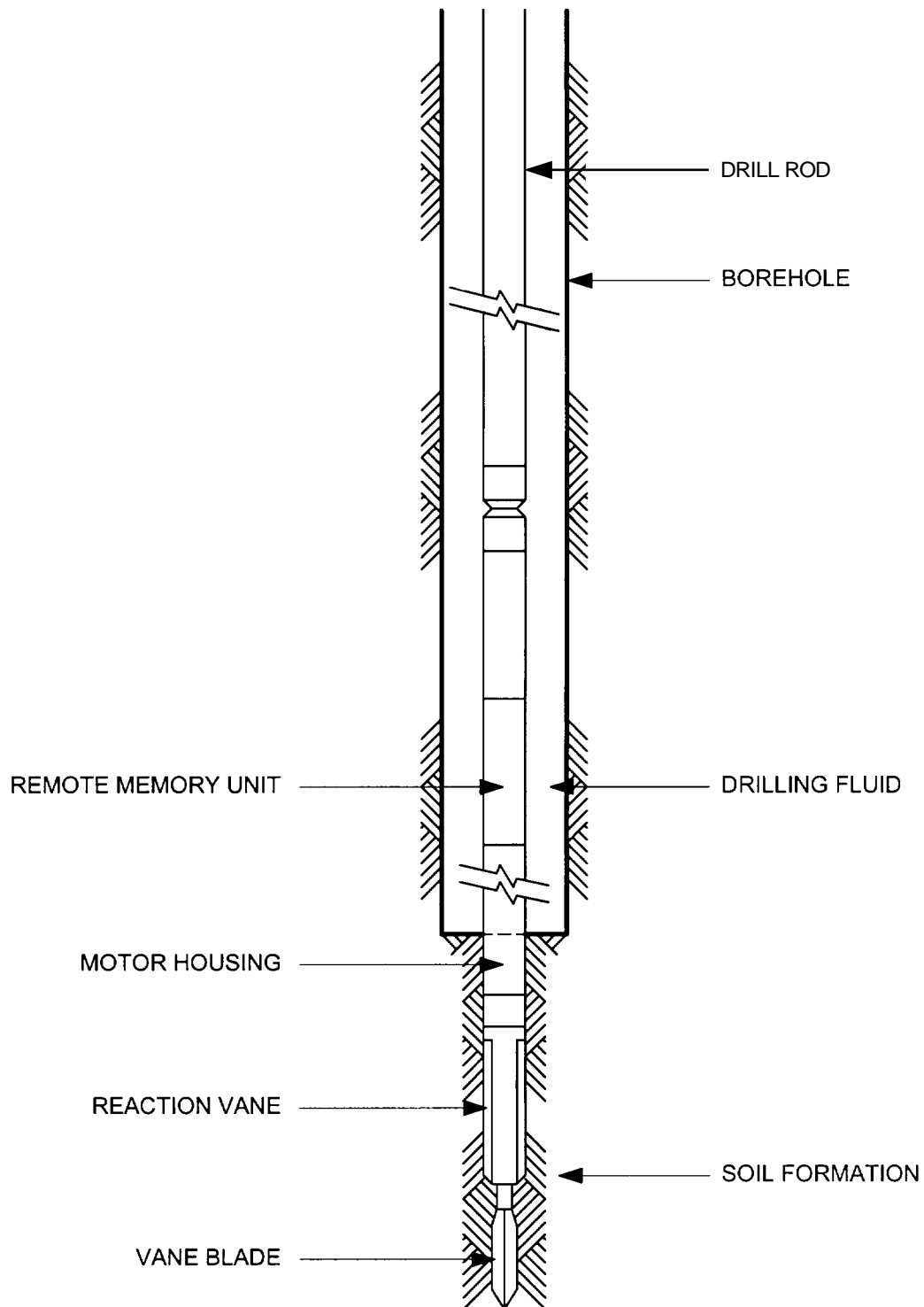




j:\caltrans\reports\finalreports\finaloaksitechar_book5\vol1\final-odb-xls\section2\plate2-1a.odb, cdean, 02/15/2001

EXPLORATION LOCATION MAP
Oakland Shore Approach
SFOBB East Span Seismic Safety Project
PLATE 2.1a





THE DOLPHIN DOWNHOLE REMOTE VANE
Oakland Shore Approach
SFOBB East Span Seismic Safety Project





TRUCK-MOUNTED CPT OPERATIONS
Oakland Shore Approach
SFOBB East Span Seismic Safety Project





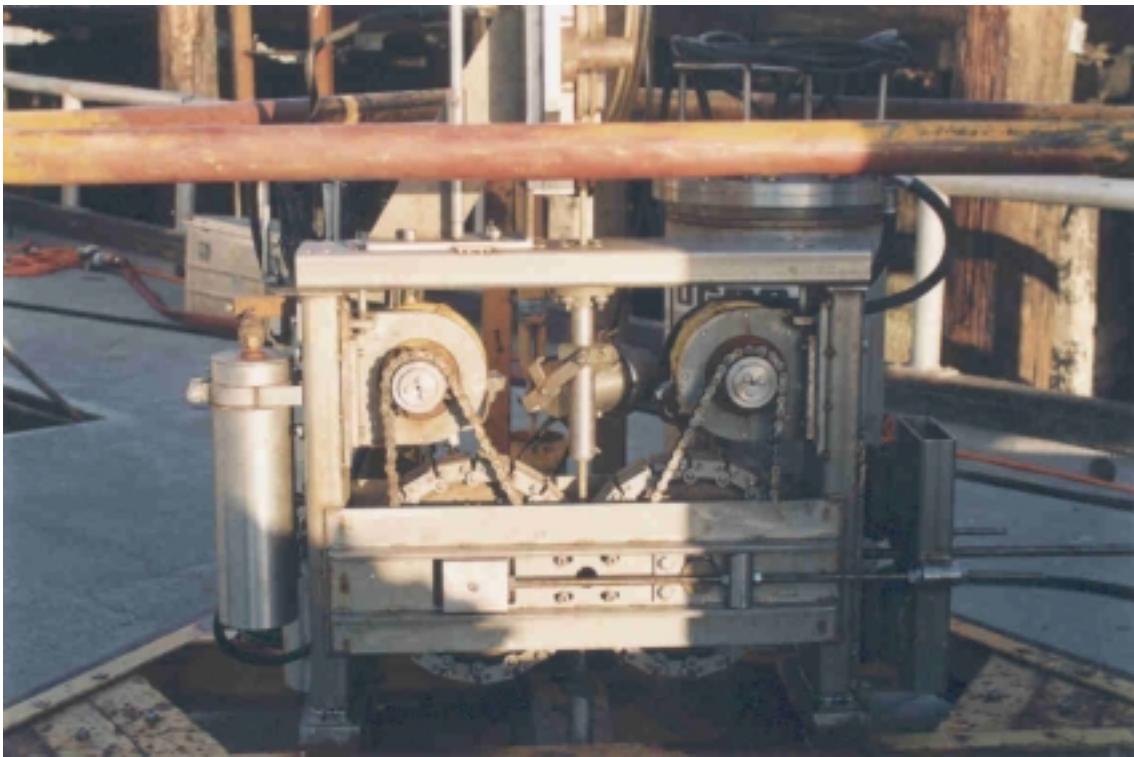
TRACK-MOUNTED CPT OPERATIONS
Oakland Shore Approach
SFOBB East Span Seismic Safety Project





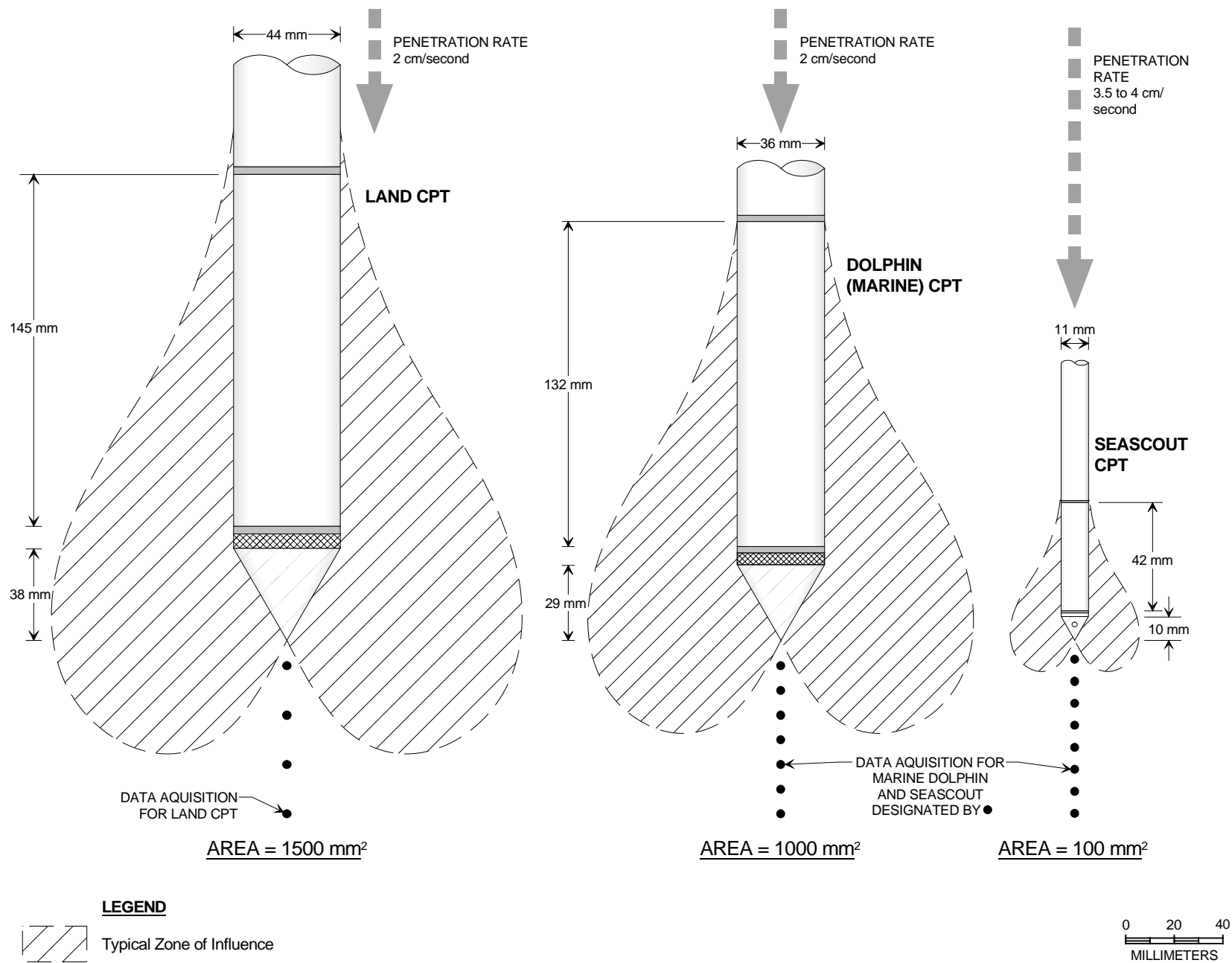
TETHERED SEASCOUT DEPLOYMENT
Oakland Shore Approach
SFOBB East Span Seismic Safety Project





TETHERED SEASCOUT RETRIEVAL
Oakland Shore Approach
SFOBB East Span Seismic Safety Project





COMPARISON BETWEEN LAND, DOLPHIN AND SEASCOUT CPTS
Oakland Shore Approach
SFOBB East Span Seismic Safety Project



Barge 32 with Seacalf at San Francisco-Oakland Bay Bridge.



Seacalf being deployed from retractable cantilever frame.

SEACALF CPT OPERATIONS
Oakland Shore Approach
SFOBB East Span Replacement Project

PLATE 2.7a





Preparation for sounding with Seacalf in raised position.

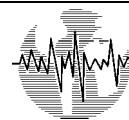
SEACALF CPT OPERATIONS
Oakland Shore Approach
SFOBB East Span Replacement Project

PLATE 2.7b



SECTION 3.0 LABORATORY TESTING

SECTION 3.0



3.0 LABORATORY TESTING

3.1 INTRODUCTION

The laboratory testing program for this study was performed in two phases. Visual classification, wet density determinations, water content determinations, and strength tests (including Torvane tests, pocket penetrometer tests, miniature vane tests, Swedish fall cone, and unconsolidated-undrained triaxial compression tests) were performed on the Fugro barge concurrently with the marine drilling and sampling operations. Additional laboratory soil testing was subsequently performed at Fugro's onshore soil mechanics laboratories in Ventura, California, and Houston, Texas. Dynamic testing was performed at the University of California at Berkeley. The onshore laboratory testing program included: classification tests (grain size, plasticity, organic content, specific gravity), consolidation tests, consolidated drained and undrained triaxial tests, cyclic direct simple shear tests, corrosion tests, and resistance value (R-value) tests.

The test procedures generally conformed to the applicable Caltrans and ASTM standards (ASTM, 1998). The following sections provide descriptions of the laboratory tests performed in the static laboratory soil testing program. The total numbers of laboratory tests that have been conducted are listed on Table 3.1. The results of most laboratory tests conducted on soil and rock samples are included in the individual boring-specific appendices provided in Volumes 2A and 2B. The report prepared by the University of California at Berkeley is included in Volume 4.

3.2 CLASSIFICATION TESTS

The method of classifying soils according to their engineering properties used in this study was ASTM Standard Test Method D2487, which is based on the Unified Soil Classification System. The classification tests performed for this project include tests for moisture content, unit weight, grain size distribution, Atterberg limits, organic content, and specific gravity. All of those data are tabulated on the Summary of Test Results provided in the boring-specific appendices (Volumes 2A and 2B), and most of the results also are plotted on the individual boring logs.

Tests for moisture content and unit weight of the soils were performed in general accordance with California Test 226. Plastic and liquid limits, collectively termed the Atterberg limits, were determined for selected cohesive soil samples and were performed in accordance with California Test 204. Wet densities of soil samples, where possible, were measured in the field by weighing soil samples of known volumes immediately after extrusion. Moisture content measurements for the above tests were from samples dried in an oven maintained at





approximately 110°C. In the onshore laboratories, potentially organic samples were dried in an oven maintained at approximately 60°C.

Specific gravity of soil tests were performed in accordance with California Test 209. Organic content tests to estimate the weight percentage of organic matter in potentially organic soils were performed in accordance with ASTM D2974.

The gradation characteristics of selected samples were estimated in general accordance with the sieve and hydrometer analysis procedures of California Tests 202 and 203, respectively. In general, sieve analysis (for sizes greater than the No. 200 sieve) were performed on primarily granular samples (sand and gravel), and hydrometer analysis was performed on primarily fine-grained samples (silt and clay). Several granular samples were tested for only the percent passing the No. 200 sieve.

3.3 SOIL SHEAR STRENGTH TESTS

3.3.1 Undrained Shear Strength

Six procedures were used in the laboratory investigation to determine the undrained shear strengths of the cohesive soils under various conditions. Undisturbed and residual shear strengths of cohesive soil samples were determined in the field with a motorized miniature vane device while the samples were still in the sample tubes. Remolded miniature vane tests, and undisturbed and remolded unconsolidated-undrained triaxial compression tests were performed in the field on selected samples after extrusion. Estimates of shear strength also were made in the field using a Torvane device, a fall cone device, and a hand-held pocket penetrometer. Additional unconsolidated-undrained triaxial compression tests were performed on selected cohesive soil samples in Fugro's Houston laboratory. Isotropically consolidated-undrained triaxial compression tests were performed on three samples in Fugro's Houston laboratory. The test procedures are described in the following paragraphs.

Torvane Test. In the Torvane test, a small hand-operated device (which consists of a metal disc with thin, radial vanes projecting from one face) is pressed against the flat surface of the soil until the vanes are fully embedded. The device is then rotated through a torsion spring until the soil is sheared. The device is calibrated to indicate the undrained shear strength of the soil directly from the rotation of the torsion spring.

Pocket Penetrometer Test. This test is performed by slowly pressing a small, flat-ended, cylindrical metal rod (6.35 mm in diameter) into the flat surface of the soil sample through a spring until it is embedded a predetermined distance. The resistance to penetration is recorded by the spring, which is calibrated to read the undrained shear strength of the soil based on spring compression.





Fall Cone Test. This test is performed by lowering a conical tool of known dimensions and weight so that the tip just makes contact with the flat surface of the soil sample. The tool is then released so that it penetrates below the surface of the sample under its own weight. The device is calibrated to indicate the undrained shear strength of the soil directly from the measured penetration of the cone. The maximum undrained shear strength that could be measured with the apparatus onboard the barge is approximately 215 kPa.

Miniature Vane Test. Miniature vane tests are performed in accordance with ASTM D4648. In performing the miniature vane test, a small, 4-bladed vane is inserted into an undisturbed or remolded cohesive specimen. Torque is applied to the vane through a calibrated spring activated by a motorized pulley and belt system, which causes the vane to rotate slowly until soil shear failure occurs. The undisturbed or remolded shear strength of the soil is computed from the torque transmitted by the calibrated spring by multiplying the net rotation, in degrees, by the spring calibration factor. The maximum undrained shear strength that could be measured with the miniature vane device used for this project is approximately 215 kPa.

In selected undisturbed miniature vane tests, residual shear strengths of very soft to firm clay soils also were measured by allowing the vane to continue rotating after the initial soil shear failure has occurred. The tests are terminated when the torque applied to the vane through the calibrated spring has reached a constant value. The residual shear strength, which represents the soil shear strength at large strain, is computed by multiplying the net rotation (in degrees) by the spring calibration factor.

Unconsolidated-Undrained Triaxial Compression Test. In this type of strength test, either an undisturbed or remolded test specimen is enclosed in a thin rubber membrane and subjected to a confining pressure at least equal to the computed effective overburden pressure. A confining pressure of about 830 kPa (the pressure limitation of the triaxial cell in the field laboratory) was used in the field for unconsolidated-undrained triaxial compression tests performed on samples encountered at deep penetration. The test specimen is not allowed to consolidate under the influence of this confining pressure prior to testing. The test specimen is then loaded axially to failure at a constant rate of strain without permitting drainage from the specimen. The undrained shear strength of the cohesive soil is computed as one-half the maximum observed deviator stress.

Undisturbed and remolded shear strengths determined by this type of test are tabulated on the Summary of Test Results in the boring-specific appendices (Volumes 2A and 2B). Values of ϵ_{50} from undisturbed unconsolidated-undrained triaxial compression tests, confining pressure, percent strain at failure, and type of failure are tabulated with the stress-strain curves in the boring-specific appendices.

Isotropically Consolidated-Undrained Triaxial Compression (CIUC) Test. Triaxial compression tests were performed to determine the stress-strain characteristics and the static





shear strength of a soil specimen under applied axial stresses. This test uses procedures recommend by ASTM D4767. Prior to setting up the test, the in situ effective vertical stress at the penetration of the sample was estimated on the basis of the interpreted unit weight profile at the boring location. The maximum past pressure that the sample had been subjected to was estimated from a consolidation test performed on a specimen from the same Shelby tube.

A cylindrical soil specimen was enclosed in a rubber membrane and placed inside a pressure chamber (triaxial cell). Tests were performed on specimens trimmed to 51.0-mm diameter (area = 20.27 cm²) and a height of about 114 mm. The test specimens were saturated through back pressuring. Specimens were then isotropically consolidated in a drained state at a controlled rate of strain (about 0.3 percent per hour) to the assigned stresses, which are greater than or equal to the estimated maximum past pressure, thus inducing an overconsolidation ratio (OCR) of 1.0. Vertically or spirally oriented, 6-mm-wide, Whitman No. 54 filter strips placed at about 6-mm spacing provided radial drainage. The chamber pressure was kept constant and specimen drainage was not permitted during shear. A loading piston was advanced against the specimen cap at an applied rate of strain slow enough to produce approximate equalization of pore water pressure throughout the specimen at failure. The static stresses and pore water pressures, measured under undrained conditions, were used to express the measured strength parameters in terms of effective stress. Load, deformation, and pore water pressure measurements were recorded during loading using a data acquisition system.

Typically, a series of three tests were performed from each selected Shelby tube sample. One specimen was consolidated to approximately its effective overburden stress (typically close to the past maximum pressure in the Young Bay Mud). A second and third test were run on specimens consolidated to stress levels two and four times the estimated effective overburden pressure.

A summary of the estimated in situ stresses, consolidation stresses, and undrained shear strengths for the CIUC triaxial compression tests is presented on Table 5.1. Additionally, the following plots are provided for each test in the boring-specific appendices:

- Axial strain versus effective vertical stress during consolidation
- Shear stress (q) versus average effective stress (p') during undrained loading
- Shear stress, excess pore water pressure, and obliquity versus axial strain during undrained loading

3.3.2 Drained Strength Tests

Multi-stage, isotropically consolidated-drained (CIDC) triaxial compression tests were performed to evaluate the frictional characteristics of the granular materials encountered in the boring. The tests were performed on samples recovered using a 57-mm-ID, 74-mm-ID, and thin-walled Shelby tube or a modified California sampler with a 61-mm-ID brass liner. The test





specimen was trimmed down to a diameter of 51 to 71 mm, a height of 96 to 140 mm, and placed in a rubber membrane with saturated filter paper strips around the perimeter of the specimen.

During the consolidation phase, the test specimen was allowed to consolidate to one of three test-confining pressures. The Young Bay Mud samples were tested at confining stresses ranging from the interpreted in situ vertical effective stress to approximately five to eight times the interpreted in situ vertical effective stress. Due to the relatively low confining stresses, it was considered relatively difficult to test these samples at stresses less than the in situ vertical stresses. The Old Bay Mud/Upper Alameda Marine (OBM/UAM) samples were tested at stresses ranging from approximately half the interpreted in situ vertical effective stress to approximately four times the interpreted in situ vertical effective stress.

After the consolidation phase for the lowest confining pressure was completed and with the drainage line remaining open, the test specimen was sheared by increasing the axial load at a constant strain rate using a 44.5-kN Wykham-Farrance compression frame. The axial load was monitored by a load cell, deformation was measured by an LVDT, and volume change readings were taken with a calibrated burette. The load and deformation readings were continuously recorded by an IBM-compatible data logger.

The above procedures were repeated for two higher confining pressures. For the first two loading stages, the specimen was sheared until failure was indicated by a decrease in load, or 5 percent strain, whichever occurred first. After reconsolidation to a higher confining stress for the third stage, the sample was sheared to failure.

Isotropically consolidated-drained triaxial (CIDC) test results, including friction angle, are summarized in Table 5.3. Additionally, plots of stress versus strain, volumetric strain versus axial strain, and Mohr diagrams for the individual tests are presented in the boring-specific appendices (Volumes 2A and 2B).

3.4 CONSOLIDATION TESTS

3.4.1 Incremental Consolidation Tests

Incremental consolidation tests were performed on selected high-quality cohesive samples to investigate the stress history of the soils at the boring location. The tests were performed in accordance with the recommendations of ASTM D2435. The consolidation test specimens were trimmed into 63.4-mm-ID stainless steel rings. The trimmed test specimen and ring were then placed in a specially designed cell where the base of the test specimen was sealed from the fluid (water) and the top of the test specimen was exposed to the fluid. A porous stone was placed on top of the test specimen and the loading ram was brought into contact with the porous stone. As the test specimen was compressed during loading, the pore fluid drained from the sample through the porous stone. The setup of the test specimen into the cell was performed





with the entire cell under water so that there was no air trapped in the system that would affect the pore pressure response during loading.

After the cell was fully assembled, it was placed in a loading frame where the test specimen would be saturated before loading. Vertical loads were added in increments that usually doubled the previous load, yielding a load increment ratio of two. Each load increment was held for a period t_{100} (primary consolidation) determined by the logarithm of time method. The data readings were used to compute the vertical strain, vertical pressure, and coefficient of consolidation. Loading was continued until the effective stress applied was greater than the maximum past pressure applied to the test specimen, and the virgin compression portion of the consolidation curve was well defined. At that point, the test specimen was unloaded and then reloaded. The test specimen was rebounded again at the end of the test to produce a second rebound curve.

3.4.2 Controlled-Rate-of-Strain (CRS) Consolidation Test

CRS consolidation tests were performed in general accordance with ASTM D4186 on selected samples from the two adjacent marine borings (98-39 and 98-44). CRS consolidation test specimens were trimmed into 63.5-mm-ID stainless steel rings. The trimmed test specimen and ring were placed in a specially designed cell. The base of the test specimen was sealed from fluid (water) and the top of the specimen was exposed to the fluid. A porous stone was placed on top of the test specimen and the loading ram was brought into contact with the porous stone. As the test specimen was compressed during loading, the pore fluid drained from the top of the sample through the porous stone. A pressure transducer was connected to the bottom of the specimen, through the test cell, to measure the excess pore pressure during loading.

After the cell had been fully assembled, it was placed in a loading frame where the test specimen was saturated after a small setting load had been applied (to prevent swelling). The rate-of-strain was selected to produce a minimum excess pore pressure of 21 kPa and to limit the ratio of maximum excess pore pressure to applied vertical pressure to less than 15 percent (more commonly 10 percent). A limit of 10 to 15 percent was selected to obtain more reliable compressibility and rate of consolidation coefficients. The pore pressure ratio was continuously monitored during the first stage of loading, and the rate of strain was automatically adjusted to keep the pore pressure ratio within the above limits. Loading was continued until the applied effective stress was greater than the estimated maximum past pressure applied to the test specimen and the virgin compression portion of the consolidation curve was well defined. The sample was loaded to between 20 and 30 percent strain, and then rebounded to produce a rebound curve.

A summary of the consolidation test results is presented in Table 5.4. Individual test results are presented in the boring-specific appendices (Volume 2) as curves of void ratio versus





effective vertical pressure. Also plotted with these curves is the computed coefficient of consolidation at each effective vertical pressure.

3.5 ADDITIONAL LABORATORY TESTING

3.5.1 R-Value Testing

The R-value tests were performed on bulk samples of pavement subgrade material obtained from selected pavement series borings (98-65, 98-68, 98-69, and 98-72). The tests were performed in accordance with California Test 301 by BTC Laboratories, Inc., Ventura, California.

The R-value is a parameter used in the design of flexible pavement sections. The test consists of four basic steps:

1. Compaction of three samples at different moisture contents in a 100-mm-ID, by 127-mm-tall mold using a mechanical compactor.
2. An exudation pressure test is performed. An increasing pressure is applied to the compacted sample. When enough moisture is expelled from the sample to turn on five moisture indicating lights on the exudation device, the pressure is recorded as the exudation pressure.
3. A swell pressure test is performed by adding 200 mL of water to the top of the mold and measuring the expansion pressure after 16 to 24 hours.
4. A stabilometer test is performed where the induced lateral pressure is measured under an applied vertical pressure of 110 kPa. The R-value is then determined from an empirical formula presented in California Test Method 216.

The results of the R-value testing are presented in the Summary of Test Results and as plots of exudation pressure versus R-value in Volume 2B.

3.5.2 Corrosion Testing

Corrosion testing was performed by Health Science Associates, Los Alamitos, California. The corrosion testing followed California Test Methods 532 and 643. A series of four tests were run, including Resistivity (ohms/cm), pH, Chloride Content (parts per million [ppm]), and Sulfate Content (ppm). Corrosivity test results are presented in the by-boring appendices provided in Volumes 2A and 2B.

3.6 UNIVERSITY OF CALIFORNIA AT BERKELEY TESTING

Sealed "SAVE" tube samples from six locations were delivered to the University of California at Berkeley to conduct a series of special cyclic simple shear and consolidation tests.



The methods and results of that testing program are described and presented in UC Berkeley (1999), which is provided in Volume 4.

3.6.1 Simple Shear Testing

The purpose of the simple shear testing was to investigate the possible effects of large cyclic straining (such as might be caused by a significant seismic event) on the subsequent stress-strain properties of the soil. To assess this directly, pairs of specimens from a given sampling tube were tested. One of the specimens was sheared monotonically, while the other specimen was first cyclically loaded at a specified strain amplitude and number of cycles, and then monotonically sheared without allowing the pore pressures from the cyclic loading to dissipate. Cyclic loading consisted of 25 strain-controlled cycles at a frequency of 0.2 Hertz (Hz), with single amplitude shear strains ranging from 1 to 3 percent. A total of six sets of two or three specimens were tested.

3.6.2 Consolidation Testing

Six special consolidation tests were performed at the University of California at Berkeley to investigate the rate of consolidation that could be expected when pore pressures are allowed to dissipate horizontally, as would be the case after the installation of wick drains. Rather than conventional oedometer tests (which are designed to consolidate horizontal slices of a tube sample using vertical drainage), the tests used a modified triaxial test apparatus to measure the consolidation response of large cylindrical specimens to isotropic increases in stress.





TABLE 3.1

Test	Number of Tests by Boring																												Totals
	98-51	98-52	98-53	98-54	98-55	98-56	98-57	98-58	98-59	98-60	98-61	98-62	98-63	98-64	98-65	98-66	98-67	98-68	98-69	98-70	98-71	98-72	98-73	98-74	98-75	98-39	98-44		
Index Tests																													
Atterberg Limits	22	13	9	9	19	17	15	19	13	15	11	7	11	9	9	--	4	4	2	8	6	1	4	--	10	34	33	304	
Unit Weight	13	8	8	6	19	8	10	12	10	10	7	8	9	8	8	--	4	1	1	5	4	2	3	--	6	35	34	239	
Water Content	31	20	21	19	30	29	23	27	22	25	19	17	20	18	18	5	12	10	10	19	11	6	9	5	21	51	48	546	
Percent Passing #200	4	4	5	3	--	5	2	6	2	3	4	5	1	--	5	--	3	3	2	3	3	1	3	--	4	--	2	73	
Sieve Analysis	3	2	3	3	2	3	5	4	3	2	8	5	4	3	1	3	3	4	4	4	--	3	2	2	6	6	3	91	
Hydrometer	--	--	--	2	1	2	--	--	1	--	7	1	4	2	1	1	1	--	--	--	--	2	--	--	3	7	4	39	
Specific Gravity	2	3	3	3	3	3	5	4	4	2	--	--	--	--	--	--	--	--	--	--	--	--	--	--	--	--	--	32	
Consolidation Tests																													
CRS Consolidation	--	--	--	--	--	--	--	--	--	--	--	--	--	--	--	--	--	--	--	--	--	--	--	--	--	4	3	7	
Incremental Consolidation	7	1	2	4	5	3	4	4	2	2	6	3	4	3	7	--	1	--	1	3	2	--	4	--	4	4	5	81	
Radial Consolidation	--	--	--	--	--	--	1	--	1	1	--	1	--	--	--	--	--	--	--	--	--	--	--	--	--	--	--	4	
Shear Strength Tests																													
Miniature Vane - Residual	--	--	1	--	--	--	--	--	2	1	1	--	2	1	--	--	--	--	--	--	--	--	1	--	--	9	6	24	
Miniature Vane - Remolded	2	1	--	2	5	3	1	2	4	1	2	3	3	3	2	--	2	--	1	1	3	1	4	--	--	1	4	51	
Miniature Vane - Undisturbed	14	7	9	10	17	11	15	14	8	13	6	6	6	8	5	--	4	--	2	5	4	1	3	--	7	24	29	228	
Torvane	13	11	9	15	18	17	7	19	12	13	10	12	7	13	9	--	9	1	4	10	5	2	8	--	6	23	23	276	
Pocket Penetrometer	9	1	2	2	10	9	6	11	--	5	2	2	4	2	3	--	--	--	--	1	--	--	--	--	5	22	24	120	
Swedish Fall Cone	--	--	--	--	--	--	--	2	--	--	--	--	--	--	--	--	2	--	--	--	--	--	--	--	1	9	4	18	
UU-Triaxial - Undisturbed	11	3	3	4	9	5	9	9	3	6	5	5	2	4	3	--	2	--	1	3	1	--	2	--	4	16	17	127	
UU-Triaxial - Remolded	4	4	5	2	4	4	5	4	3	3	1	2	2	3	2	--	--	--	--	2	--	--	--	--	4	7	6	67	
ICUC-Triaxial	--	--	--	--	--	--	1	--	--	--	--	--	--	1	--	--	1	--	--	--	--	--	--	--	--	--	--	3	
ICDC-Triaxial	--	--	--	--	--	--	--	*	--	--	--	--	--	--	--	--	--	--	--	--	--	--	--	--	--	--	--	0	
Remote Vane	19	13	7	12	18	8	11	14	13	15	--	--	--	--	--	--	--	--	--	--	--	--	--	--	--	7	2	139	
Direct Shear	--	--	--	--	--	--	--	--	--	--	--	--	1	--	--	--	--	--	--	--	--	--	--	--	--	--	--	1	
Monotonic Direct Simple Shear	--	2	--	--	3	2	--	--	2	3	--	3	--	--	--	--	--	--	--	--	--	--	--	--	--	--	--	15	
Cyclic Direct Simple Shear	--	1	--	--	1	1	--	--	1	1	--	1	--	--	--	--	--	--	--	--	--	--	--	--	--	--	--	6	
Other Tests																													
Corrosivity	--	--	--	--	--	--	--	--	--	--	1	--	1	--	--	1	--	--	1	--	--	1	--	--	--	--	--	5	
R-Value	--	--	--	--	--	--	--	--	--	--	1	--	--	--	--	1	--	1	1	--	--	1	--	--	--	--	--	5	
Compaction (CA 216)	--	--	--	--	--	--	--	--	--	--	1	--	--	--	--	1	--	1	1	--	--	1	--	--	--	--	--	5	
Sand Equivalent	--	--	--	--	--	--	--	--	--	--	1	--	--	--	--	--	1	1	--	--	1	--	--	--	--	--	--	4	

* Test in progress.

SUMMARY OF LABORATORY TESTING PROGRAM
Oakland Shore Approach
SFOBB East Span Seismic Safety Project

SECTION 4.0 SITE CHARACTERIZATION



4.0 SITE CHARACTERIZATION

4.1 SITE HISTORY

4.1.1 Mole Key

The original Key System Mole was constructed (filled) on a former shallow water tidal flat prior to the construction of the existing SFOBB in the 1930s. The original Key System Mole served as a roadway and railroad trackbed for a ferry terminal that extended into the bay to the west of the western end of the Mole (see Plate 4.1).

4.1.2 Northern Mole Extension

Based on Trask and Rolston (1961), the construction of a northern extension to the then existing Key System Mole started on January 8, 1934. The approximate location of the original Mole key and the 1930s-circa northern extension relative to the existing Mole are shown on Plates 4.1 and 4.2. (Note that the historical overlay has been obtained from a small-scale, page-size drawing Caltrans [1932].)

To allow for the construction of the approaches to the current bridge, the westerly 610 meters (approximately from the existing western tip of the Mole to the proposed westbound Stations 89+00 to 90+00) were constructed first. Within this westerly segment of the northern extension, the historical documentation suggests that the fill was placed directly on the bay bottom. East of this limit, work reportedly began with the dredging of about 3 meters of the Young Bay Mud (YBM) from the bay bottom. The current investigation suggests that YBM was excavated around westbound Station 89+00, but does not appear to have been excavated east of westbound Station 89+50. Material for the northern extension fill was dredged from the Oakland Outer Harbor.

The Caltrans annual progress report reports for construction of the existing SFOBB (Caltrans, 1934) indicate that the northern extension fill was built in three stages:

1. The first-stage fill was placed hydraulically without containment up to about El. ± 0 MSL. Upon completion of the first-stage fill, a temporary 1.2-meter-high bulkhead was constructed during periods of low tide. This bulkhead served the dual purpose of reducing the amount of rock needed to retain further fill and retaining the second stage of the fill.
2. The second stage fill was placed to about El. +1.2 meters MSL and served as a roadway for the operation of the rock contractor. Core rock was moved into position beyond the temporary bulkhead to an elevation slightly above El. +1.2 meters MSL. Face rock was then placed on the exposed face and the remainder of the core rock





was placed to between El. +3 and El. +3.7 meters MSL. This roughly shaped wall was then backed with sand to prevent excess leakage through it during the pumping of the third-stage fill.

3. The final stage was placed to an elevation sufficiently above the grade line of El. +3 meters MSL to allow for the anticipated settlement and consolidation that the fill would experience in the years to come. The remainder of the face rock was then placed by dumping from the top of the fill. The dredged fill was completed on December 28, 1934, with a total of approximately 2.9 million cubic meters having been pumped.

Post-Extension Modifications. As recorded on aerial photos, the northern side of the Oakland Mole has undergone several changes since construction of the northern extension. Significant changes on the northern portion of the Mole were observed in historical photographs as follows:

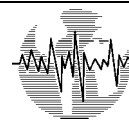
- By the late 1940s, the mudflat area to the north and northwest of the current Toll Plaza had been filled.
- By 1957, the northern edge of the Mole near the western tip (where early photos from 1936 show a docking pier) had been filled out to the north to form a new "pad" measuring approximately 30 by 60 meters. The western fill knob, subsequently referred to as the "western jughandle" in this report, is at proposed westbound Station 86+20.
- A second smaller filled area, located on the northern edge of the Mole farther to the east, was created by the late 1960s and is currently used as a "jughandle" traffic turnaround for the Caltrans maintenance road. The eastern knob (referred to as "eastern [turnaround] jughandle" in this report) and is at proposed westbound Station 88+30.
- By 1963, the portion of the western end of the Mole located beneath the SFOBB was extended to the west by approximately 90 meters.

Since approximately 1969, the geometry of the northern side of the Mole has remained basically unchanged.

Failure of Mole Fill. In the winter of 1947-1948, the underlying mud failed during the construction of the Mole fill to the north of the Toll Plaza. At the time of failure, the fill sank at least 6 meters. The mud reportedly thrust itself upward in places through the previous sand fill.

Settlement of Existing Fill. Plate 4.3 shows fill settlement along the Mole at 1, 5, and 20 years after construction. It appears that the settlement varies almost directly with the thickness of the underlying Young Bay Mud. After 20 years, the average settlement is approximately 10 percent of the thickness of Young Bay Mud. The total settlement could have





been more than that shown on Plate 4.3 since the settlement incurred during fill placement was not recorded and long-term (post-20-year) data are not available.

Since most of the filling occurred decades ago, primary settlement of the underlying Young Bay Mud has likely occurred, thus minimizing the possibility of significant future long-term settlement under the existing stress state. In addition, the Young Bay Mud underlying the fill will be stronger than its nearby marine counterpart due to consolidation under the weight of the Mole fill.

4.2 TOPOGRAPHY

The Oakland Mole is relatively flat except near the shoreline. Ground surface elevations on the Mole are typically between about El. +1.5 and El. +3.5 meters. In the western 150 meters, however, the ground surface slopes slightly to the west. In addition, as shown on Plate 4.3, the ground surface on the western jughandle is lower and slopes northward. Beyond and west of the toe of the western jughandle, there is an intermittently exposed, northwesterly-sloping beach.

4.3 BATHYMETRY

A bathymetric survey of the shallow tidal flat areas to the north and west of the Oakland Mole was conducted on August 23 and 24, 2000. A description of the survey equipment and procedures is presented in Appendix E of the Final Marine Geophysical Survey (Fugro-EM, 2001c). Bathymetric contours are shown on Plate 4.4.

The tidal flat to the north and west of the Mole extends from the toe of the northern and western Mole slopes to form a broad platform with a surface elevation of between about El. 0 and El. -1.3 meters. At low tide along the toe of the Mole, there is a strip of emergent land, the width of which decreases to the east. Locally, the emergent land strip is largest on the western sides of the jughandles. The extent of this emergent land generally corresponds to the El. -1.0 meter (MSL) contour (approximately MLLW elevation), which roughly parallels the Mole shoreline about 10 to 30 meters north of the toe of the Mole. The El. -1.3 meter (MSL) contour, which approximately corresponds to the lowest tide levels, typically runs about 50 meters north from the toe of the Mole. At the western jughandle, however, this contour deviates to the north to form a relatively shallow nob that extends approximately 100 meters from the jughandle shoreline.

Of the proposed overwater piers in the vicinity of the Oakland Shore Approach (Piers E17 and E18 Eastbound and Westbound, and Piers 19 through 20 Westbound), the bathymetry data show that Piers E20 and E21 Westbound will be exposed during most low tide cycles. It is likely that Piers E19 Westbound and E18 Eastbound will only be exposed during extreme low tide periods.





Local topographical variation on the tidal flat occurs as local features whose relief is greater than the general slope or changes on the tidal flat. These features are likely due to the ongoing, dynamic coastal and beach erosional and depositional processes around the tidal flat areas of the Mole. The bathymetry, therefore, is likely subject to seasonal variations.

A comparison of the current bathymetry on the tidal flat and the bathymetry shown on the Caltrans' 1933 map shows that the water depth has decreased to the north of the Mole. Those data show that the current bathymetry is as much as 2.2 meters shallower than the bathymetry prior to construction of the Mole extension. Review of the Seascout CPT sounding results suggests that the additional sediment accumulated on the tidal flat includes: a) sands that were deposited below water prior to the construction of the northern perimeter containment structure (during the northern Mole extension fill), b) very recent fine-grained sediments (subsequently referred to as "historical bay mud"), and c) a local surface sand layer.

4.4 GENERAL SUBSURFACE SOIL CONDITIONS

4.4.1 Stratigraphic Sequence Under Mole

The present subsurface site soils consist of the following sequence of major units (in descending order):

- Granular fill
- Soft to stiff clay (Young Bay Mud [YBM])
- Dense sand with layers of stiff sandy clay (Merritt-Posey-San Antonio [MPSA] Formations)
- Stiff to very stiff clay (Old Bay Mud [OBM])
- Very stiff to hard marine clays (Upper Alameda Marine [UAM] Formation)
- Dense to very dense alluvial sands (Lower Alameda Alluvium [LAA] Formation)

This sequence of marine and alluvial sediments unconformably overlies bedrock of the Franciscan Formation.

4.4.2 Stratigraphic Relationships

Longitudinal and transverse stratigraphic cross sections were constructed to assist with geologic characterization. The locations and orientation of those sections are shown on Plate 4.5 and a key to the symbols used on the cross sections is included on Plate 4.6. The cross sections are provided on Plates 4.7 through 4.12.





The following list summarizes the locations and data presented on the cross sections:

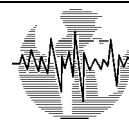
Plate No.	Section Designation	Location (see Plate 4.5 for cross section locations)	Data Shown on Cross Section
4.7a	M1-M1'	N6 Eastbound Alignment, Marine Areas, Piers E16 through E18 Eastbound	S_u and q_c
4.7b	M2-M2'	N6 Westbound Alignment, Marine Areas, Piers E16 through E19 Westbound	S_u and q_c
4.7c, 4.7d	A-A' through B-B'	Approximately the N6 Eastbound Alignment, Mole Areas	S_u and q_c
4.7e, 4.7f	A1-A1' through B1-B1'	Approximately the N6 Westbound Alignment, Mole Areas	S_u and q_c
4.8	C-C'	Perpendicular to Alignment - Approximately at Pier E20	S_u and q_c
4.9	D-D'	Perpendicular to Alignment - Between East and West Jughandles, Approximately "W" Station 87+10	S_u and q_c
4.10	E-E'	Perpendicular to Alignment - Approximately "W" Station 87+90	S_u and q_c
4.11	F-F'	Perpendicular to Alignment - Approximately "W" Station 89+90	S_u and q_c
4.12	A-A'	Approximately the N6 Eastbound Alignment, Mole Areas	q_c and V_s

The cross sections provide graphical representations of the soil units, measured cone tip resistance, and measured and calculated undrained shear strengths. The measured undrained shear strengths include in situ measurements from the remote vane shear tests and laboratory test results. Undrained shear strengths calculated from the measured CPT tip resistances (corrected for unequal end area and overburden effects) also are shown. Those calculated shear strengths are based on a bearing capacity factor (N_k) with a range of 12 to 15.

The variations in the stratigraphic sequence and thickness of strata as illustrated on the cross sections include the following:

- A distinct Young Bay Mud paleochannel crosses beneath the proposed new bridge alignment between about exploration locations 98C-54 and 98C-18 (approximately between proposed eastbound Stations 86+00 and 88+00). The paleochannel is interpreted to be a north-south-trending tributary to the east-west-trending paleochannel that crosses San Francisco Bay to the north of the existing East Span alignment. The ATV-mounted CPT soundings on the tidal flat to the north of the Mole suggest that the width of the paleochannel increases significantly to the north. Those data also suggest that the thalweg of the paleochannel deepens rapidly to the north.
- An additional east-west-trending tributary channel that begins just west of proposed Pier location E17 and deepens to the west was delineated based on the Phase 3 field investigation. The western edges of the Eastbound and Westbound Piers E17 appear to lie on the flank of this channel.





- The continuity of the MPSA Formations is interrupted where the Young Bay Mud-filled paleochannel is incised through the MPSA Formations. The CPT data suggest that MPSA sand layers generally are not present within that particular tributary paleochannel.
- The base of the fill is deeper and the thickness of the fill is greater where the Young Bay Mud paleochannel has incised into and through the MPSA Formations. This is due to the differential settlement of the greater thickness of Young Bay Mud clay within the paleochannels.
- Except where removed by channeling, the MPSA Formations frequently include a distinct 3- to 5-meter-thick very dense sand (Merritt) layer. The sand layer is often overlain by a limited thickness of clayey sand (or sandy clay) and is underlain by variable amounts of stiff to very stiff clay and sandy clay. The MPSA Formations are generally present between about El. -8 and El. -20 meters. Locally, on the eastern flank of the Young Bay Mud paleochannel, the very dense sand layer (or a separate sand layer with similar characteristics that was probably deposited inside an older paleochannel) within the sequence appears to be displaced about 5 meters downward.
- The Old Bay Mud includes a distinct crust at its surface. The data provide direct evidence of other deeper crust layers. The crusts are typically flat-lying and relatively continuous, although the crusts will be discontinuous where channels locally have eroded through the crust layers.

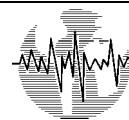
4.4.3 Tidal Flat Sediments

Mudline elevations to the north of the Mole are typically higher than the top of the Young Bay Mud beneath the Mole. This is due to the consolidation of the Young Bay Mud beneath the Mole under the weight of the Mole fill. Examination of the data suggests that the difference in elevation between the top of the Young Bay Mud under the tidal flat and beneath the Mole fill is between 0.5 and 2 meters. That magnitude of elevation difference is consistent with the reported settlement of the Mole fill.

To the north of the Mole, the Young Bay Mud sediments are overlain by sediments deposited during and since the construction of the northern extension of the Mole. Those tidal flat sediments locally include some or all of the following sediments:

- A locally continuous layer of sand that was probably deposited during the hydraulic placement of the lower submerged Mole fill, but prior to construction of the containment structure for the subsequent upper fill lifts.
- A layer of very soft clay that is subsequently referred to as the "historical bay mud" in order to differentiate that layer from the geologically-recent Young Bay Mud.
- A layered deposit of the sands and historic mud.





A surface sand in the western portion of the tidal flat, subsequently referred to as the "beach sand" layer.

4.5 GEOLOGIC AND CULTURAL FEATURES

4.5.1 Mole Fills

The northern portion of the Oakland Mole consists of primarily hydraulic (not engineered) fill placed during bridge construction in the 1930s. That fill predominantly consists of granular, poorly graded sand with silt and silty fine sand. The fill includes variable amounts of debris, rubble, cobbles, boulders, and shore protection riprap. The thickness of the fill typically varies from 4.5 to 9.0 meters. Locally, the fill is as thick as 12.5 meters.

Fill extends beyond the 1930s' northern extension at the present western and eastern "jughandles" (see Plate 1.2). Those subsequent fills consist of similar sands that locally extend northward and create beach areas at the toe of the existing slopes. These areas probably also contain rock of the former extended Mole dike. The present slopes of the Mole are protected by a blanket of riprap.

4.5.2 Buried Rock Dikes

The northern portion of the Mole is believed to be underlain by the buried remnants of at least two prior east-west-trending rock dikes. A 1932 Caltrans map shows the alignment of the northern edge of the original Mole (or key) as well as the proposed Mole extension to the north (see Plate 4.2). Several borings that penetrated gravel and rock appear to approximately correlate to the locations of the northern edge of the original and extended Mole as shown on the 1933 map.

Trench excavations conducted in April 1999 verified the existence of pre-1950 rock dikes buried beneath the existing east and west jughandles. The trench locations are provided on Plates 2.1a and 2.1b. The dikes are approximately in line with the existing shoreline on either side of the jughandles. The dike was found to be approximately 0.9 meter below the existing ground surface at the trench locations. The dike thicknesses were measured to be about 3 meters at the eastern jughandle and about 2.4 meters at the western jughandle. The excavation revealed the dike to be covered with angular and rounded riprap 0.6 to 1.2 meters in size. The dike core materials were composed of round to angular cobbles, 300 to 600 mm in size, with smaller cobbles and gravel filling the voids. Further detail from the trench excavations can be found in the memorandum included in Volume 4.

4.5.3 Tidal Flat to the North of the Mole

The data suggest that the Young Bay Mud, Merritt-Posey-San Antonio, and Old Bay Mud strata (see below) continue to the north of the Mole. The CPT soundings show that up to





several meters of sand and clay, collectively defined as the tidal flat sediments, overlie the Young Bay Mud immediately to the north of the Mole edge. The data suggest that the surface sand layer is discontinuous and decreases in thickness to the north and east.

4.5.4 Paleochannels

The stratigraphic sequence described in Section 4.4.1 is generally present under most of the site, although some formations have been locally eroded and complicated by various episodes of channeling. A main Young Bay Mud-infilled, east-west-trending paleochannel crosses San Francisco Bay to the north of the existing East Span alignment and is joined by several tributary paleochannels along the proposed SFOBB alignment. One north-south-trending tributary paleochannel (referred to hereafter as the tributary Mole paleochannel) crosses beneath the proposed new bridge alignment on the Mole approximately between boring locations 98-54 and 98-18 (at approximately westbound Stations 86+50 to 87+70).

The CPT data suggest that this paleochannel is filled with Young Bay Mud and that the channel appears to be incised through the Merritt-Posey-San Antonio Formations. With the exception of one relatively continuous 1- to 1.5-meter-thick sand layer, no other continuous sand seams or layers are observed from the available data within this channel.

In the vicinity of the Oakland Shore Approach, there is another Young Bay Mud-infilled paleochannel that lies in a southeast-northwest-trending tributary channel between proposed Piers E17 and E18 and runs west, eventually veering north to meet the main east-west-trending paleochannel.

4.5.5 Description of Stratigraphic Units

Fill. The Mole fill consists predominantly of poorly graded fine sand with silt to silty fine sand. The sands are generally dense above groundwater and medium dense with loose layers below groundwater.

The fill was dredged from the outer Oakland Harbor during the construction and subsequent extension of the Mole in the 1930s. Similarities in grain size characteristics suggest that the primary source of the Mole fill is the Merritt Sand deposits, a unit of the Merritt-Posey-San Antonio Formations. The data show that the fill is slightly coarser, with less fines than the average grain size of the Merritt Sand. That observation is considered to be consistent with the unconfined hydraulic placement of much of the Mole extension fill. The fill sands typically include about 5 to 14 percent fines. Local layers, however, include up to about 30 percent fines.

The thickness of the fill generally varies from 4.5 to 9.0 meters, but is as thick as 12.5 meters near the location of CPT 98C-105. The location of 98C-105 appears to correspond to the location where the Young Bay Mud was apparently excavated prior to the placement of the fill in the 1930s. The bottom of the fill typically ranges from El. -3.5 to El. -8.8 meters. The base of





the fill is deeper and the thickness of the fill greater where the Mole overlies a buried paleochannel. This is primarily due to the additional fill that was placed to compensate for the consolidation settlement of the thicker layers of compressible Young Bay Mud within the paleochannel.

The fill includes variable amounts of debris, rubble, cobbles and boulders, and shore protection riprap. The northern portion of the Mole is also believed to be underlain by buried remnants of the prior east-west-trending rock dikes that served as the edge of the original Key System Mole. In addition, former rock dikes placed before 1950 were left in place in the two jughandle areas. The dikes are approximately in line with the visible slopes east and west of the jughandles.

Tidal Flat Sediments. The tidal flat sediments to the north of the Mole consist of a sequence of Recent sand and very soft clay historical bay mud deposits overlying the Young Bay Mud. A deposit of surface beach sand extends along the northern shore of the Mole between the jughandles and to the west of the western jughandle. The beach sand is up to 1 meter thick at the shoreline. The data suggest that the surface sand layer is discontinuous and decreases in thickness to the north. The beach sand is generally thicker and extends farther north in the western portion of the tidal flat. Local variations in the beach sand thickness are likely due to littoral drift and other beach environment processes. Plate 4.13 shows the approximate beach sand thickness encountered in the tethered Seascout and ATV-mounted CPT soundings.

Throughout the tidal flat area to the north of the Mole and underlying the beach sand (where present) is historical bay mud that is comprised of very soft clay with interspersed seams and layers of sand. A comparison of the current bathymetry on the tidal flat and the bathymetry shown on a 1933 Caltrans map (provided in Volume 4) suggests that the historical bay mud has been deposited since the construction of the bridge in the 1930s. The historical bay mud deposits appear to be 0.3 to 3.0 meters thick.

A locally continuous layer of sand underlies the historical bay mud along the northern Mole shoreline between the jughandles and to the east of the eastern jughandle. This sand was likely deposited during the hydraulic placement of the lower submerged fill. The lower submerged fill was placed prior to the construction of the containment structure for the upper Mole fill of the northern Mole extension constructed in the 1930s. The sand layer is evident in many of the Seascout CPT soundings immediately north of the Mole and extends as far as 120 meters north of the Mole shoreline. The sand layer is as much as 1.5 meters thick at the northern shore of the Mole and thins northward. Plate 4.14 shows the approximate thickness of fill sand encountered in tethered Seascout and ATV-mounted CPT soundings. Plate 4.15 provides a schematic cross section through the northern tidal flats and Mole, and shows the relationship of the sand and historical bay mud deposits that overlie the Young Bay Mud.





Throughout the tidal flat area, the sequence of Recent sands and soft clays is underlain by the Young Bay Mud deposits. The tethered Seascout and ATV-mounted CPT data show that the top of the Young Bay Mud typically ranges in elevation from El. -3.5 to -5.0 meters.

Young Bay Mud (YBM). The Mole fill and tidal flat are underlain by a soft to stiff, Holocene-age marine clay deposit referred to as Young Bay Mud. Those compressible clay sediments have consolidated under the weight of the Mole fill since the 1930s.

The base of the Young Bay Mud typically occurs, where encountered in the borings, at about El. -9.5 to El. -14.5 meters throughout the site. In the paleochannel area (approximately Stations 86+50 to 87+70), the Young Bay Mud thickens and extends approximately El. -24.5 meters at the deepest point.

The deposits encountered in the tidal flat area farther to the north of the Mole predominantly consist of very soft to stiff clay with silt, sand, and shells deposited after construction was completed (around 1934). Seascout CPT data suggest abundant thin seams of silt, sand, or shells at various depths within the Young Bay Mud.

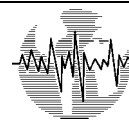
The data on the Mole and adjacent tidal flat confirm that the consolidation of the Young Bay Mud varies with the presence or absence of fill as well as with the age of the overlying fill. Beneath the northern Mole extension, the Young Bay Mud appears to be normally consolidated under the weight of the 1930s' fill. Beneath the more recent jughandle extensions, however, the data suggest that the Young Bay Mud is slightly underconsolidated relative to the weight of the 1950s' and 1960s' fill. The degree of underconsolidation in the Young Bay Mud at those locations appears to increase with depth. To the north of the Mole, the CPT data suggest that the upper portion of the Young Bay Mud is slightly overconsolidated relative to the much lower stress state that is present in the unfilled areas.

Merritt-Posey-San Antonio (MPSA) Formations. Beneath the Young Bay Mud, a layered sequence of sands and clays is present over portions of eastern San Francisco Bay. The term "Merritt-Posey-San Antonio (MPSA) Formations" is preferred over the more simplified designation of Merritt Sand in recognition of the layered and interbedded characteristics of the sequence.

The MPSA Formations include dense to very dense sand with layers of stiff to very stiff sandy clay and clay that underlie the Young Bay Mud throughout most of the site area. Except where removed by channeling, this sequence frequently includes a distinct 3- to 4.5-meter-thick, very dense sand (Merritt) layer. This sand layer is often overlain by a limited thickness of clayey sand (or sandy clay) and is underlain by variable amounts of stiff to very stiff clay and sandy clay with sand layers.

The MPSA Formations are generally present between about El. -7.6 and El. -19.8 meters. Locally, on the eastern flank of the Young Bay Mud paleochannel, the very dense sand layer (or





a separate layer of similar characteristics) within the sequence appears to be displaced about 5 meters downward.

Two deep marine borings at the western tip of the Mole, ATV-mounted CPT soundings, and Seacalf CPT soundings all show that the MPSA Formations continue to the north of the Mole.

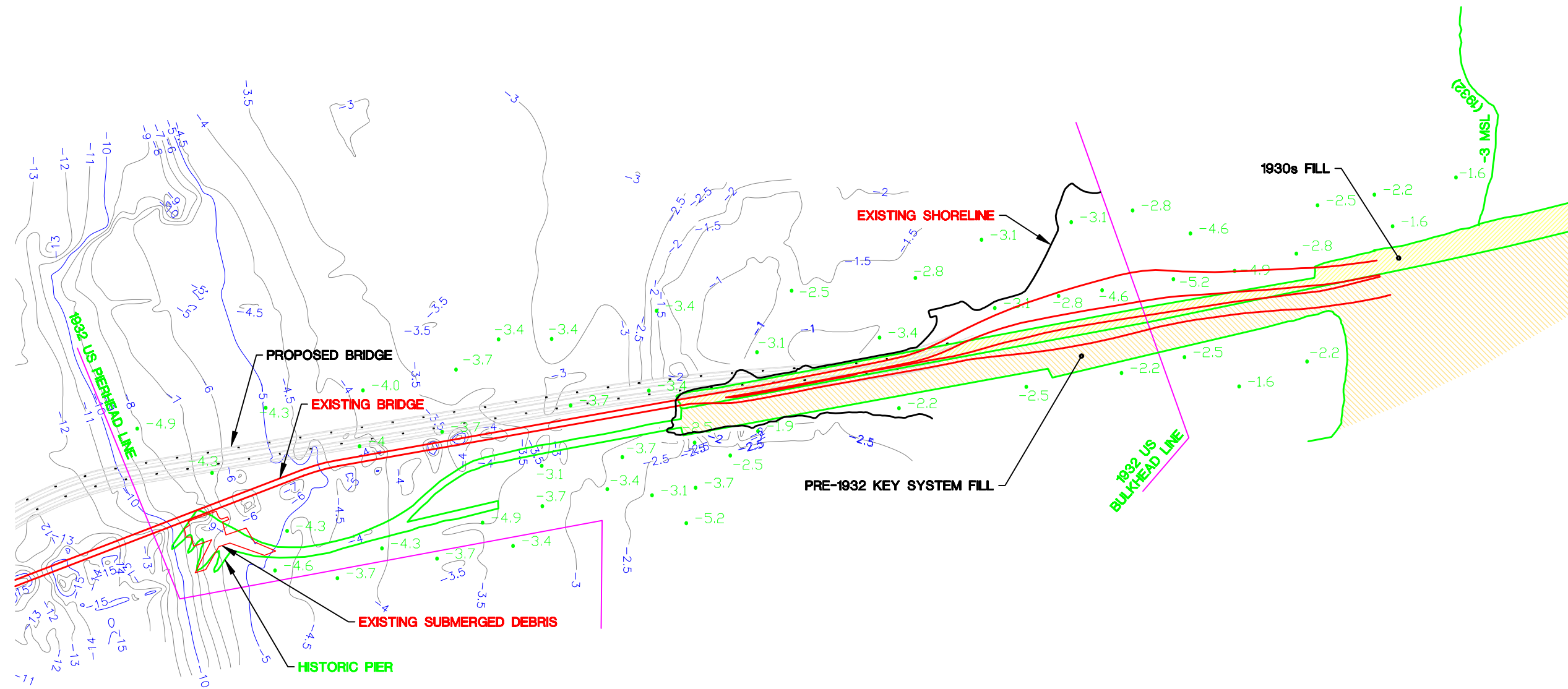
Old Bay Mud/Upper Alameda Marine Sediments. The Old Bay Mud/Upper Alameda Marine sequence (OBM/UAM) is an older marine stratum that underlies the entire site and its surrounding area. The OBM/UAM consist primarily of very stiff to hard fat clay and includes a distinct crust at its surface. Because the composition and geotechnical properties of the two units are similar and the definition of the interface between the two formations is tenuous, the two formations have been discussed and mapped as one combined sequence of sediments. Except where eroded by channeling, the top of the sequence typically is present from about El. -18 to El. -25 meters. The data provide evidence of other deeper crust layers. The crusts are typically flat-lying and relatively continuous, although locally the crusts will be discontinuous where channels have eroded through the crust layers.

Lower Alameda Alluvial Sediments. The Upper Alameda Marine sediments are underlain by dense to very dense alluvial sands with hard lean clay layers that are referred to as the Lower Alameda Alluvial (LAA) Formation. These primarily dense, granular sediments overlie the Franciscan Formation bedrock. The top of the LAA was encountered at about El. -75 meters in nearby marine Boring 98-44. The characteristics of the LAA are discussed in greater detail in the Final Marine Geotechnical Site Characterization Report (Fugro-EM, 2001d).

Bedrock. The Jurassic/Cretaceous-age Franciscan Formation forms the bedrock that underlies the Alameda Formation. Bedrock gently slopes to the east-southeast and was encountered at El. -135 meters (approximately 131.5 meters below existing top grade) at the western tip of the Mole and at El. -150 meters (approximately 146.5 meters below existing grade) at the Toll Plaza, which is located east of the subject project site.

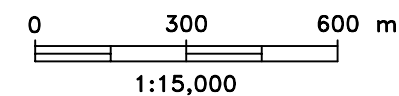
For the Phase 1 and Phase 2 investigations (see Section 2.1), borings were not advanced to bedrock because deep foundations for the Oakland Shore Approach structures are not anticipated to reach bedrock. Bedrock was encountered by Caltrans (Caltrans, 1994) in three test borings at the western tip of the Mole and in one boring at the present Toll Plaza location as part of the Oakland Bay Bridge Seismic Retrofit program. According to those borehole logs and the marine boring logs by Fugro (see Volume 2), bedrock consists of weathered (brown/olive-colored) to fresh (dark gray-colored) sandstone with laminated interbeds of black-colored siltstone, claystone, and shale. The top of the bedrock includes varying degrees and depths of weathering.





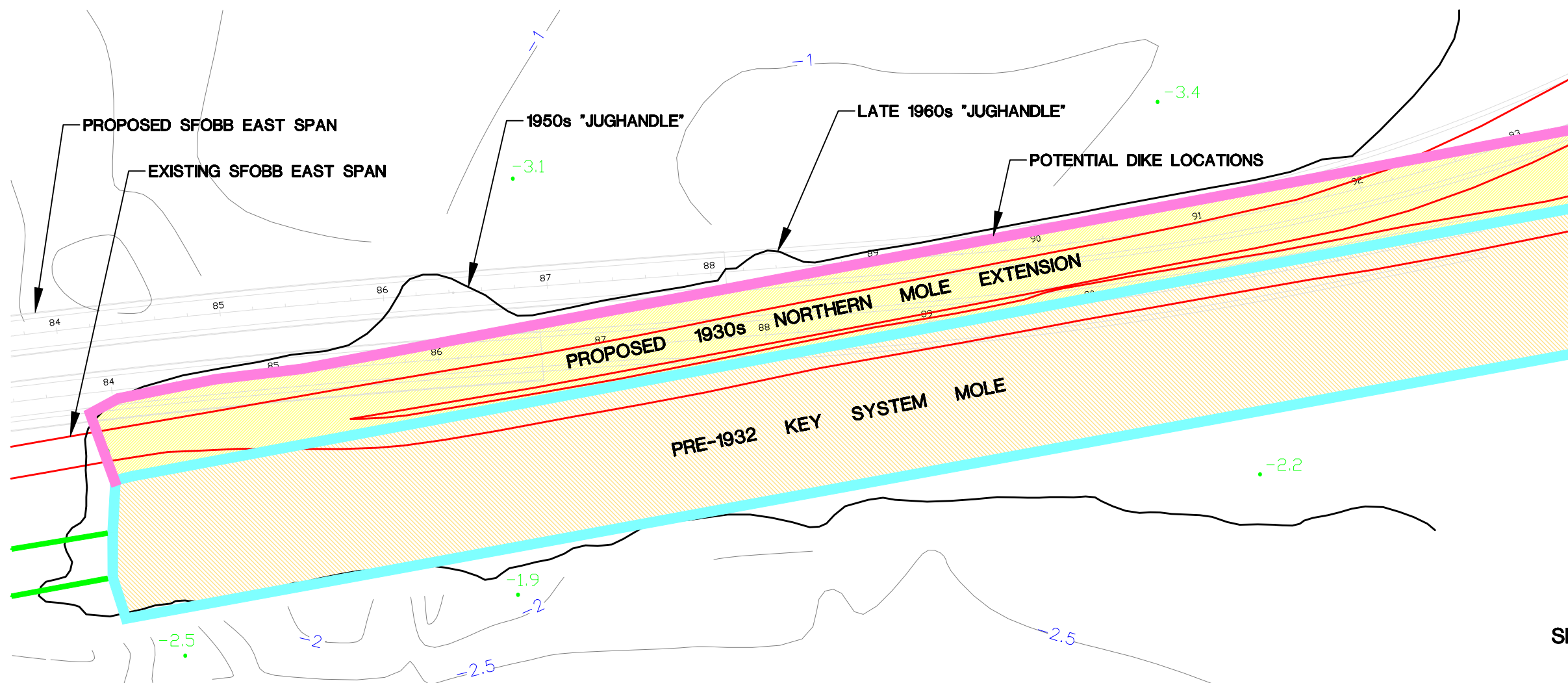
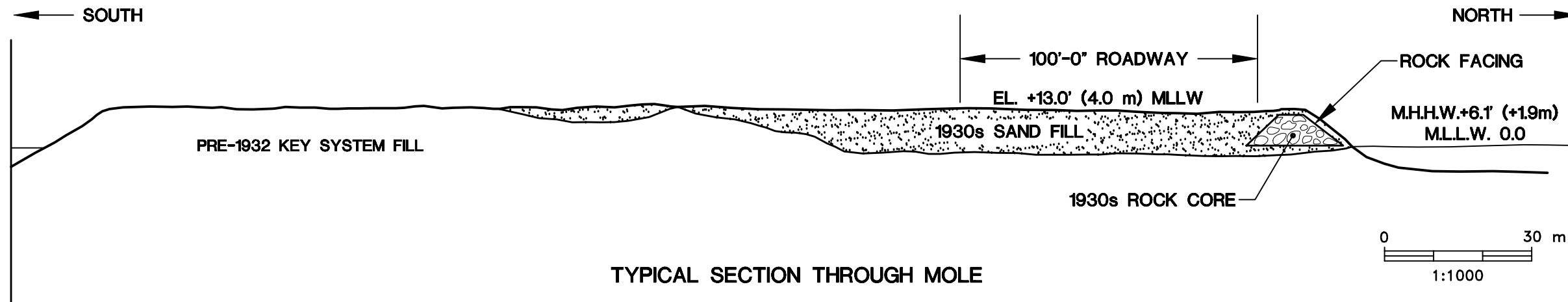
LEGEND

- -5.2 1930s Bathymetry, meters (MSL)
- 10— 1997 Bathymetry Contours, meters (MSL)
- 11—



MORPHOLOGY OF OAKLAND MOLE
Oakland Shore Approach
SFOBB East Span Seismic Safety Project

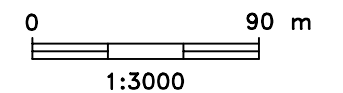




LEGEND

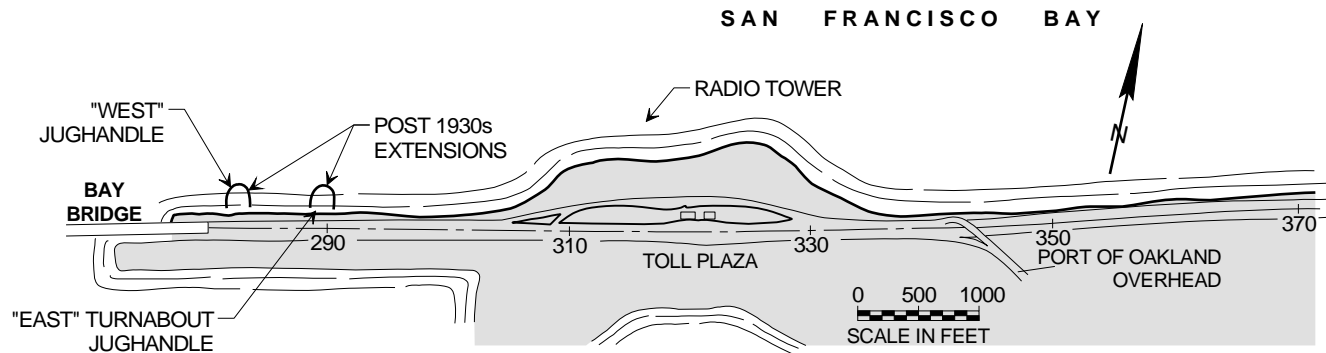
- -5.2 1930s Bathymetry
- 10 -11 1997 Bathymetry Contours

NOTE: Historical overlay was obtained from a small-scale page-size drawing in Caltrans (1932).

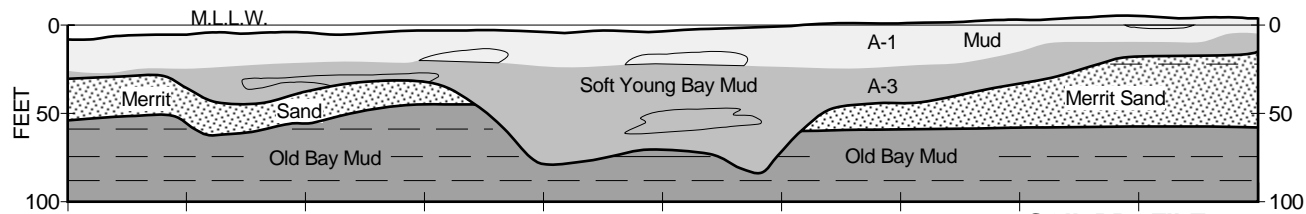


**NORTHERN EXTENSION OF
KEY SYSTEM MOLE**
Oakland Shore Approach
SFOBB East Span Seismic Safety Project

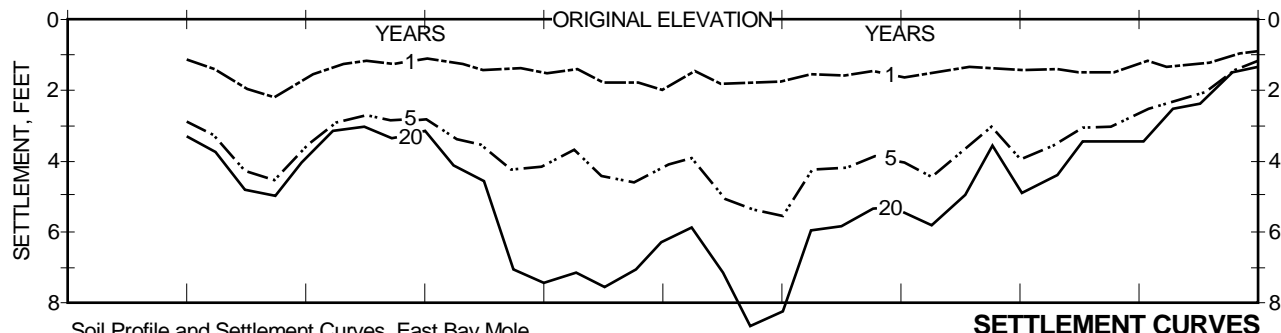




PLAN OF MOLE



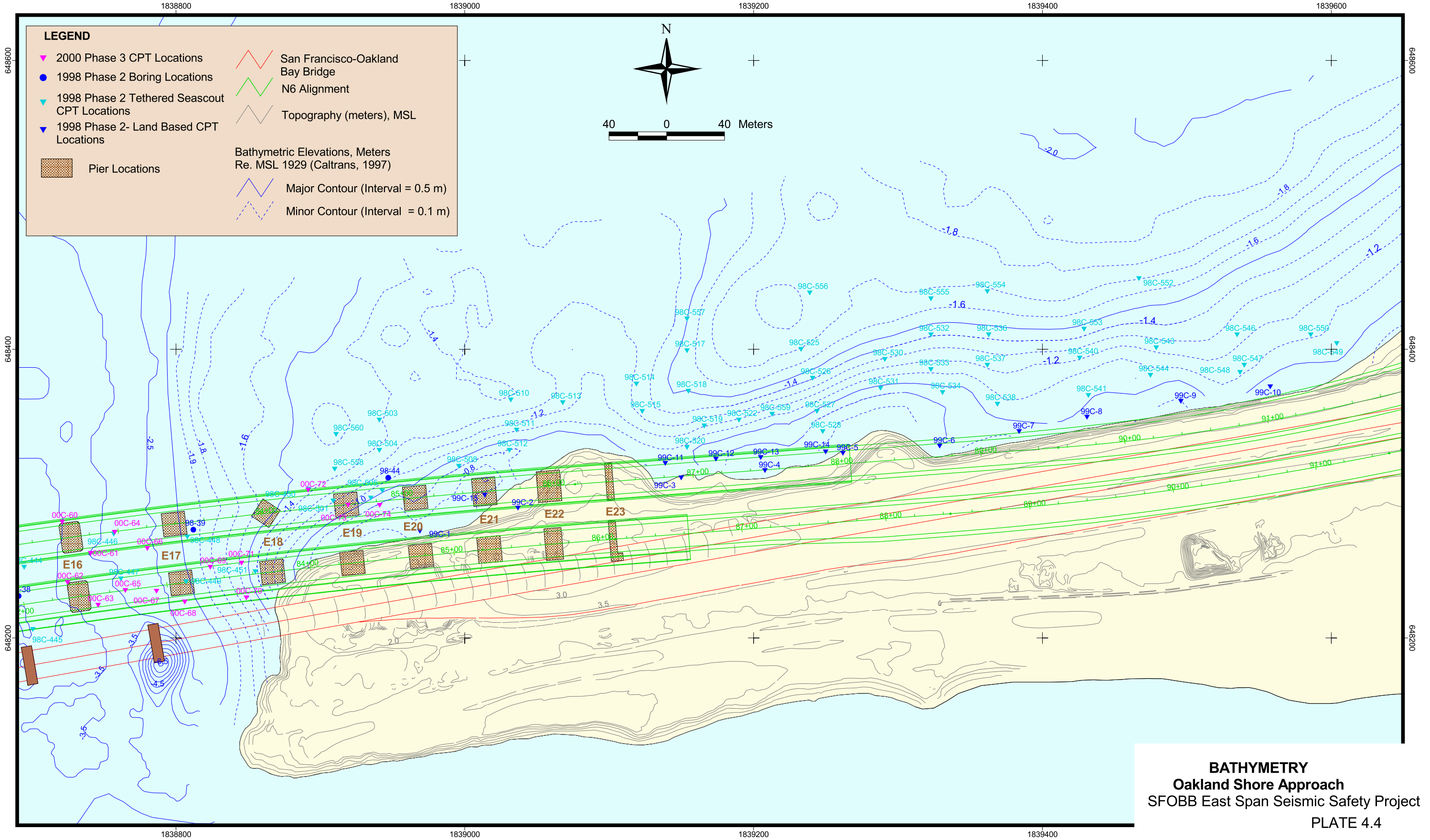
SOIL PROFILE

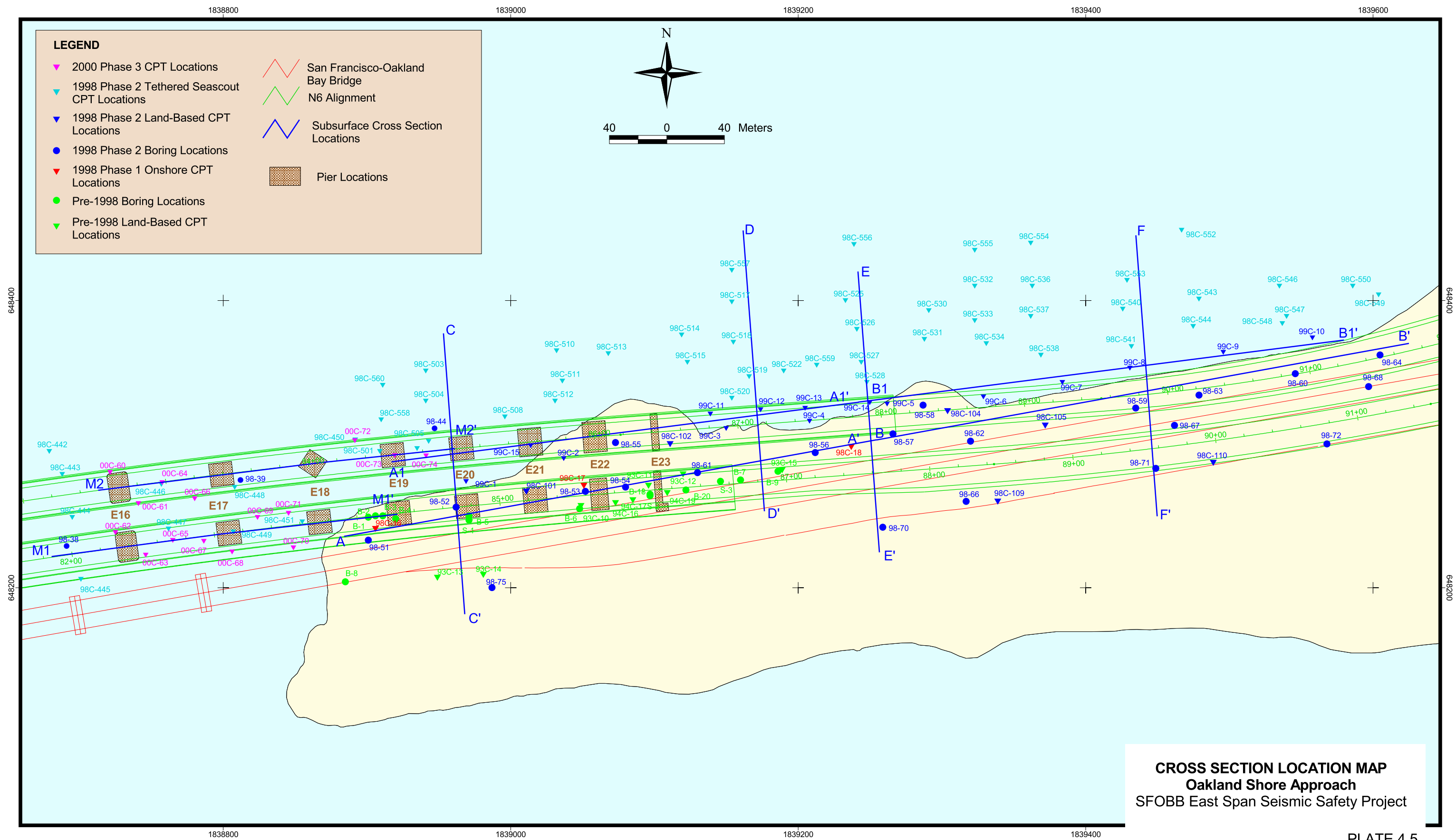


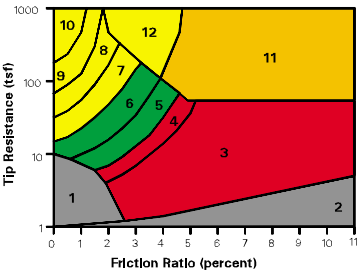
SETTLEMENT CURVES

Soil Profile and Settlement Curves, East Bay Mole,
San Francisco-Oakland Bay Bridge (from Caltrans).

OAKLAND MOLE HISTORIC SETTLEMENT PROFILE
Oakland Shore Approach
SFOBB East Span Seismic Safety Project





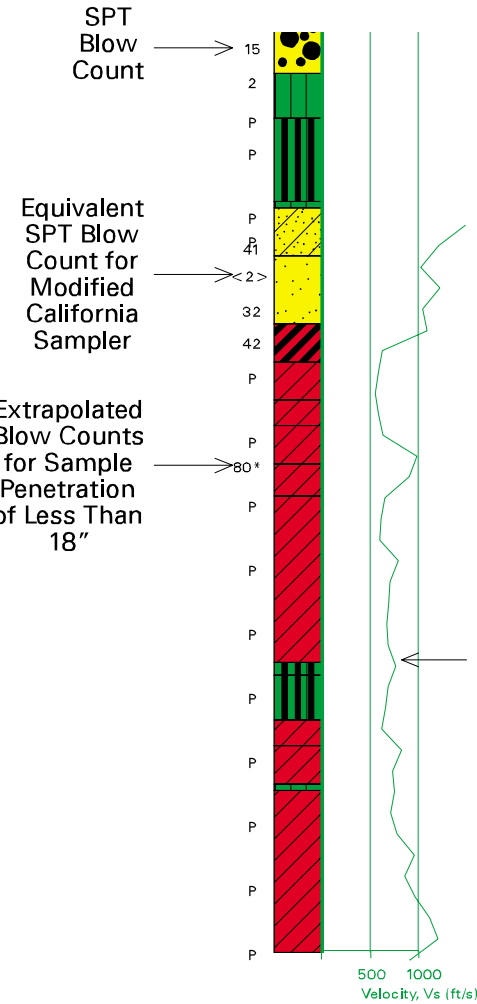
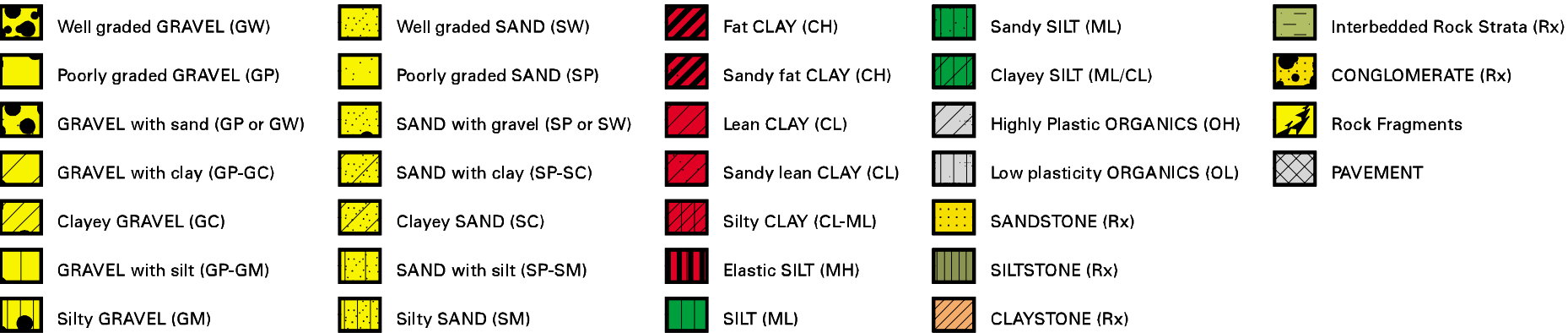


CPT CORRELATION CHART (Robertson and Campanella, 1984)

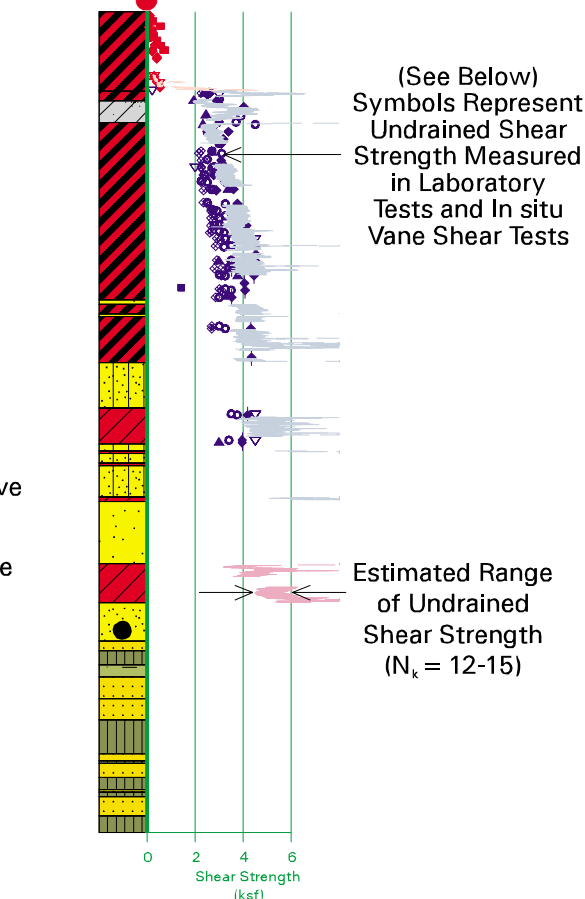
Zone	Soil Behavior Type	U.S.C.S.
1	Sensitive Fine-grained	OL-CH
2	Organic Material	OL-OH
3	Clay	CH
4	Silty Clay to Clay	CL-CH
5	Clayey Silt to Silty Clay	MH-CL
6	Sandy Silt to Clayey Silt	ML-MH
7	Silty Sand to Sandy Silt	SM-ML
8	Sand to Silty Sand	SM-SP
9	Sand	SW-SP
10	Gravelly Sand to Sand	SW-GW
11	Very Stiff Fine-grained *	CH-CL
12	Sand to Clayey Sand *	SC-SM

* overconsolidated or cemented

KEY TO CROSS SECTIONS



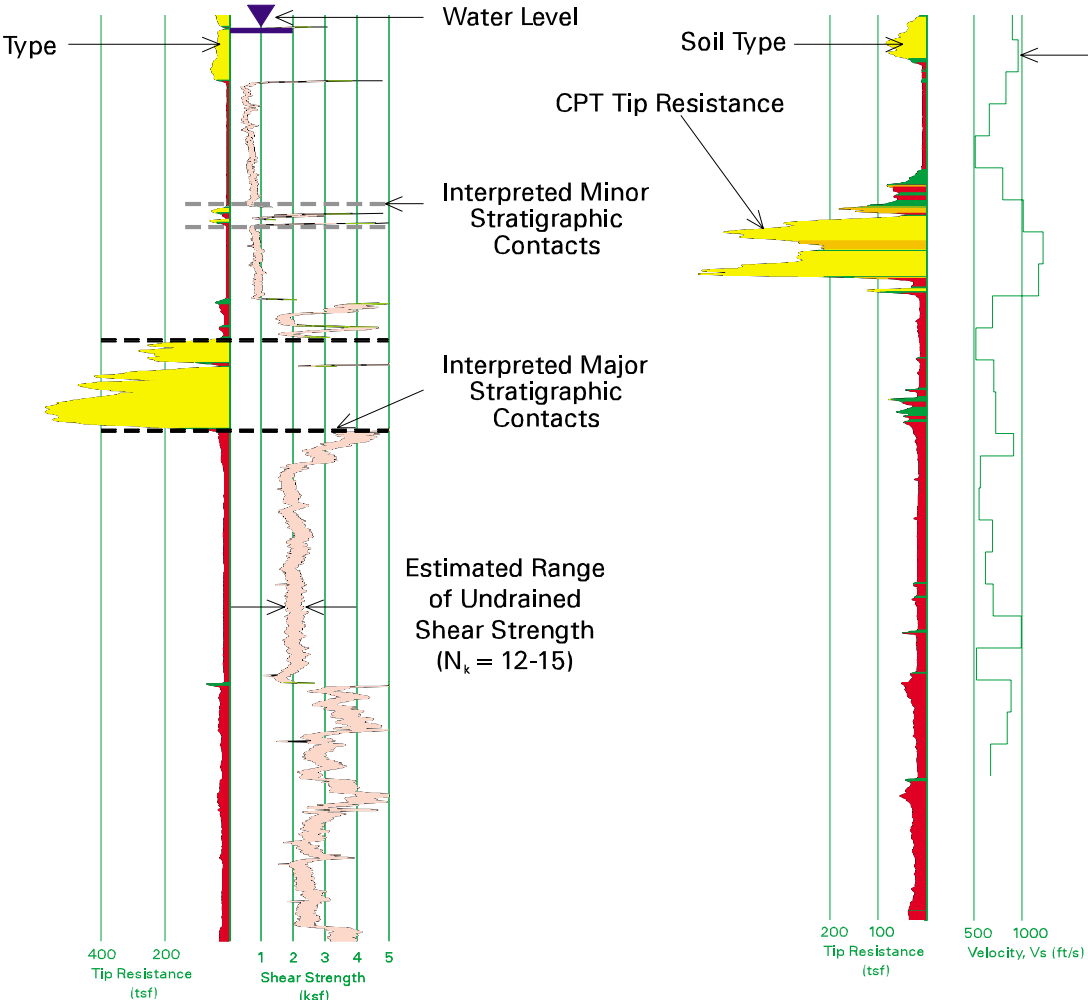
SOIL BORING
LITHOLOGY WITH
SHEAR WAVE VELOCITY



SOIL BORING
LITHOLOGY WITH
UNDRAINED SHEAR STRENGTH

Key to Undrained Shear Strength Symbols

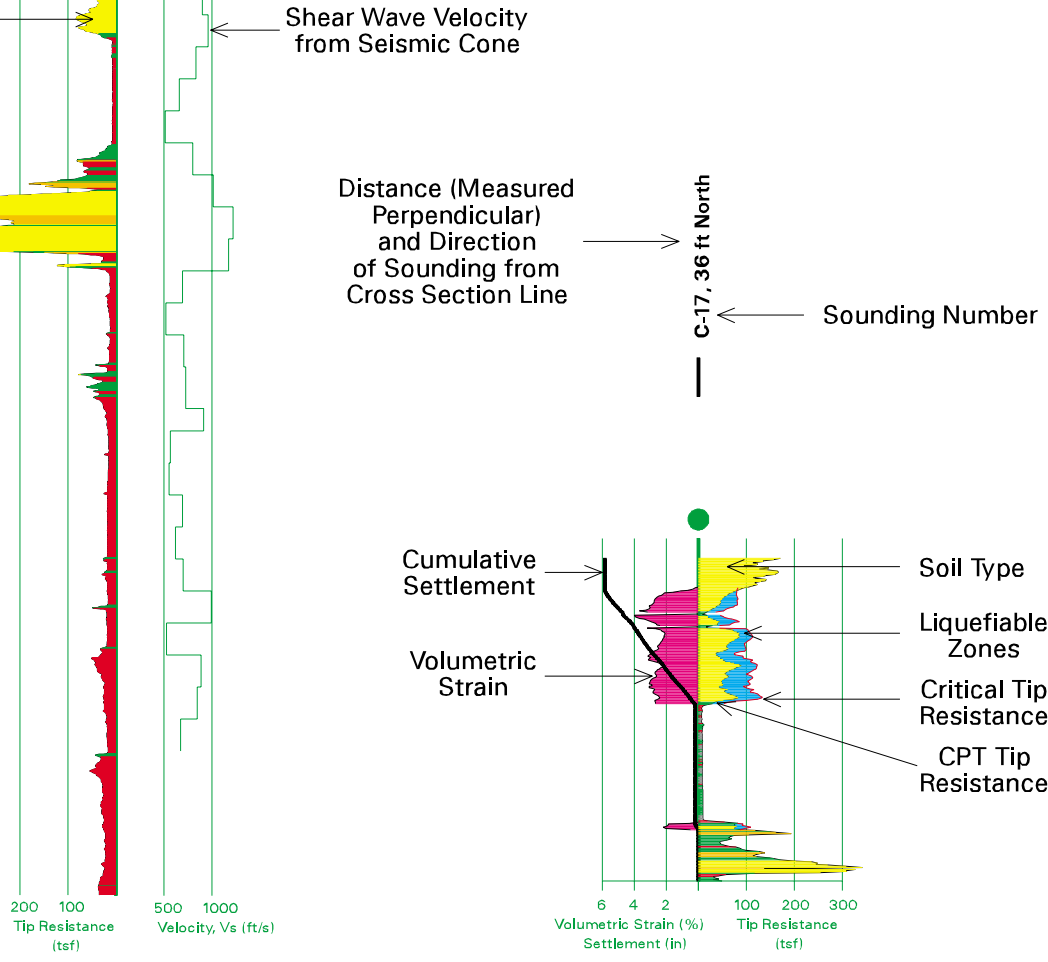
- ▲ Unconsolidated Undrained (UU)
- △ Unconfined Compression (UC)
- Pocket Penetrometer (PP)
- ◆ Torvane (TV)
- ◆ Miniature Vane (MV)
- Remote Vane (RV)
- ▽ Fall Cone (FC)



CPT SOUNDING
WITH UNDRAINED SHEAR STRENGTH
AND INTERPRETED LITHOLOGY

Metric Conversions:

tsf = 0.0958 MPa
ksf = 47.9 KPa
ft/s = 0.3048 m/s
foot = 0.3048 m
inch = 2.54 cm



CPT SOUNDING
WITH SHEAR WAVE
VELOCITY

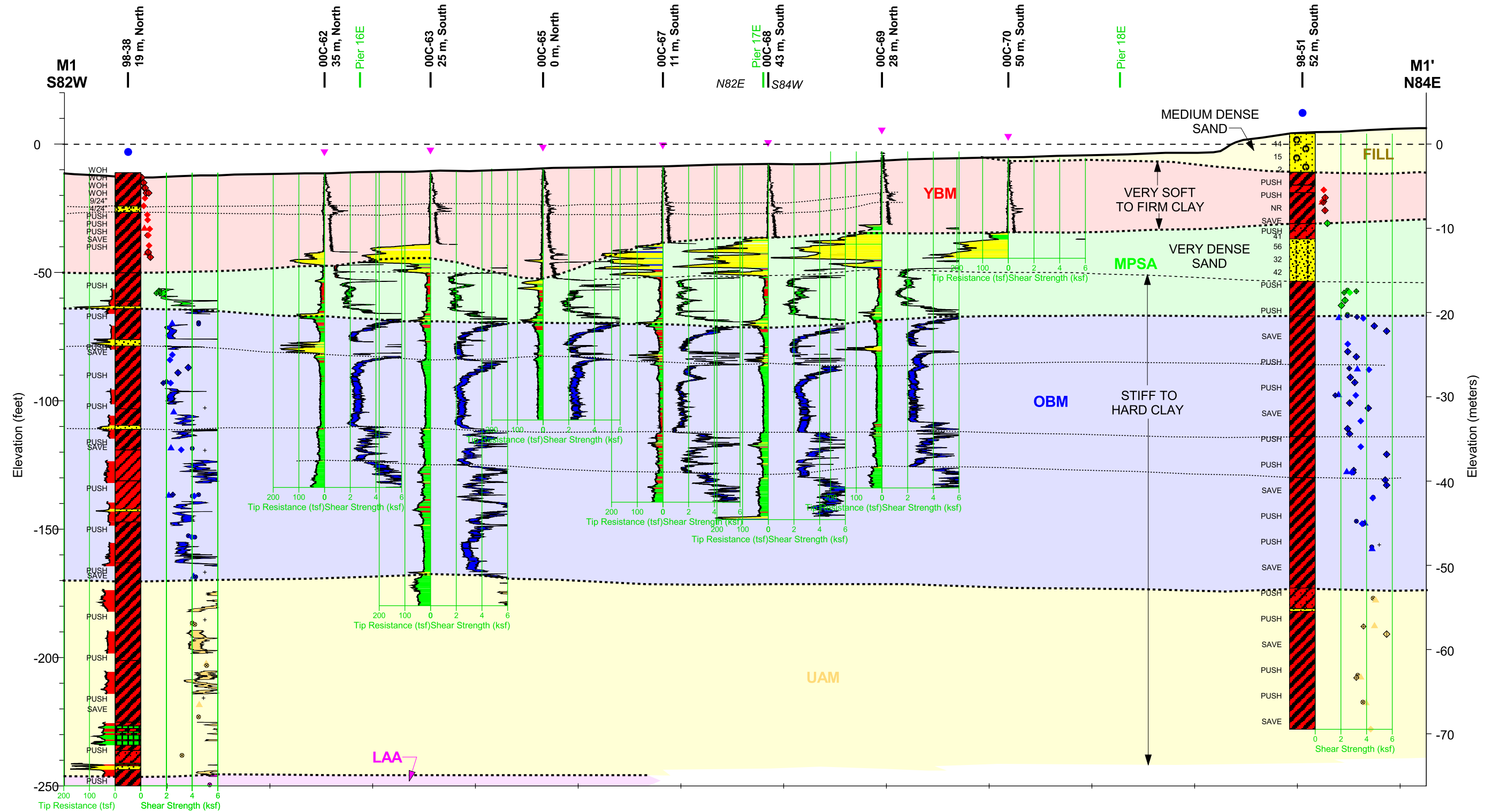
CPT SOUNDING
WITH LIQUEFACTION
EVALUATION

KEY TO CROSS SECTIONS

Oakland Shore Approach

SFOBB East Span Seismic Safety Project





GENERAL NOTES:

- 1) Stratigraphic contacts are approximate and are interpreted from CPT soundings, borings, and seismic reflection survey data. Conditions vary both along and perpendicular to the section line.
- 2) Refer to Key to Cross Sections (Plate 4.6) for descriptions of boring and CPT data shown above.

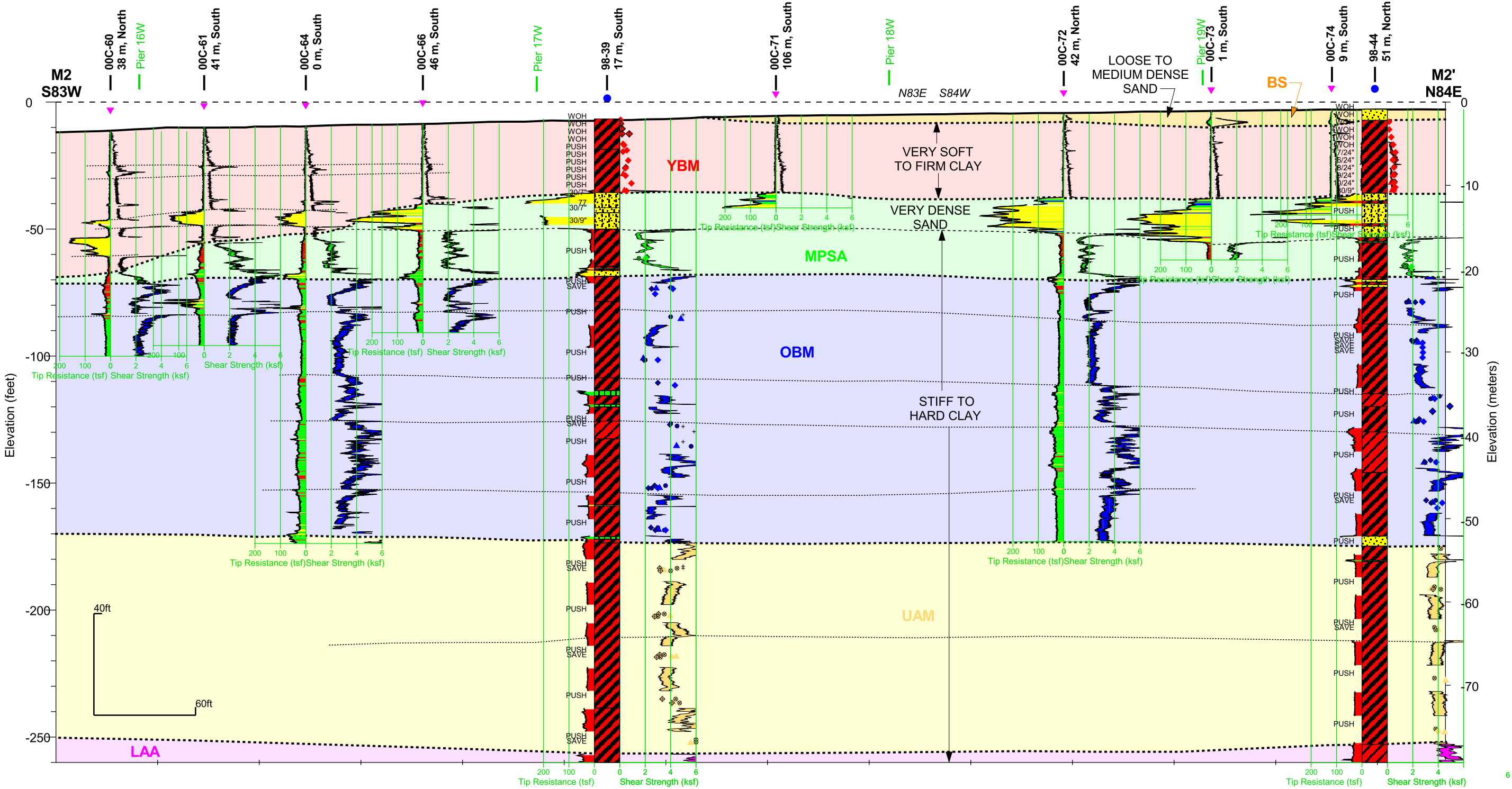
SHEAR STRENGTH SYMBOLS

- ▲ Unconsolidated Undrained (UU)
- Unconfined Compression (UC)
- ⊗ Pocket Penetrometer (PP)
- ⊕ Torvane (TV)
- ◆ Miniature Vane (MV)
- ◇ Remote Vane (RV)
- + Strength Exceeds Capacity of Measuring Device

KEY TO GEOLOGIC UNITS

- | | | | |
|------|--------------------------------------|-----|------------------------|
| FILL | Fill/Buried Sand Fill | OBM | Old Bay Mud |
| YBM | Young Bay Mud | UAM | Upper Alameda Marine |
| MPSA | Merritt-Posey-San Antonio Formations | LAA | Lower Alameda Alluvial |

SUBSURFACE CROSS SECTION M1-M1'
With Undrained Shear Strength
SFOBB East Span Seismic Safety Project



GENERAL NOTES:

- 1) Stratigraphic contacts are approximate and are interpreted from CPT soundings, borings, and seismic reflection survey data. Conditions vary both along and perpendicular to the section line.
- 2) Refer to Key to Cross Sections (Plate 4.6) for descriptions of boring and CPT data shown above.

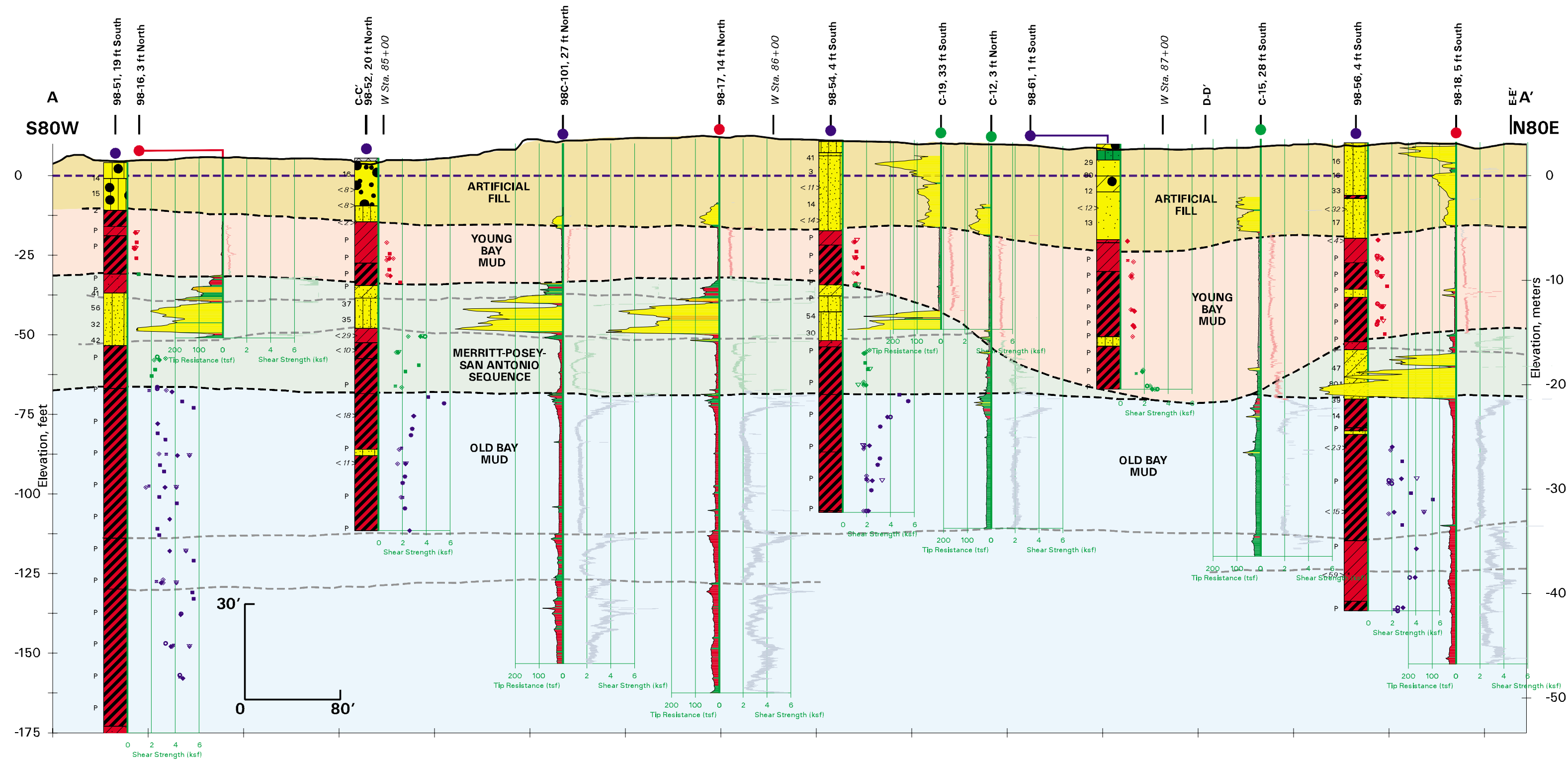
SHEAR STRENGTH SYMBOLS

- ▲ Unconsolidated Undrained (UU)
- Unconfined Compression (UC)
- ⊗ Pocket Penetrometer (PP)
- ⊕ Torvane (TV)
- ◆ Miniature Vane (MV)
- ◇ Remote Vane (RV)
- ⊕ Strength Exceeds Capacity of Measuring Device

KEY TO GEOLOGIC UNITS

- | | | | |
|------|--------------------------------------|-----|------------------------|
| BS | Beach Sand | OBM | Old Bay Mud |
| YBM | Young Bay Mud | UAM | Upper Alameda Marine |
| MPSA | Merritt-Posey-San Antonio Formations | LAA | Lower Alameda Alluvial |

SUBSURFACE CROSS SECTION M2-M2'
With Undrained Shear Strength
SFOBB East Span Seismic Safety Project



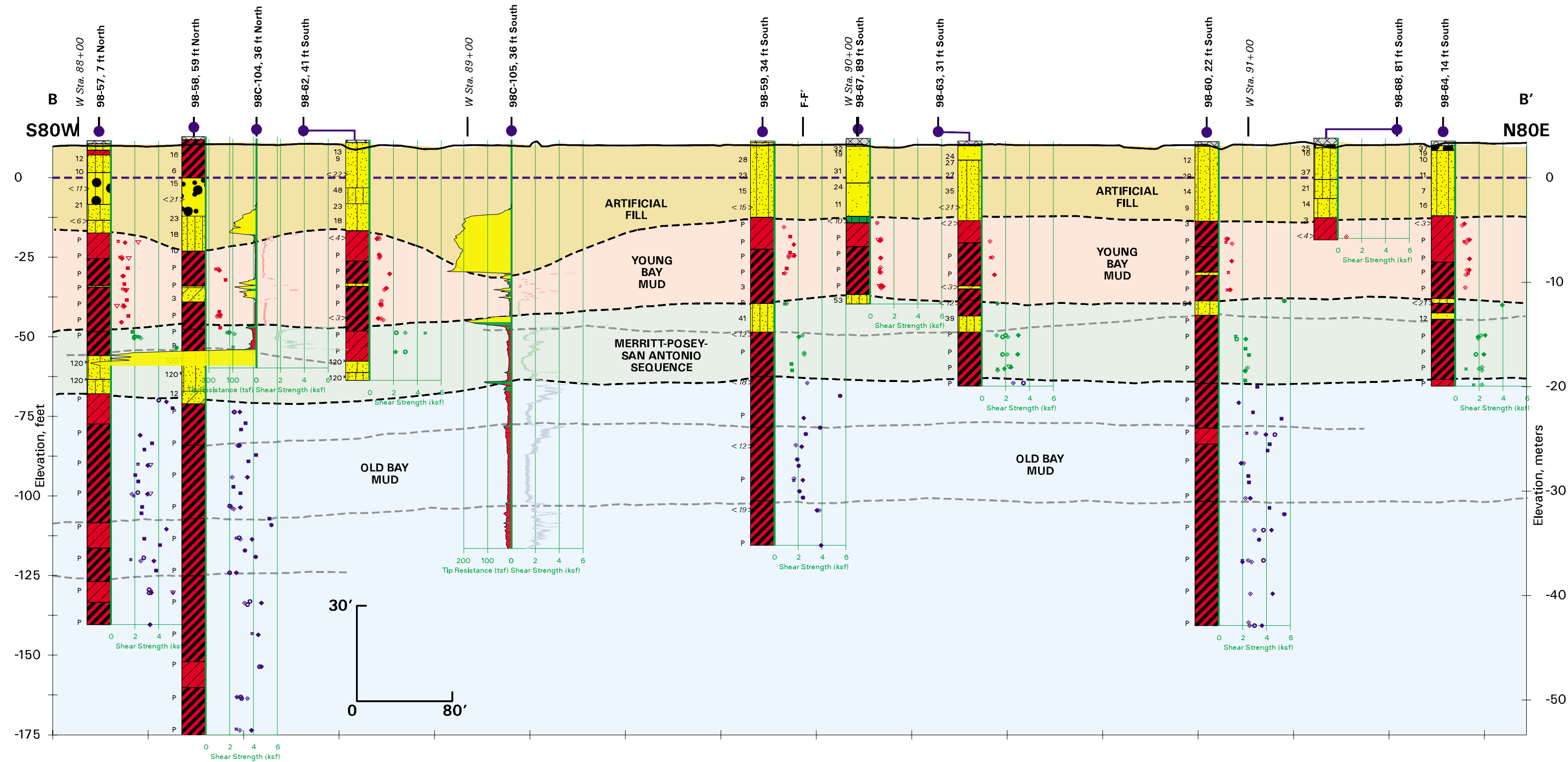
- GENERAL NOTES:
- 1) Stratigraphic contacts are approximate and are interpreted from lithology in borings and CPT soundings. Conditions vary both along and perpendicular to the cross section.
 - 2) Strata descriptions are generalized. Individual logs of borings and CPT soundings should be consulted for details.
 - 3) Refer to Key to Cross Sections (Plate 4.6) for details of data plotted on cross-sections. Note that lithologies for pre-1998 boring and CPT logs are as shown on Caltrans' Log of Test Boring Sheets.
 - 4) The CPT lithologies are based on the empirical correlation between tip resistance and friction ratio (Robertson and Campanella, 1984) shown on Plate 4.6.

UNDRAINED SHEAR STRENGTH LEGEND

- | | | | |
|---|-------------------------------|---|---------------------|
| ▲ | Unconsolidated Undrained (UU) | ◆ | Miniature Vane (MV) |
| △ | Unconfined Compression (UC) | ■ | Remote Vane (RV) |
| ○ | Pocket Penetrometer (PP) | ▽ | Fall Cone (FC) |
| ◇ | Torvane (TV) | | |

SUBSURFACE CROSS SECTION A-A'
With Undrained Shear Strength
SFOBB East Span Seismic Safety Project





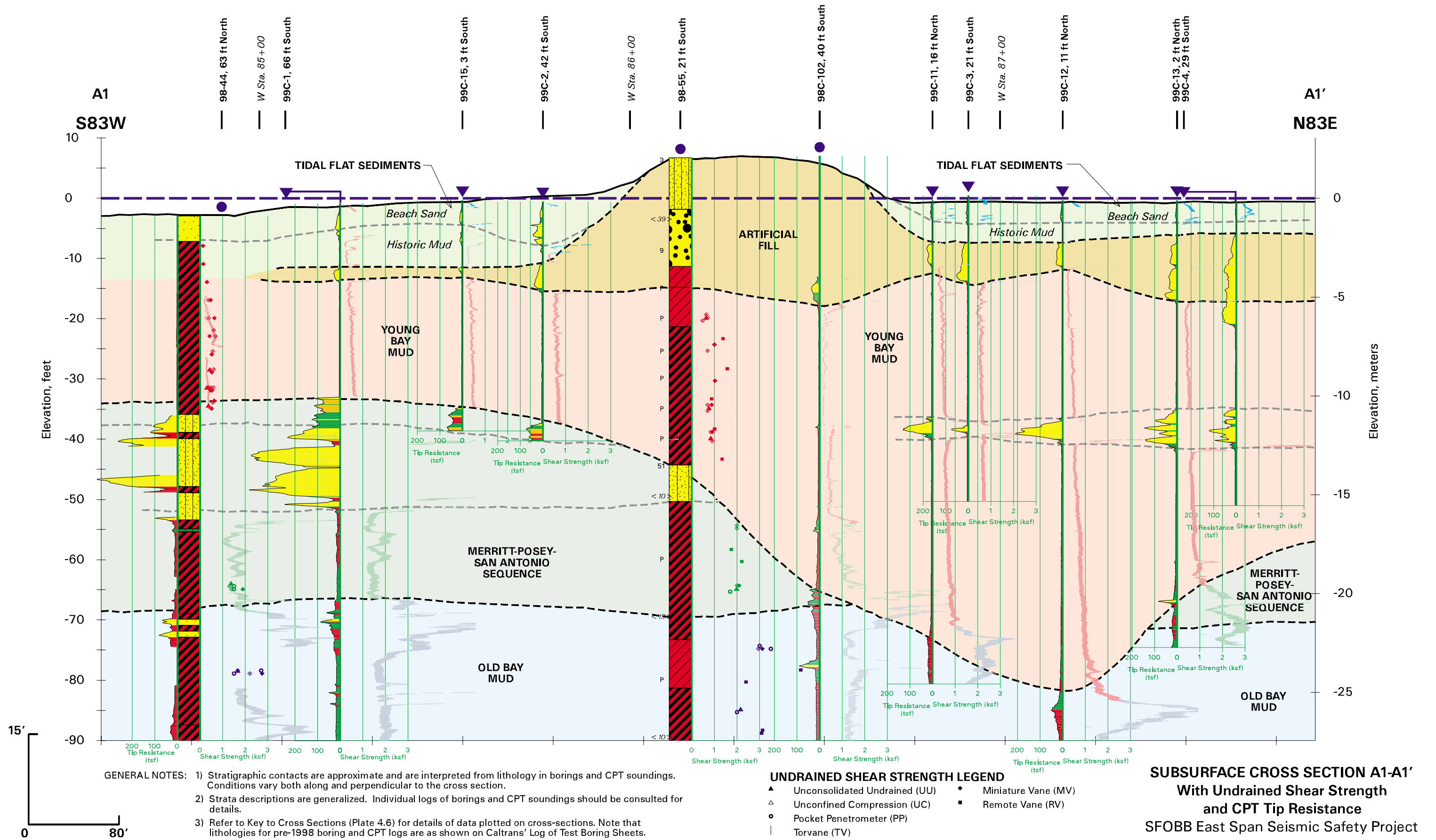
GENERAL NOTES: 1) Stratigraphic contacts are approximate and are interpreted from lithology in borings and CPT soundings. Conditions vary both along and perpendicular to the cross section.
2) Strata descriptions are generalized. Individual logs of borings and CPT soundings should be consulted for details.
3) Refer to Key to Cross Sections (Plate 4.6) for details of data plotted on cross-sections. Note that lithologies for pre-1998 boring and CPT logs are as shown on Caltrans' Log of Test Boring Sheets.
4) The CPT lithologies are based on the empirical correlation between tip resistance and friction ratio (Robertson and Campanella, 1984) shown on Plate 4.6.

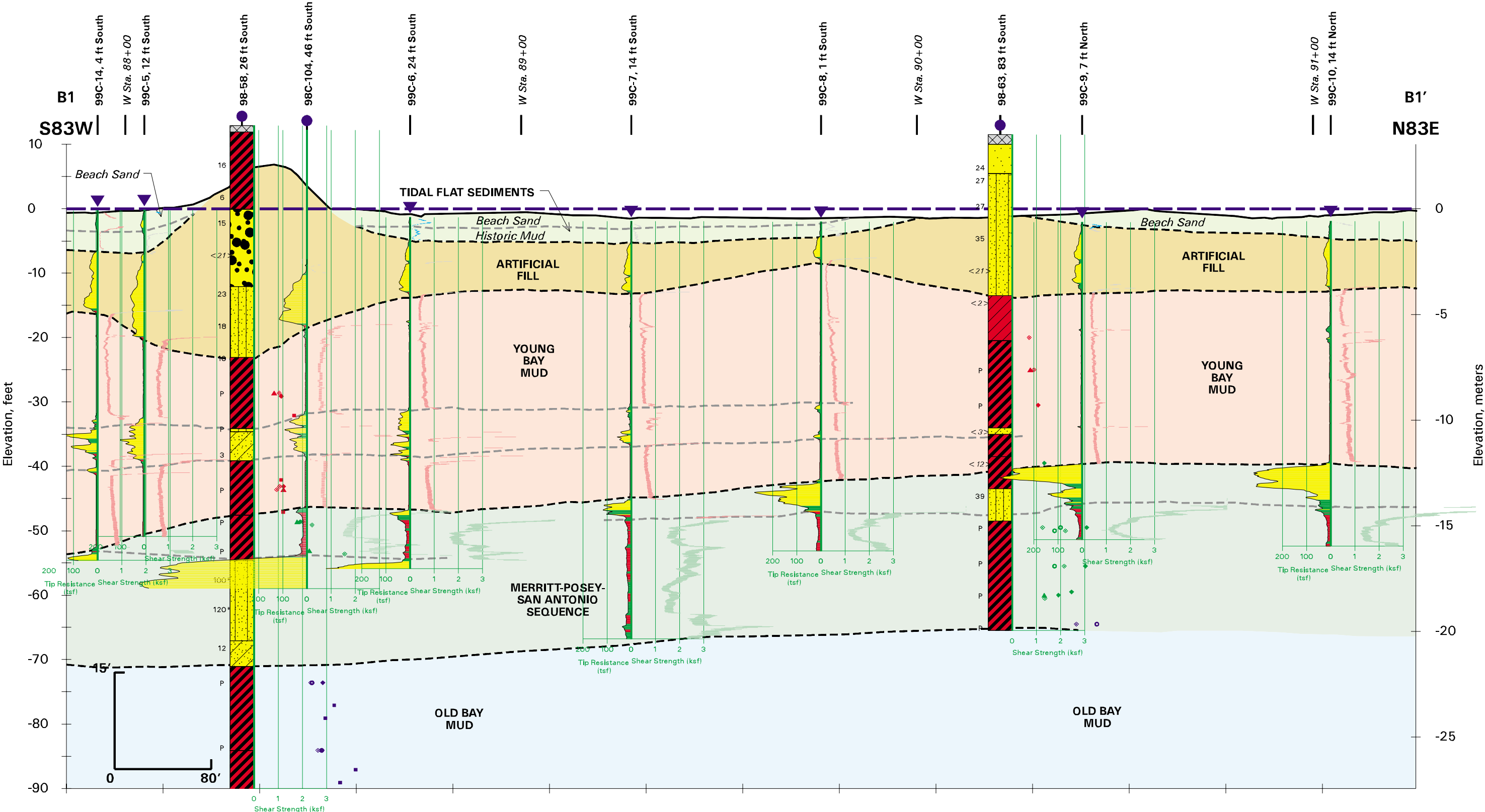
UNDRAINED SHEAR STRENGTH LEGEND

- | | |
|---------------------------------|-----------------------|
| ▲ Unconsolidated Undrained (UU) | ◆ Miniature Vane (MV) |
| △ Unconfined Compression (UC) | ■ Remote Vane (RV) |
| ● Pocket Penetrometer (PP) | ▽ Fall Cone (FC) |
| ◇ Torvane (TV) | |

SUBSURFACE CROSS SECTION B-B'
With Undrained Shear Strength
SFOBB East Span Seismic Safety Project







GENERAL NOTES: 1) Stratigraphic contacts are approximate and are interpreted from lithology in borings and CPT soundings. Conditions vary both along and perpendicular to the cross section.
2) Strata descriptions are generalized. Individual logs of borings and CPT soundings should be consulted for details.
3) Refer to Key to Cross Sections (Plate 4.6) for details of data plotted on cross-sections. Note that lithologies for pre-1998 boring and CPT logs are as shown on Caltrans' Log of Test Boring Sheets.
4) The CPT lithologies are based on the empirical correlation between tip resistance and friction ratio (Robertson and Campanella, 1984) shown on Plate 4.6.

UNDRAINED SHEAR STRENGTH LEGEND

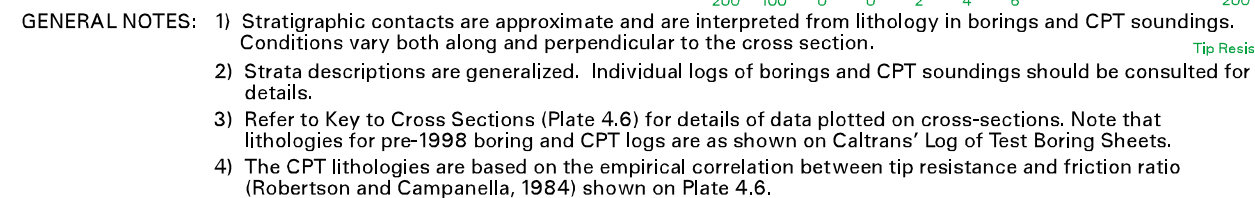
- ▲ Unconsolidated Undrained (UU)
- △ Unconfined Compression (UC)
- Pocket Penetrometer (PP)
- | Torvane (TV)
- ◆ Miniature Vane (MV)
- Remote Vane (RV)

SUBSURFACE CROSS SECTION B1-B1'

With Undrained Shear Strength
and CPT Tip Resistance

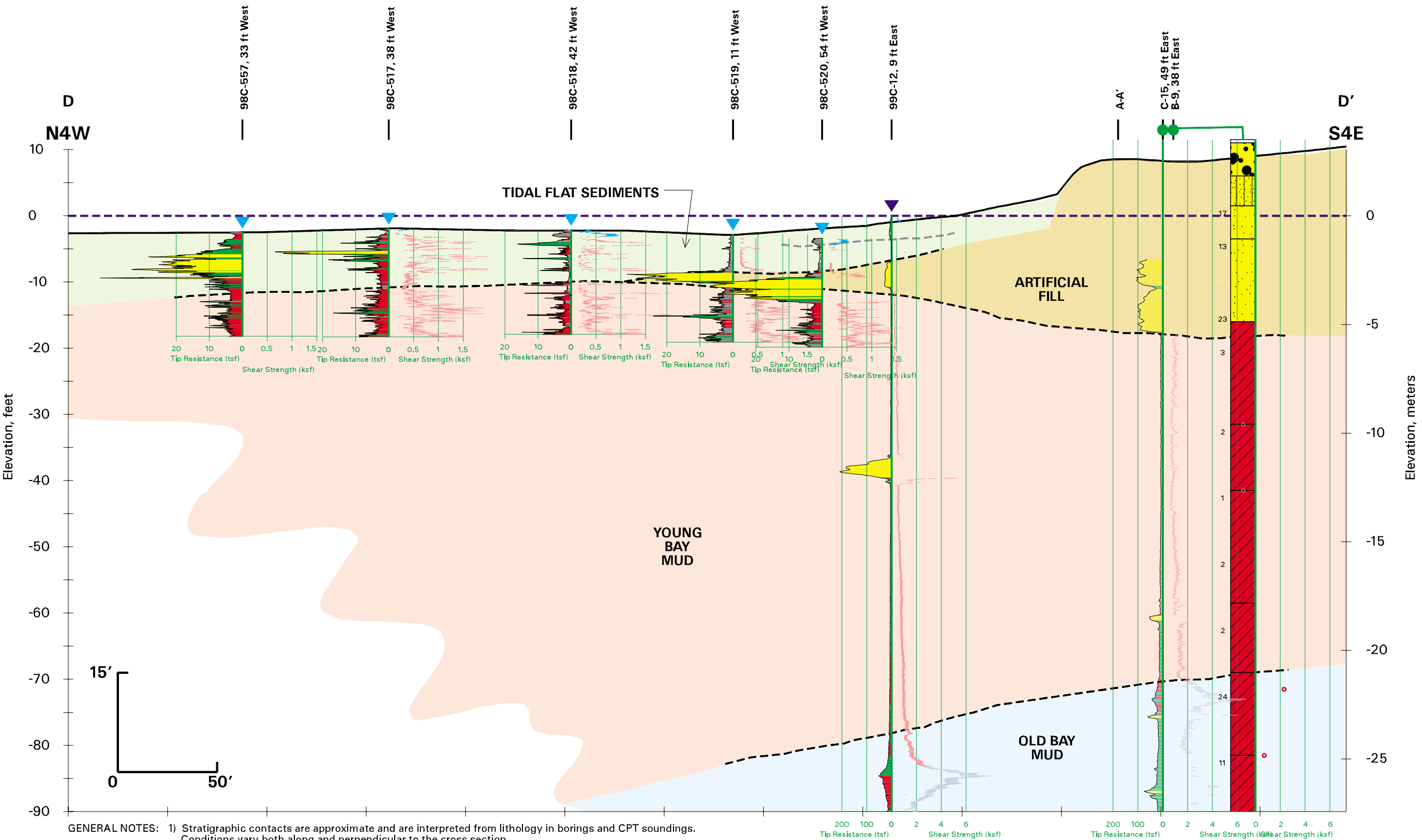
SFOBB East Span Seismic Safety Project





▲	Unconsolidated Undrained (UU)	◆	Miniature Vane (MV)
△	Unconfined Compression (UC)	■	Remote Vane (RV)
●	Pocket Penetrometer (PP)	▽	Fall Cone (FC)
◇	Torvane (TV)		

PLATE 4.8



GENERAL NOTES: 1) Stratigraphic contacts are approximate and are interpreted from lithology in borings and CPT soundings. Conditions vary both along and perpendicular to the cross section.
2) Strata descriptions are generalized. Individual logs of borings and CPT soundings should be consulted for details.
3) Refer to Key to Cross Sections (Plate 4.6) for details of data plotted on cross-sections. Note that lithologies for pre-1998 boring and CPT logs are as shown on Caltrans' Log of Test Boring Sheets.
4) The CPT lithologies are based on the empirical correlation between tip resistance and friction ratio (Robertson and Campanella, 1984) shown on Plate 4.6.

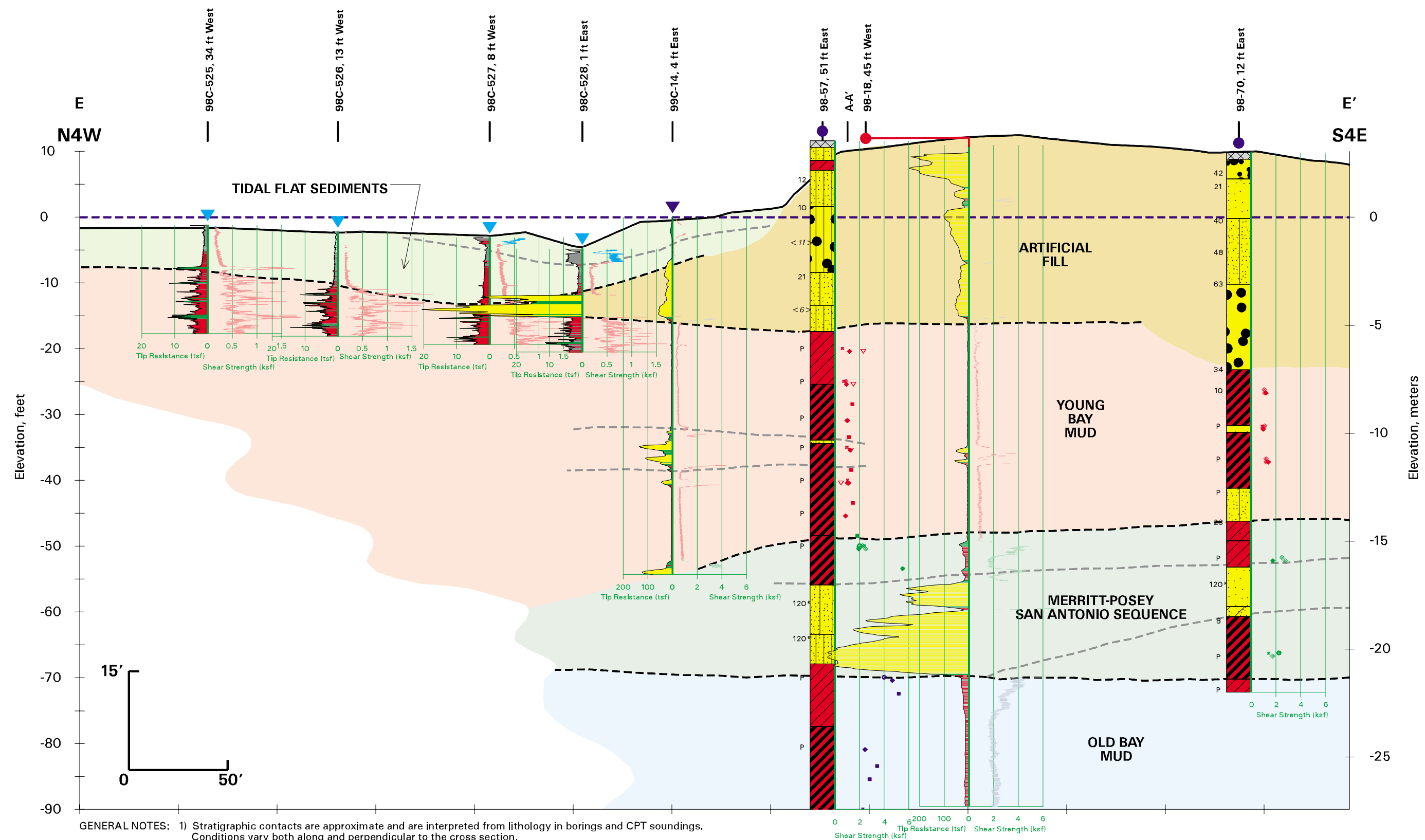
UNDRAINED SHEAR STRENGTH LEGEND

- | | | | |
|---|-------------------------------|---|---------------------|
| ▲ | Unconsolidated Undrained (UU) | ◆ | Miniature Vane (MV) |
| △ | Unconfined Compression (UC) | ■ | Remote Vane (RV) |
| ○ | Pocket Penetrometer (PP) | ▽ | Fall Cone (FC) |
| ◇ | Torvane (TV) | | |

SUBSURFACE CROSS SECTION D-D'

With Undrained Shear Strength
SFOBB East Span Seismic Safety Project





- GENERAL NOTES:
- 1) Stratigraphic contacts are approximate and are interpreted from lithology in borings and CPT soundings. Conditions vary both along and perpendicular to the cross section.
 - 2) Strata descriptions are generalized. Individual logs of borings and CPT soundings should be consulted for details.
 - 3) Refer to Key to Cross Sections (Plate 4.6) for details of data plotted on cross-sections. Note that lithologies for pre-1998 boring and CPT logs are as shown on Caltrans' Log of Test Boring Sheets.
 - 4) The CPT lithologies are based on the empirical correlation between tip resistance and friction ratio (Robertson and Campanella, 1984) shown on Plate 4.6.

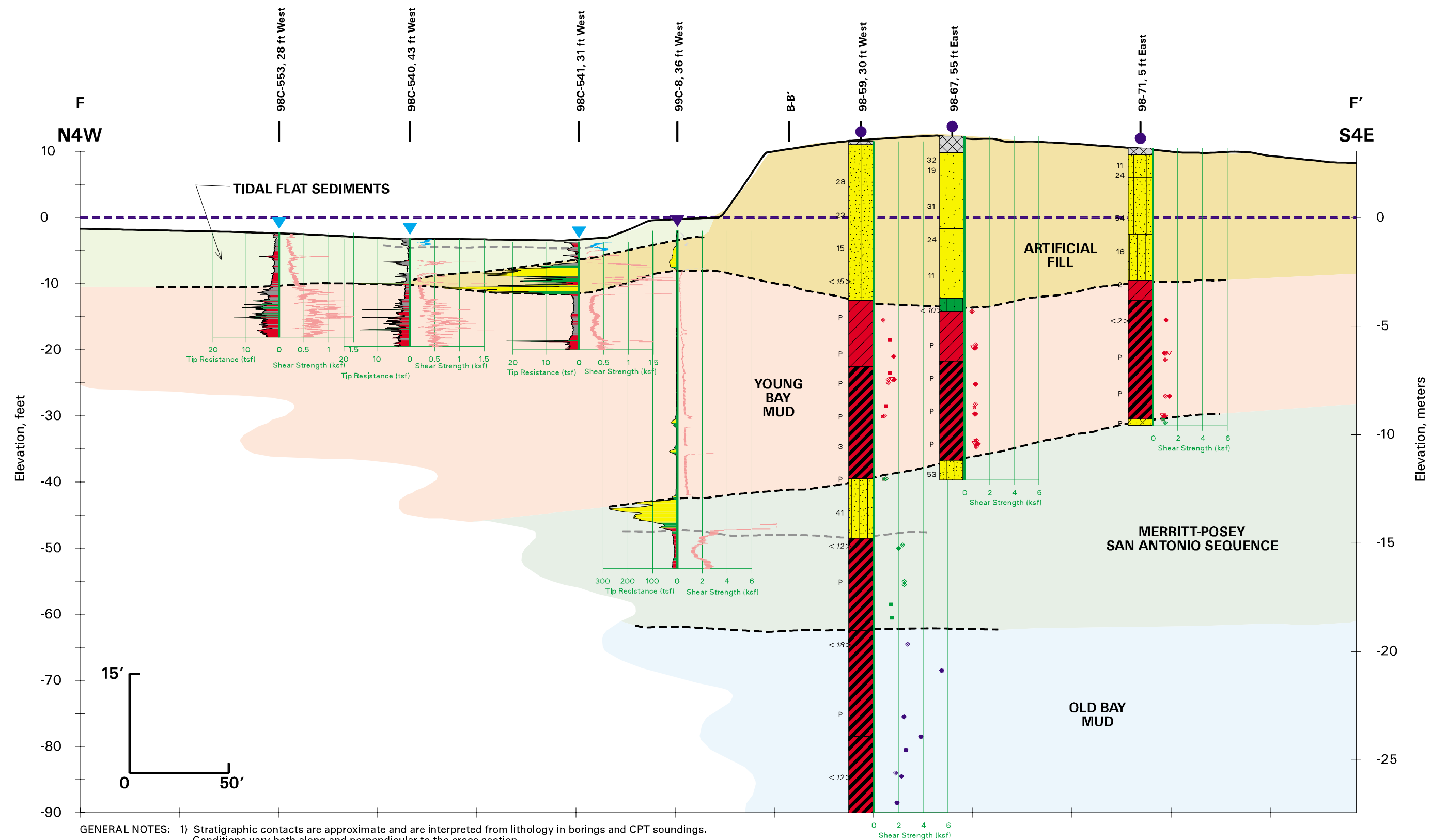
UNDRAINED SHEAR STRENGTH LEGEND

- | | | | |
|---|-------------------------------|---|---------------------|
| ▲ | Unconsolidated Undrained (UU) | ◆ | Miniature Vane (MV) |
| △ | Unconfined Compression (UC) | ■ | Remote Vane (RV) |
| ● | Pocket Penetrometer (PP) | ▽ | Fall Cone (FC) |
| ◆ | Torvane (TV) | | |

SUBSURFACE CROSS SECTION E-E'

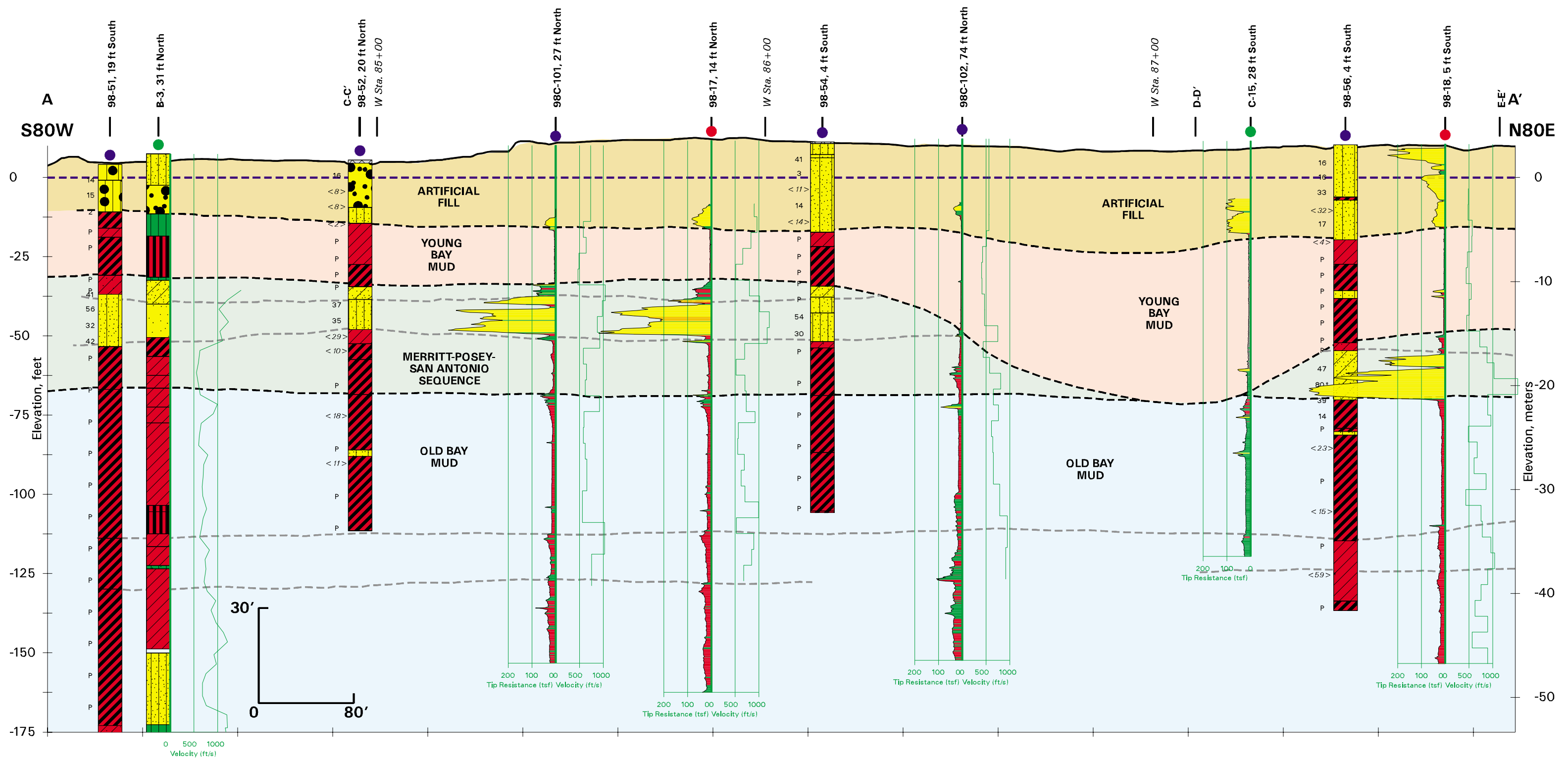
With Undrained Shear Strength
SFOBB East Span Seismic Safety Project





SUBSURFACE CROSS SECTION F-F'
With Undrained Shear Strength
SFOBB East Span Seismic Safety Project

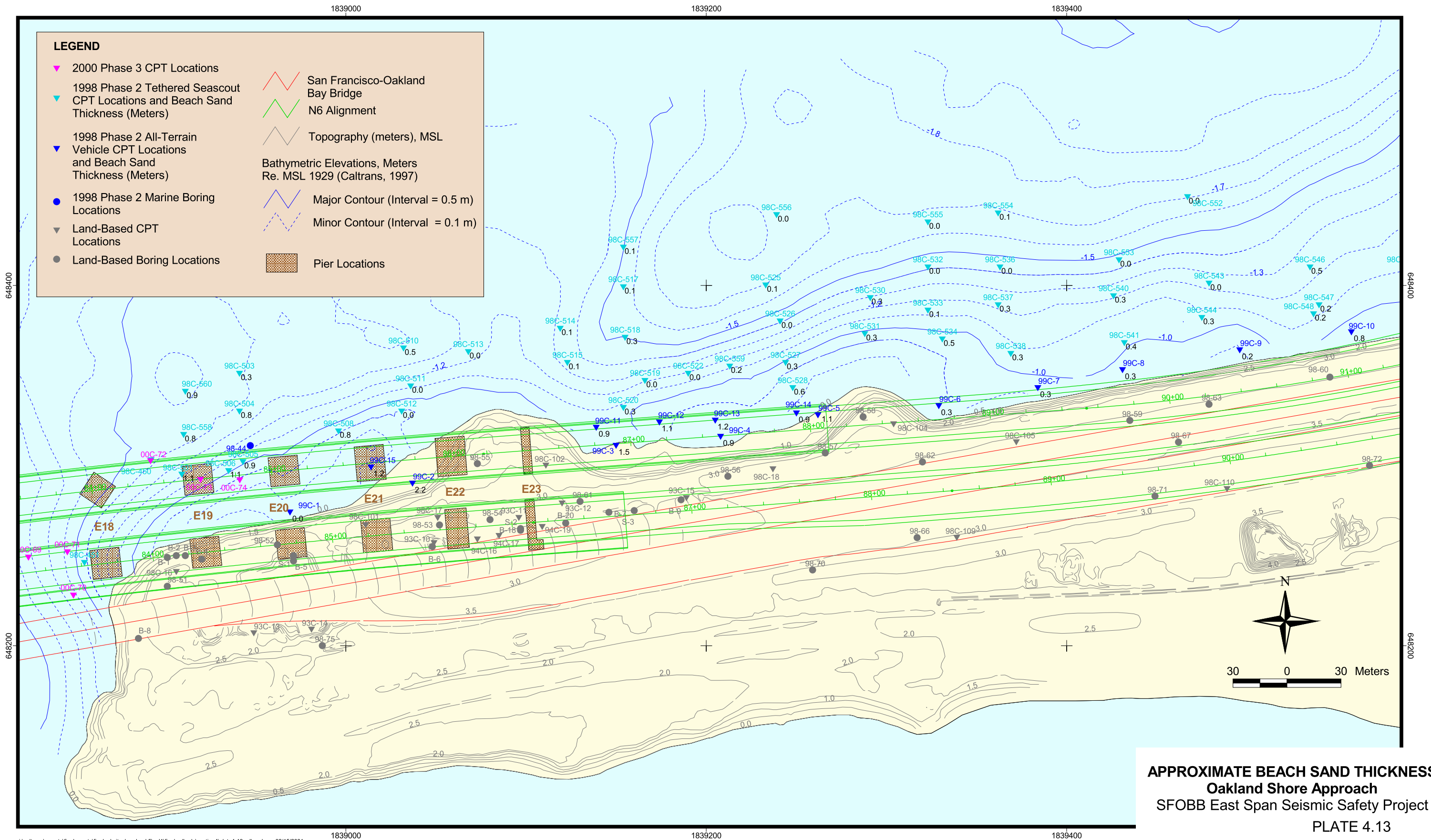


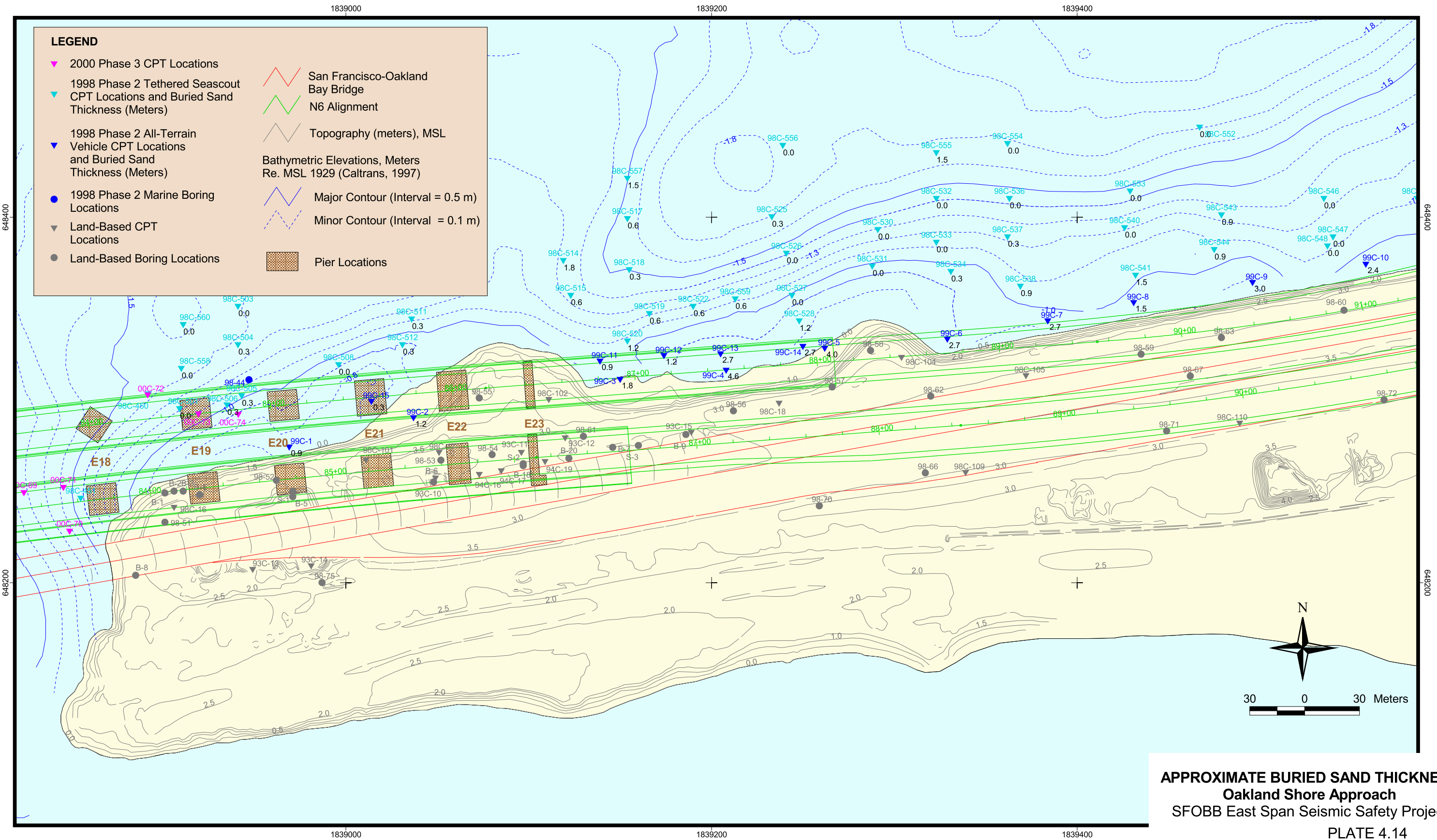


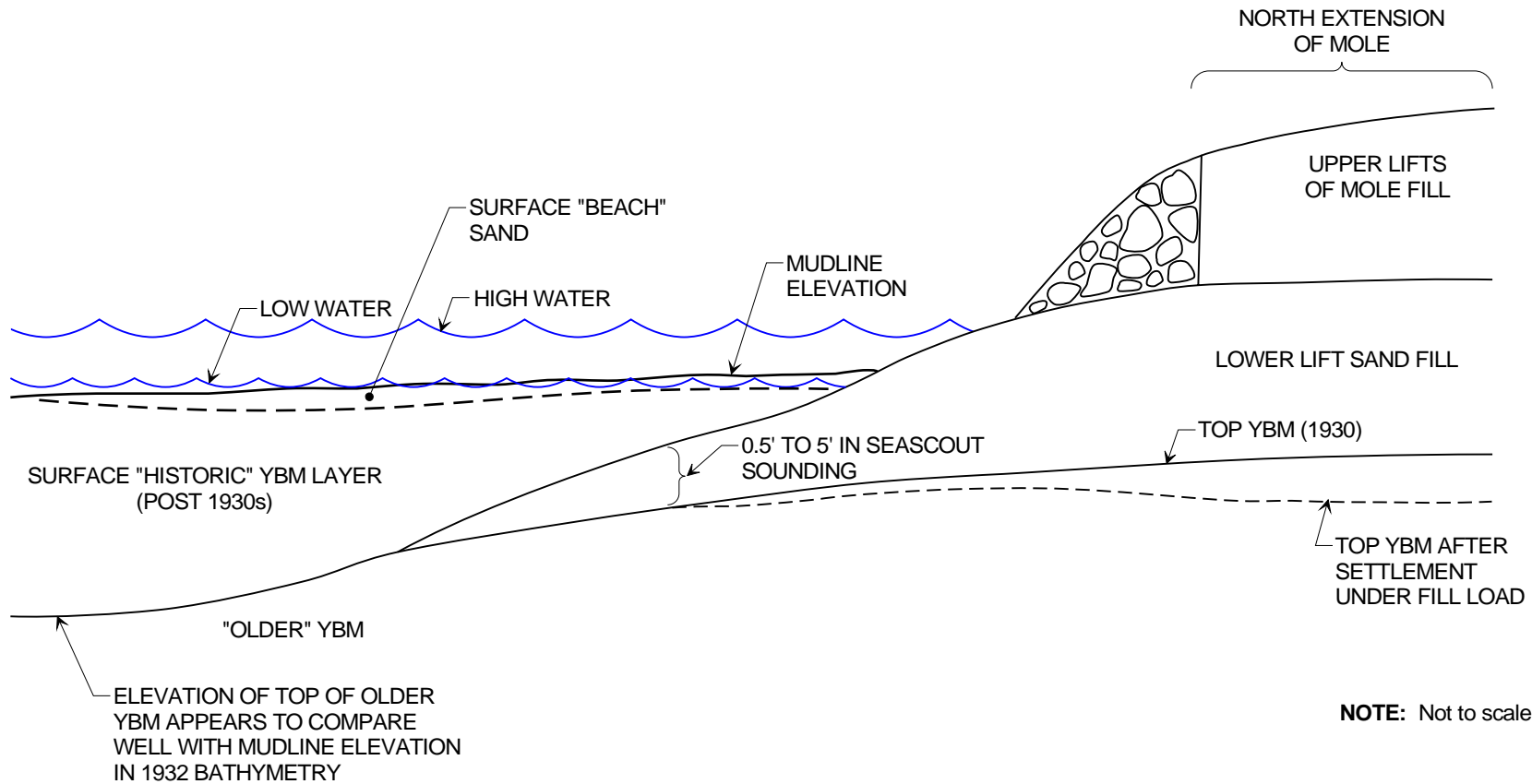
- GENERAL NOTES:
- 1) Stratigraphic contacts are approximate and are interpreted from lithology in borings and CPT soundings. Conditions vary both along and perpendicular to the cross section.
 - 2) Strata descriptions are generalized. Individual logs of borings and CPT soundings should be consulted for details.
 - 3) Refer to Key to Cross Sections (Plate 4.6) for details of data plotted on cross-sections. Note that lithologies for pre-1998 boring and CPT logs are as shown on Caltrans' Log of Test Boring Sheets.
 - 4) The CPT lithologies are based on the empirical correlation between tip resistance and friction ratio (Robertson and Campanella, 1984) shown on Plate 4.6.

SUBSURFACE CROSS SECTION A-A'
With Shear Wave Velocity
SFOBB East Span Seismic Safety Project
PLATE 4.12

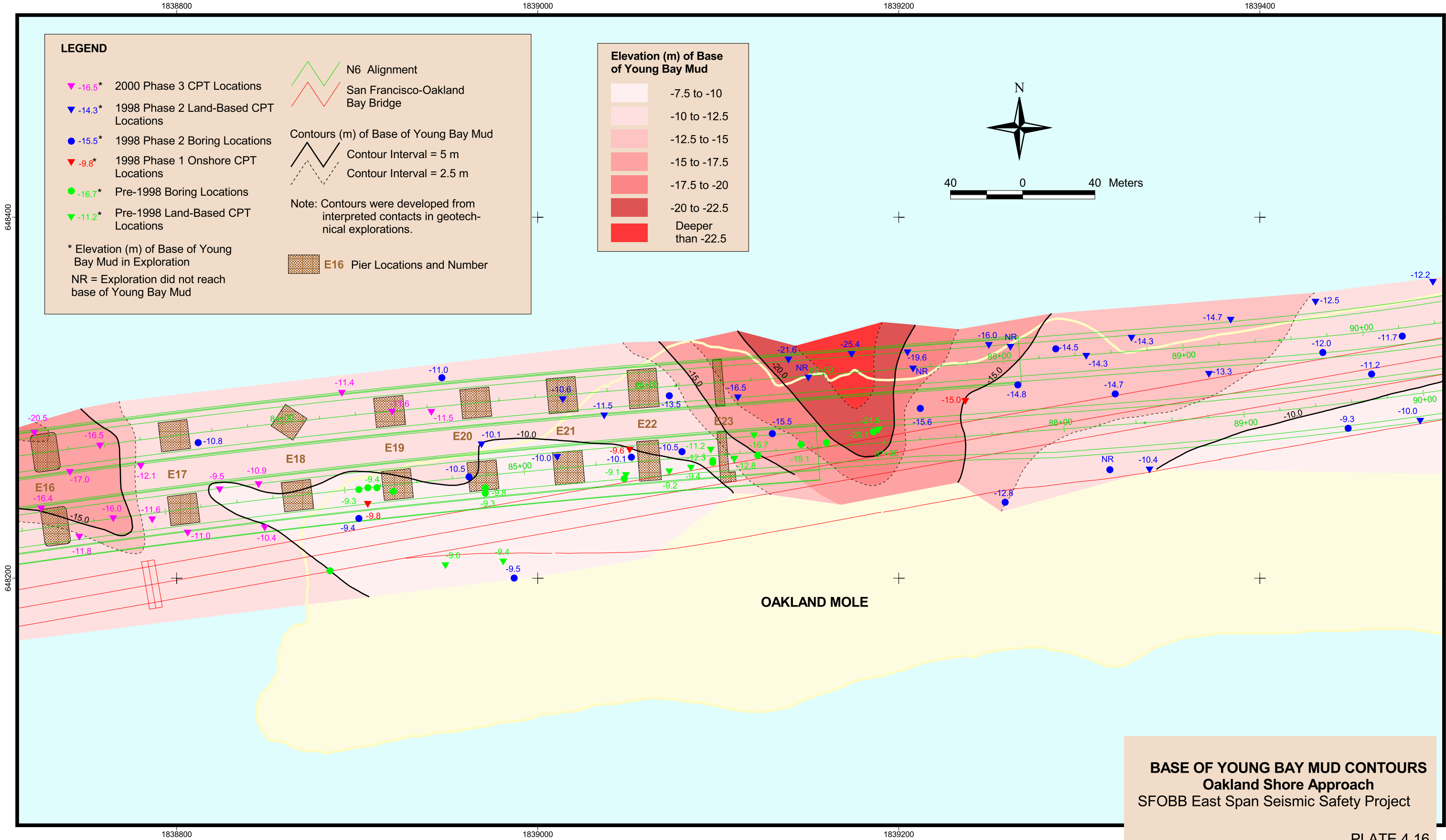




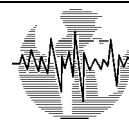




**SIMPLIFIED CROSS-SECTION THROUGH
NORTHERN TIDAL FLAT AND OAKLAND SHORE APPROACH**
Oakland Shore Approach
SFOBB East Span Seismic Safety Project



SECTION 5.0 ENGINEERING SOIL PROPERTIES



5.0 ENGINEERING SOIL PROPERTIES

5.1 CLASSIFICATION PROPERTIES AND UNIT WEIGHT OF SEDIMENTS

5.1.1 Classification Properties of Fine-Grained Sediments

In the vicinity of the Oakland Mole, marine clay sediments compose about 75 to 90 percent of the stratigraphic sequence that lies above the deep Lower Alameda Alluvial sediments. The fine-grained sediments are composed primarily of fat clay with lesser amounts of lean clays.

Plasticity. Consistent with the marine characterization program, the sediments comprising most of the Young Bay Mud (YBM), Old Bay Mud (OBM), and much of the Upper Alameda Marine (UAM) sequences are predominantly fat clays. Lower plasticity lean clay layers within those strata are predominantly encountered in crustal, overconsolidated zones. Outside of these crustal zones, the liquid limits of the fat clay sediments are generally similar.

The Atterberg limits for the sediments from the borings plot above the A-line of the plasticity chart, as shown on Plate 5.1. The liquid limits of the clay sediments typically range from about 40 to 82, and approximately 65 percent of the test specimens had a liquid limit of more than 50. The Young Bay Mud was typically less plastic and plots closer to the A-line of the plasticity chart than the Old Bay Mud. The upper few meters of the Young Bay Mud are typically siltier than the underlying clay deposits and tend to have a lower liquid limit. The plasticity index typically ranges from about 18 to 55.

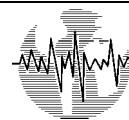
Liquid limit and plasticity index data are plotted versus elevation by formation on Plates 5.2 and 5.3, respectively. The typical ranges of soil plasticity are summarized as follows:

- **Young Bay Mud** - A liquid limit of 40 to 70 and a plasticity index of 18 to 42. There is a noticeable trend of increasing plasticity with depth, due to generally decreasing silt content with depth.

The liquid limit and plasticity index of several Young Bay Mud samples collected at all-terrain CPT locations along the foot of the Mole were similar to the sediments recovered from the land borings. The liquid limit of the Young Bay Mud underlying the tidal flat was generally higher than that encountered in land borings and ranged from 50 to 90.

- **Clay Layers in the Merritt-Posey-San Antonio (MPSA) Formations** - A liquid limit of 35 to 75 and a plasticity index of 25 to 50. The large range in plasticity within the MPSA Formations is due to the presence of both fat clays and sandy lean clays. The sandy clays typically have a liquid limit of 35 to 45 and a plasticity index





of 25 to 35. The fat clays are generally similar to the clay layers within the Young and Old Bay Muds.

- **Old Bay Mud/Upper Alameda Marine (OBM/UAM) Sediments** - Typically the OBM/UAM sediments have a liquid limit of 55 to 90 and a plasticity index of 35 to 60, with crust layers having a liquid limit of 35 to 45 and plasticity index of 20 to 30.
- **Tidal Flat Sediment** - The liquid limits and plasticity index of samples of historical bay mud collected at ATV-mounted CPT locations underlying the tidal flat to the north of the Mole were generally similar to the Young Bay Mud. The liquid limits were 62 and 92 with plasticity indexes of 38 and 55.

Grain Size. The grain-size characteristics of the fat clay, which comprises the majority of the Young Bay Mud and Old Bay Mud/Upper Alameda Marine sediments, show that: a) the percent minus the No. 200 sieve typically exceeds 85 percent, and b) the percent of clay-size particles that are finer than 0.002 mm generally ranges from about 30 to 55 percent. Lean clay layers within the Young Bay Mud typically contain about 15 to 30 percent clay-size particles that are finer than 0.002 mm. Those results are generally comparable to the results from the marine investigation and characterization program. The grain size of the historical bay mud underlying the tidal flat to the north of the Mole is judged to be generally similar to the fat clays and Young Bay Mud grain size properties. A sample of historical mud collected at an all-terrain CPT location shows that: a) the percent minus the No. 200 sieve exceeds 75 percent, and b) the percent of clay-size particles that are finer than 0.002 mm is about 22 percent. The typical ranges of grain size for the fat and lean clays from the Young and Old Bay Muds are shown on Plate 5.4.

5.1.2 Classification Properties of Granular Sediments

Granular soils were encountered down to the maximum depth explored in the Mole borings: a) as the artificial fill that comprises the majority of the top several meters of the subsurface, b) within the Merritt-Posey-San Antonio Formations as Merritt Sand, and c) as layers within the Old Bay Mud and Upper Alameda Marine sediments. Poorly-graded fine sand with silt and silty fine sand layers also are locally present above the Young Bay Mud on the tidal flat to the north of the Mole.

Typical grain-size characteristics of the granular materials are shown on Plate 5.4, the fines content data are plotted on Plate 5.5, and the mean grain size (D_{50}) data are plotted on Plate 5.6. The grain-size characteristics are summarized as follows:

- **Artificial Fill** - The fill typically consists of poorly graded fine sand with silt and silty fine sand with shell fragments. The poorly graded fine sand with silt and silty fine sand typically contain 5 to 14 percent finer than the No. 200 sieve and have a mean grain size of about 0.22 to 0.3 mm. Less prevalent, siltier layers contain up to





30 percent finer than the No. 200 sieve and have a mean grain size of between 0.12 and 0.22 mm.

- **Gravel and Rock in Artificial Fill** - The fill locally includes layers, pockets, and zones of gravel with sand, cobbles, and rubble. Riprap, cobbles, and gravel are present at the locations of buried rock dikes that were constructed during the placement of the Mole fill during the 1930s. Observations in the trench excavations indicate that the rock dike consists of a facing of angular and rounded riprap and quarry-run size round and angular cobbles. The face rock ranged from 0.6 to 1.2 meters in size and the core material ranged from 300 to 600 mm in size with small angular gravel filling the voids.
- **Merritt-Posey-San Antonio Formations** - The Mole investigation borings suggest that the sands within the MPSA Formations are typically poorly graded fine sand to silty fine sand with 6 to 25 percent finer than a No. 200 sieve and a mean grain size of about 0.18 to 0.26 mm.
- **Sand and Silt Layers in Old Bay Mud and Upper Alameda Marine** - In the sequence of primarily marine clays, sand layers were typically poorly graded fine sand with silt or silty fine sand with 5 to 15 percent finer than a No. 200 sieve.
- **Tidal Flat Sands** - Poorly-graded fine sand with silt and silty fine sand are locally present above the Young Bay Mud on the tidal flat to the north of the Mole. Grain size tests on a limited number of samples suggest that those tidal flat sands typically contain 4 to 10 percent finer than the No. 200 sieve and have a mean grain size of about 0.2 to 0.25 mm.

5.1.3 Water Content and Unit Weights

Water Content. The measured water content data are summarized on Plate 5.7. The typical range of water content data are summarized as follows:

- **Artificial Fill** - Water content of the sand fill above the water table ranges from 4 to 13 percent. Below the water table, the water content of the fill is typically between about 15 to 26 percent. In the transition zone between the emergent and submerged fill, the water content typically ranges from 10 to 24 percent.
- **Tidal Flat Sediments** - The available water content data of the historical bay mud on the tidal flat to the north of the Mole typically ranges from about 40 to 100.
- **Young Bay Mud Beneath Mole** - The measured water content of the Young Bay Mud (YBM) beneath the Mole typically ranges from about 32 to 62 percent. Water content of up to 80 percent exists in local layers. The water content is frequently near the liquid limit. The water content is generally lower than the YBM data from the marine samples, where the water content generally ranges from 40 to 100 percent.





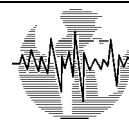
The difference is due to the consolidation of the YBM under the weight of the fill and the increased silt content in the upper few meters of the YBM underlying the Mole.

- **Young Bay Mud Beneath Tidal Flat** - Samples collected from the top 3 meters of Young Bay Mud to the north of the Mole indicate the water content typically ranges from about 65 to 75 percent.
- **Merritt-Posey-San Antonio Formations** - The water content in the Merritt Sand typically ranges from 20 to 32 percent, which is comparable to the marine characterization results. Water content of the fine-grained layers of the sequence typically is between 38 and 55 percent.
- **Old Bay Mud/Upper Alameda Marine Sediments** - Water content in the OBM/UAM sediments generally ranges from 35 to 55 percent. Lower values were measured in crustal zones and zones with a higher sand content. Although the water content has significant variability due to the presence of crust layers, there is a trend of decreasing water content with depth. The occasional granular layers generally have a water content of about 18 to 25 percent. This compares favorably with the results from the marine site characterization program where water content within the OBM/UAM sediments typically ranged from approximately 40 to 60 percent.

Unit Weights. The measured total unit weights are summarized on Plate 5.8. The typical range of unit weight data are summarized as follows:

- **Artificial Fill** - The total unit weights of the submerged fill ranges from 19.5 to 20.5 kilonewtons per cubic meter (kN/m^3). Unit weights as high as 21.8 kN/m^3 were measured in the fill.
- **Recent Young Bay Mud** - The total unit weights of the Young Bay Mud are generally between 16.4 and 18.4 kN/m^3 , and generally decrease in depth due to the decreased silt and sand content.
- **Merritt-Posey-San Antonio Formations** - Total unit weights of the Merritt Sand range from 18.5 to 20.6 kN/m^3 . The data compare favorably with the marine site characterization, where the unit weights of granular layers are generally between 18.6 and 20.2 kN/m^3 . Unit weights within the fine-grained portions of the sequence typically range from 16.2 to 18.0 kN/m^3 .
- **Old Bay Mud/Upper Alameda Marine Sediments** - Total unit weights in the OBM/UAM sediments range from 16.4 to 19.4 kN/m^3 . The unit weights have significant variability due to the presence of crust layers, but there is a trend of increasing unit weight with depth. The occasional granular layers generally have submerged unit weights in excess of 19.4 kN/m^3 .





5.2 CONSISTENCY AND SHEAR STRENGTH OF FINE-GRAINED SEDIMENTS

5.2.1 Undrained Shear Strengths From Laboratory and Remote Vane Testing

Both undrained shear strength measurements from laboratory tests on samples collected from land borings and in situ remote vane tests conducted in the land borings are summarized on Plates 5.9 through Plate 5.12. Plate 5.9 is a summary of all shear strength data plotted by test type. Plates 5.10 through 5.12 show shear strength data plotted by boring for the western, central, and eastern portions of the explored area of the Mole.

Some of the laboratory tests were conducted on driven samples. Examination of the data clearly shows that those test results are lower than the results of tests conducted on pushed samples or in situ vane shear tests. Those disturbance effects were recognized when formulating these interpretations of the in situ undrained shear strengths of the various sediments. In addition, the undrained shear strengths from laboratory miniature vane and in situ remote vane tests shown on Plates 5.9 through 5.12 include some tests on clay samples with sand seams and shells. The possibility that those test results, where sand seams are present within the test depth or specimen, may overestimate the strength also has been considered in these interpretations of the typical undrained shear strengths.

5.2.2 Undrained Shear Strengths Interpreted From CPT Testing

Undrained shear strengths have been estimated from the CPT measurements using the following expression:

$$S_u = (q_c - \sigma_{vo}) / N_k$$

Where: S_u = Undrained shear strength, kPa
 q_c = Corrected cone tip resistance, kPa
 σ_{vo} = Estimated in situ total vertical stress, kPa
 N_k = Empirical cone bearing factor

Undrained shear strengths interpreted from CPT tip resistances are plotted on Plate 5.13. The data presented on Plate 5.13 are based on an empirical cone bearing capacity factor (N_k) of 12. The undrained shear strengths are calculated from tip resistances that are corrected for unequal cone end area effects.

Although the CPT data were filtered to exclude non-cohesive strata shown on the boring logs, the data presented on Plate 5.13 include scattered data points in thin sand seams and layers (plotting higher than the trend). Those abnormal test results were discounted when typical undrained shear strengths were interpreted.





5.2.3 Isotropically Consolidated-Undrained Triaxial Compression (CIUC) Results

Three series of CIUC tests were performed on Young Bay Mud samples. In each test series, three samples were consolidated to consecutively higher stress levels before being sheared in compression. Typically, one sample was consolidated to approximately the effective overburden pressure, while the second and third samples were consolidated to pressures approximately two and four times the effective overburden stress.

The results of the CIUC testing are summarized in Table 5.1. The measured undrained strengths of the samples consolidated to the effective overburden pressures ranged from 34 to 43 kPa, which is slightly higher than the undrained shear strength found in the field, laboratory, and CPT testing in the same borings. As expected, the results show that the undrained strength increases with increasing consolidation stress.

5.2.4 Variability of Undrained Shear Strength Measurements

Statistical evaluations of the variations in different types of undrained shear strength measurements were conducted to evaluate the results of the Mole data. A summary of the observations and conclusions is presented below.

Driven Samples, Pushed Samples, and In Situ Measurement Comparison. The undrained strength data from the Mole exploration plotted versus elevation (Plate 5.9) were evaluated by test type. The following observations are made relative to the differences among the laboratory vane test data on driven and pushed samples and the in situ vane testing data:

- The in situ remote vane measurements are consistently greater than the laboratory measurements on the samples.
- The laboratory measurements on the driven samples are consistently the lowest of the three measurements.
- The ratio of the laboratory miniature vane test measurements on pushed samples to the in situ vane results is less in the firm to stiff Young Bay Mud than in the stronger clay layers in the Merritt-Posey-San Antonio Formations or the Old Bay Mud.
- The difference between the laboratory measurements on the lower quality, driven modified California samples and the higher quality push samples is greater in the very stiff to hard Old Bay Mud than the soft to stiff Young Bay Mud.
- The ratio of laboratory measurement to in situ measurement is summarized below:

	<u>Driven Samples</u>	<u>Pushed Samples</u>
Young Bay Mud	0.4 to 0.7	0.6 to 0.85
Merritt-Posey-San Antonio Clay Layers	0.5 to 0.8	0.7 to 0.9
Old Bay Mud	0.65 to 0.8	0.75 to 0.95





The above observations are consistent with the sensitivity and potential for disturbance of the softer Young Bay Muds.

Comparison of Measurements From Different Test Types. In addition to evaluating the effect of different sampling procedures, the differences between different types of tests were also evaluated. To evaluate the data, cumulative frequency distributions of the different types of measurements were prepared for both the Young and Old Bay Muds. In addition, the cumulative frequency distributions were computed for the interpreted undrained shear strengths from the land CPT data based on an assumed N_k of 12. The cumulative frequency plots for the Young and Old Bay Muds are presented on Plates 5.14 and 5.15, respectively.

The following observations are made relative to the differences among the various types of measurements:

- In the firm to stiff Young Bay Mud, the CPT data and remote vane data suggest that about 10 percent of those measurements are affected by sand seams.
- After deleting that 10 percent of the data from the Young Bay Mud distributions and removing the measurements on driven samples from the data, the remaining data suggest that:
 - The ratio of unconsolidated-undrained triaxial test results to in situ vane results is about 75 percent.
 - The ratio of laboratory miniature vane results to in situ vane results is about 90 percent.
- In the very stiff Old Bay Mud, data from the CPT soundings, UU triaxial tests, and remote vane tests suggest that about 30 to 40 percent of those measurements are either in hard crust layers or affected by sand seams. Because laboratory miniature vane shear tests were frequently not performed in the hard crust layers, that data does not contain those higher strength layers.
- After the measurements in the crust and on driven samples are removed from the data, the Old Bay Mud distributions suggest that:
 - The ratio of unconsolidated-undrained triaxial test results to in situ vane results is about 80 percent.
 - The ratio of laboratory miniature vane results to in situ vane results is about 100 percent.

The cumulative frequency distributions also can be used to determine an appropriate N_k value for interpreting undrained shear strength from the CPT data. As noted earlier, recognizing that some of the unconsolidated-undrained triaxial measurements will underestimate the in situ shear strength and that some of the in situ vane tests may overestimate the undrained shear strength in layers with sand seams, N_k in the range of 10 to 13 for Young Bay Mud and 11 to 14 for Old Bay Mud appear applicable. Therefore, the interpreted undrained shear strengths based





on an N_k of 12 and plotted on Plate 5.13 are likely to be a slightly conservative estimate. The range of interpreted undrained shear strengths shown on the cross sections based on an N_k range of 12 to 15 are similarly slightly conservative.

5.2.5 Spatial Variability of Undrained Strength

Beneath the Mole. Plates 5.10 through 5.12 show undrained shear strengths by borings grouped in the western, central, and eastern portions of the Mole. As shown, the undrained shear strengths are generally similar throughout the Mole exploration area. With two exceptions, no significant spatial variations are observed.

The first exception is in the Young Bay Mud in the western portion of the site. In that area, the undrained shear strengths in the Young Bay Mud typically range from 23 to 60 kPa. In comparison, a range of 28 to 70 kPa appears to be more representative of the central and eastern areas. The lower undrained shear strengths in the western Mole area are interpreted to be due to: 1) lower overburden stresses (Borings 98-51 and 98-52) due to thinner fill sections, and 2) a thinner and younger fill section at Boring 98-55 on the western jughandle. As described subsequently, the consolidation data suggest that the Young Bay Mud is not fully consolidated under the weight of the more recent fill at that jughandle location.

The second exception is in the central area where the Young Bay Mud is thicker in the paleochannel. The data suggest that within the deeper portion of the paleochannel fill, the rate of increase in undrained shear strength with depth is less than elsewhere within the Young Bay Mud.

Differences Between Young Bay Mud Beneath the Mole and Adjacent Marine Areas

The interpreted undrained shear strengths from the CPT data on the Mole and at the toe of the Mole slope are shown on Plates 5.16a and 5.16b. The results indicate that the undrained strengths of the Young Bay Mud measured on the tidal flats north of the Mole are typically 15 to 25 kPa lower than the shear strength beneath the Mole (Plate 5.16a). The higher shear strength beneath the Mole is primarily due to the consolidation of Young Bay Mud under the weight of the fill. The differences in undrained shear strength at the western end of the Mole and the western jughandle are quite small due to the relatively thin fill thicknesses at those locations (see Plate 5.16b). Similarly, lower shear strengths were computed from Seacalf CPT data in Young Bay Mud layers in areas to the north and west of the Mole than were measured in Young Bay Mud layers beneath the Mole. In general, the undrained shear strengths computed from Seacalf and ATV-mounted CPT data compare favorably. However, the undrained shear strengths from the Seacalf CPTs were typically slightly lower than undrained shear strengths measured from ATV-mounted tidal flat CPTs. This difference is attributed to the fact that the Seacalf CPTs generally encountered lesser thicknesses of sand overburden than the ATV-mounted CPTs. In areas of thicker sand overburden, the Young Bay Mud has likely consolidated to somewhat higher stresses and consequently has a higher undrained shear strength.





5.2.6 Summary of Undrained Strength

The consistency and undrained shear strength of fine-grained sediments is summarized as follows:

- **Young Bay Mud Beneath the Mole** - The Young Bay Mud beneath the Mole is typically firm to stiff with an undrained shear strength that increases with depth. The undrained shear strength typically ranges from 20 to 40 kPa at the top of the layer, and increases to about 35 to 60 kPa at the base of the layer. Where the paleochannel exists, the clay increases in strength with additional depth, albeit at a more gradual rate of increase. At the thalweg of the paleochannel, the interpreted undrained shear strength is 43 to 60 kPa.
- **Historical Bay Mud and Young Bay Mud Beneath the Adjacent Marine Areas** - The historical mud is typically very soft to soft with undrained shear strength (interpreted from CPT tip resistances) ranging from less than 5 to 20 kPa. As discussed above, the undrained shear strength of the Young Bay Mud beneath the tidal flat and the marine areas to the west of the Mole is less than the Young Bay Mud underlying the fill. The CPT data suggests that the undrained strength of the Young Bay Mud beneath these adjacent marine areas increases with depth from 15 to 35 kPa at the top of the layer to about 40 to 75 kPa at the bottom of the layer.
- **Clay Layers Within the Merritt-Posey-San Antonio Formations** - Clay layers within the MPSA Formations typically are stiff to very stiff sandy clay and clay with undrained shear strengths typically between about 60 and 120 kPa.
- **Old Bay Mud/Upper Alameda Marine Sequence** - These marine clays are generally very stiff to hard with shear strengths increasing from approximately 80 to 150 kPa near the top of the sequence to about 150 to 200 kPa at El. -69.5 meters where Boring 98-51 terminated. The adjacent marine Boring 98-44 reached the base of the OBM/UAM sequence at approximately El. -76.8 meters where the undrained shear strengths ranged from 144 to 215 kPa. The sequence includes several crust layers, generally including one at the top, where the undrained shear strengths are at least 25 to 70 kPa higher than the adjacent layers.

5.2.7 Effect of Cyclic Loading on Undrained Shear Strength of Young Bay Mud

A series of six pairs of simple shear tests (UC Berkeley, 1999 [reproduced in Volume 4]) were conducted to evaluate the effect of cyclic loading on the undrained shear strength of the Young Bay Mud. The test results are summarized in Table 5.2.

The test results suggest that for the range of cyclic shear stress amplitudes tested (single amplitude shear strains of from 1 to 3 percent), the ratio of the undrained shear strength after 25 cycles of load to the undrained shear strength prior to cyclic loading ranges from about 85 to 100



percent. The results did, however, show a significant degradation in the low strain shear modulus.

5.2.8 Strain Rate Effects

The undrained shear strength is affected by the rate of strain. Tests at different strain rates were conducted as part of the marine site characterization (Fugro-EM, 2001d). Those test results suggest that the undrained shear strength of the clay sediments beneath the project site generally increases by about 10 to 12 percent per log cycle of strain rate.

Idriss (1991) studied the stress-strain-strength behavior of clays under earthquake and wave loading conditions to understand strain-rate effects. Two frequencies (1 Hz and 0.05 Hz) were used to conduct cyclic loading in a laboratory. As reported in Idriss (1991), the cyclic shear stress with a 1 Hz frequency was about 68 percent higher than the static shear stress at 2-percent shear strain for Icy Bay Mud from Alaska. Even with a 0.05 Hz frequency, the tests show a 46-percent increase over the static shear stress.

Based on those studies, it is believed that strain-rate effects are inherent in the University of California at Berkeley cyclic simple shear tests because they were conducted with a loading frequency of 0.2 Hz. However, only a limited number of cyclic tests were conducted for the Young Bay Mud; thus, it is not possible to quantitatively assess the strain-rate effects from the University of California at Berkeley set of tests. A 40-percent increase from the static shear strength is proposed to account for strain-rate effects in the Young Bay Mud for the purpose of analysis of ground stability and lateral spreading issues.

5.2.9 Sensitivity and ϵ_{50}

Soil Sensitivity. Soil sensitivity is defined as the ratio of the undrained shear strength of an undisturbed sample to the shear strength of a remolded sample. This ratio is important in the prediction of soil resistance to pile driving. The ratio also can be used to evaluate possible disturbance of abnormally low values of undrained shear strength.

The sensitivities calculated from laboratory tests on samples from the Mole exploration borings are shown on Plate 5.17. The sensitivity is typically between about 2 and 4 in the Young Bay Mud and the upper 10 meters of the Old Bay Mud/Upper Alameda Marine sequence. Occasional lower sensitivities are inferred to suggest that the measurements of undisturbed shear strength have been adversely affected by sample disturbance. Most of those values were obtained in tests conducted on driven samples. Occasional higher sensitivities may be spurious, due to the presence of sand seams and shells in vane shear test specimens.

A range of 1.5 to 2 is more typical of the sensitivity of the clay layers in the Merritt-Posey-San Antonio Formations and the lower portion of the Old Bay Mud/Upper Alameda Marine sequence.





Sensitivity data also were analyzed from the remote vane testing conducted in the foundation borings (98-51 to 98-60). Sensitivity was taken as the peak undrained shear strength divided by the residual strengths (remote vane data are provided in the Volume 2 by-boring appendices). The sensitivities from the remote vane data form a relatively narrow band and typically range from 1.5 to 2.5 in the Young Bay Mud and Old Bay Mud sequences. These sensitivity estimates are generally less than the sensitivity calculated from the laboratory data. The lower values from the remote vane data may be due to the fact that remote vane residual shear strengths are not indicative of the completely remolded state achieved in the laboratory testing.

ϵ_{50} Value. The ϵ_{50} value is defined as the strain at 50 percent of the failure stress. The ϵ_{50} strain is used in the formulation of p-y curves for prediction of the lateral load-deflection response of pile foundation. Measured ϵ_{50} strains (as shown on Plate 5.18) typically range from 0.5 to 2.5 percent.

The following table summarizes the measured ϵ_{50} strains, the comparable values typically used (when high quality test data are not available) in conjunction with the methods of API RP 2A (1993), and the recommended ϵ_{50} values for p-y analyses:

Material	Typical Measured ϵ_{50} Strains (%)	Typical API Value (%)	Suggested ϵ_{50} Strain for p-y Formulation (%)
Soft to Firm Young Bay Mud	0.6 to 2.4	1 to 2	1.0
Firm Clay Layers in Merritt-Posey-San Antonio	0.5 to 3	1	0.75
Very Stiff (Old Bay Mud) Clay	0.5 to 2.5	0.5	0.5
Very Stiff to Hard (Upper Alameda Marine) Clay	0.5 to 2	0.5	0.5

The above interpretation of the representative ϵ_{50} strains for use in p-y formulation recognizes that the sampling process can lead to a softening of the stress-strain response, but not a stiffening.

5.3 DENSITY AND CONDITION OF GRANULAR SEDIMENTS

As noted previously, granular soils were encountered: a) as artificial fill that comprises the majority of the Mole, b) as thin layers within the Young Bay Mud and paleochannel clays, c) within the Merritt-Posey-San Antonio Formations, d) as layers within the Old Bay Mud and Upper Alameda Marine sediments, and e) within the tidal flat sediments to the north of the Mole.

5.3.1 Relative Density

Relative density (D_r) is defined as the ratio of the difference of the in situ void ratio and the maximum void ratio to the difference of the maximum and minimum void ratios. Relative density is a useful parameter in determining the frictional characteristic of granular soil and is





indicative of a soil's resistance to settlement and liquefaction. An assessment of relative density of granular soils encountered in the soil borings was carried out using correlations with CPT cone tip resistance and SPT blow count measurements.

CPT Cone Tip Resistance. Relative density from the CPT measurements was estimated using an empirical expression recommended by Robertson and Campanella (1989), and is given below:

$$D_r = [1/2.41] \ln [q_c / (157 * (\sigma'_{vo})^{0.55})]$$

where: D_r = Relative density, decimal
 q_c = Cone tip resistance, kPa
 σ'_{vo} = Estimated in situ effective vertical stress, kPa

The above expression is based on studies originally performed by Schmertmann (1976) and later modified by Baldi et al. (1986). The expression has some limitations, including:

- Applies only to normally consolidated (coefficient of lateral earth pressure at rest of 0.45), moderately compressible, uncemented, unaged quartz sands with about 5 percent mica by volume.
- Is limited to an in situ effective vertical stress of about 500 kilonewtons per square meter (kN/m^2) (10 kips per square foot [ksf]).

It is noted that overburden stresses within the Upper and Lower Alameda sequences are generally in excess of the range used to generate the referenced correlation between tip resistance, overburden stress, and relative density. For the marine site characterization where cone data is available from the Alameda sequences, the expression was extrapolated for use at higher in situ effective vertical stresses.

Where appropriate, a correction has been applied to the measured q_c values to allow for fines content, using the correction procedure proposed by Robertson and Campanella (1989).

Cone tip resistance (q_c) values that have been calculated for relative densities of 15, 35, 65, 85, and 100 percent using the above expression are plotted on Plate 5.19. The average measured q_c values from field CPT data also are plotted on Plate 5.19 with the corresponding in situ σ'_{vo} , which is computed from an interpreted unit weight profile.

Blow Count Data. Relative density also can be estimated from a number of correlations with SPT blow counts in granular soils. A plot of normalized (to an overburden pressure of 95.8 kPa [1 ton per square foot]) N_1 -values versus elevation sand deposits is shown on Plate 5.20.





A simple and often used correlation was presented by Terzaghi and Peck (1967). The correlation provides an approximation of the relative density for ranges of blow counts. The correlations are provided in the table below:

SPT N-value (blows/foot)	Relative Density	D _r (%)
0 to 4	Very loose	0 to 15
4 to 10	Loose	15 to 35
10 to 30	Medium Dense	35 to 65
30 to 50	Dense	65 to 85
> 50	Very Dense	85 to 100

Another correlation between blow count and relative density was presented by Kulhawy and Mayne (1990) and is given below:

$$D_r = \left[\left((N_1)_{60} / (60 + 25 \log D_{50}) \right) \right]^{0.5}$$

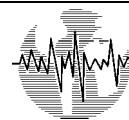
where: D_r = Relative density, decimal
 $(N_1)_{60}$ = Normalized SPT blow count with 60-percent energy correction
 D_{50} = Mean grain size, mm

In the above expression, D_{50} was taken to be 0.22 mm in the fine sands with silt and silty fine sand (which comprise the majority of the fill) and the Merritt Sand within the Merritt-Posey-San Antonio Formations. A plot of relative density versus elevation from SPT blow count data is presented on Plate 5.21.

Conclusions. Our interpretation of the typical density of the granular layers or strata are as follows:

- **Emergent Artificial Fill** - Above the water table, the fill is generally medium dense to dense with average SPT N-values ranging from 15 to 45 and measured cone tip resistances of between 6 and 29 MPa. The estimated relative density ranges from 65 to over 85 percent.
- **Submerged Hydraulic Fill** - Below the water table, the fill is generally loose to medium dense with SPT N-values ranging from 4 to 25 and measured cone tip resistances of between 1 and 10 MPa. The interpreted average N-value is about 15. The relative density is interpreted to range from 35 to 65 percent. In CPT sounding 98C-105, the fill encountered below El. -3 meters is dense to very dense. The measure cone tip resistances are over 20 MPa with an interpreted relative density of about 85 to 90 percent.





- **Tidal Flat Sediments** - The granular layers within the tidal flat sediments generally consist of a relatively thin surface layer of beach sand (up to 1 meter thick) and a locally continuous layer of sand along the northern Mole shoreline, which was likely deposited during the hydraulic placements of the lower submerged Mole fill (buried fill). The beach sand is generally loose to medium dense with relative densities ranging from 30 to 65 percent and measured cone tip resistances generally under 2.5 MPa. The buried fill is generally medium dense with relative densities varying from 40 to 70 MPa and measured cone tip resistances ranging from 2 to 5 MPa.
- **Sand Layers in Young Bay Mud** - A continuous sand layer measuring 0.3 to 1.5 meters thick is present in the Young Bay Mud between Borings 98-56 and 98-62, beginning along the eastern margin of the paleochannel. The sand layer is located approximately in the middle of the Young Bay Mud deposit at an elevation of approximately El. -10.5 meters. The CPT data indicate that this layer is dense with tip resistances ranging from 12 to 15 MPa. The relative density is interpreted to range from 65 to 70 percent.
- **Merritt-Posey-San Antonio Formations** - The Merritt Sand is generally dense to very dense with SPT N-values that range from 30 to greater than 50, and measured cone tip resistances of between 11.5 and 33.5 MPa. The interpreted relative density range is from 85 to over 100 percent.
- **Sand Layers in Old Bay Mud and Upper Alameda Marine** - Sand layers in the Old Bay Mud and Upper Alameda Marine sequences were encountered in the Mole exploration (Borings 98-51 and 98-52). The marine geotechnical site characterization (Fugro-EM, 2001d) indicates that these sand layers are generally dense to very dense with relative densities in excess of 75 percent, SPT N-values in excess of 50, and measured cone tip resistances of 20 to 45 MPa.

5.3.2 Drained Strength

Laboratory Data. Limited laboratory testing was performed to assess the frictional characteristics of the granular sediment encountered in the Mole explorations. A direct shear test was performed in the fine sand fill in Boring 98-63. The sample was obtained from a modified California liner sampler that was driven with a 63-kilogram hammer. Plots of the direct shear test are presented in the boring-specific appendices (Volume 2).

The direct shear test indicated an effective cohesion of 24 kPa and an effective friction angle of approximately 40 degrees. It is unlikely that the fill deposits are cemented and the apparent effective cohesion is interpreted to indicate non-linearity of the failure envelope with some reduction in effective friction angles at the higher confining stresses.

In addition, one isotropically consolidated-drained triaxial compression (CIDC) test was performed on a sample of fine sand fill from Boring 98-59. The sample also was obtained from





a modified California liner sample. Results are plotted in the boring-specific appendices (Volume 2A) and summarized in Table 5.3. The CIDC test indicated an effective cohesion of 10 (0.2 ksf) and an effective friction angle of approximately 47 degrees.

To assist in the interpretation of the drained strength of granular sediments, a total of 32 CIDC tests were performed on samples recovered from the 1998 marine borings. The test specimens included: 16 samples from sand layers in the Young Bay Mud, 7 samples from the Merritt-Posey-San Antonio Formations, 9 samples from sand layers in the Old Bay Mud/Upper Alameda Marine sequence, and 5 samples from the Lower Alameda Alluvial sequence. The test specimens were generally obtained from 54-mm-diameter tube samples driven with a 79-kilogram downhole hammer. Other specimens were obtained from 72-mm-diameter push samples.

A summary of the CIDC test results along with the results of classification tests performed on the specimen are presented in the Final Marine Geotechnical Site Characterization report (Fugro-EM, 2001d). Plots of consolidated-drained triaxial test results are presented in the boring-specific appendices.

Effective cohesion ranging from approximately 10 to as high as 150 kPa were interpreted from CIDC test results performed on sand samples from the Young Bay Mud, Merritt-Posey-San Antonio Formations, and Upper Alameda Marine sediments. While it is possible that these sediments may be slightly cemented, the apparent effective cohesion is interpreted to indicate non-linearity of the failure envelope with some reduction in effective friction angle at the higher confining stresses. Interpreted effective friction angle values were calculated by assuming no effective cohesion and considering only the failure stresses at the confinement that most closely approximated the in situ stresses. The laboratory data on marine boring samples and CPT test data indicate that the interpreted effective friction angle ranges from 34 to 40 in the sand layers within the Young Bay Mud, from 39 to 45 degrees in the Merritt-Posey-San Antonio Formations, and from 35 to 42 degrees in the Lower Alameda Alluvial sediments.

CPT Cone Tip Resistance. To supplement the laboratory test data, effective friction angles in the granular strata also were estimated using in situ CPT q_c data and the empirical expression recommended by Kulhawy and Mayne (1990):

$$\phi' = 17.6 + 11.0 \log \left[\frac{q_c / p_a}{\left(\sigma'_{vo} / p_a \right)^{0.5}} \right]$$

where: ϕ' = Effective friction angle
 q_c = Measured cone tip resistance





$$\begin{aligned}\sigma'_{vo} &= \text{Effective overburden pressure} \\ p_a &= \text{Atmospheric pressure}\end{aligned}$$

Cone tip resistance (q_c) values were calculated for ϕ' of 35°, 37.5°, 40°, 42.5°, and 45°, using the above expression, and are plotted versus effective vertical stress on Plate 5.22 along with the measured cone tip resistances (corrected for fines as described above).

Conclusions. Our interpretation of the typical frictional characteristics for those granular layers or strata are as follows:

- **Artificial Fill** - Above the water table, the effective friction angle of the fill is interpreted to range from approximately 40 to 45 degrees. Below the water table, the effective friction angle is interpreted to range from approximately 36 to 47 degrees. In CPT sounding 98C-105, the effective friction angle of the fill encountered below El. -3 meters is interpreted to be about 42 degrees.
- **Merritt-Posey-San Antonio Formations** - The effective friction angle of the Merritt Sand interpreted from the CPT data ranges from approximately 40 to 45 degrees, which is in general agreement with the data from the marine investigation.

5.4 CONSOLIDATION AND COMPRESSIBILITY PROPERTIES OF SEDIMENTS

5.4.1 State of Consolidation

Basis of Interpretation. The stress history of a soil formation can be evaluated by comparing the preconsolidation stresses with the existing overburden stresses. Preconsolidation stresses were estimated from 67 incremental consolidation tests. Those tests were performed (primarily) on relatively undisturbed SAVE tube samples and samples from Shelby tubes that were extruded in the field and stored in plastic quarts. Consolidation test results are presented in the boring-specific appendices (Volume 2). Table 5.4 summarizes the interpretations made from those tests and provides data from index tests performed on those samples.

The preconsolidation pressures (maximum past pressures) are interpreted from the consolidation test results using the Casagrande (1936) procedure and the Work Per Unit Volume Method proposed by Becker et al. (1987). Preconsolidation pressures also were estimated from CPT data using the following empirical correlation (Kulhawy and Mayne, 1990):

$$\sigma'_p = 0.33 (q_c - \sigma'_{vo})$$

where: σ'_p = Preconsolidation pressure
 q_c = Cone tip resistance
 σ'_{vo} = Effective overburden pressure





Preconsolidation data from the laboratory and CPT data from the land exploration are presented on Plate 5.23. The data are plotted versus effective vertical stress and show lines of constant OCR (which is the ratio of the preconsolidation pressure to the in situ effective overburden pressure). OCRs for all the laboratory data are plotted versus elevation on Plate 5.26. Similar data from the tidal flat CPTs and marine Borings 98-39 and 98-44 are provided on Plates 5.24 and 5.25. The preconsolidation stresses interpreted from CPT data generally agree favorably with those interpreted from the consolidation tests and can be used to extrapolate the state of consolidation between consolidation tests.

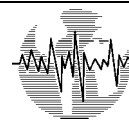
Interpretation. Out interpretation of the typical state of consolidation for the sediment underlying and adjacent to the Mole are as follows:

- **Young Bay Mud** - The laboratory test results indicate that the Young Bay Mud is generally normally consolidated with respect to the stresses imposed by the 1930s fill. The interpreted OCR values in the Young Bay Mud generally range from about 0.9 to 1.3 in the areas outside of the paleochannel. In the deeper portions of the paleochannel that cross beneath the Mole, the OCR of the lower portion of the Young Bay Mud is more typically about 0.8 to 1.1, which suggests that the deeper Young Bay Mud present within the lower section of the paleochannel may be slightly underconsolidated. This would indicate that these areas of the Mole may still be experiencing additional settlement due to the weight of the existing Mole fill.

Beneath the western jughandle, the preconsolidation stresses interpreted from CPT sounding 98C-102 suggest that the Young Bay Mud sediments underlying that newer fill are underconsolidated. At that location, an OCR of about 0.6 to 0.8 is interpreted. The lower OCR agrees with the lower shear strength measurements from adjacent Boring 98-55 and may be due to relatively more recent filling of the jughandle area. The consolidation test run on a Young Bay Mud sample from Boring 98-55 indicates an OCR of 1.4, which matches the preconsolidation stress in the CPT sounding 98C-102 data at the same elevation. Interpreted CPT data (98C-104) and laboratory test data indicate that the Young Bay Mud underlying the eastern jughandle may also be slightly underconsolidated with an OCR ranging from 0.8 to 1.1.

- **Young Bay Mud Beneath the Tidal Flat** - Offshore from the Mole, the consolidation data from adjacent marine Borings 98-39 and 98-44 suggest that the Young Bay Mud is normally consolidated with an OCR of around 1. This is consistent with the data from the rest of the characterization where the OCR in the Young Bay Mud typically ranges from 0.9 to 2.0. The interpretation of the OCR from the ATV-mounted CPTs on the tidal flat indicate that the Young Bay Mud underlying the tidal flat is normally to slightly overconsolidated with OCRs typically decreasing from 2 to 3 at the top of the sequence to approximately 1.0 to 1.8 at the bottom of the sequence (see Plate 5.24). The higher OCR, however, does not necessarily represent overconsolidation. Due to the relatively low overburden





pressures at the top of the Young Bay Mud sequence, the estimated past pressures are only on the order of 40 to 80 kPa in excess of the estimated vertical overburden pressure.

- **Merritt-Posey-San Antonio Formations and Old Bay Mud/Upper Alameda Sequence** - The clay layers within the Merritt-Posey-San Antonio Formations, the Old Bay Mud, and the Upper Alameda Marine sediments are generally overconsolidated. Beneath the Mole, the OCR of the clay layers in the Merritt-Posey-San Antonio (MPSA) Formations is typically between about 1.2 and 2.5. The interpreted OCR typically ranges from about 2.5 to 3.5 in the various crust layers within the Old Bay Mud and top of the Upper Alameda Marine sediments. Below the crust layers, the interpreted OCR of the Old Bay Mud and top of the Upper Alameda Marine sediments typically ranges from about 1.3 to 1.8. The CPT data also show that the preconsolidation stresses in the crustal zones of the Old Bay Mud sequence are up to 500 kPa greater than the preconsolidation pressures in the rest of the sequence.

The preconsolidation pressures in the MPSA, Old Bay Mud, and Upper Alameda Marine interpreted for the sediments beneath the Mole are similar to the values interpreted from the marine borings. The OCRs of those sediments, however, are lower beneath the Mole than beneath the San Francisco Bay farther to the west. The lower OCR is attributable to the additional stresses imposed by the weight of the Mole fill. Because those additional stresses likely did not exceed the preconsolidation pressure of the older deposits, it is logical to assume that the majority of the settlement that occurred below the Mole was due to consolidation of the Young Bay Mud.

- **Clay Layers Within the Lower Alameda Alluvial Sediments** - The marine geotechnical site characterization (Fugro-EM, 2001d) indicated that the OCRs tended to reduce with depth and are on the order of 1 to 2 at the base of the Lower Alameda Alluvial sequence. Although the majority of the sediments appear to have OCRs on the order of 2 to 3, overconsolidated crustal zones with OCRs on the order of 3 to 5 are common within these sequences. The relatively low OCRs at greater depths are not strictly indicative of normal or light overconsolidation, since the interpreted maximum past pressures are on the order of 300 to 800 kPa higher than the estimated overburden stresses.

5.4.2 Compressibility

Undisturbed Samples. The compression (C_{ec}) and recompression (C_{er}) ratios interpreted from consolidation tests are summarized on Table 5.4 and plotted on Plate 5.27.

The compression ratios for the primarily fat clays of the Young Bay Mud sequence range from approximately 0.12 to 0.30. The majority of the data for the Young Bay Mud are between





approximately 0.14 and 0.25. In the Old Bay Mud and Upper Alameda Marine sequences, the compression ratios for the primarily fat clays range from approximately 0.12 to 0.35.

Recompression ratios were estimated for tests on samples that included an intermediate rebound/recompression loop. The recompression ratios are generally between about 0.01 and 0.04.

Remolded Consolidation Tests. Two series of incremental consolidation tests were conducted on samples that were remolded at their natural water content and at their natural water content plus 5 to 8 percent. Plate 5.28 shows the results of a series of tests performed on Young Bay Mud samples taken from Boring 98-73, where a series of four incremental consolidation tests were run on samples between 7.9 and 9.4 meters. Three tests were run on a sample obtained from a driven modified California sampler, one from the extruded sample, and two remolded tests at water contents of 40 percent (natural water content) and 48 percent. The fourth test was run on a relatively undisturbed push tube sample. The results on Plate 5.28, show the effects of increasing sample disturbance and illustrates the effects of remolding on the compressibility of the Young Bay Mud. At a load of 120 kPa (near the preconsolidation stress), the driven sample and the sample remolded at a water content of 40 percent strained approximately 200 to 250 percent more than the relatively undisturbed sample. The sample remolded at a water content of 48 percent strained approximately 500 percent more than the relatively undisturbed sample. The results of the remolded consolidation tests are summarized in Table 5.4.

5.4.3 Coefficient of Consolidation

Vertical Samples. The coefficient of consolidation (c_v) was estimated from incremental consolidation tests. The coefficient of consolidation is generally highest in the overconsolidated range prior to the load reaching the preconsolidation pressure, and then decreases as the loading reaches and exceeds the preconsolidation pressure. The measured c_v values at the interpreted effective overburden pressure (which are typically between the c_v values in the overconsolidated range and those in the normally consolidated range) are plotted on Plate 5.29.

In general, the c_v values ranged from approximately 1 to 40 square meters per year (m^2/yr), although some values over 100 m^2/yr were calculated at stresses lower than the interpreted preconsolidation stress and along the intermediate reloading loops. At the effective overburden stress, approximately two-thirds of the c_v values are between 1 and 10 m^2/yr . In the normally consolidated range, at loads greater than the preconsolidation stress, the c_v data range from approximately 1 to 15 m^2/yr , but are typically less than 5 m^2/yr .

Multi-Oriented Samples. For Phase 2 of the marine geotechnical site characterization program (Fugro-EM, 2001d), a series of 14 multi-orientation consolidation tests were performed. In each series of tests, either two or three consolidation tests were performed from the same sample with the only variable being the orientation of the trimmed sample. In the two-test series,





the central axis of the specimen was either parallel or perpendicular to the axis of the boring (i.e., the specimen's orientation was vertical or horizontal, respectively). In the three-test series, an additional specimen with a 45-degree orientation also was tested.

The multi-orientation testing indicated that in the normally consolidated range of loading, the ratio of the horizontal c_v to the vertical c_v ranged between about 1 and 5 with an average value of approximately 2. The ratio of the 45-degree c_v to the vertical c_v ranged between 0.5 and 2.4 with an average of 1.1, indicating that the change in c_v with specimen orientation is relatively minor until there is a 90-degree change in orientation. This is consistent with the interpretation that the differences in c_v are primarily attributable to minor layering of the sediments.

Radial Consolidation Tests. Radial consolidation tests were performed by the University of California at Berkeley (1999) on conventional Shelby tube samples of the Young Bay Mud to evaluate the time rate of radial consolidation under applied isotropic stress increments with radial drainage. The procedures, method of interpretation, and results of these tests are discussed in Volume 4.

Two samples from depths of approximately 10 and 12 meters were tested under both convergent flow (towards the sample) and divergent flow (outward from the sample) conditions. The rates of consolidation for convergent flow and divergent flow were 1.8 and 3.6 m^2/yr and 0.3 and 1 m^2/yr , respectively. These c_v values are similar to the horizontal c_v measured in the multi-orientation consolidation tests discussed above. The lower rates from divergent flow were subsequently discounted due to technical difficulties encountered in the laboratory in maintaining a free-draining boundary on the circumference of the soil sample. As a result, the higher rates for convergent flow (with an average rate of about 2.7 m^2/yr) are considered more representative of horizontal radial flow conditions, such as those that would occur around a drainage well or wick drain.

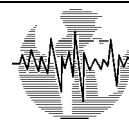
5.5 SHEAR WAVE VELOCITY OF SEDIMENTS

Downhole shear wave velocities (V_s) were measured in five seismic CPTs (98C-17, 98C-18, 98C-101, 98C-102, and 98C-109) on the Mole and in two seismic CPTs (99C-13 and 99C-15) on the tidal flat to the north of the Mole. The measured V_s data are plotted versus elevation on Plate 5.30 and are also shown on the CPT logs in Volume 3. Only a limited amount of shear wave velocity data were obtained in the Mole fill due to the necessity of predrilling through the rubble in the fill.

The V_s data as measured in the different soil layers are summarized below:

- **Mole Fill Below El. 0** - Variable V_s between about 150 and 280 meters per second (m/sec).





- **Young Bay Mud Beneath Mole** - Vs typically between about 130 and 180 m/sec, with locally higher measurements at the top of the Young Bay Mud in some locations and in the bottom of the paleochannel in others.
- **Young Bay Mud Beneath Tidal Flat** - Vs data from two seismic CPTs (98C-13 and 98C-15) indicate that Vs is typically between about 100 and 160 m/sec, with lower measurements at the top of the sequence ranging from 60 to 80 m/sec.
- **Merritt-Posey-San Antonio Formations** - Variable Vs between 140 and 350 m/sec due to layered nature of sequence. In primarily clay zones, the Vs is typically less than 230 m/sec, while in dense sand layers the Vs is typically in excess of 260 m/sec.
- **Old Bay Mud** - In the Old Bay Mud, the Vs measurements tend to increase with depth. At the top of the layer (about El. -20 meters), the Vs typically ranges from about 180 to 230 m/sec. At about El. -35 meters, the Vs measurements are typically about 200 to 250 m/sec. Vs values of 280 to 320 m/sec were obtained in crust layers.

The shear wave velocities, obtained from the seismic CPTs, generally correlate favorably with the different strata identified from the CPT and boring explorations.

The Vs values in the Young Bay Mud under the Mole are slightly higher than those found in the marine investigation. This is due to the Young Bay Mud under the Mole being more consolidated due to the overlying fill and the higher silt content in the upper several meters of the sequence. The maximum Vs values in the Merritt Sand also are slightly higher than those from the marine investigation (Fugro-EM, 2001d). The Vs values in Old Bay Mud generally fall within the range of values found in the marine investigation.

Shear wave velocity data also are available from a previous Caltrans boring (B-1) located near the western end of the Mole. Those Vs data were collected in the Merritt Sand and underlying Old Bay Mud. No data were available in the Young Bay Mud. The Vs for the Merritt Sand was about 305 to 460 m/sec, which compares well with the seismic CPT results. Measured Vs values in the Old Bay Mud ranged from about 180 to 335 m/sec and generally increased with depth.

5.6 CYCLIC PROPERTIES OF YOUNG BAY MUD

5.6.1 Test on Mole Boring Samples

A total of six soil samples extruded from Shelby tubes collected within the Young Bay Mud were tested to investigate the stress-strain behavior under large cyclic strain and the post-earthquake properties at the University of California at Berkeley. The purpose of this program was to understand the stress-strain behaviors before and after an earthquake. One of the specimens was sheared monotonically from a virgin state, while the other was cyclically loaded to a specified strain amplitude and number of cycles and then monotonically sheared without





allowing the specimen to reconsolidate. The results of those tests are presented in the University of California at Berkeley report (1999) reproduced in Volume 4.

5.6.2 Tests on Phase 1 Marine Boring Samples

In addition to the dynamic tests conducted at UC Berkeley on selected SAVE tube samples from the Mole borings, dynamic tests were conducted on Young Bay Mud samples during the Phase 1 preliminary site investigation phase. During Phase 1, dynamic tests were conducted on both Young Bay Mud and Old Bay Mud samples at Fugro's Houston laboratory and at the University of Texas at Austin. Those tests included Resonant Column, Torsional Shear, and Cyclic Simple Shear tests. Our interpretation of the test results is provided in the Final Marine Geotechnical Site Characterization report (Fugro-EM, 2001d). The test results are provided in reports by Fugro South (1998) and the University of Texas at Austin (1998), which are reproduced in Volume 4 of the Phase 1 Subcontractor reports (Fugro-EM, 1998).





Boring Number	98-57			98-64			98-67		
Sample Number	20A	20B	20C	13A	13B	13C	12A	12B	12C
Penetration									
meters	16.9	17.1	17.2	11.0	10.9	10.7	11.1	11.0	10.8
feet	55.6	56.0	56.4	36.2	35.6	35.2	36.5	36.0	35.6
Unit	YBM	YBM	YBM	YBM	YBM	YBM	YBM	YBM	YBM
Moisture Content (%)									
Initial, W_0	53	49	53	45	44	45	52	46	45
Final, W_f	50	38	37	42	39	33	47	38	33
Atterberg Limits									
Liquid Limit, LL	57	57	57	43	43	43	53	53	53
Plastic Limit, PL	22	22	22	21	21	21	23	23	23
Initial Total Unit Weight, $\gamma_{t,0}$									
kN/m ³	16.7	16.8	16.5	17.4	17.4	17.4	16.8	17.4	17.4
pcf	107	107	105	111	111	111	107	111	111
Interpreted In Situ Preconsolidation Stress, σ'_p									
kPa (Casagrande Method, 1936)	158	158	158	144	144	144	153	153	153
ksf	3.3	3.3	3.3	3.0	3.0	3.0	3.2	3.2	3.2
Interpreted In Situ Preconsolidation Stress, σ'_p									
kPa (Work per Unit Volume, Becker et al, 1987)	148	148	148	141	141	141	158	158	158
ksf	3.1	3.1	3.1	3.0	3.0	3.0	3.3	3.3	3.3
Estimated In Situ Effective Vertical Stress, σ'_{v0}									
kPa	182	182	182	137	137	137	141	141	141
ksf	3.8	3.8	3.8	2.9	2.9	2.9	2.9	2.9	2.9
Estimated In Situ Overconsolidation Ratio, OCR									
OCR - Casagrande Method	0.9	0.9	0.9	1.0	1.0	1.0	1.1	1.1	1.1
OCR - Becker Method	0.8	0.8	0.8	1.0	1.0	1.0	1.1	1.1	1.1
Estimated In Situ Coeff. of Horizontal Stress (k_0)									
	0.4	0.4	0.4	0.5	0.5	0.5	0.5	0.5	0.5
Pre-Shear Effective Stress, σ'_{vc}									
kPa	177	383	766	134	240	479	134	240	479
ksf	3.7	8.0	16.0	2.8	5.0	10.0	2.8	5.0	10.0
Measured Undrained Shear Strength (S_u)									
kPa	87	145	262	78	109	179	71	102	181
ksf	1.8	3.0	5.5	1.6	2.3	3.7	1.5	2.1	3.8
Failure Strain, ϵ_f (%)									
	2.9	4.8	6.2	3.8	4.7	6.5	3.5	7.3	6.3
Undrained Strength Ratio									
S_u/σ'_{vc}	0.49	0.38	0.34	0.59	0.46	0.37	0.53	0.43	0.38
S_u/σ'_m [$\sigma'_m = (\sigma'_{vc} + 2\sigma'_{hc})/3$]	1.47	1.14	1.03	1.76	1.37	1.12	1.58	1.28	1.13
Undrained Shear Strength at In Situ Stresses									
kPa	89	69	62	80	62	51	74	60	53
ksf	1.9	1.4	1.3	1.7	1.3	1.1	1.5	1.3	1.1
Effective Cohesion									
kPa	13			12			15		
ksf	0.3			0.3			0.3		
Estimated Effective Friction Angle (ϕ') [degrees]									
	30			33			32		

**SUMMARY RESULTS OF
CONSOLIDATED-UNDRAINED TRIAXIAL COMPRESSION TESTING
Oakland Shore Approach
SFOBB East Span Seismic Safety Project**

TABLE 5.1





Boring No.	Sample Pair	Depth (m)	Static Shear Strength (Pre-Cyclic) (kPa)	Cyclic Strain (%)	Initial Cyclic Stress (kPa)	Final Cyclic Stress @ 25th Cycle (kPa)	Static Shear Strength (Post Cyclic) (kPa)
98-55	1	10.98	45	1	40	33	42
98-52	2	10.98	50	2	52	33	50
98-59	3	9.15	47	1	45	33	56
98-60	4	10.98	48	1.5	45	33	48
98-56	5	18.60	72	3	73	45	60
98-62	6	12.50	51	3	52	33	47

SUMMARY OF CYCLIC SHEAR TESTING PROGRAM ON YOUNG BAY MUD
Oakland Shore Approach
SFOBB East Span Seismic Safety Project

TABLE 5.2





Boring Number	98-59
Sample Number	4
Penetration	
meters	6.4
feet	21.0
Strata Designation	Artificial Fill
Moisture Content (%)	
Initial, W_o	22
Gradation	
-200 (%)	8
D_{50} (mm)	0.23*
Wet Unit Weight	
kN/m^3	20.2
pcf	128
Dry Unit Weight	
kN/m^3	16.6
pcf	105
Effective Cohesion	
kPa	10
ksf	0.2
ϕ' (degrees)	47
In Situ Effective Overburden	
kPa	97
ksf	2.0
Test Confining Stresses	
kPa	28
ksf	0.6
kPa	55
ksf	1.2
kPa	110
ksf	2.3
ϕ' (degrees) -at σ'_{vo} & $c' = 0$	48

SUMMARY OF CONSOLIDATED-DRAINED TRIAXIAL TEST RESULTS
Boring 98-59
Oakland Shore Approach
SFOBB East Span Seismic Safety Project

TABLE 5.3





Boring Number	98-51	98-51	98-51	98-51	98-51	98-51	98-51	98-52	98-53	98-53
Sample Number	10	24	32	39	47	54	62	36	12	28
Penetration										
meters	10.9	24.8	33.8	42.9	49.2	61.5	70.3	35.5	11.2	29.5
feet	35.9	81.4	111.0	140.6	161.3	201.6	230.7	116.4	36.6	96.6
Unit	YBM	YBM	OBM/UAM	OBM/UAM	OBM/UAM	OBM/UAM	OBM/UAM	OBM/UAM	YBM	OBM/UAM
Moisture Content (%)										
Initial, W_0	49	46	46	26	38	48	42	44	45	57
Final, W_f	31	37	39	22	36	46	42	35	32	46
Atterberg Limits										
Liquid Limit, LL	50	66	66	42	76	79	68	64	48	77
Plastic Limit, PL	21	25	27	19	27	27	27	24	20	24
Initial Total Unit Weight, $\gamma_{t,0}$										
kN/m ³	17.1	17.3	17.3	19.3	18.3	17.3	17.7	17.7	17.5	16.6
pcf	109	110	110	123	116	110	113	113	111	106
Void Ratio										
Initial, e_0	1.35	1.28	1.28	0.77	1.03	1.31	1.17	1.19	1.23	1.55
Final, e_f	0.86	1.00	1.04	0.59	0.97	1.24	1.15	0.94	0.89	1.25
Interpreted Preconsolidation Pressure, σ'_p										
kPa (Casagrande Method, 1936)	139	407	623	575	1150	719	814	503	168	479
ksf	2.9	8.5	13.0	12.0	24.0	15.0	17.0	10.5	3.5	10.0
Interpreted Preconsolidation Pressure, σ'_p										
kPa (Work per Unit Volume, Becker et al, 1987)	134	383	584	589	1178	671	790	489	168	450
ksf	2.8	8.0	12.2	12.3	24.6	14.0	16.5	10.2	3.5	9.4
Estimated Effective Vertical Stress, σ'_{v0}										
kPa	109	243	321	399	458	560	630	321	145	301
ksf	2.3	5.1	6.7	8.3	9.6	11.7	13.2	6.7	3.0	6.3
Overconsolidation, OCR										
OCR - Casagrande Method	1.3	1.7	1.9	1.4	2.5	1.3	1.3	1.6	1.2	1.6
OCR - Becker Method	1.2	1.6	1.8	1.5	2.6	1.2	1.3	1.5	1.2	1.5
Compression Index, C_c										
$C_{c,c}$	0.56	0.64	0.77	0.26	0.65	0.73	0.66	0.65	0.47	0.48
$C_{c,s}$	0.24	0.28	0.34	0.15	0.32	0.32	0.30	0.30	0.21	0.19
Swelling Index, C_s										
$C_{e,s}$	0.08	0.13	0.12	0.05	0.13	0.16	0.15	0.12	0.05	0.14
$C_{e,r}$	0.03	0.06	0.05	0.03	0.06	0.07	0.07	0.05	0.02	0.06
Recompression Index, C_r										
$C_{e,r}$	-	-	-	-	-	-	-	-	0.06	-
$C_{e,r}$	-	-	-	-	-	-	-	-	0.03	-
Coefficient of Consolidation, C_v (at σ'_{v0})										
m ² /year (square root of time method)	6.1	13.0	37.0	97.6	42.0	6.3	5.3	9.6	12.9	9.2
ft ² /year (square root of time method)	65.67	139.94	398.30	1050.66	452.13	67.82	57.05	103.34	138.87	99.04

* Sample trimmed at 45 degree angle, representing in situ loading at 45 degree angle.

** Sample trimmed vertically, representing horizontal in situ loading.

sample remolded at natural water content

sample remolded at natural water content plus 5 to 8%

SUMMARY OF CONSOLIDATION TEST RESULTS

Oakland Shore Approach

SFOBB East Span Seismic Safety Project

TABLE 5.4a



Boring Number	98-54	98-54	98-54	98-54	98-55	98-55	98-55	98-55	98-55	98-55
Sample Number	13a**	13b	26	35	17	26	39	47	55	63
Penetration										
meters	12.9	12.9	26.3	35.5	14.0	21.5	34.0	43.1	52.3	61.4
feet	42.2	42.4	86.4	116.4	46.0	70.5	111.4	141.5	171.5	201.5
Unit	YBM	YBM	OBM/UAM	OBM/UAM	YBM	MPSA	OBM/UAM	OBM/UAM	OBM/UAM	OBM/UAM
Moisture Content (%)										
Initial, W_0	54	55	23	48	36	44	48	31	16	43
Final, W_f	38	43	21	18	36	32	38	25	14	34
Atterberg Limits										
Liquid Limit, LL	59	59	37	48	71	50	63	51	31	68
Plastic Limit, PL	22	22	13	18	29	22	25	21	13	25
Initial Total Unit Weight, $\gamma_{t,0}$										
kN/m ³	16.7	16.7	20.0	17.9	17.1	15.9	17.2	18.5	20.6	17.6
pcf	106	106	127	114	109	101	110	118	131	112
Void Ratio										
Initial, e_0	1.49	1.51	0.65	1.08	1.13	1.20	1.32	0.91	0.51	1.19
Final, e_f	1.02	1.16	0.58	0.71	0.59	0.86	1.02	0.68	0.38	0.93
Interpreted Preconsolidation Pressure, σ'_p										
kPa (Casagrande Method, 1936)	168	172	685	316	196	378	503	1054	790	719
ksf	3.5	3.6	14.3	6.6	4.1	7.9	10.5	22.0	16.5	15.0
Interpreted Preconsolidation Pressure, σ'_p										
kPa (Work per Unit Volume, Becker et al, 1987)	153	172	651	311	206	354	493	1059	771	699
ksf	3.2	3.6	13.6	6.5	4.3	7.4	10.3	22.1	16.1	14.6
Estimated Effective Vertical Stress, σ'_{v0}										
kPa	151	151	265	331	139	201	297	374	455	522
ksf	3.1	3.1	5.5	6.9	2.9	4.2	6.2	7.8	9.5	10.9
Overconsolidation, OCR										
OCR - Casagrande Method	1.1	1.1	2.6	1.0	1.4	1.9	1.7	2.8	1.7	1.4
OCR - Becker Method	1.0	1.1	2.5	0.9	1.5	1.8	1.7	2.8	1.7	1.3
Compression Index, C_c										
$C_{e,c}$	0.57	0.75	0.21	0.41	0.62	0.44	0.70	0.30	0.16	0.47
	0.23	0.30	0.13	0.20	0.29	0.20	0.30	0.16	0.10	0.21
Swelling Index, C_s										
$C_{e,s}$	0.07	0.08	0.06	0.08	0.09	0.05	0.12	0.06	0.05	0.13
	0.03	0.03	0.04	0.04	0.04	0.02	0.05	0.03	0.04	0.06
Recompression Index, C_r										
$C_{e,r}$	-	-	-	-	0.06	-	-	-	-	-
	-	-	-	-	0.03	-	-	-	-	-
Coefficient of Consolidation, C_v (at σ'_{v0})										
m ² /year (square root of time method)	5.4	12.0	19.2	7.1	2.5	14.8	20.5	47.0	30.8	2.1
ft ² /year (square root of time method)	58.13	129.18	206.69	76.43	26.91	159.32	220.68	505.95	331.56	22.61

* Sample trimmed at 45 degree angle, representing in situ loading at 45 degree angle.

** Sample trimmed vertically, representing horizontal in situ loading.

sample remolded at natural water content

sample remolded at natural water content plus 5 to 8%

SUMMARY OF CONSOLIDATION TEST RESULTS

Oakland Shore Approach

SFOBB East Span Seismic Safety Project

TABLE 5.4b



Boring Number	98-56	98-56	98-56	98-57	98-57	98-57	98-57	98-58	98-58	98-58
Sample Number	17b**	17a	47	20	30	38	46	11	17	36
Penetration										
meters	13.8	13.9	38.6	17.2	28.1	37.0	46.0	12.5	16.9	32.5
feet	45.4	45.5	126.8	56.5	92.2	121.4	151.0	41.0	55.5	106.5
Unit	YBM	YBM	OBM/UAM	YBM	OBM/UAM	OBM/UAM	OBM/UAM	YBM	YBM	OBM/UAM
Moisture Content (%)										
Initial, W_0	53	59	28	52	49	20	52	47	53	52
Final, W_f	36	41	24	36	39	17	49	41	28	43
Atterberg Limits										
Liquid Limit, LL	55	55	50	57	66	44	82	59	70	72
Plastic Limit, PL	24	24	19	22	25	61	25	28	28	23
Initial Total Unit Weight, $\gamma_{t,0}$										
kN/m ³	16.9	16.6	19.2	16.7	17.1	20.4	16.8	17.0	16.8	17.0
pcf	108	106	123	107	109	130	107	108	107	108
Void Ratio										
Initial, e_0	1.43	1.57	0.79	1.45	1.34	0.59	1.43	1.28	1.41	1.42
Final, e_f	0.98	1.08	0.65	0.97	1.04	0.48	1.32	0.61	0.92	1.17
Interpreted Preconsolidation Pressure, σ'_p										
kPa (Casagrande Method, 1936)	148	177	766	158	378	671	719	163	153	527
ksf	3.1	3.7	16.0	3.3	7.9	14.0	15.0	3.4	3.2	11.0
Interpreted Preconsolidation Pressure, σ'_p										
kPa (Work per Unit Volume, Becker et al, 1987)	144	180	790	148	364	623	675	172	163	503
ksf	3.0	3.8	16.5	3.1	7.6	13.0	14.1	3.6	3.4	10.5
Estimated Effective Vertical Stress, σ'_{v0}										
kPa	158	158	349	182	283	354	429	153	188	325
ksf	3.3	3.3	7.3	3.8	5.9	7.4	9.0	3.2	3.9	6.8
Overconsolidation, OCR										
OCR - Casagrande Method	0.9	1.1	2.2	0.9	1.3	1.9	1.7	1.1	0.8	1.6
OCR - Becker Method	0.9	1.1	2.3	0.8	1.3	1.8	1.6	1.1	0.9	1.5
Compression Index, C_c										
$C_{c,c}$	0.51	0.69	0.35	0.58	0.67	0.20	0.95	0.55	0.51	0.87
$C_{c,s}$	0.21	0.27	0.20	0.24	0.29	0.13	0.39	0.24	0.21	0.36
Swelling Index, C_s										
$C_{e,s}$	0.08	0.08	0.08	0.09	0.13	0.06	0.19	0.09	0.12	0.14
$C_{e,r}$	0.03	0.03	0.05	0.04	0.06	0.04	0.08	0.04	0.05	0.06
Recompression Index, C_r										
$C_{e,r}$	-	-	-	-	-	-	-	0.07	0.05	-
$C_{e,r}$	-	-	-	-	-	-	-	0.03	0.02	-
Coefficient of Consolidation, C_v (at σ'_{v0})										
m ² /year (square root of time method)	12.6	12.0	22.0	4.6	6.2	11.0	3.9	1.9	1.5	25.5
ft ² /year (square root of time method)	135.64	129.18	236.83	49.52	66.74	118.41	41.98	20.45	16.15	274.51

* Sample trimmed at 45 degree angle, representing in situ loading at 45 degree angle.

** Sample trimmed vertically, representing horizontal in situ loading.

sample remolded at natural water content

sample remolded at natural water content plus 5 to 8%

SUMMARY OF CONSOLIDATION TEST RESULTS

Oakland Shore Approach

SFOBB East Span Seismic Safety Project

TABLE 5.4c



Boring Number	98-58	98-58	98-58	98-59	98-59	98-60	98-60	98-61	98-61	98-61	98-61
Sample Number	46	55	63	28	38	33	40	16 rt	16	304	24
Penetration											
meters	41.7	50.7	59.9	26.4	38.5	34.1	43.3	14.1	14.1	17.1	20.1
feet	136.8	166.3	196.5	86.7	126.3	112.0	142.0	46.3	46.4	56.0	65.8
Unit	OBM/UAM	OBM/UAM	OBM/UAM	YBM	OBM/UAM	OBM/UAM	OBM/UAM	YBM	YBM	YBM	MPSA
Moisture Content (%)											
Initial, W_o	43	18	45	48	37	46	21	53	41	48	40
Final, W_f	38	19	41	40	26	37	22	35	30	34	39
Atterberg Limits											
Liquid Limit, LL	74	44	76	71	55	62	43	37	37	65	81
Plastic Limit, PL	24	17	27	28	21	22	16	19	19	26	31
Initial Total Unit Weight, γ_{t0}											
kN/m ³	17.1	20.7	17.4	17.2	18.1	17.3	20.3	16.8	17.7	16.7	18.2
pcf	109	132	111	110	115	110	129	107	113	106	116
Void Ratio											
Initial, e_o	1.26	0.54	1.24	1.32	1.03	1.27	0.60	1.45	1.15	1.49	1.06
Final, e_f	1.09	0.51	1.10	1.09	0.70	1.00	0.59	0.95	0.81	0.80	1.05
Interpreted Preconsolidation Pressure, σ'_p											
kPa (Casagrande Method, 1936)	455	1102	742	340	642	484	671	172	141	180	354
ksf	9.5	23.0	15.5	7.1	13.4	10.1	14.0	3.6	3.0	3.8	7.4
Interpreted Preconsolidation Pressure, σ'_p											
kPa (Work per Unit Volume, Becker et al, 1987)	441	1054	685	354	632	489	666	168	137	177	366
ksf	9.2	22.0	14.3	7.4	13.2	10.2	13.9	3.5	2.9	3.7	7.7
Estimated Effective Vertical Stress, σ'_{v0}											
kPa	393	460	537	268	361	338	421	163	163	186	212
ksf	8.2	9.6	11.2	5.6	7.5	7.1	8.8	3.4	3.4	3.9	4.4
Overconsolidation, OCR											
OCR - Casagrande Method	1.2	2.4	1.4	1.3	1.8	1.4	1.6	1.1	0.9	1.0	1.7
OCR - Becker Method	1.1	2.3	1.3	1.3	1.8	1.4	1.6	1.0	0.8	1.0	1.7
Compression Index, C_c											
C_{ec}	0.68	0.17	0.78	0.68	0.52	0.72	0.21	0.58	0.37	0.76	0.35
C_{es}	0.30	0.11	0.35	0.29	0.26	0.32	0.13	0.24	0.17	0.31	0.17
Swelling Index, C_s											
C_{es}	0.14	0.04	0.14	0.16	0.08	0.11	0.07	0.11	0.05	0.10	0.15
C_{er}	0.06	0.03	0.06	0.07	0.04	0.05	0.04	0.05	0.02	0.04	0.08
Recompression Index, C_r											
C_{er}	-	-	-	-	-	-	-	0.06	-	-	-
C_{er}	-	-	-	-	-	-	-	0.02	-	-	-
Coefficient of Consolidation, C_v (at σ'_{v0})											
m ² /year (square root of time method)	2.9	7.0	6.0	3.9	23.0	13.8	2.9	4.5	2.6	6.9	1.1
ft ² /year (square root of time method)	31.22	75.35	64.59	41.98	247.59	148.56	31.22	48.44	27.99	74.71	11.84

* Sample trimmed at 45 degree angle, representing in situ loading at 45 degree angle.

** Sample trimmed vertically, representing horizontal in situ loading.

sample remolded at natural water content

sample remolded at natural water content plus 5 to 8%

SUMMARY OF CONSOLIDATION TEST RESULTS

Oakland Shore Approach

SFOBB East Span Seismic Safety Project



Boring Number	98-61	98-61	98-62	98-62	98-62	98-63	98-63	98-63	98-63	98-64	98-64	98-64	98-65	98-65	98-65	98-65
Sample Number	24c	24d**	15	25 rt	25	9	18	30rt	30	13	13rt	29	9a	9b#	9c##	10 rt
Penetration																
meters	20.0	19.9	12.7	16.9	16.9	7.9	12.7	20.2	20.3	11.1	11.1	20.3	9.6	9.6	9.6	11.1
feet	65.7	65.3	41.5	55.5	55.5	26.0	41.5	66.4	66.5	36.5	36.3	66.5	31.5	31.5	31.5	36.4
Unit	MPSA	MPSA	YBM	YBM	YBM	YBM	YBM	MPSA	MPSA	YBM	YBM	YBM	YBM	YBM	YBM	YBM
Moisture Content (%)																
Initial, W_0	35	33	53	56	58	57	40	26	25	43	46	31	62	62	69	34
Final, W_f	35	34	39	37	41	26	26	21	21	29	31	26	-	-	-	21
Atterberg Limits																
Liquid Limit, LL	81	81	51	58	58	42	42	42	42	43	43	60	74	74	74	41
Plastic Limit, PL	31	31	24	22	22	22	18	17	17	21	21	17	29	29	29	19
Initial Total Unit Weight, $\gamma_{t,0}$																
kN/m ³	18.8	18.8	16.8	16.5	16.5	18.5	18.0	20.1	20.3	17.8	17.5	19.3	16.5	16.2	15.6	18.2
pcf	120	120	107	105	105	118	115	128	129	113	111	123	105	103	99	116
Void Ratio																
Initial, e_0	0.94	0.90	1.45	1.55	1.57	1.56	1.09	0.69	0.65	1.16	1.25	0.83	1.65	1.65	1.85	0.98
Final, e_f	0.94	0.90	1.08	0.99	1.11	0.74	0.72	0.54	0.55	0.77	0.85	0.71	1.00	0.94	1.03	0.61
Interpreted Preconsolidation Pressure, σ'_p																
kPa (Casagrande Method, 1936)	354	292	163	117	101	115	105	527	436	144	153	292	81	-	-	139
ksf	7.4	6.1	3.4	2.5	2.1	2.4	2.2	11.0	9.1	3.0	3.2	6.1	1.7	-	-	2.9
Interpreted Preconsolidation Pressure, σ'_p																
kPa (Work per Unit Volume, Becker et al, 1987)	350	297	172	139	101	129	108	479	438	141	153	283	96	-	-	144
ksf	7.3	6.2	3.6	2.9	2.1	2.7	2.3	10.0	9.2	3.0	3.2	5.9	2.0	-	-	3.0
Estimated Effective Vertical Stress, σ'_{v0}																
kPa	212	212	153	183	183	116	151	214	214	137	139	209	122	122	122	132
ksf	4.4	4.4	3.2	3.8	3.8	2.4	3.2	4.5	4.5	2.9	2.9	4.4	2.6	2.6	2.6	2.8
Overconsolidation, OCR																
OCR - Casagrande Method	1.7	1.4	1.1	0.6	0.5	1.0	0.7	2.5	2.0	1.0	1.1	1.4	0.7	-	-	1.1
OCR - Becker Method	1.7	1.4	1.1	0.8	0.5	1.1	0.7	2.2	2.0	1.0	1.1	1.4	0.8	-	-	1.1
Compression Index, C_c																
$C_{e,c}$	0.31	0.29	0.61	0.48	0.46	0.41	0.33	0.25	0.21	0.39	0.48	0.28	0.60	0.52	0.72	0.27
	0.16	0.15	0.25	0.19	0.18	0.16	0.16	0.15	0.13	0.18	0.21	0.15	0.23	0.20	0.25	0.14
Swelling Index, C_s																
$C_{e,s}$	0.13	0.12	0.12	0.09	0.09	0.05	0.06	0.07	0.07	0.08	0.05	0.09	0.11	0.10	-	0.05
	0.07	0.06	0.05	0.04	0.03	0.02	0.03	0.04	0.04	0.04	0.02	0.05	0.04	0.04	-	0.02
Recompression Index, C_r																
$C_{e,r}$	0.07	0.11	-	0.05	-	0.05	-	0.05	-	-	0.06	-	0.09	0.06	0.08	0.03
	0.04	0.06	-	0.02	-	0.02	-	0.03	-	-	0.03	-	0.04	0.02	0.03	0.01
Coefficient of Consolidation, C_v (at σ'_{v0})																
m ² /year (square root of time method)	12.0	-	8.3	2.5	2.3	8.2	3.5	4.1	4.0	7.1	7.5	1.5	1.3	1.1	1.2	6.0
ft ² /year (square root of time method)	129.18	-	89.35	26.91	24.76	88.27	37.68	44.14	43.06	76.43	80.74	16.15	13.99	11.84	12.92	64.59

* Sample trimmed at 45 degree angle, representing in situ loading at 45 degree angle.

** Sample trimmed vertically, representing horizontal in situ loading.

sample remolded at natural water content

sample remolded at natural water content plus 5 to 8%

SUMMARY OF CONSOLIDATION TEST RESULTS

Oakland Shore Approach

SFOBB East Span Seismic Safety Project



Boring Number	98-65	98-65	98-65	98-67	98-69	98-70	98-70	98-70	98-71	98-71	98-73	98-73	98-73	98-73	98-75
Sample Number	10	15	15 rt	12	9	303	312	325	14rt	14	7##	8a	8b#	9	8
Penetration															
meters	11.2	13.9	13.9	11.2	11.0	11.0	15.7	24.9	11.2	11.2	7.9	8.1	8.1	9.5	11.0
feet	36.6	45.5	45.5	36.8	36.0	36.0	51.7	81.6	36.6	36.8	26.0	26.5	26.5	31.0	36.0
Unit	YBM	YBM	YBM	YBM	YBM	YBM	MPSA	MPSA	YBM	YBM	YBM	YBM	YBM	YBM	YBM
Moisture Content (%)															
Initial, W_0	37	56	58	49	45	46	22	25	36	37	48	40	39	39	32
Final, W_f	25	37	39	34	8	-	16	21	25	25	25	-	-	28	20
Atterberg Limits															
Liquid Limit, LL	41	56	56	53	55	59	Sand	44	35	35	51	44	44	48	32
Plastic Limit, PL	19	24	24	23	29	23		20	18	18	24	24	24	24	16
Initial Total Unit Weight, $\gamma_{t,0}$															
kN/m ³	18.1	16.6	16.5	17.2	17.3	18.2	20.7	20.0	18.4	18.4	17.0	17.9	18.1	17.9	18.9
pcf	116	106	105	109	110	116	132	128	117	117	108	114	115	114	120
Void Ratio															
Initial, e_0	1.03	1.54	1.57	1.33	1.26	1.26	0.58	0.68	0.99	1.00	1.29	1.08	1.02	1.06	0.88
Final, e_f	0.68	1.02	1.06	0.94	0.52	0.80	0.48	0.56	0.68	0.68	0.61	0.62	0.58	0.66	0.57
Interpreted Preconsolidation Pressure, σ'_p															
kPa (Casagrande Method, 1936)	153	134	153	153	158	168	-	637	201	220	-	101	-	115	259
ksf	3.2	2.8	3.2	3.2	3.3	3.5	-	13.3	4.2	4.6	-	2.1	-	2.4	5.4
Interpreted Preconsolidation Pressure, σ'_p															
kPa (Work per Unit Volume, Becker et al, 1987)	158	141	163	158	153	172	-	599	206	235	-	120	-	120	249
ksf	3.3	3.0	3.4	3.3	3.2	3.6	-	12.5	4.3	4.9	-	2.5	-	2.5	5.2
Estimated Effective Vertical Stress, σ'_{v0}															
kPa	132	149	149	141	143	147	182	269	133	133	105	105	105	115	142
ksf	2.8	3.1	3.1	2.9	3.0	3.1	3.8	5.6	2.8	2.8	2.2	2.2	2.2	2.4	3.0
Overconsolidation, OCR															
OCR - Casagrande Method	1.2	0.9	1.0	1.1	1.1	1.1	-	2.4	1.5	1.7	-	1.0	-	1.0	1.8
OCR - Becker Method	1.2	0.9	1.1	1.1	1.1	1.2	-	2.2	1.6	1.8	-	1.1	-	1.0	1.8
Compression Index, C_c															
$C_{c,c}$	0.28	0.58	0.61	0.54	0.57	0.47	0.14	0.21	0.29	0.30	0.28	0.28	0.28	0.33	0.26
$C_{c,s}$	0.14	0.23	0.24	0.23	0.25	0.21	0.09	0.12	0.15	0.15	0.12	0.14	0.14	0.16	0.14
Swelling Index, C_s															
$C_{e,s}$	0.05	0.17	0.10	0.09	-	0.08	0.01	0.05	0.27	0.02	0.06	0.05	0.05	0.06	0.02
$C_{e,r}$	0.02	0.07	0.04	0.04	-	0.04	0.01	0.03	0.14	0.01	0.02	0.03	0.02	0.03	0.01
Recompression Index, C_r															
$C_{e,r}$	-	-	-	0.03	0.05	0.04	0.01	0.02	0.03	-	0.03	0.04	0.03	0.03	0.03
$C_{e,r}$	-	-	-	0.01	0.02	0.02	0.01	0.01	0.01	-	0.01	0.02	0.02	0.01	0.01
Coefficient of Consolidation, C_v (at σ'_{v0})															
m ² /year (square root of time method)	6.7	3.6	10.0	8.2	4.0	2.4	56.0	4.7	14.00	22.7	3.0	10.5	3.6	6.5	1.5
ft ² /year (square root of time method)	72.13	38.75	107.6	88.27	43.06	25.84	602.84	50.60	150.71	244.36	32.19	113.03	38.75	69.97	16.15

* Sample trimmed at 45 degree angle, representing in situ loading at 45 degree angle.

** Sample trimmed vertically, representing horizontal in situ loading.

sample remolded at natural water content

sample remolded at natural water content plus 5 to 8%

SUMMARY OF CONSOLIDATION TEST RESULTS

Oakland Shore Approach

SFOBB East Span Seismic Safety Project



Boring Number	98-75	98-75	98-75	98-39	98-39	98-39	98-39	98-39	98-39	98-39
Sample Number	20	27	34	5	10	36a	50a	63a	71	80
Penetration										
meters	21.8	26.4	31.0	3.0	4.9	20.9	37.4	54.6	64.6	75.5
feet	71.6	86.6	101.6	10.0	16.0	68.5	122.6	179.1	212.0	247.7
Unit	MPSA	OBM/UAM	OBM/UAM	YBM	YBM	OBM/UAM	OBM/UAM	OBM/UAM	OBM/UAM	LAA
Moisture Content (%)										
Initial, W_0	62	34	50	57	31	45	23	79	41	20
Final, W_f	48	28	40	-	23	43	24	74	36	19
Atterberg Limits										
Liquid Limit, LL	38	61	70	46	33	70	41	81	61	66
Plastic Limit, PL	14	20	22	22	17	25	17	26	26	17
Initial Total Unit Weight, γ_{t0}										
kN/m ³	16.3	18.5	16.8	15.4	17.9	17.4	20.1	16.5	17.8	19.9
pcf	104	118	107	98	114	111	128	105	113	127
Void Ratio										
Initial, e_0	1.68	0.95	1.40	1.54	1.00	1.23	0.64	1.93	1.13	0.63
Final, e_f	1.29	0.75	1.09	-	0.58	1.18	0.65	1.68	1.00	0.54
Interpreted Preconsolidation Pressure, σ'_p										
kPa (Casagrande Method, 1936)	326	575	460	53	86	479	853	862	623	1557
ksf	6.8	12.0	9.6	1.1	1.8	10.0	17.8	18.0	13.0	32.5
Interpreted Preconsolidation Pressure, σ'_p										
kPa (Work per Unit Volume, Becker et al, 1987)	335	560	450	56	91	465	877	833	671	1533
ksf	7.0	11.7	9.4	1.2	1.9	9.7	18.3	17.4	14.0	32.0
Estimated Effective Vertical Stress, σ'_{v0}										
kPa	250	278	311	19	31	160	300	455	536	637
ksf	5.2	5.8	6.5	0.4	0.6	3.3	6.3	9.5	11.2	13.3
Overconsolidation, OCR										
OCR - Casagrande Method	1.3	2.1	1.5	2.8	2.8	3.0	2.8	1.9	1.2	2.4
OCR - Becker Method	1.3	2.0	1.4	2.9	3.0	2.9	2.9	1.8	1.3	2.4
Compression Index, C_c										
$C_{e,c}$	0.97	0.38	0.79	0.76	0.27	0.66	0.18	1.20	0.47	0.24
$C_{e,s}$	0.36	0.20	0.33	0.30	0.13	0.29	0.11	0.41	0.22	0.15
Swelling Index, C_s										
$C_{e,s}$	0.17	0.14	0.14	0.09	0.03	0.13	0.05	0.17	0.18	0.05
$C_{e,s}$	0.06	0.07	0.06	0.04	0.01	0.06	0.02	0.07	0.08	0.02
Recompression Index, C_r										
$C_{e,r}$	0.03	0.01	0.01	-	-	-	-	-	-	-
$C_{e,r}$	0.01	0.01	0.01	-	-	-	-	-	-	-
Coefficient of Consolidation, C_v (at σ'_{v0})										
m ² /year (square root of time method)	10.8	16.0	12.0	17.0	17.5	-	-	-	2.0	3.5
ft ² /year (square root of time method)	116.26	172.24	129.18	183	188	-	-	-	22	38

* Sample trimmed at 45 degree angle, representing in situ loading at 45 degree angle.

** Sample trimmed vertically, representing horizontal in situ loading.

sample remolded at natural water content

sample remolded at natural water content plus 5 to 8%

SUMMARY OF CONSOLIDATION TEST RESULTS

Oakland Shore Approach

SFOBB East Span Seismic Safety Project



Boring Number	98-39	98-44	98-44	98-44	98-44	98-44	98-44	98-44	98-44	98-44
Sample Number	106a	16	36a**	36b	50a**	50b	54	68	79	90
Penetration										
meters	99.0	5.0	9.3	9.3	28.5	28.5	29.8	47.7	63.0	81.2
feet	324.6	16.5	30.4	30.5	93.5	93.6	97.7	156.6	206.5	266.3
Unit	LAA	YBM	YBM	YBM	OBM/UAM	OBM/UAM	OBM/UAM	OBM/UAM	OBM/UAM	LAA
Moisture Content (%)										
Initial, W_0	20	39	59	60	46	50	47	46	49	18
Final, W_f	21	29	39	39	35	41	35	42	39	15
Atterberg Limits										
Liquid Limit, LL	45	42	53	53	70	70	56	76	67	29
Plastic Limit, PL	17	22	21	21	28	28	23	26	23	17
Initial Total Unit Weight, γ_{t0}										
kN/m ³	20.5	18.4	16.3	16.3	17.4	17.1	17.2	17.3	16.9	20.3
pcf	130	117	104	104	111	109	109	110	108	129
Void Ratio										
Initial, e_0	0.58	1.19	1.61	1.64	1.26	1.36	1.30	1.27	1.38	0.56
Final, e_f	0.58	0.79	1.08	1.06	0.93	1.09	0.94	1.13	1.05	0.43
Interpreted Preconsolidation Pressure, σ'_p										
kPa (Casagrande Method, 1936)	1485	-	67	62	479	407	393	766	958	1389
ksf	31.0	-	1.4	1.3	10.0	8.5	8.2	16.0	20.0	29.0
Interpreted Preconsolidation Pressure, σ'_p										
kPa (Work per Unit Volume, Becker et al, 1987)	1542	-	77	65	474	455	407	790	1035	1533
ksf	32.2	-	1.6	1.4	9.9	9.5	8.5	16.5	21.6	32.0
Estimated Effective Vertical Stress, σ'_{v0}										
kPa	881	37	64	64	227	227	236	387	501	647
ksf	18.4	0.8	1.3	1.3	4.7	4.7	4.9	8.1	10.5	13.5
Overconsolidation, OCR										
OCR - Casagrande Method	1.7	-	1.0	1.0	2.1	1.8	1.7	2.0	1.9	2.1
OCR - Becker Method	1.8	-	1.2	1.0	2.1	2.0	1.7	2.0	2.1	2.4
Compression Index, C_c										
$C_{e,c}$	0.23	0.29	0.59	0.58	0.58	0.66	0.63	0.82	1.07	0.16
$C_{e,s}$	0.14	0.13	0.23	0.22	0.26	0.28	0.28	0.36	0.45	0.10
Swelling Index, C_s										
$C_{e,s}$	0.10	4.11	3.06	3.06	4.70	6.46	4.23	7.87	4.94	0.99
$C_{e,s}$	0.04	0.04	0.03	0.03	0.04	0.06	0.04	0.07	0.04	0.01
Recompression Index, C_r										
$C_{e,r}$	-	-	-	-	-	-	-	-	-	-
$C_{e,r}$	-	-	-	-	-	-	-	-	-	-
Coefficient of Consolidation, C_v (at σ'_{v0})										
m ² /year (square root of time method)	-	8.0	3.5	3.6	24.0	21.5	6.0	-	-	43.0
ft ² /year (square root of time method)	-	86	38	39	258	231	65	-	-	463

* Sample trimmed at 45 degree angle, representing in situ loading at 45 degree angle.

** Sample trimmed vertically, representing horizontal in situ loading.

sample remolded at natural water content

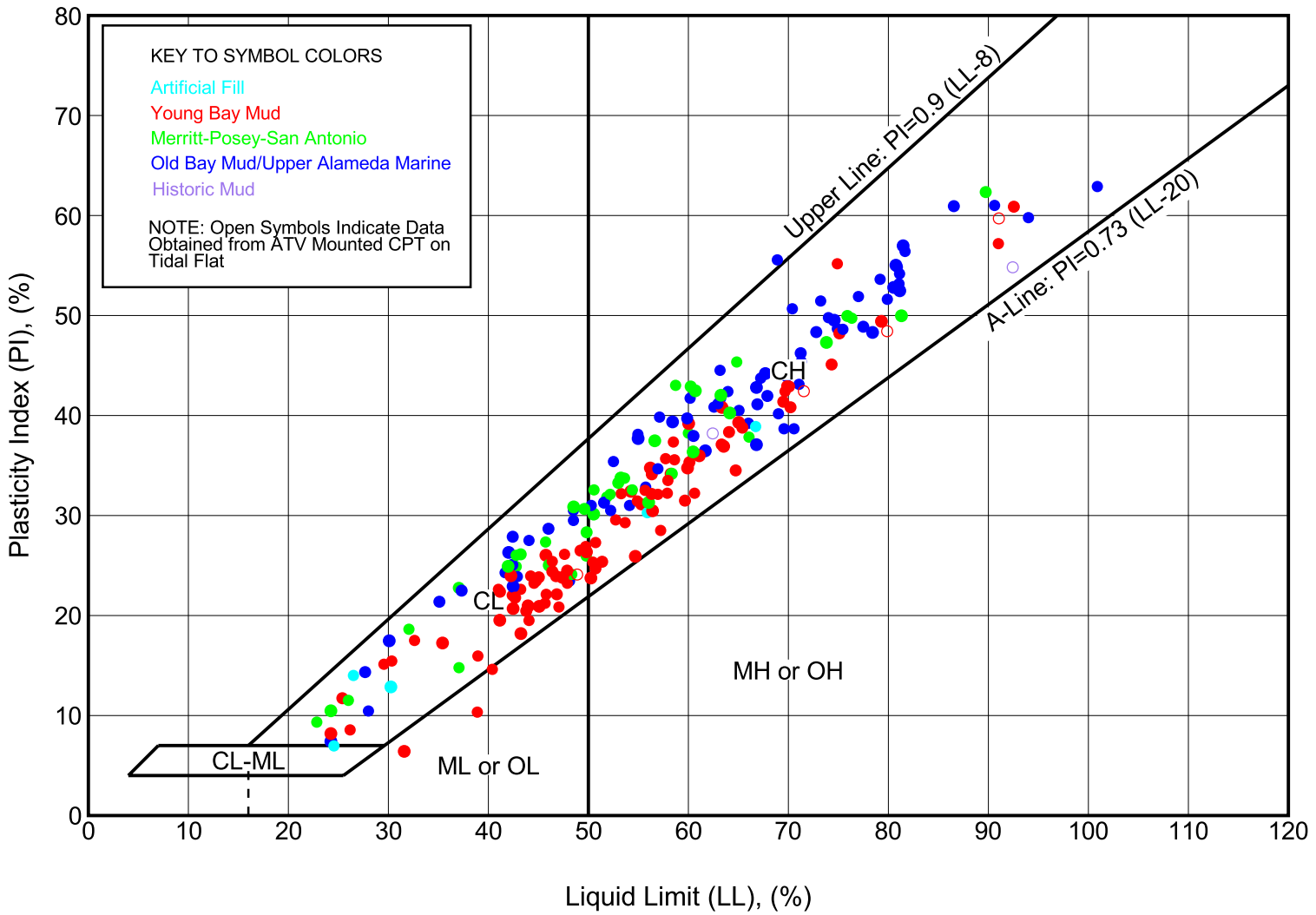
sample remolded at natural water content plus 5 to 8%

SUMMARY OF CONSOLIDATION TEST RESULTS

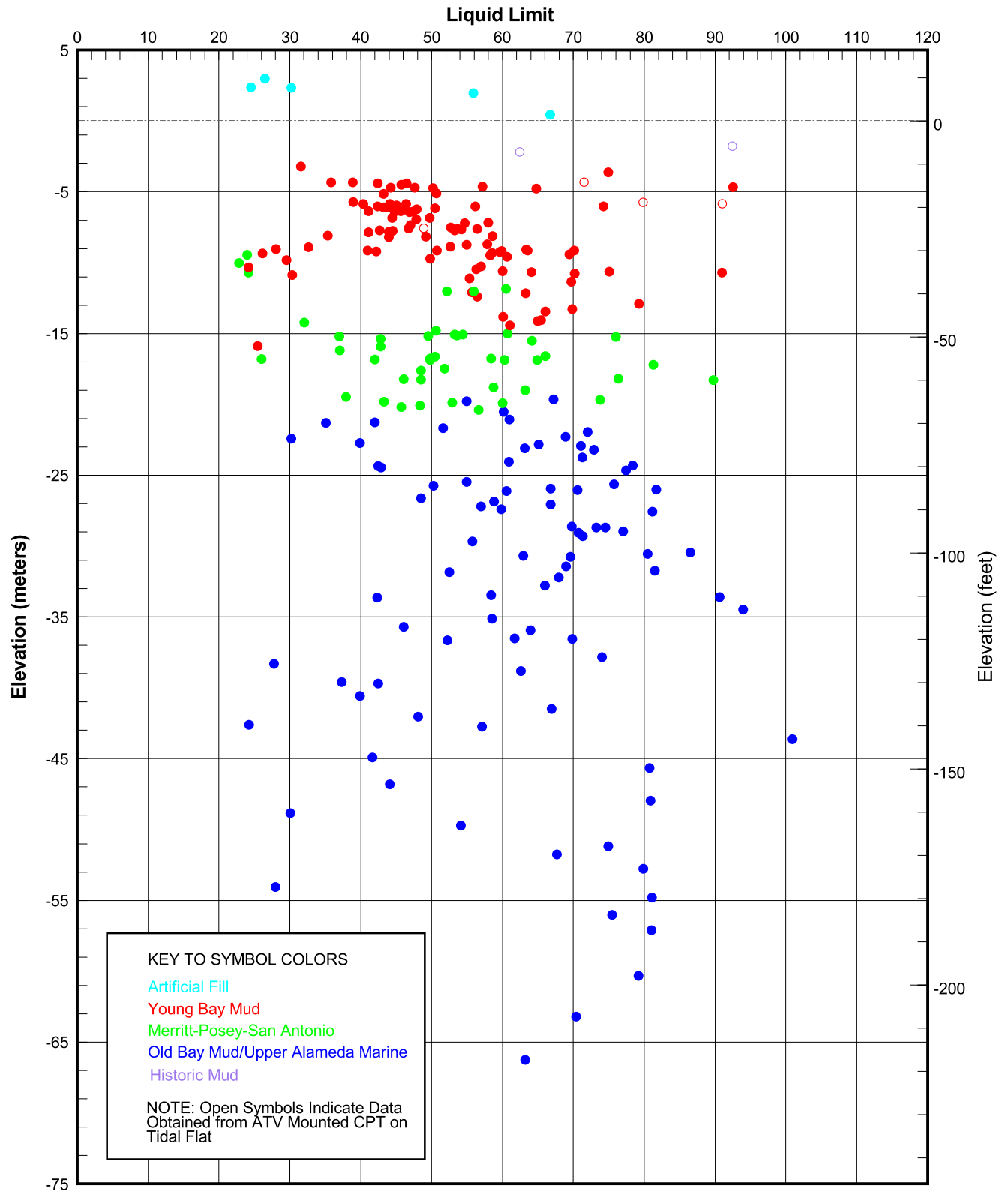
Oakland Shore Approach

SFOBB East Span Seismic Safety Project

TABLE 5.4h

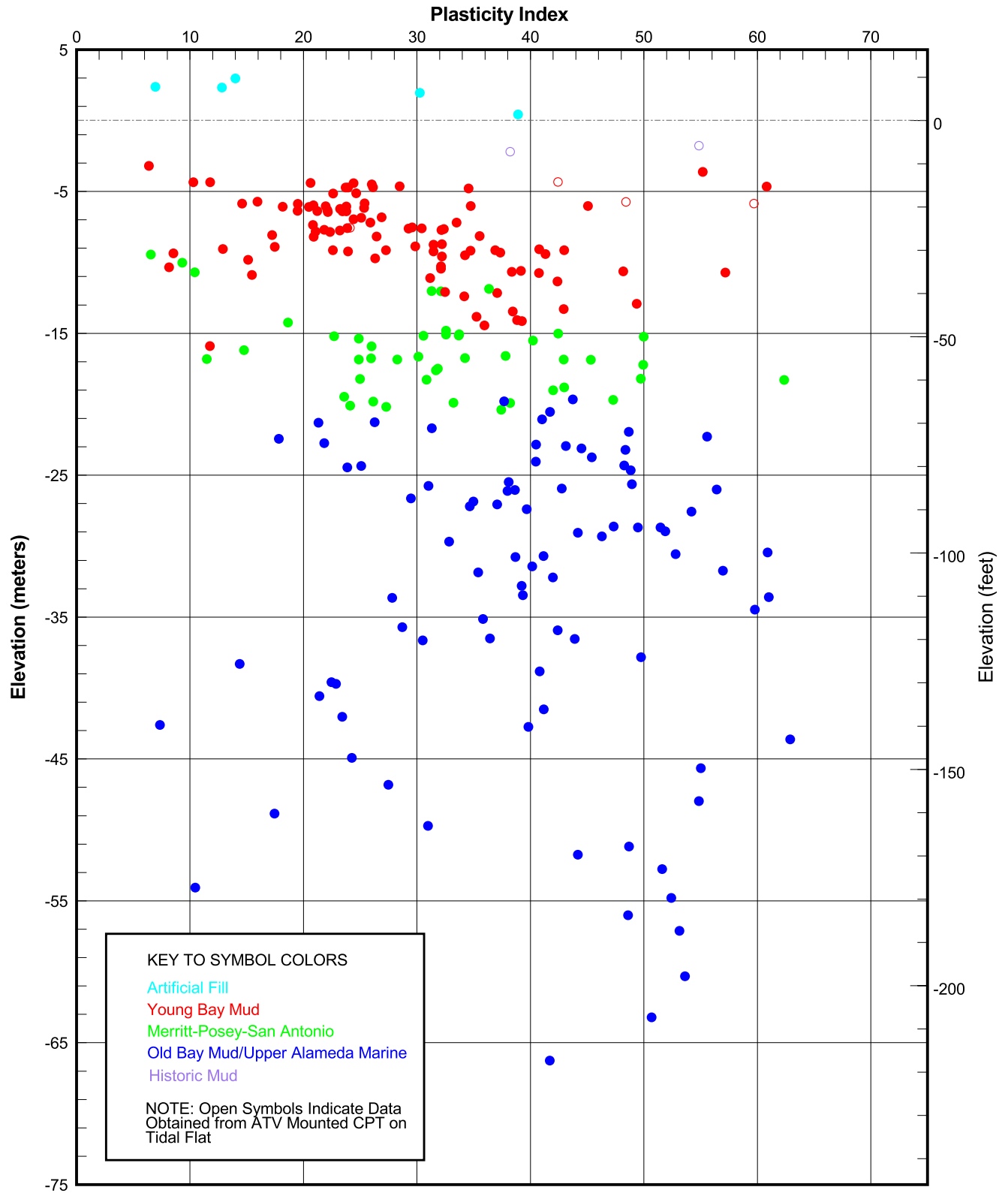


PLASTICITY CHART
Oakland Shore Approach
SFOBB East Span Seismic Safety Project



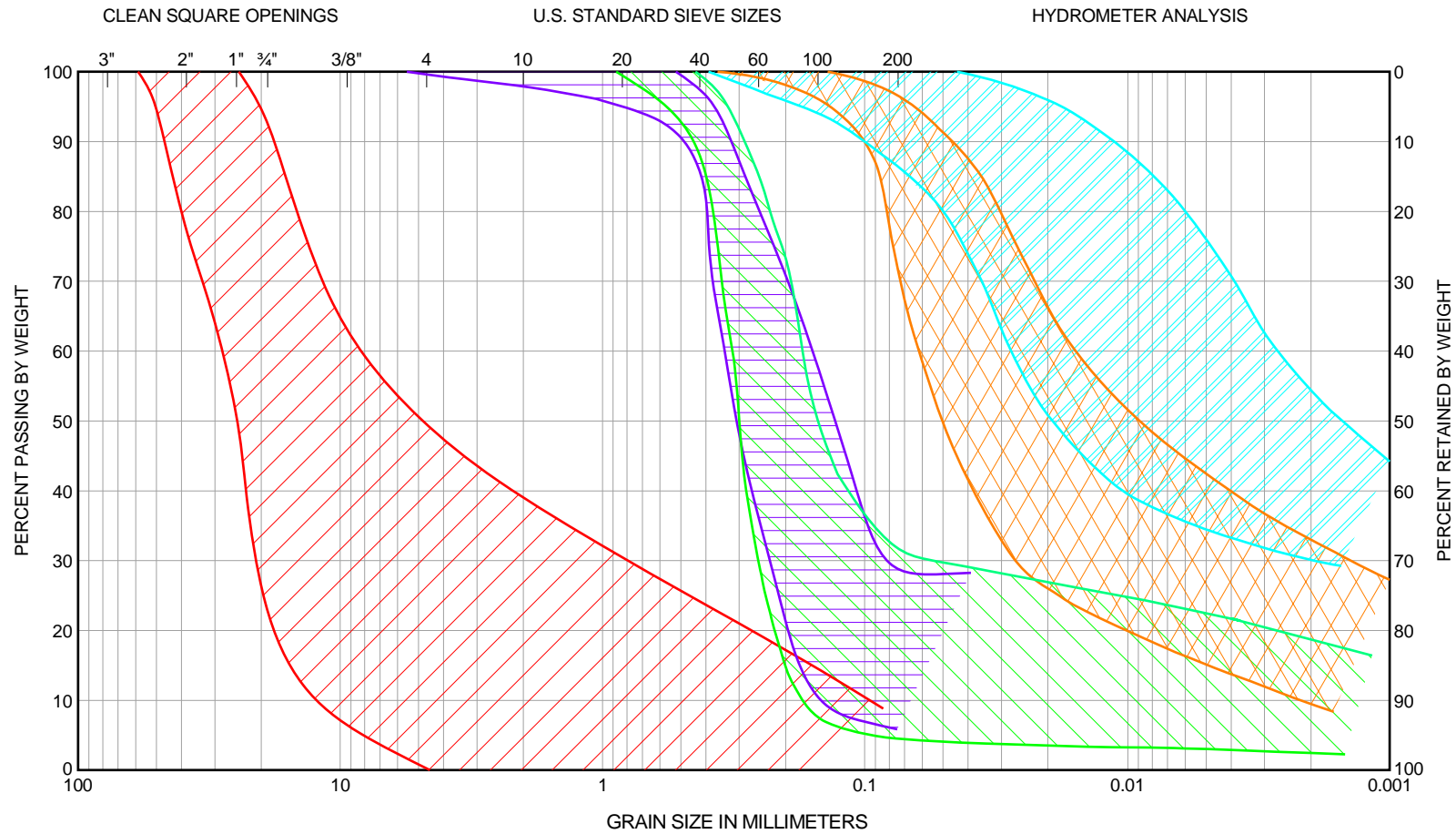
LIQUID LIMIT PROFILE
Oakland Shore Approach
SFOBB East Span Seismic Safety Project





PLASTICITY INDEX PROFILE
Oakland Shore Approach
SFOBB East Span Seismic Safety Project





GRAVEL		SAND			SILT (nonplastic) to CLAY (plastic)
COARSE	FINE	COARSE	MEDIUM	FINE	

Typical Range: Merritt Sand in Merritt-Posey-San Antonio Formation

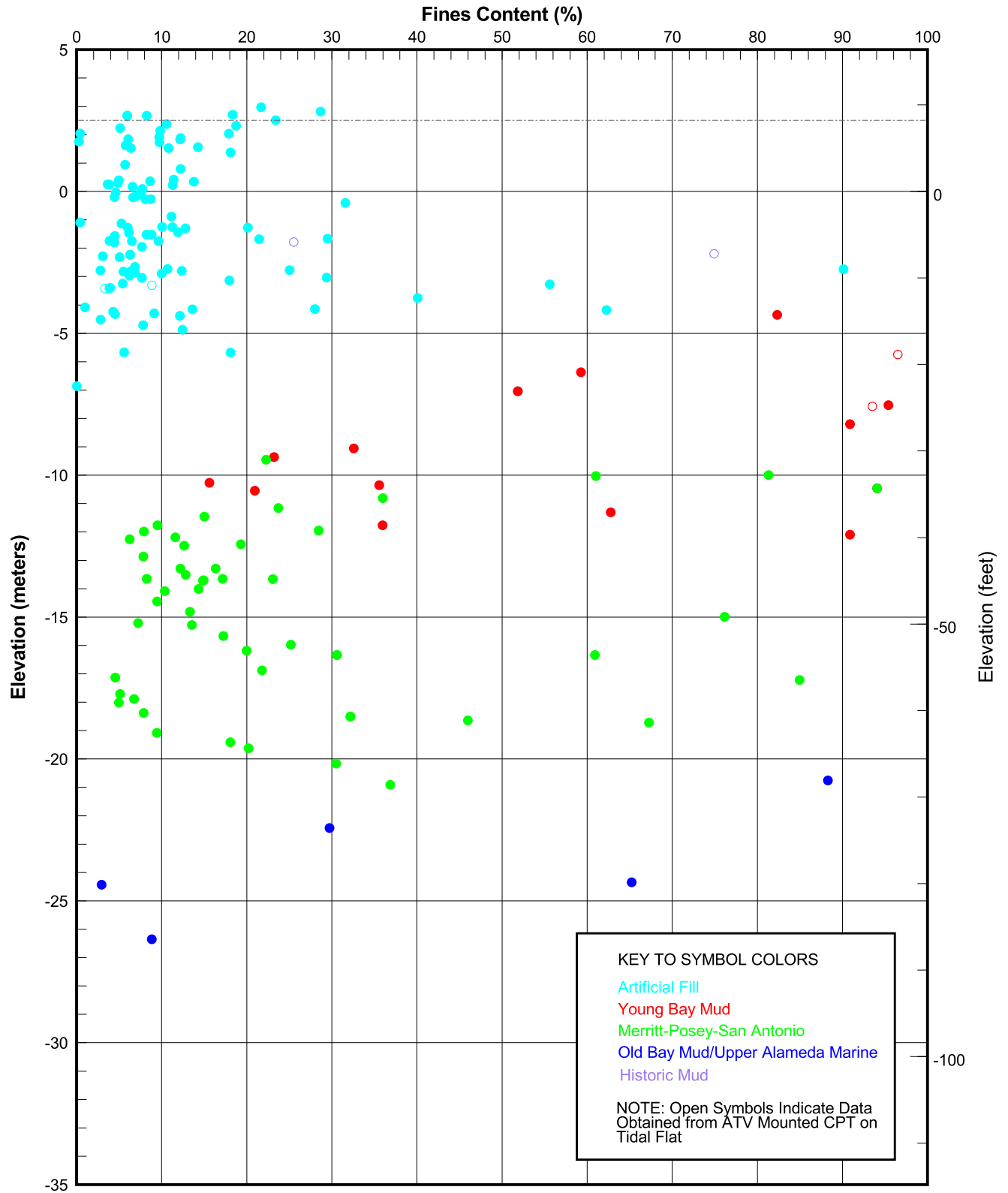
Typical Range: Fine Sands in Artificial Fill

Typical Range: Gravel in Artificial Fill

Typical Range: Lean Clay in Young Bay Mud, Old Bay Mud and Upper Alameda Sediments

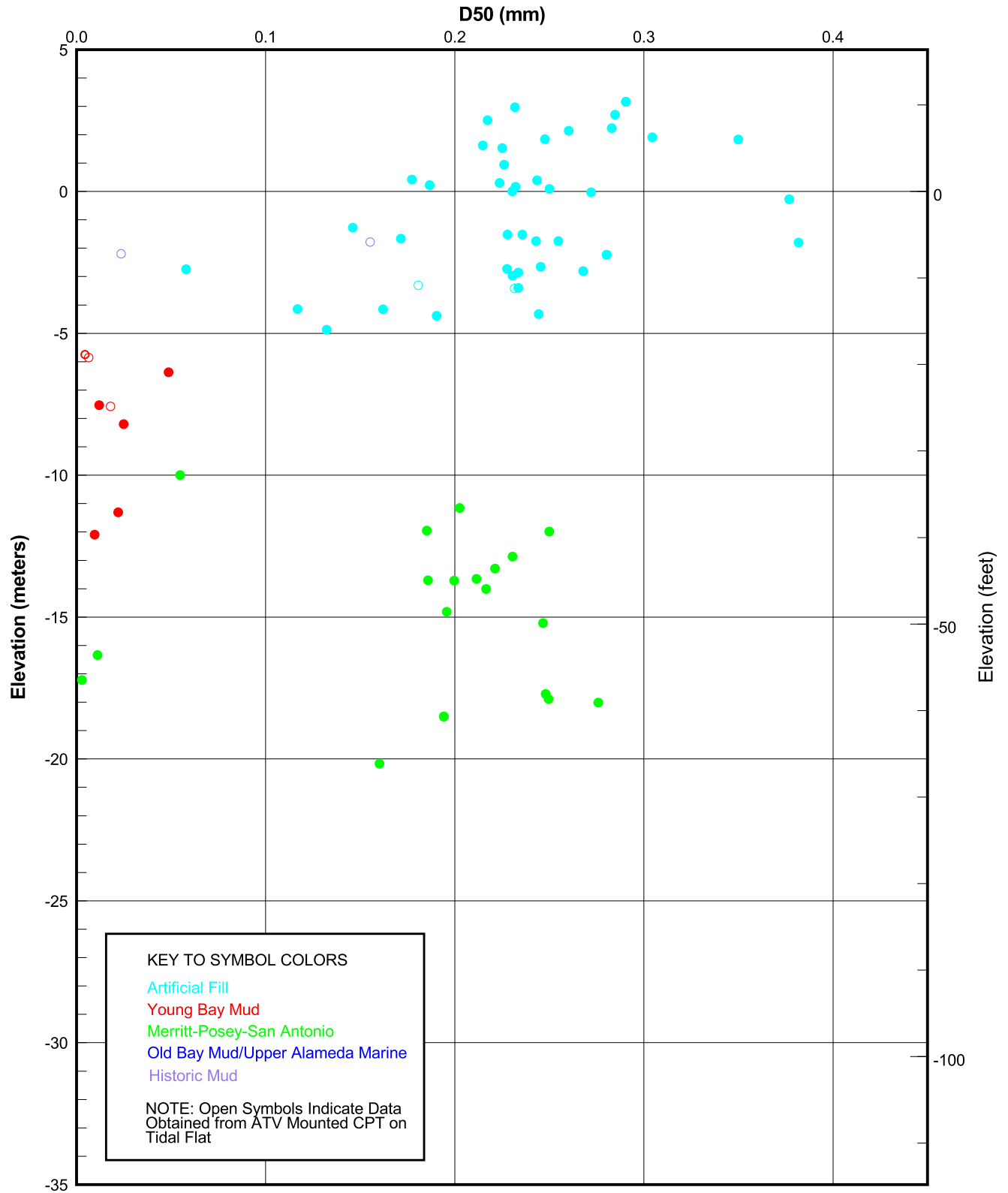
Typical Range: Fat Clay in Young Bay Mud, Old Bay Mud and Upper Alameda Sediments (From Marine Characterization)

TYPICAL GRAIN SIZE DISTRIBUTION CURVES Oakland Shore Approach SFOBB East Span Seismic Safety Project



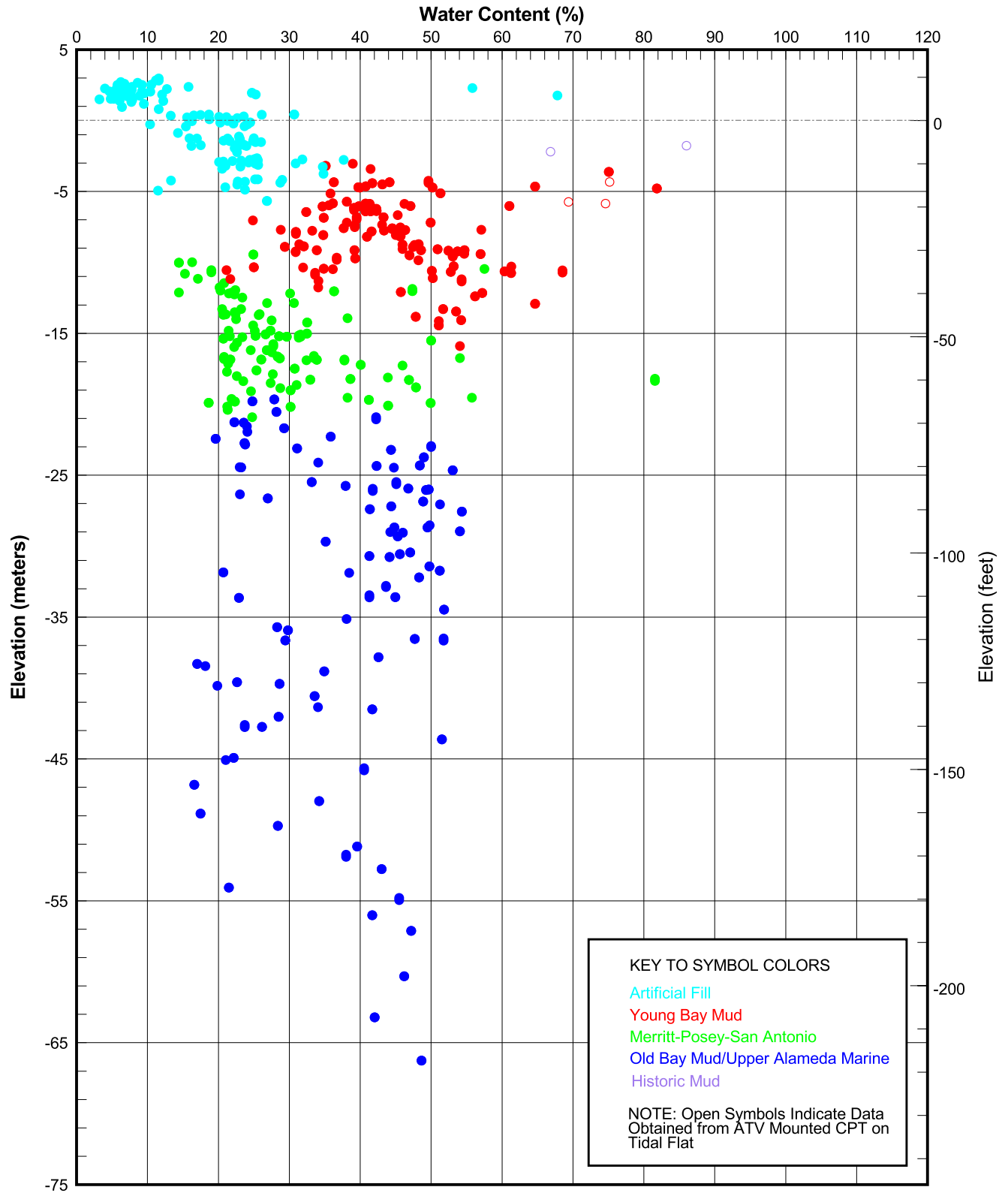
FINES CONTENT PROFILE
Oakland Shore Approach
SFOBB East Span Seismic Safety Project





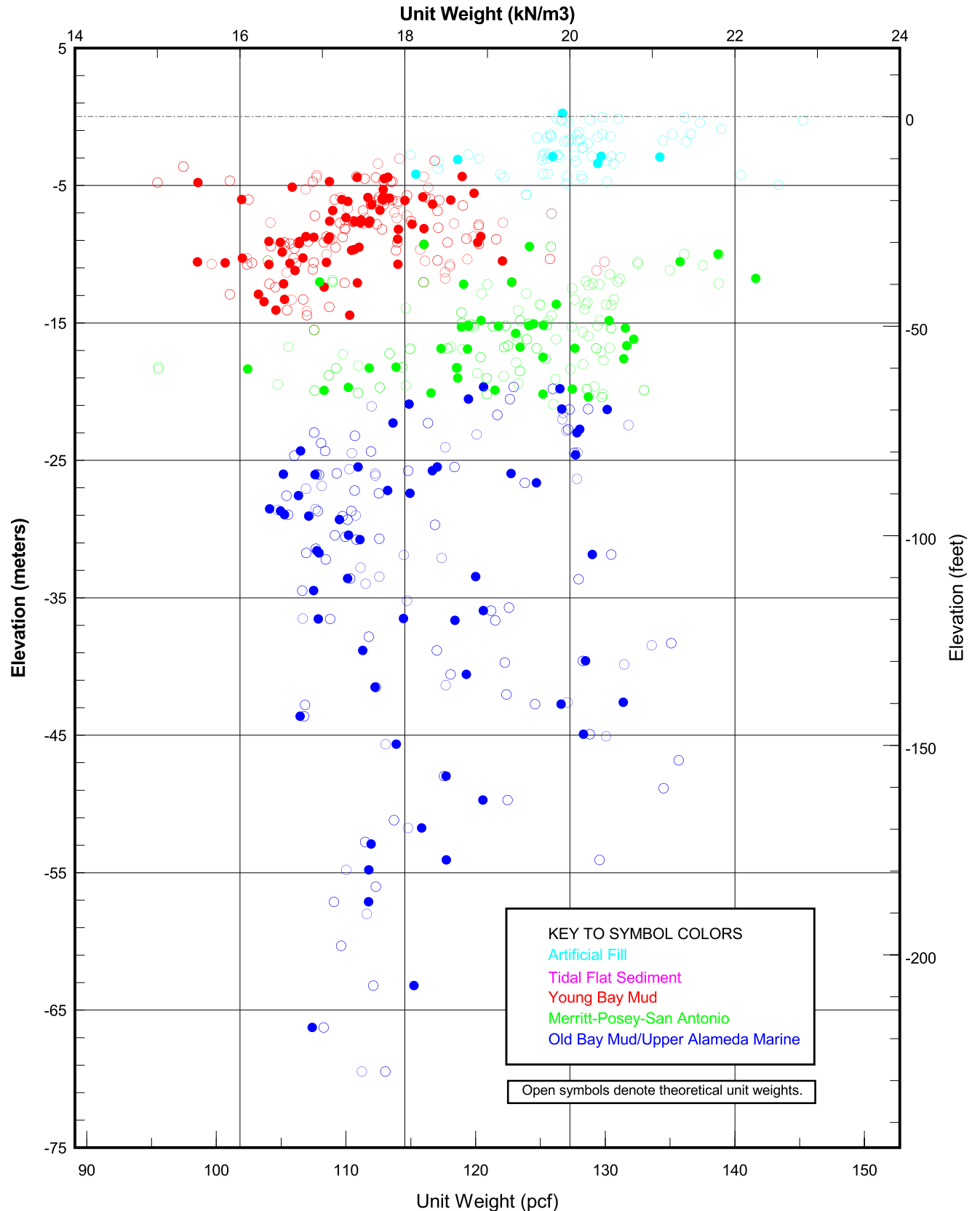
D50 PROFILE
Oakland Shore Approach
SFOBB East Span Seismic Safety Project





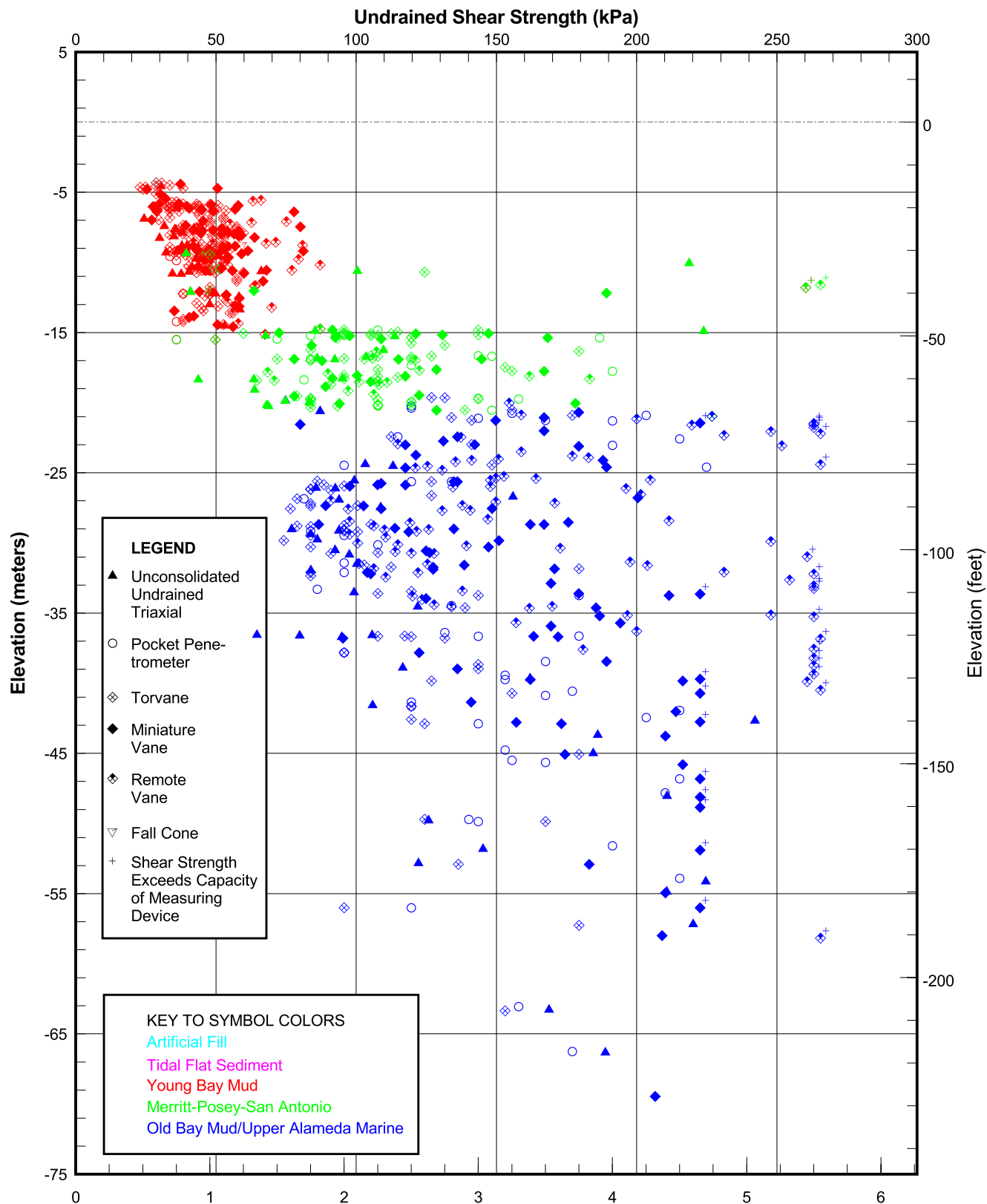
WATER CONTENT PROFILE
Oakland Shore Approach
SFOBB East Span Seismic Safety Project





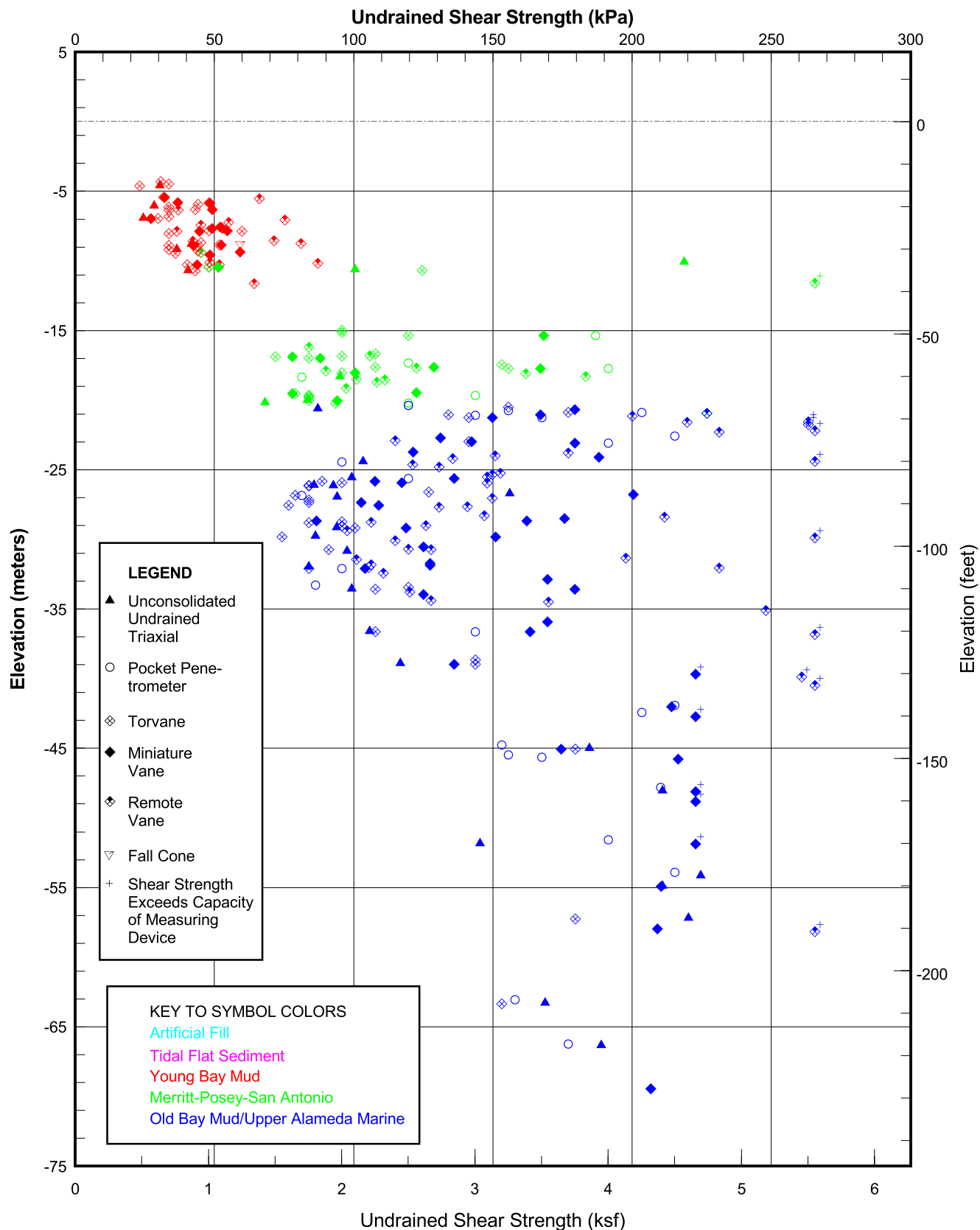
UNIT WEIGHT PROFILE
Oakland Shore Approach
SFOBB East Span Seismic Safety Project

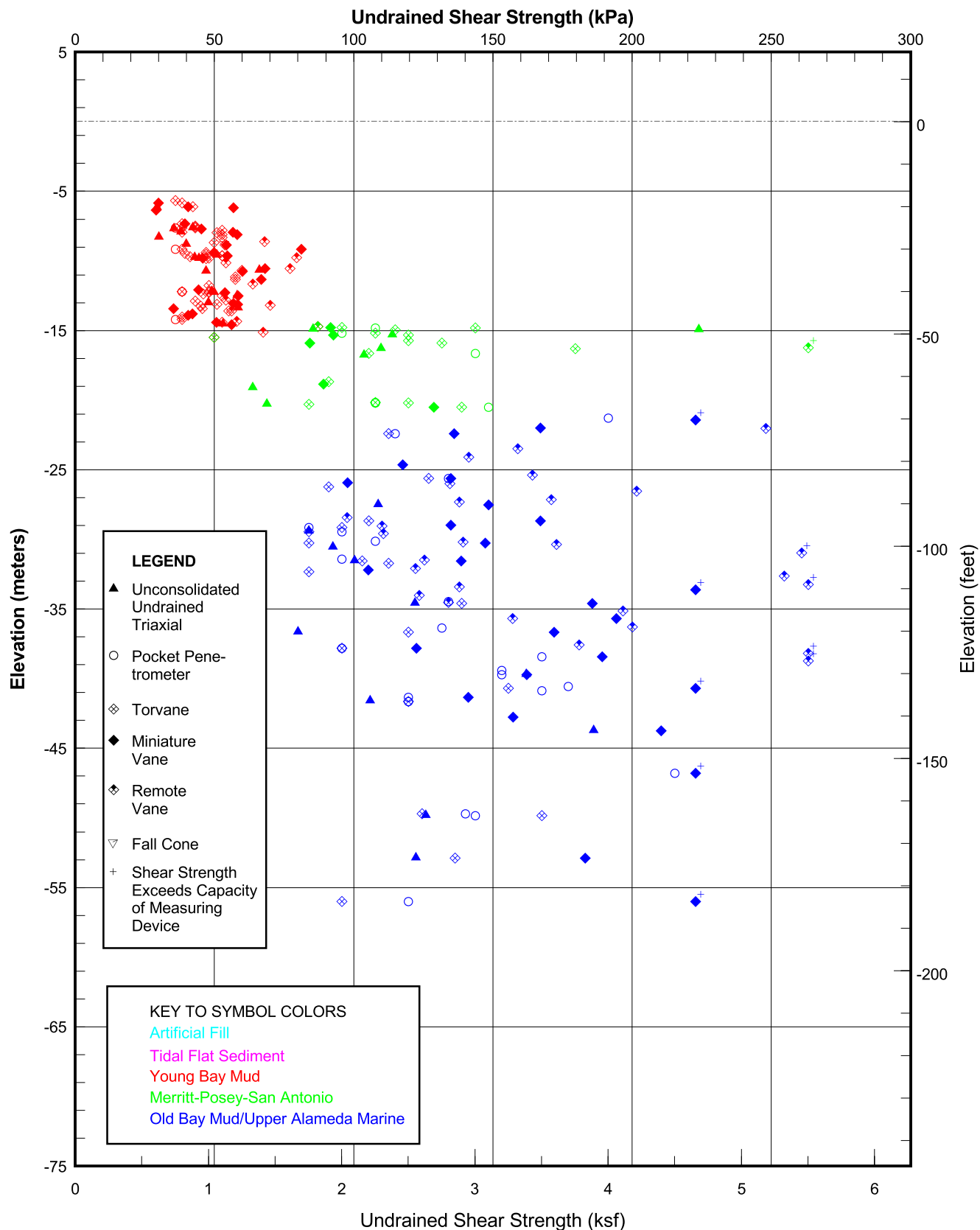




UNDRAINED SHEAR STRENGTH PROFILE
Oakland Shore Approach
SFOBB East Span Seismic Safety Project

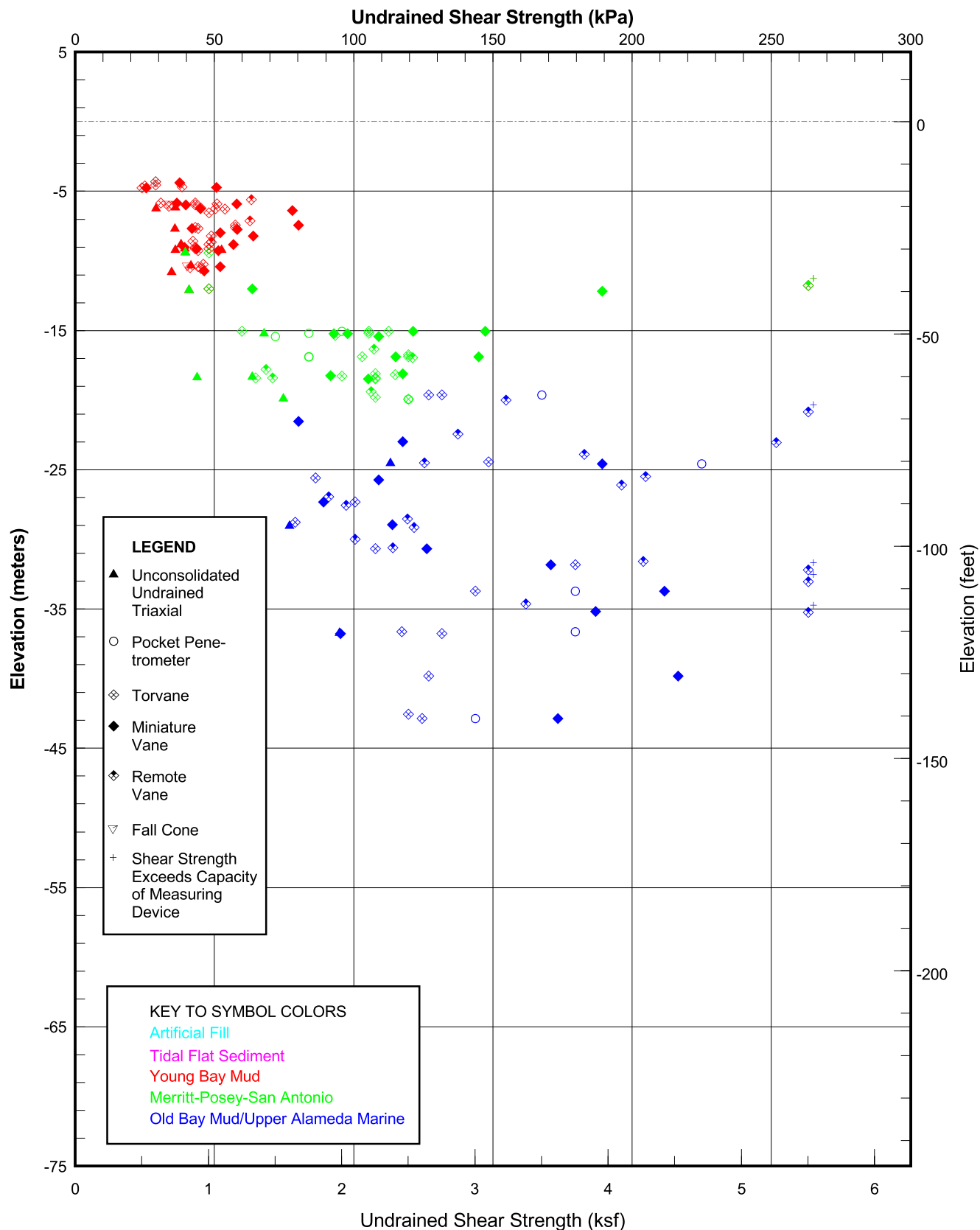






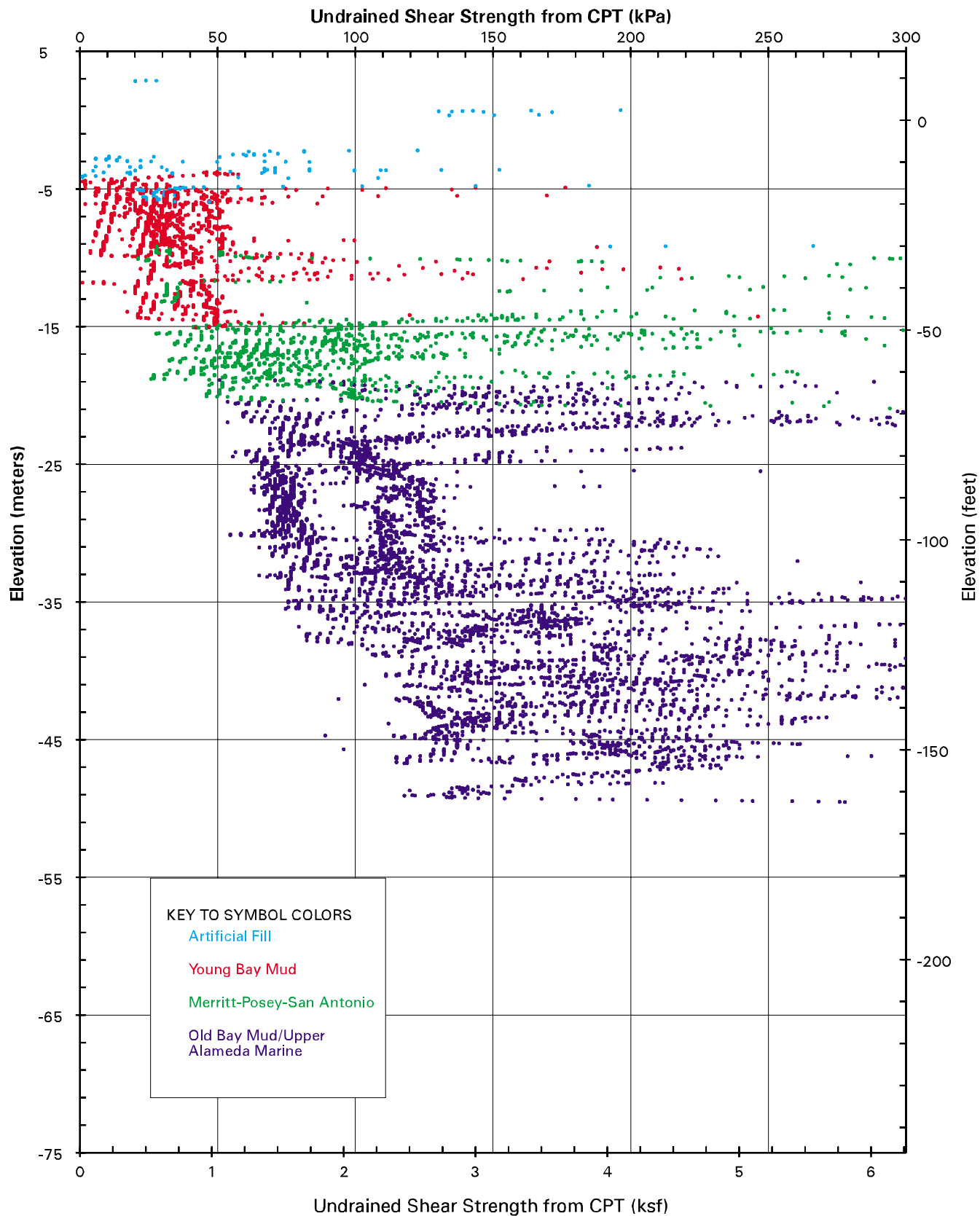
UNDRAINED SHEAR STRENGTH PROFILE FOR CENTRAL PORTION OF MOLE
Borings 98-56, 98-57, 98-58, 98-61, 98-62, 98-66, and 98-70
 SFOBB East Span Seismic Safety Project





UNDRAINED SHEAR STRENGTH PROFILE FOR EASTERN PORTION OF THE MOLE
Borings 98-59, 98-60, 98-63, 98-64, 98-67, 98-71, and 98-72
 SFOBB East Span Seismic Safety Project





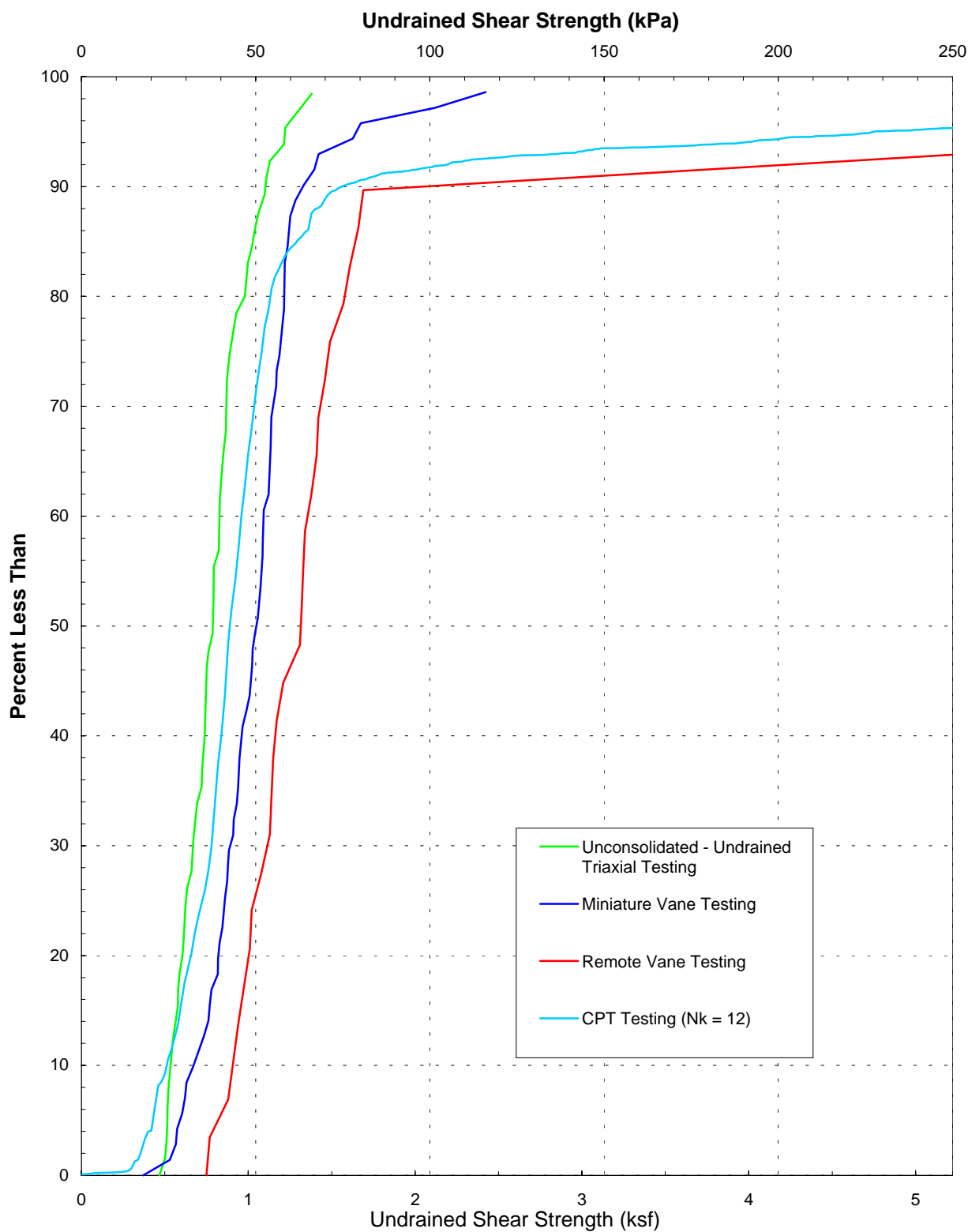
UNDRAINED SHEAR STRENGTH PROFILE FROM CPT TIP RESISTANCE ($N_k = 12$)

Oakland Shore Approach

SFOBB East Span Seismic Safety Project

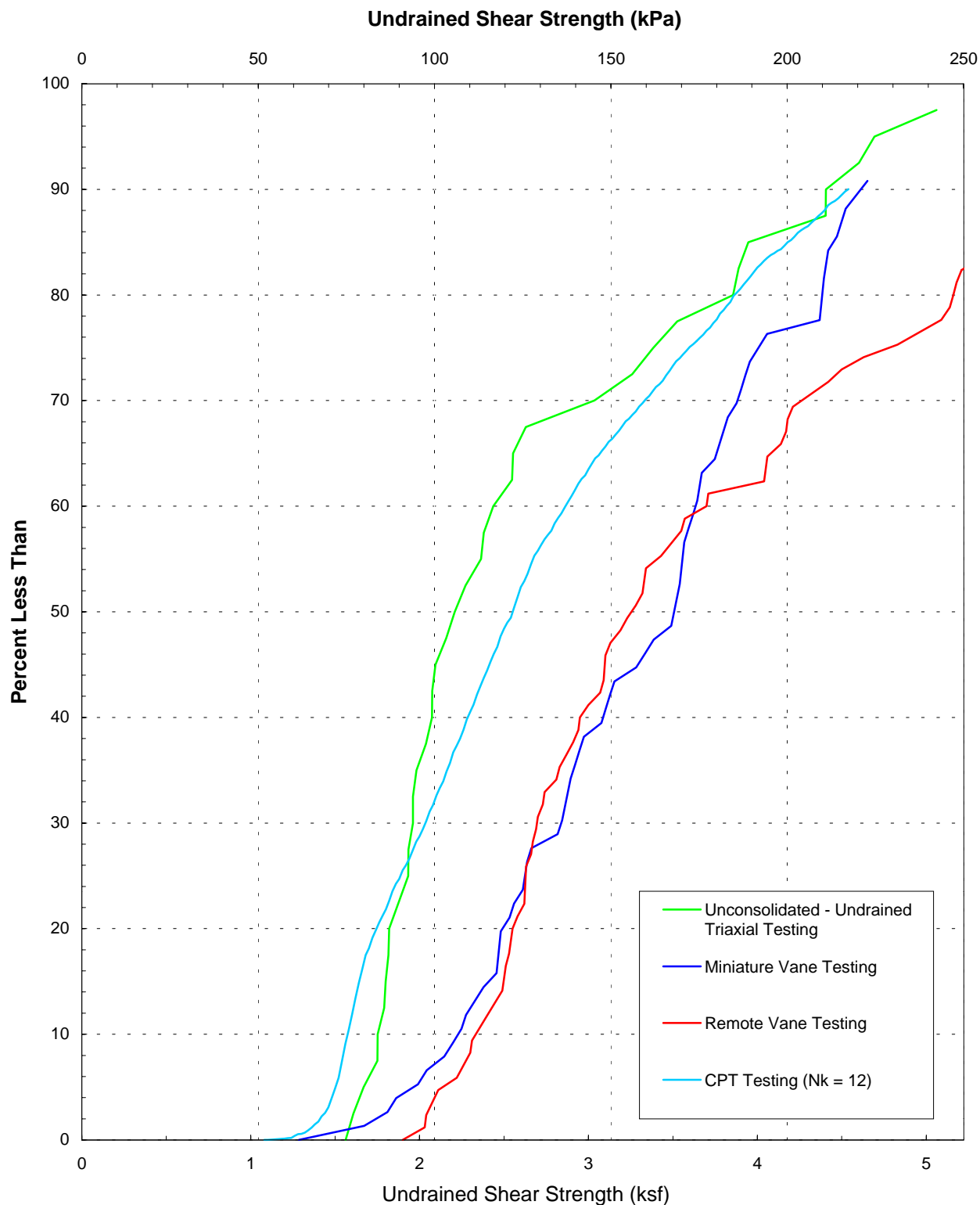
PLATE 5.13





**CUMULATIVE FREQUENCY OF UNDRAINED SHEAR STRENGTH
YOUNG BAY MUD
Oakland Shore Approach
SFOBB East Span Seismic Safety Project**

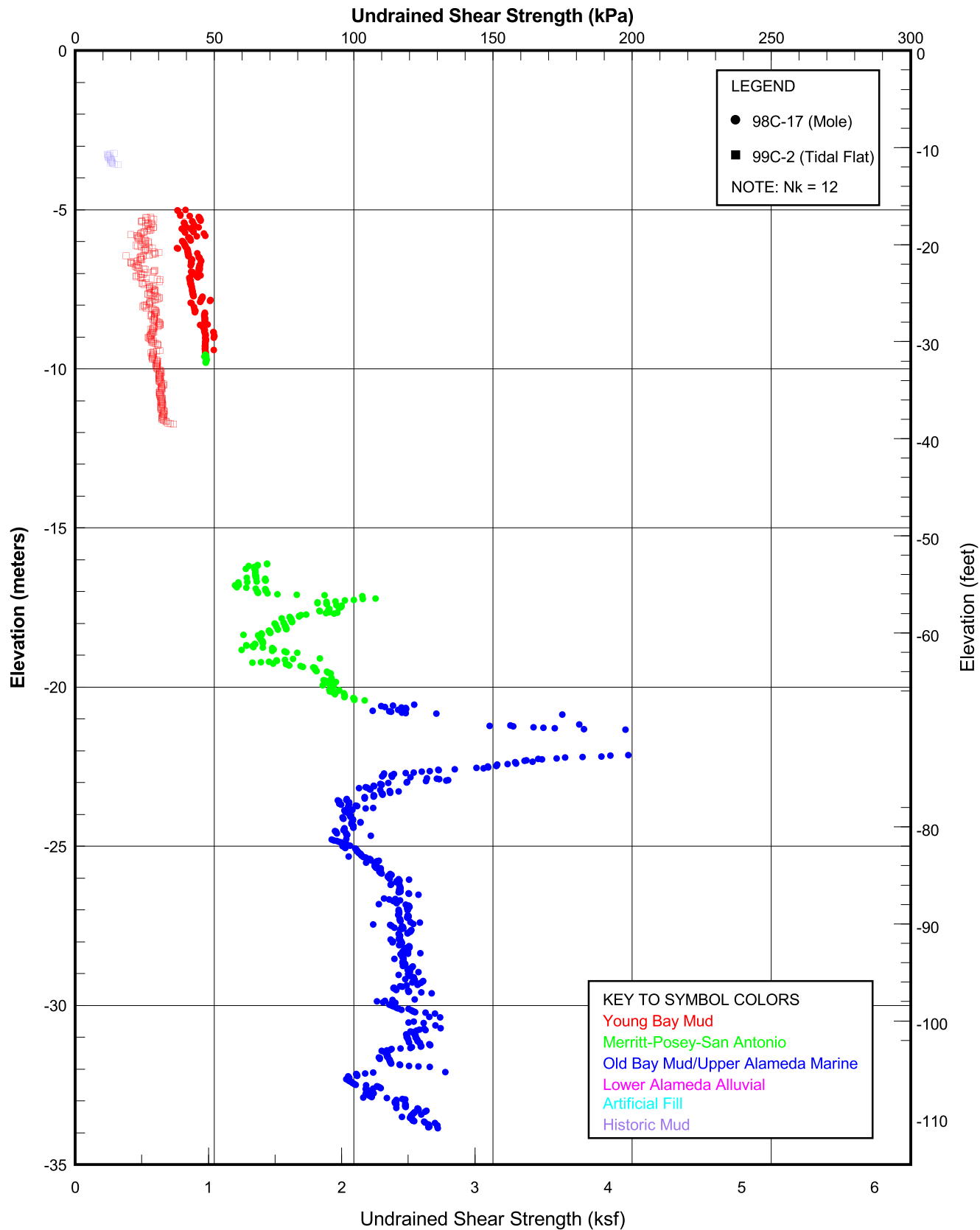




**CUMULATIVE FREQUENCY OF UNDRAINED SHEAR STRENGTH
OLD BAY MUD**

**Oakland Shore Approach
SFOBB East Span Seismic Safety**

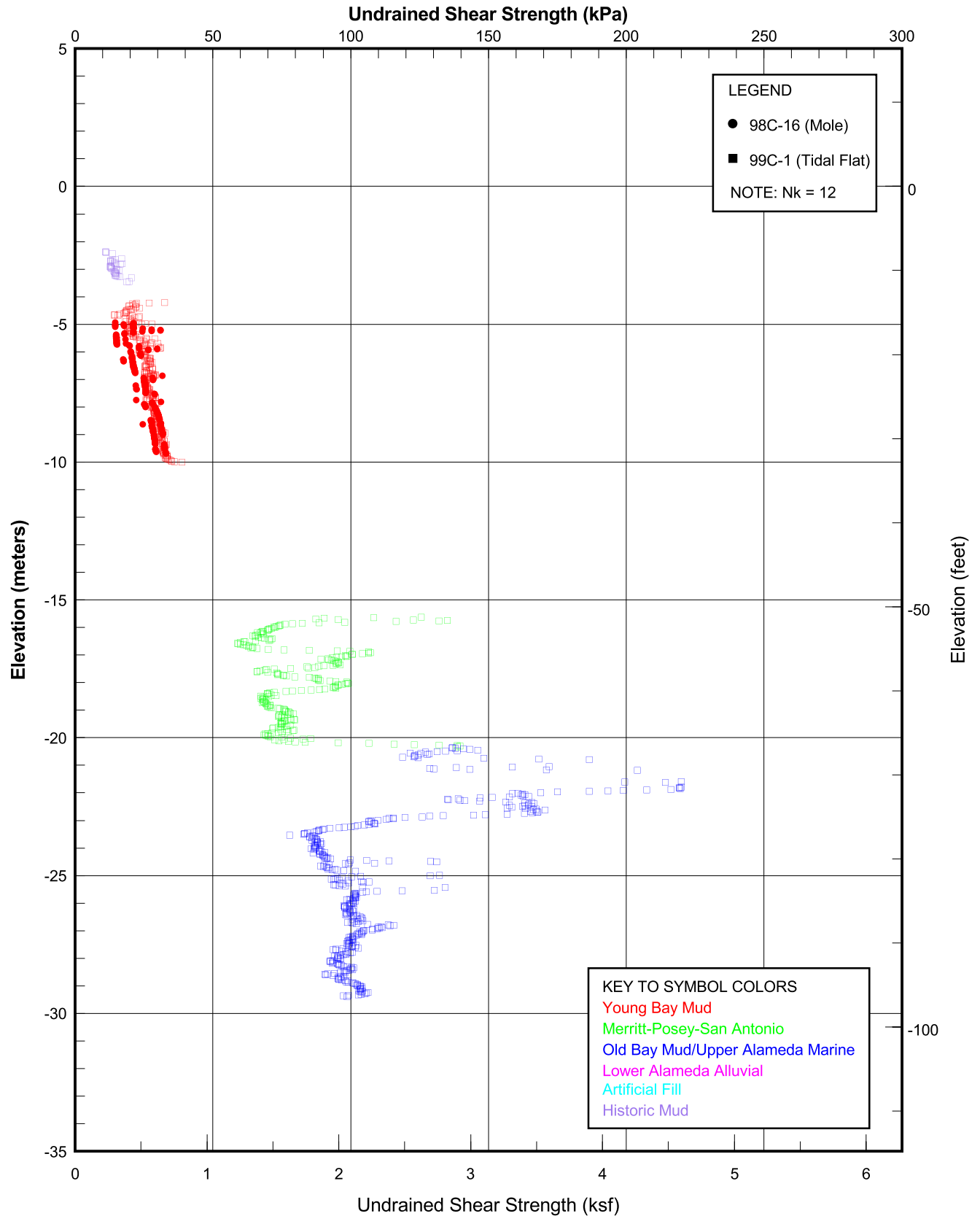




UNDRAINED SHEAR STRENGTH FROM CPT DATA ON THE MOLE AND TIDAL FLAT
Soundings 98C-17 and 99C-2

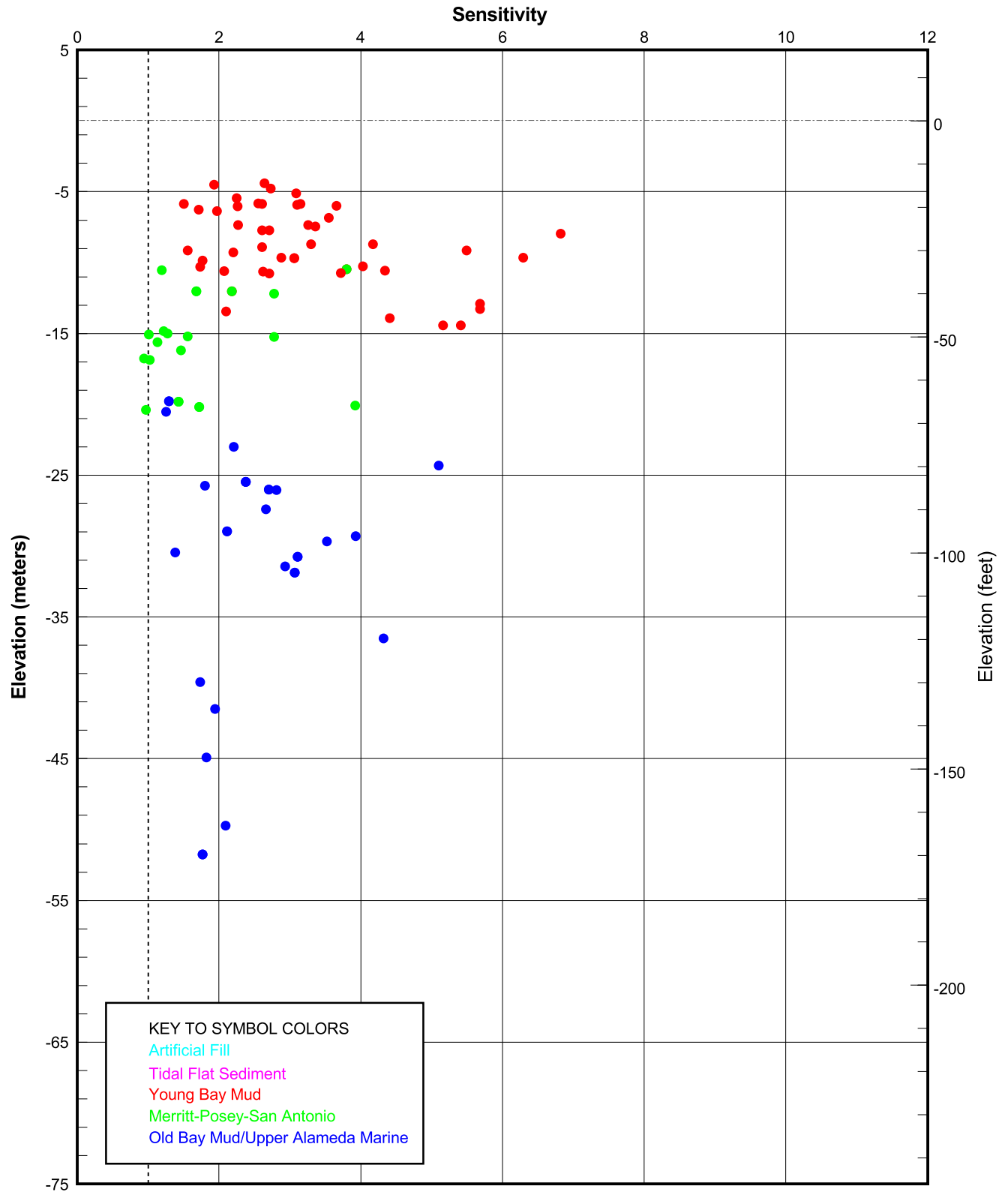
SFOBB East Span Seismic Safety Project





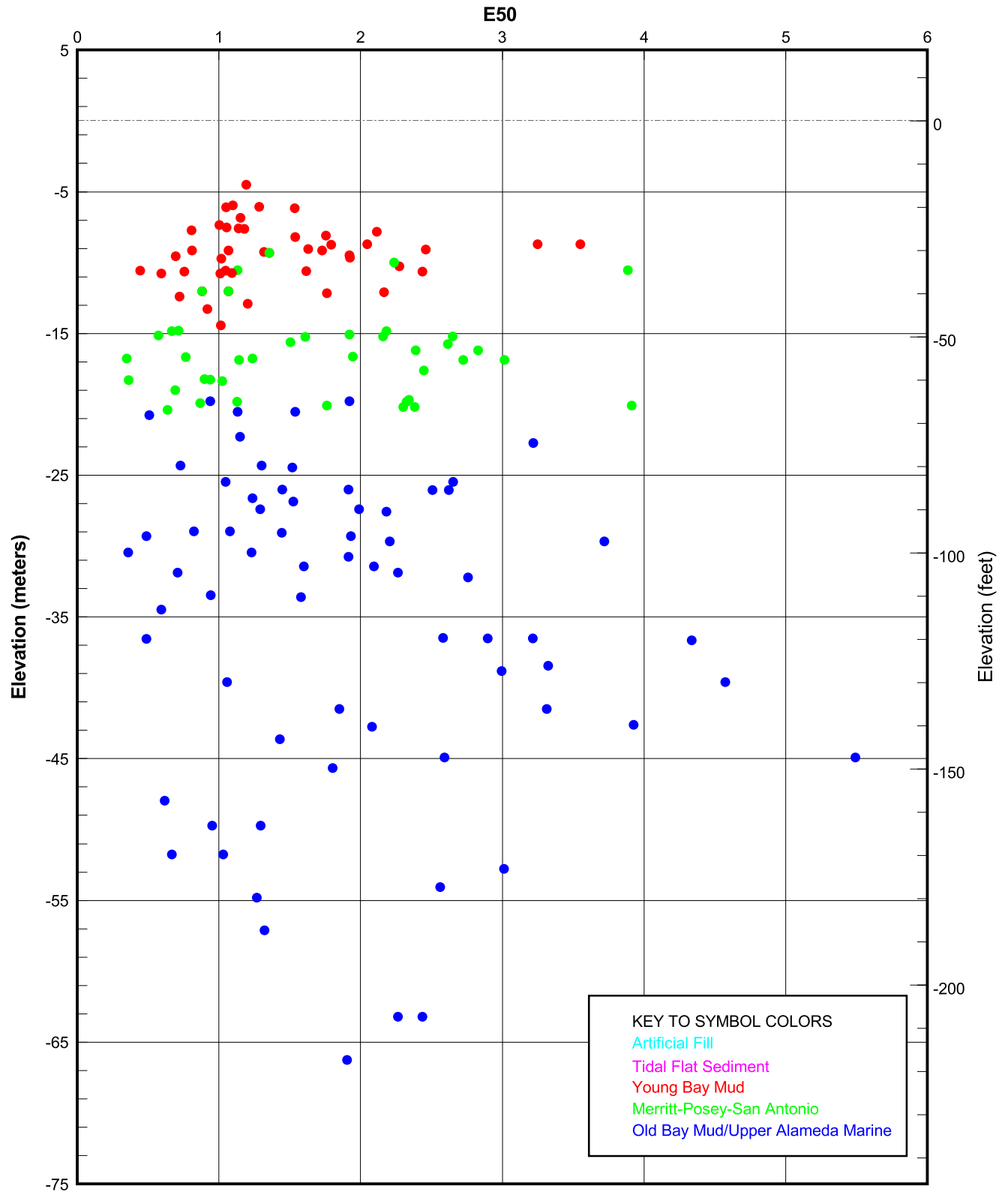
UNDRAINED SHEAR STRENGTH PROFILE
Borings 98C-16 and 99C-1
SFOBB East Span Seismic Safety Project





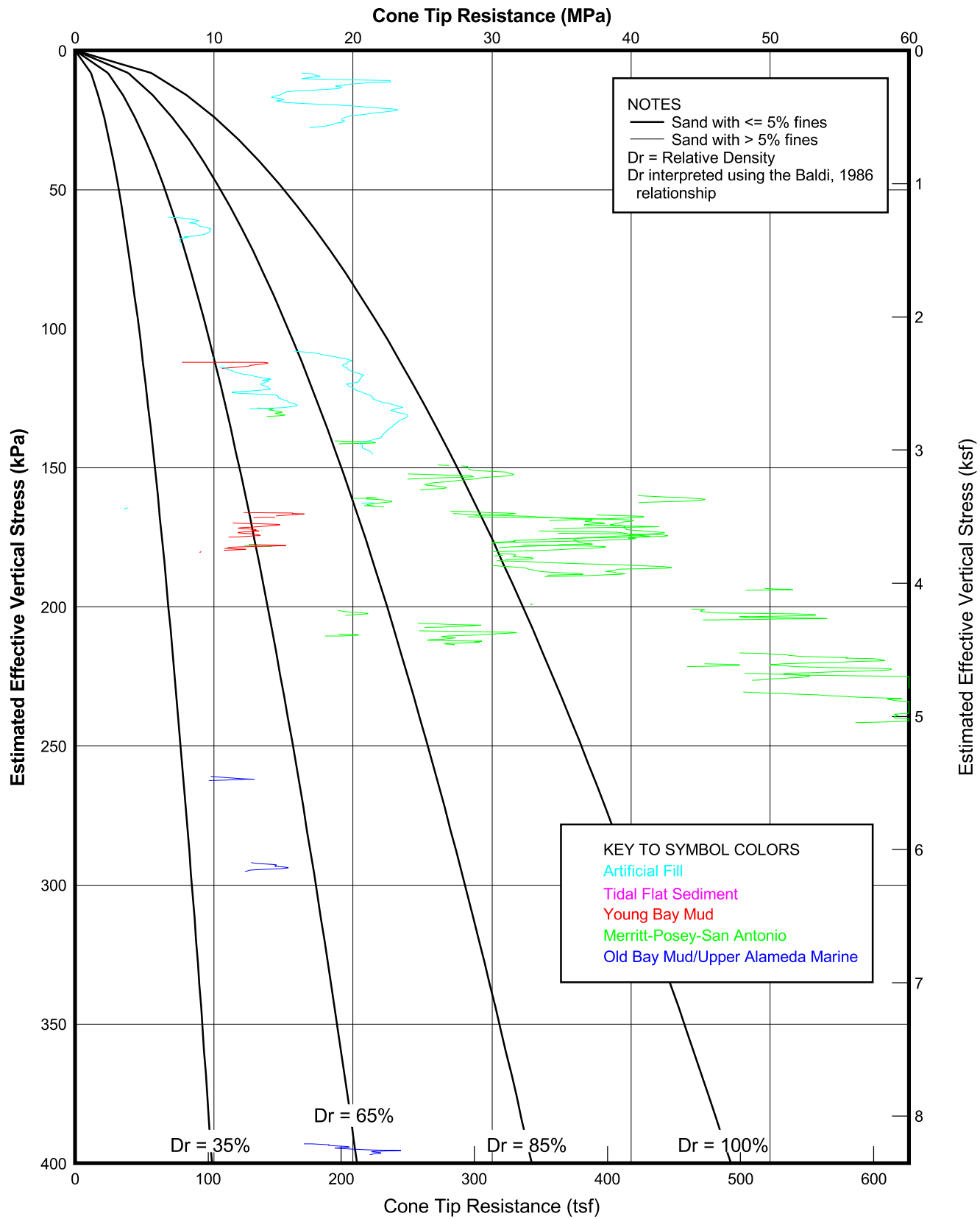
SENSITIVITY PROFILE
Oakland Shore Approach
SFOBB East Span Seismic Safety Project

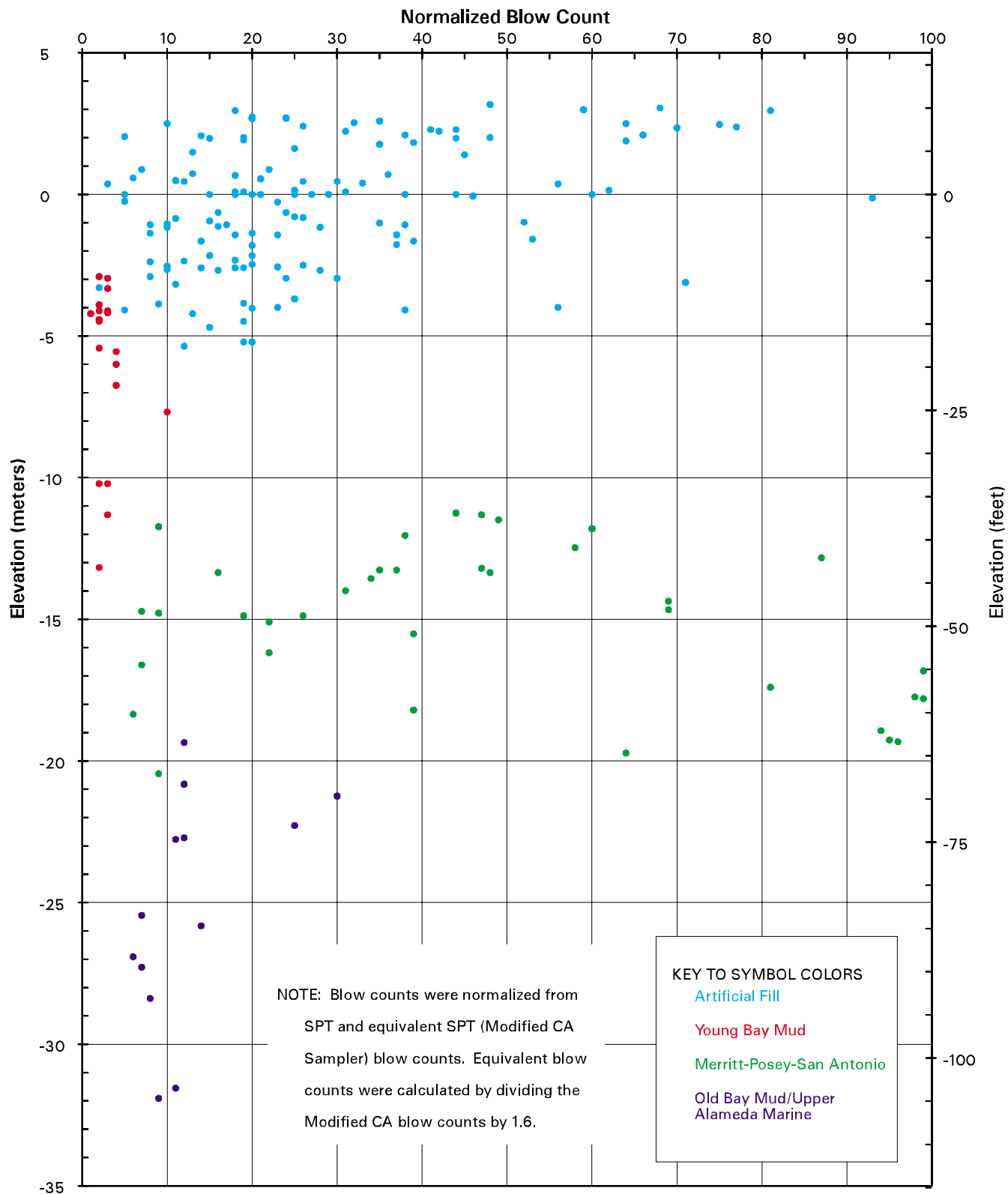




E50 PROFILE
Oakland Shore Approach
SFOBB East Span Seismic Safety Project

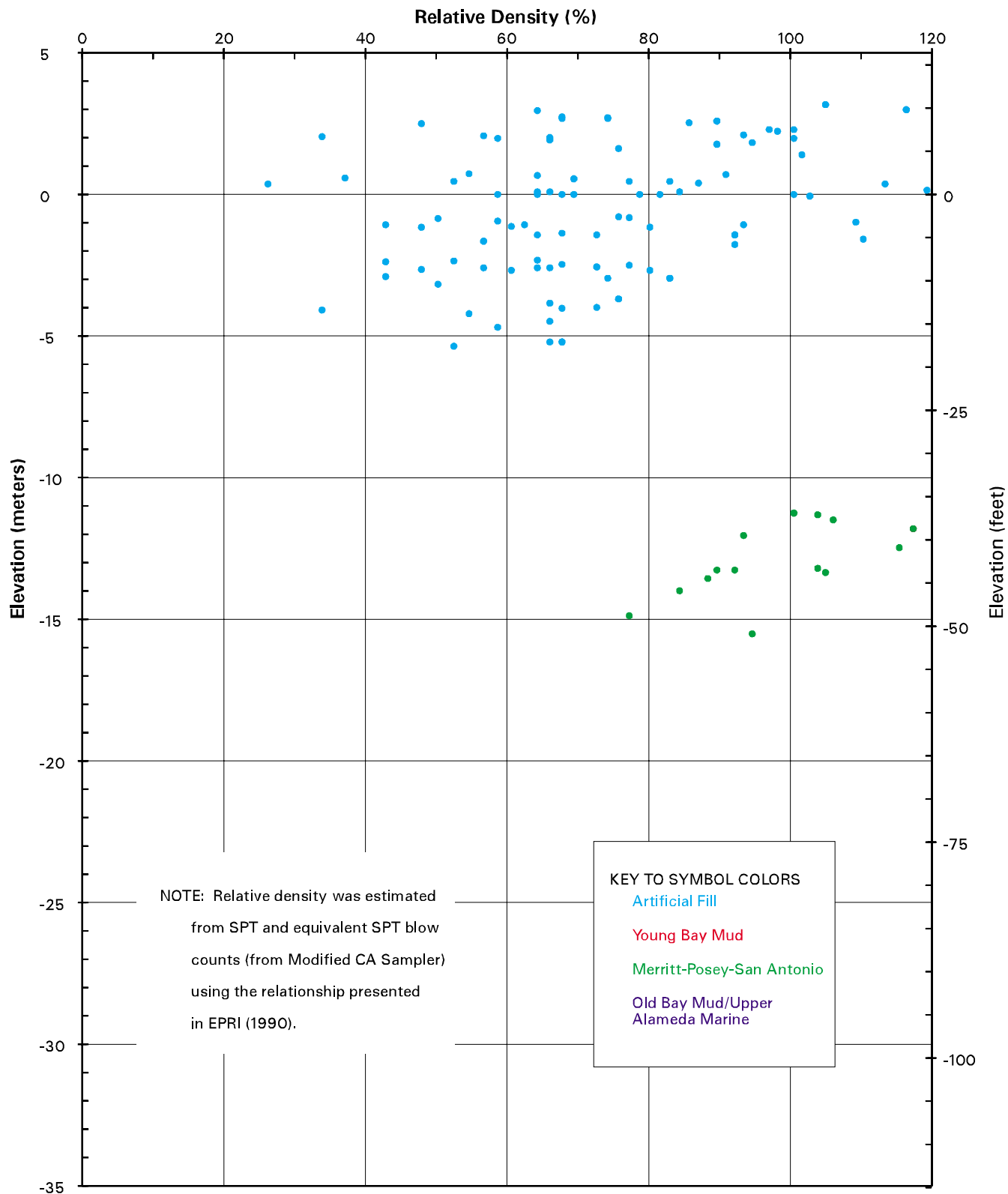






NORMALIZED BLOW COUNT PROFILE
Oakland Shore Approach
SFOBB East Span Seismic Safety Project





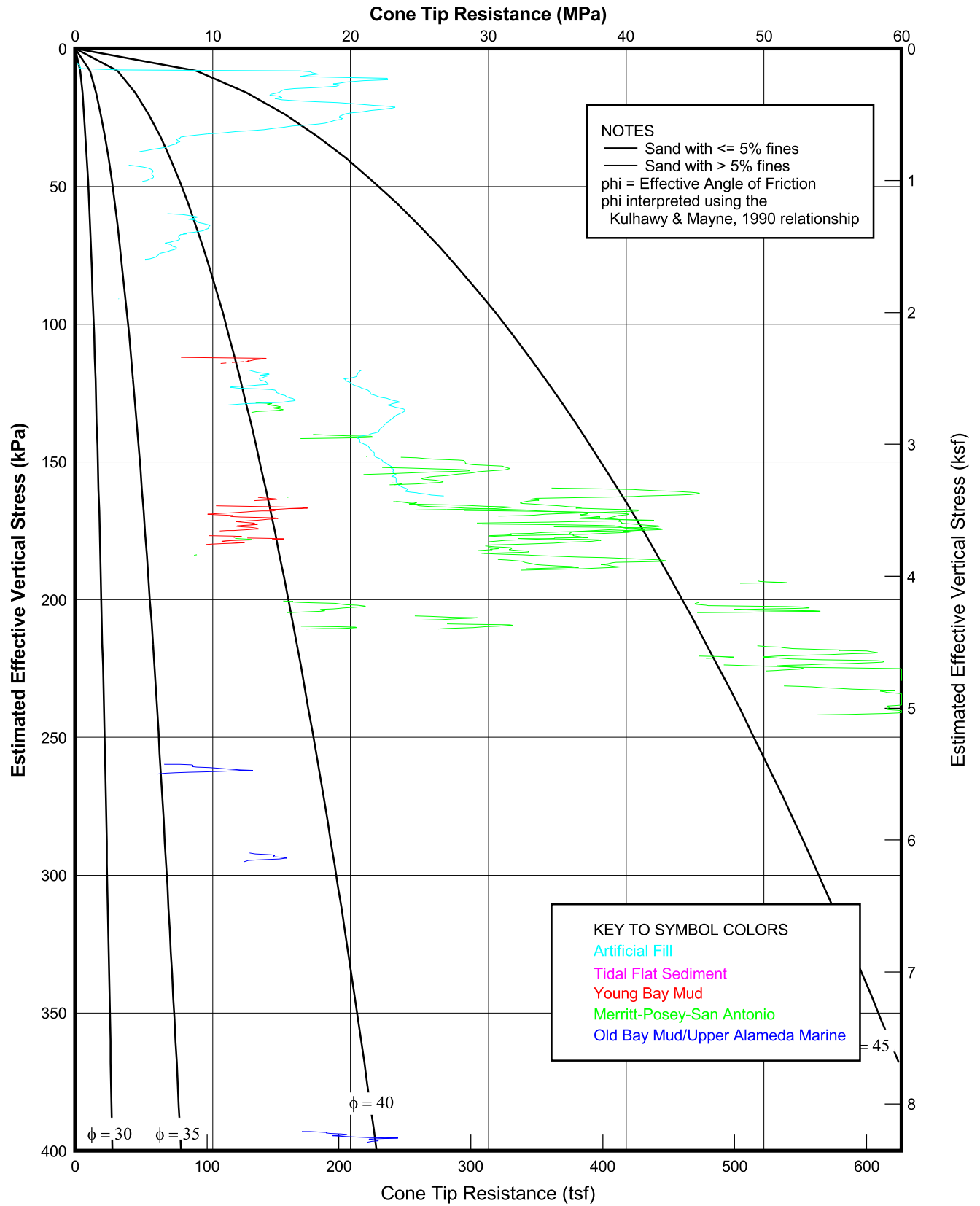
RELATIVE DENSITY PROFILE INTERPRETED FROM BLOW COUNTS

Oakland Shore Approach

SFOBB East Span Seismic Safety Project

PLATE 5.21



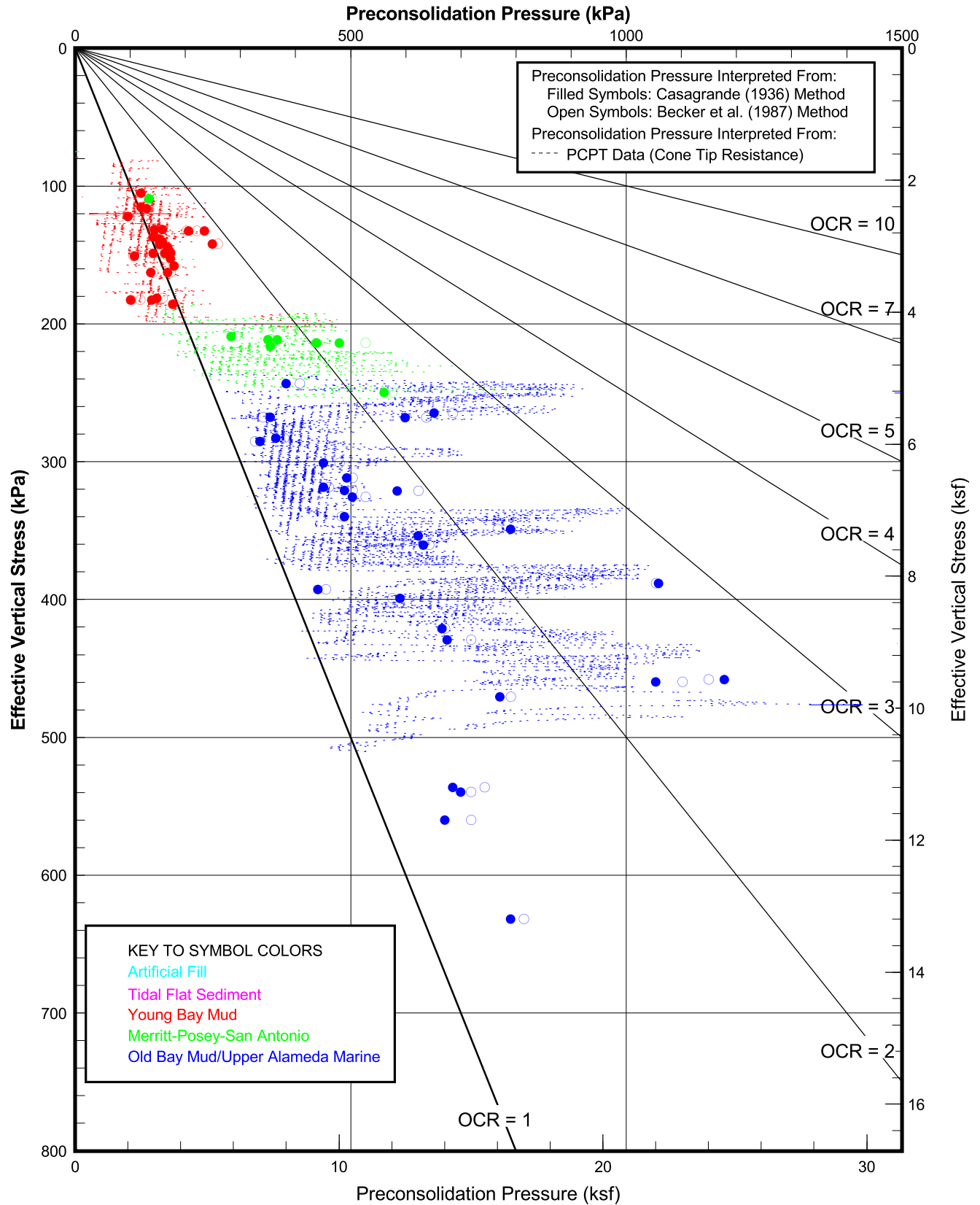


EFFECTIVE ANGLE OF FRICTION INTERPRETED FROM CPT DATA

Oakland Shore Approach

SFOBB East Span Seismic Safety Project





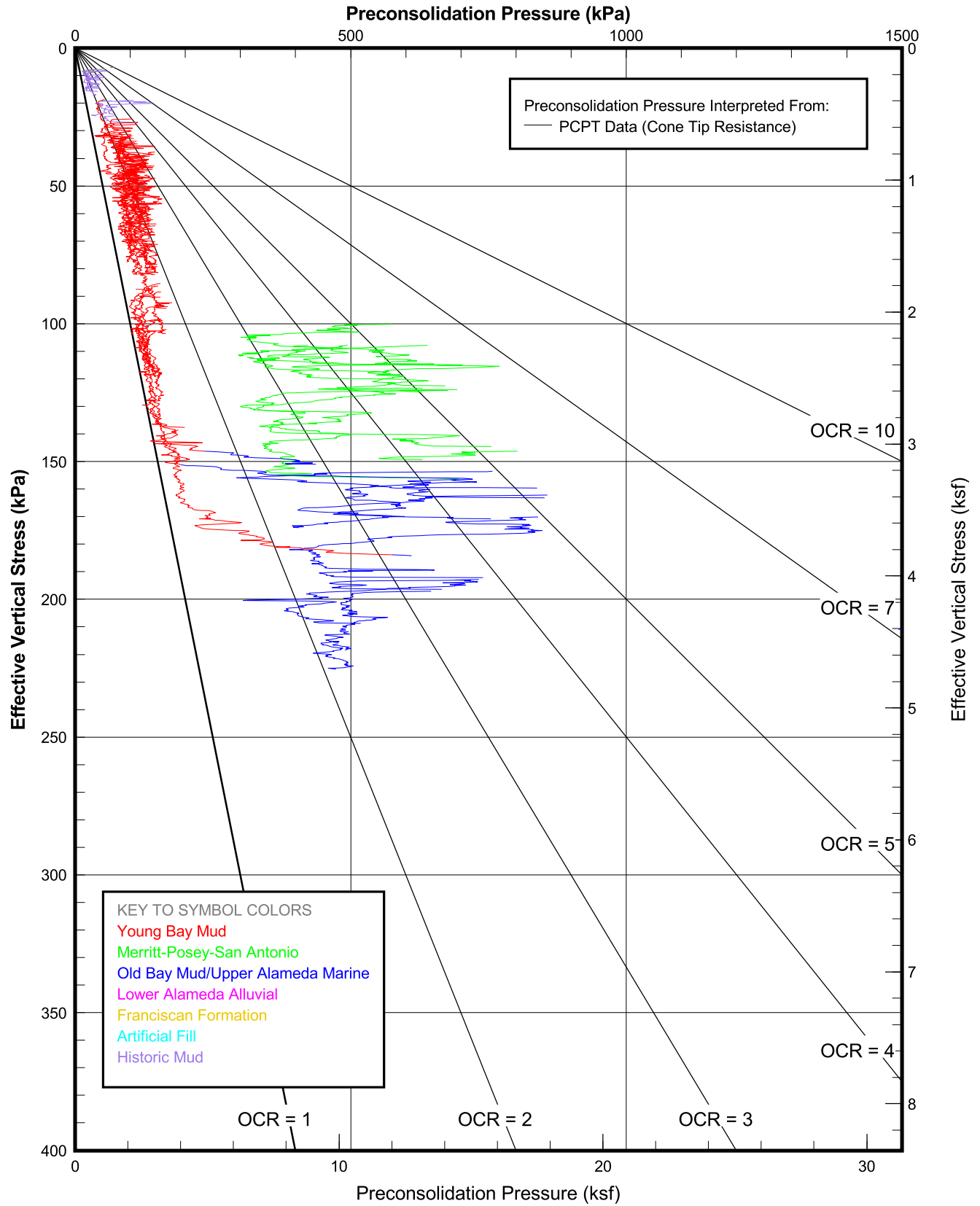
PRECONSOLIDATION STRESS INTERPRETED FROM CPT AND LABORATORY DATA

Oakland Shore Approach

SFOBB East Span Seismic Safety Project

PLATE 5.23





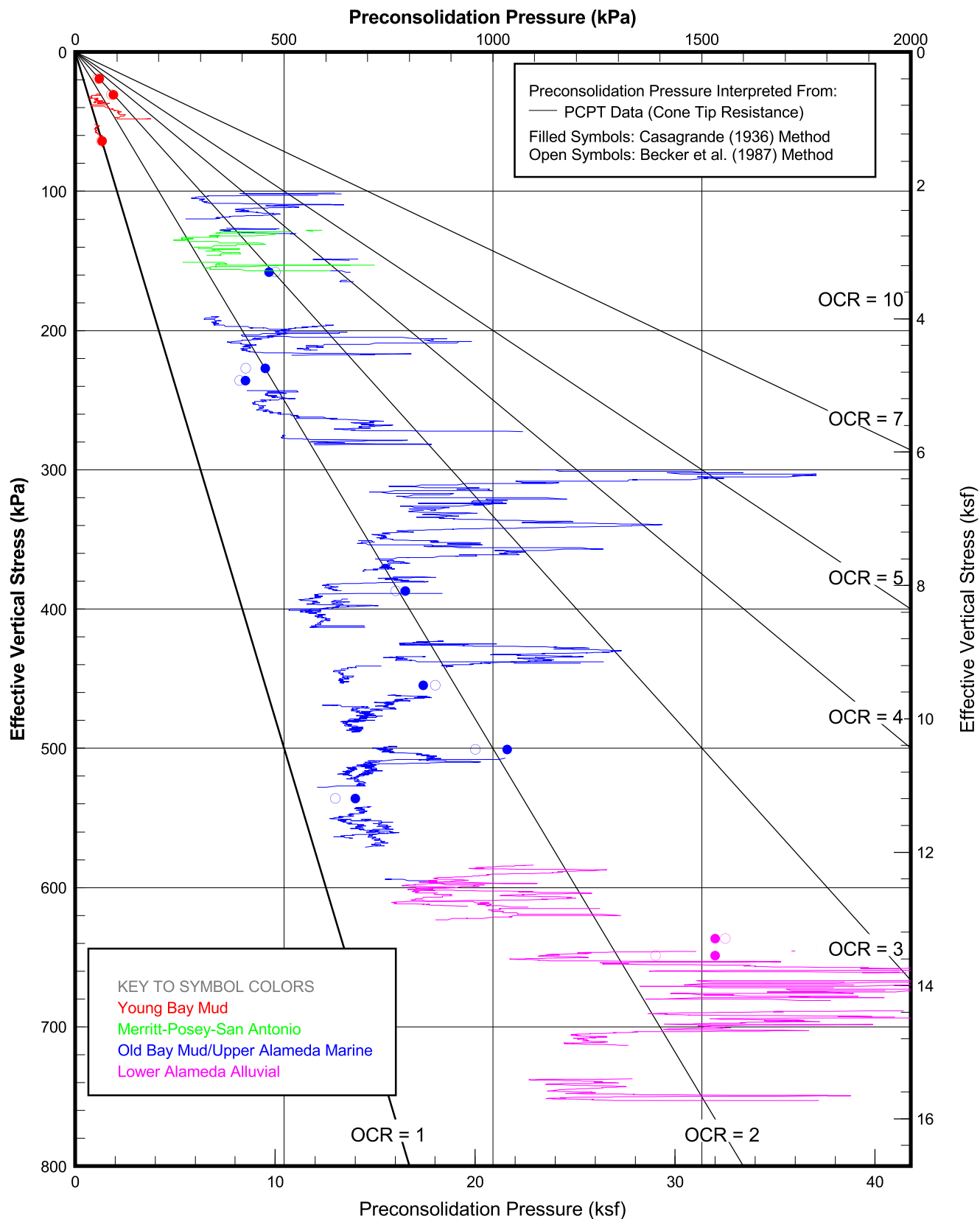
PRECONSOLIDATION PRESSURE INTERPRETED FROM CPT DATA

Borings 99C-1 through 99C-15

SFOBB East Span Seismic Safety Project

PLATE 5.24

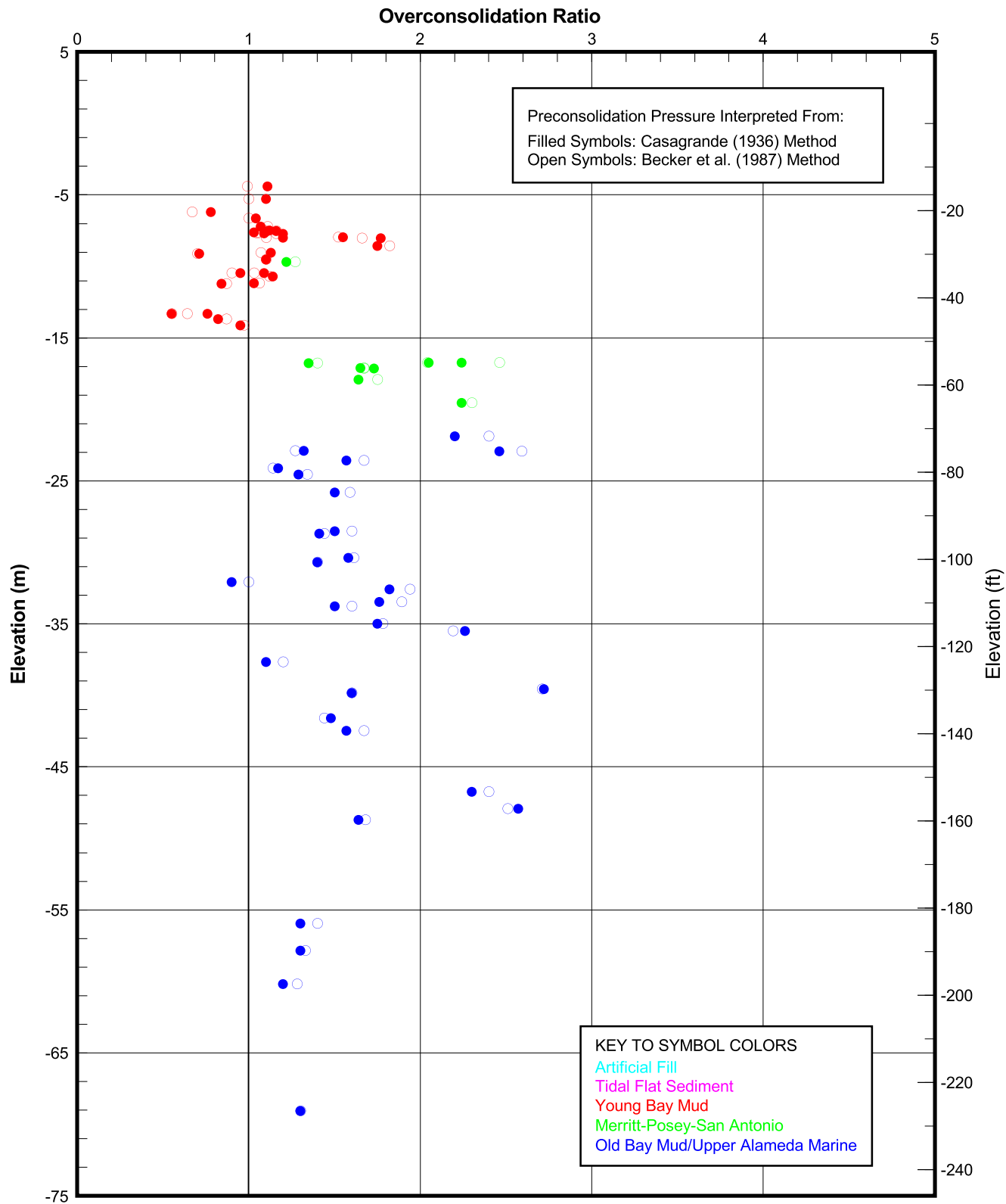




PRECONSOLIDATION STRESS FROM CPT AND LABORATORY DATA
Marine Borings 98-44 and 98-39
Oakland Shore Approach

SFOBB East Span Seismic Safety Project





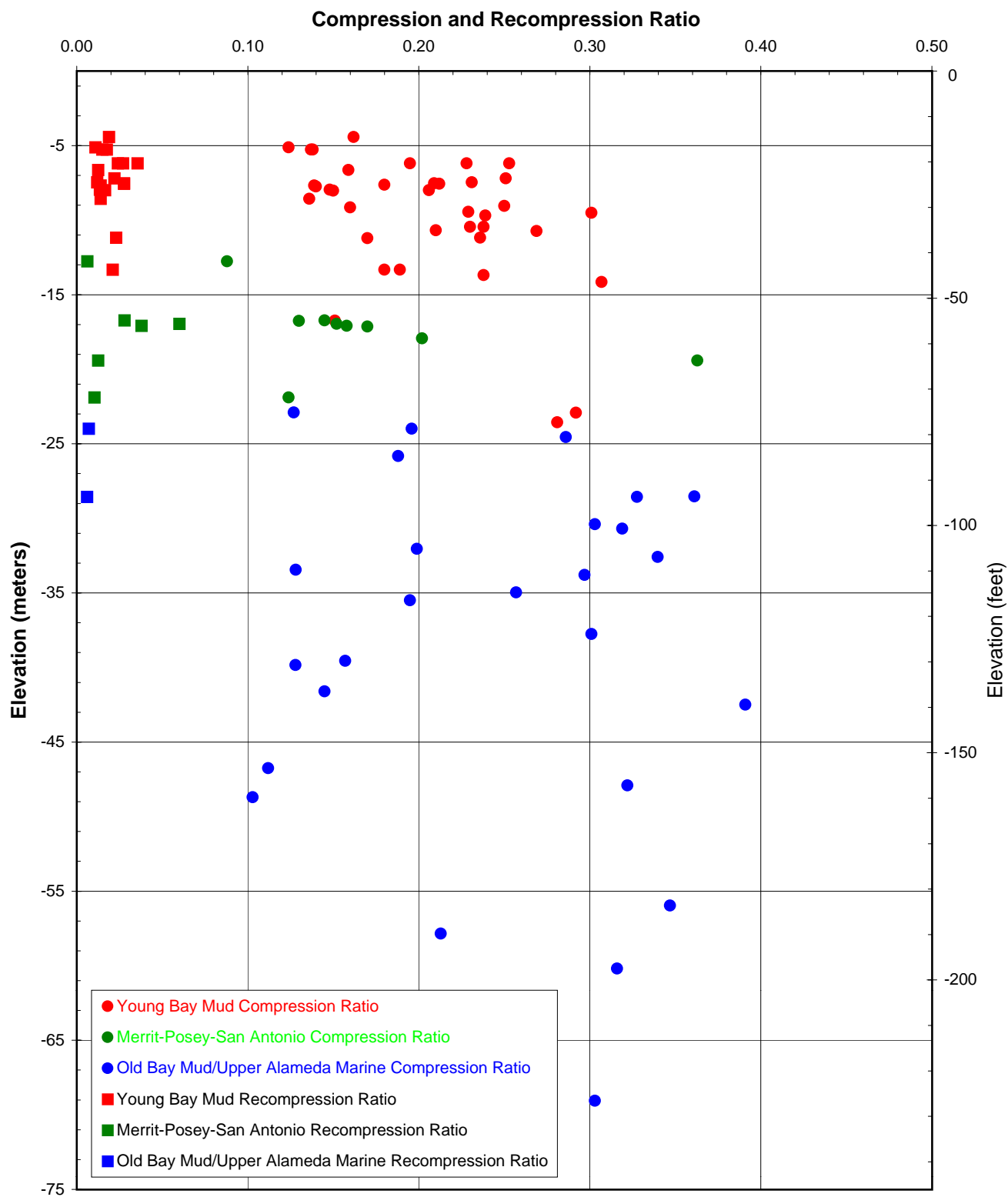
OVERCONSOLIDATION RATIO INTERPRETED FROM LABORATORY DATA

Oakland Shore Approach

SFOBB East Span Seismic Safety Project

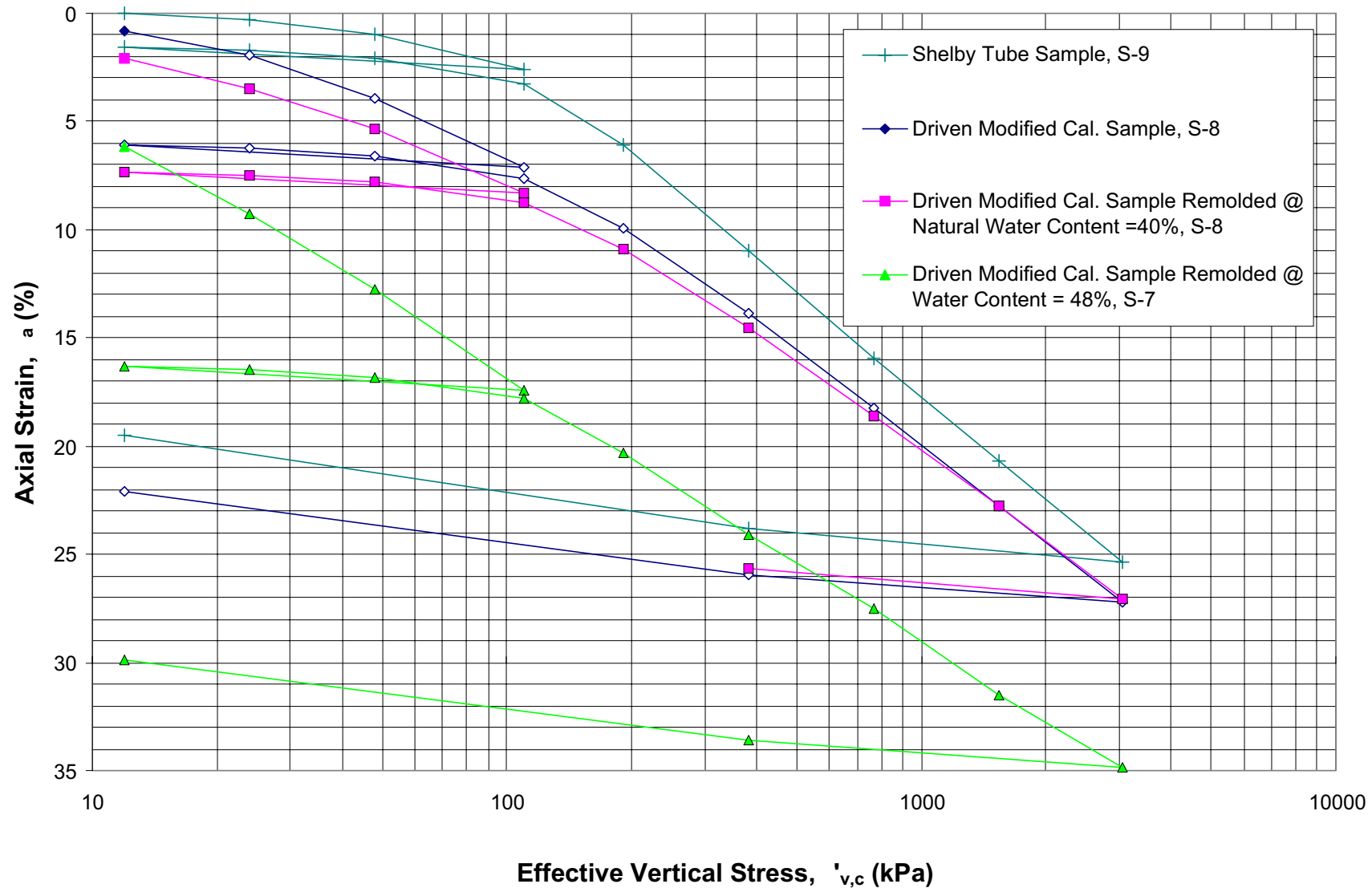
PLATE 5.26



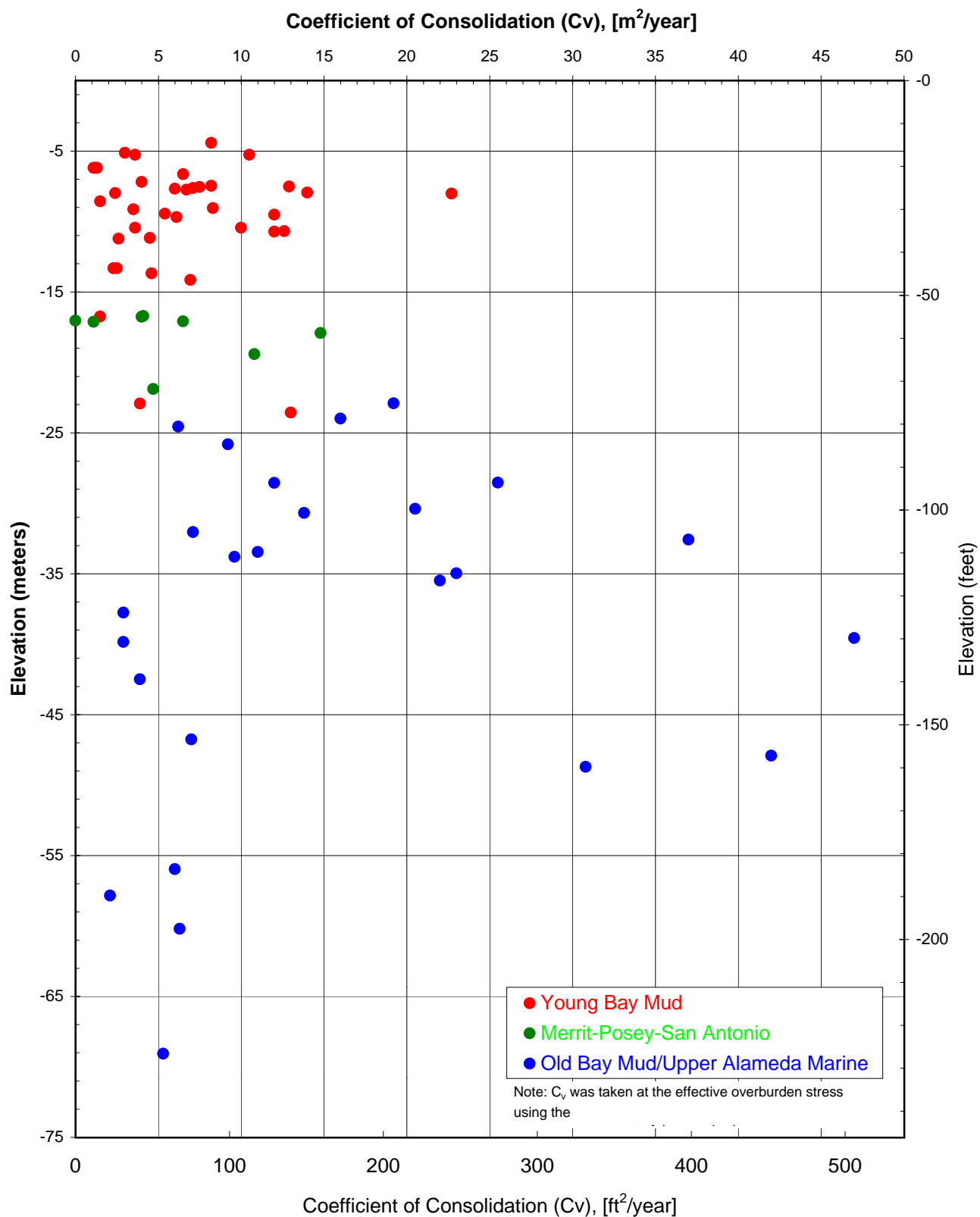


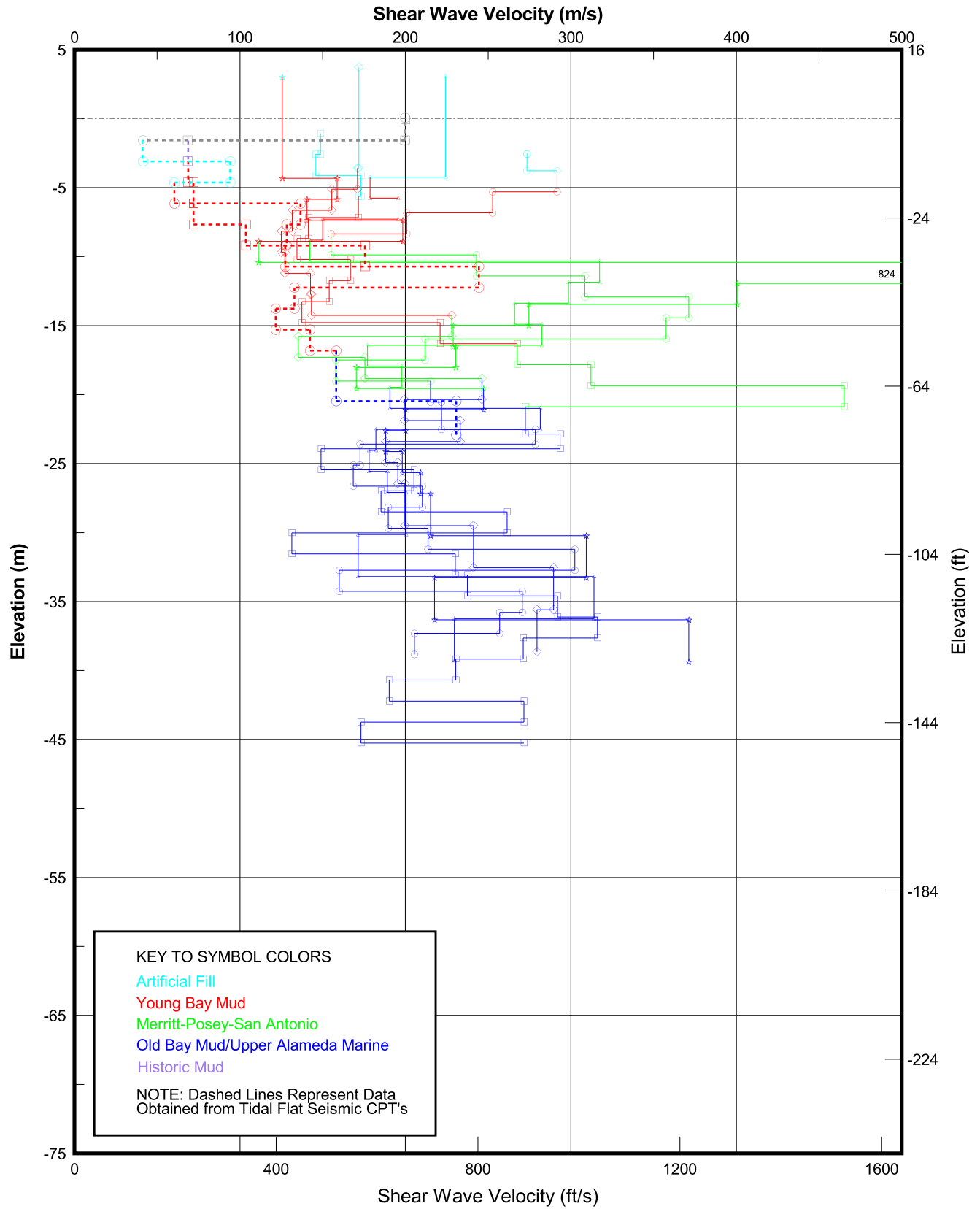
COMPRESSION AND RECOMPRESSION RATIO PROFILE
Oakland Shore Approach
SFOBB East Span Seismic Safety Project





REMOLDED CONSOLIDATION TEST RESULTS
 Boring 98-73; Sample 7 - Depth: 26 ft, Sample 8 - Depth: 26.5 ft, Sample 9 - Depth: 31 ft
 Oakland Shore Approach
 SFOBB East Span Seismic Safety Project

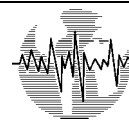




SHEAR WAVE VELOCITY PROFILE
Oakland Shore Approach
SFOBB East Span Seismic Safety Project



SECTION 6.0 OAKLAND MOLE STABILITY ISSUES



6.0 OAKLAND MOLE STABILITY ISSUES

6.1 INTRODUCTION

6.1.1 Description of Anticipated New Approach Fills

As described in Section 1.0, the limits of the structural and fill-supported components of the Oakland Shore Approach have varied during design. However, Caltrans has indicated that the 100-percent design will be for the Short Structure Alternative with a fill-supported roadway linking the structure to existing roads on the Oakland Mole.

The approximate location of the transition from the Short Structure Alternative to the new fill sections is shown on Plate 1.2. Along the eastbound alignment, the fill section is anticipated to begin at about eastbound Station 86+11. In that area, the eastbound alignment is underlain by the existing 1930-circa northern extension of the Mole. At the eastbound abutment, the proposed roadway surface is anticipated to be at about El. +6.9 meters, which would require up to about 4 meters of new approach fill. Along the westbound alignment, it is understood that the bridge abutment is to be located on the western jughandle at westbound Station 86+42. At the westbound abutment, the proposed roadway surface is anticipated to be at about El. +6.8 meters, which would require up to about 5 meters of new approach fill. East of the transition, the northern edge of the new fill section will extend out onto the existing tidal flat to the north of the Mole.

6.1.2 Overview of Subsurface Conditions

The Oakland Mole is a filled area consisting primarily of granular soils with high groundwater overlying Young Bay Mud. The lower, submerged portion of the granular fill is typically loose to medium dense. As shown on Plate 4.7 and described in Section 4.0, both the existing fill and underlying Young Bay Mud are thickest where the Mole overlies a buried Holocene paleochannel between the western and eastern jughandles.

As discussed in Section 5.0, the Young Bay Mud is essentially normally consolidated under the weight of the 1930s' northern Mole extension fill. Under the newer jughandles that extend farther to the north, however, the test data show the Young Bay Mud to be underconsolidated under the weight of the more recently placed fill.

To the north of the Oakland Mole, the exploration shows that the geologically Recent Young Bay Mud is overlain by 2 to 5 meters of very recent tidal flat sediments. The overlying, post-1930s sediments include local accumulations of beach sand and very soft clay (historical bay mud). Underlying those surface materials, there is a semicontinuous layer of sand that was deposited during the construction of the northern Mole extension in the 1930s.





6.1.3 Implications of Subsurface Conditions

The subsurface conditions have a number of geotechnical implications for the stability of the Oakland Mole and any new fill that might be placed to either raise or extend the Mole. The stability issues include both settlement and seismic performance considerations.

Static stability issues include considerations of:

- Compression and settlement due to the weight of additional fill;
- Variations of the total settlement due to the variable thicknesses of both the historical and Young Bay Muds, and the variations in the existing state of consolidation of the Young Bay Mud; and
- The time rate of settlement.

There is potential for seismic shaking to cause several problems, including:

- Liquefaction of the saturated fill;
- Ground surface settlement due to seismic shaking;
- Differential settlement and gapping between the proposed bridge abutment or slab deck and adjacent ground;
- Cyclic degradation and loss of strength in the Young Bay Mud; and
- Lateral spreading or large lateral soil displacements if liquefaction or other strength degradation occurs behind the present slopes.

6.2 SETTLEMENT CONSIDERATIONS

6.2.1 Sources and Implications

Ground settlements will result from volume change in compressible soils due to the primary consolidation under the weight of the existing fill, consolidation under the weight of new fill, and secondary consolidation (creep) under the existing and/or additional stresses. The effects of ground settlement include: a) pile downdrag, b) gapping and related movement, c) damage to roadway pavements and foundations, and d) damage to structures as a result of differential settlements.

Where the existing ground surface of the Mole will be raised, significant short-term and long-term ground settlements are expected as a result of consolidation of the Young Bay Mud. Some additional settlement also may be realized due to consolidation in the deeper clay layers in the Merritt-Posey-San Antonio Formations and the underlying Old Bay Mud. Because the test data suggest that the Young Bay Mud is underconsolidated beneath the jughandle extensions, the





settlement due to the placement of additional fill is anticipated to be greater beneath those newer fill areas. Short-term ground settlement also could occur in the Mole fill in the areas underlain by rock dikes or riprap, rubble, debris, and where underground voids and burrows exist in the fill.

The settlements beneath new fill to the north of the existing Mole will be influenced by the same factors described above. However, to the north of the existing Mole, the thickness of new fill will be much greater than that required to raise the existing Mole to the same elevation. Further, the underlying Young Bay Mud to the north of the existing mole is consolidated to a much lower stress state than it is beneath the Mole. Therefore, the settlements beneath the new fill to the north of the existing Mole will be larger. Additional settlements also should be expected due to the consolidation of the historical bay mud layer.

6.2.2 Historical Settlement of 1930s Northern Mole Extension

Historical settlement measurements (Caltrans, 1933) following construction of the northern Mole extension in the 1930s are reproduced on Plate 4.3. As shown, those records indicate that:

- Outside of the paleochannels, as much as 1 meter of settlement occurred within the first 5 years, but little additional settlement occurred afterwards.
- Above the paleochannel to the west of the turnaround jughandle, about 1.5 meters of settlement occurred within the first 5 years, and about 0.1 to 0.2 meter of additional settlement occurred over the next 15 years.
- In the radio tower area farther to the east, about 1.5 to 2 meters of settlement occurred in the first 5 years over the deeper paleochannel present at that location, and as much as 1 meter of additional settlement occurred over the next 15 years.

The historical data illustrate that the total settlement will be proportional to the thickness of the Young Bay Mud, and the rate of settlement will be inversely proportional to the thickness of the Young Bay Mud.

6.2.3 Predicted Total Settlement Due to New Fill

A preliminary assessment of potential settlement due to the weight of new fill (reproduced in Volume 4) was conducted to assist in a cost comparison of the slab-on-pile versus the fill-supported slab roadway options. This assessment is presented in Volume 4. Caltrans will conduct further studies to finalize the design of the new approach fill. The preliminary settlement assessment for the new fill included:

- Research on construction of the existing Mole,
- Review of settlement history of the existing Mole,





- Review of the failure of the existing Mole during construction,
- Consideration of the construction sequence,
- Settlement analyses for the new fill along the eastbound alignment, and
- Settlement analyses for the new fill along the westbound alignment.

Based on the historical settlement data, total ground settlement from new approach fill being placed on existing soils north of the present slopes (up to El. +4 meters) will be on the order of 10 percent of the underlying Young Bay Mud thickness. The primary conclusions drawn from the study are as follows:

- For an assumed 5.5 meters of new fill on the new westbound alignment, the maximum ultimate settlement is anticipated to be about 1.5 meters.
- Along the northern edge of the existing westbound roadway, the maximum additional settlement is expected to be on the order of 0.15 meter.
- The ultimate settlement at the abutment fill for the new eastbound approach is expected to be about 0.6 meter.
- Secondary settlements are estimated to be on the order of about 6 mm per year.
- The use of lightweight fill may be a feasible option for the proposed eastbound abutment backfill and approach embankment.

Detailed evaluations and design of fill-supported roadway sections on the Mole are being performed by Caltrans.

6.2.4 Time Rate of Settlement Considerations

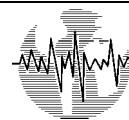
According to historical settlement measurements (refer to Volume 4), a settlement period of over 15 years would be required to achieve 90-percent consolidation in the Young Bay Mud. Based on preliminary studies (presented in Volume 4), the settlement period potentially can be reduced to less than 1 year using a wick drain design based on 1-meter, on-center spacing. The selection and design of appropriate ground improvement (drainage) methods (including wick drain systems) and construction sequences are being performed by Caltrans.

6.3 SOIL LIQUEFACTION

6.3.1 Definition

Liquefaction is the loss of strength that can occur in a loose, saturated sand during (or immediately following) seismic shaking. As loose granular soils are shaken, their tendency to contract and compress leads to the development of positive pore pressures. If the intensity or duration of the shaking is great enough, the buildup in pore pressure can produce a significant loss of shear strength. If the shaking continues after the onset of liquefaction, liquefaction can





produce a number of ground effects (e.g., sand boils, settlement, lurching, and lateral deflection). Liquefaction also can cause a loss of axial capacity of shallow or deep (due to downdrag) foundations, loss of lateral pile capacity, and lateral ground spreading.

The susceptibility of a granular soil to liquefaction is a function of the gradation, density, and fines content of the soil. Susceptibility to liquefaction decreases with respective increases in: a) distribution of grain size, b) soil density, c) fines content, and d) clay-size fraction of the fines. The susceptibility to liquefaction also tends to decrease as a function of the age of the deposit.

6.3.2 Method of Evaluation

Overview. Evaluation of the liquefaction susceptibility of coarse-grained layers and deposits primarily was based on the empirical procedure recommended by the National Center for Earthquake Engineering Research (NCEER, 1997). In the NCEER procedure, potentially liquefiable soil strata are identified as being those layers that are relatively loose, submerged granular sediments. Soil strata above the assumed groundwater level were considered not susceptible to liquefaction.

NCEER recommendations were used to compute liquefaction susceptibility using both boring SPT and CPT data. The available cyclic shear resistance of the potentially liquefiable strata encountered (based on the normalized SPT N-value or CPT tip resistance) was compared to the estimated cyclic shear stress that would be induced by a given earthquake. The estimated factor of safety against liquefaction is the ratio of the available cyclic shear resistance to the induced cyclic shear stress.

The estimated factors of safety against liquefaction at various depths are a function of the estimated overburden pressure at that depth. In general, higher factors of safety against liquefaction are calculated for higher overburden pressures. We note that most of the liquefaction analyses were performed using the existing Mole geometry and a groundwater level at El. 0 meter MSL. Several analyses, however, also were conducted for the assumed new ground surface elevation. When the profiles of the new fill sections are finalized, additional evaluations should be performed to check the validity of the results presented below.

Boring SPT Data. For use with the NCEER procedure, sample depths, fines contents, soil unit weights, and field SPT N-values were interpreted and summarized from the borings. The SPT data were then normalized to an overburden pressure of 0.1 MPa and corrected for fines content. Because the SPT sampling procedure consisted of a standard rope and cathead SPT hammer, the energy delivered to the sampler was assumed to be consistent with the conventional 60-percent efficiency for the SPT sampling procedure.

For this evaluation, sublayers were identified at each boring location. Typically, the overall stratigraphic description was obtained from the descriptions presented on the logs, and





sublayers were created on the basis of SPT blow counts and fines contents. Usually, one sublayer was created for each sample obtained in the boring and that layer was assigned the blow count associated with the sample. A fines content value was assigned to each of those sublayers on the basis of either laboratory tests performed on the sample or the nearest fines content measurement considered to be representative of the sublayer. Unless bounded by one of the stratigraphic layers shown on the boring logs or the estimated groundwater table, sublayer boundaries were selected midway between adjacent samples.

CPT Data. Liquefaction susceptibility also was calculated using the NCEER procedure based on the CPT tip resistance. For those analyses, the measured tip resistances were corrected for fines content using the procedures suggested in NCEER (1997) and normalized to an overburden pressure of 0.1 MPa.

6.3.3 Earthquake Ground Motion Assumed for Analyses

The seismic hazard analyses for the project (Fugro-EM, 2001g) have defined the following design earthquakes: a) a magnitude 7.5 event on the Hayward fault, and b) a magnitude 8 event on the San Andreas fault. Either of those two events is capable of producing a peak horizontal ground acceleration (PGA) on rock of at least 0.52g. The preliminary liquefaction analyses results presented subsequently assumed that an earthquake magnitude of 7.5 produced a PGA of 0.52g at the Oakland Mole. In addition, a limited number of analyses were conducted using lesser ground motions to evaluate the threshold ground motions that might be expected to produce liquefaction at the Mole.

6.3.4 Presentation of Results

Using the NCEER (1997) procedure, liquefaction analyses were performed for the borings and CPTs along longitudinal cross sections A-A' and B-B' as well as perpendicular cross sections C-C' and E-E' (the locations of which are shown on Plate 4.5; the geologic cross sections are included in Section 4.0). The results of the analyses of a magnitude 7.5 earthquake producing a PGA of 0.5g are shown on Plates 6.1 through 6.4. A key to the symbols used on the liquefaction analyses cross sections is provided on Plate 4.6.

Also shown on each plate is the respective equivalent PGA that would likely induce similar levels of cyclic shear stress for earthquake magnitudes of 6.0, 6.5, and 7.0. The equivalent PGAs were estimated using the Idriss Magnitude Scaling Factors (as recommended by the NCEER [1997] committee as a lower bound).

On the liquefaction analyses cross sections, the tip resistance and SPT N-values (or equivalent N-values [blow count divided by 1.6] for the California modified sampler) are shown as yellow bars to the right of the axis for each boring and CPT location. Also shown on each plot are the estimated SPT blow count and CPT tip resistance (red line) that would be required (based on NCEER, 1997) to prevent the occurrence of liquefaction for the assumed earthquake





magnitude and PGA. In general, layers and zones where the SPT or tip resistance required to preclude the occurrence of liquefaction is less than the normalized measured tip resistance are considered liquefiable. Where the resistance required to prevent liquefaction is less than the measured resistance, the zone that represents the deficiency is shaded blue.

6.3.5 Conclusions

Submerged Fill. As described in Section 5.0, the saturated granular Mole fill is generally loose to medium dense. The N_1 -values in the submerged fill typically are between about 9 and 23, and average about 14.

The analyses results indicate that liquefaction of the Mole fill beneath the water table (El. 0 meter MSL) is likely to occur under the design seismic conditions. As shown on Plates 6.1 through 6.4, about 3.5 to 5 meters of the fill appear to be liquefiable under the analyzed ground motions. As shown, the measured resistances are typically about one-third to two-thirds of the resistances required to prevent liquefaction. The cross sections suggest that the liquefiable submerged fill layers are generally continuous beneath the Mole. The analyses results also show that the layer of sand placed to the north of the Mole during the 1930s Mole construction also is liquefiable.

Although not presented, analyses for other levels of ground shaking suggest that localized zones of the submerged fill are likely to experience liquefaction during a magnitude 7.5 earthquake at a PGA of about 0.2g. The analyses also suggest that widespread liquefaction will begin to occur during a magnitude 7.5 earthquake at a PGA of about 0.25 to 0.3g.

Those results are considered generally consistent with historical observations following the 1939 and 1981 (Loma Prieta) earthquakes, which probably produced PGAs of about 0.2 to possibly 0.3g at the site. Following the 1981 Loma Prieta event, sand boils and other ground deformations were observed to the east of the project site at the Toll Plaza. Documented records of those two historic earthquakes, however, show no reports of damage to the bridge or roadways in that area.

Native Merritt Sand. Merritt Sand is typically dense to very dense sand with an uncorrected SPT N-value of from 30 to more than 50 blows per 0.3 meter. As shown on Plates 6.1 through 6.4, the evaluation suggests that the Merritt Sand layer is unlikely to liquefy under the design seismic shaking.

6.4 GROUND SETTLEMENT DUE TO EARTHQUAKE SHAKING

Ground settlement (and other ground effects) during seismic shaking can occur due to: a) liquefaction, b) lateral spreading, and c) the compression of loose fill with rubble, voids, animal burrows, or other similar conditions. Settlements due to liquefaction and/or in loose, dry fill can be estimated using empirical procedures. Those estimates are based on level ground





conditions and are described below. Because the Mole is adjacent to a slope and lateral spreading is a significant possibility, the total ground settlements should be expected to be larger than estimated below for level ground conditions. Earthquake-induced settlement can cause downdrag on deep foundations, distress to pavements, gaps between ground support pavements and approach slab or abutments, and structural damage to structures founded on shallow foundations on or within the fill.

6.4.1 Liquefaction-Induced Settlement

The liquefaction cross sections provided on Plates 6.1 through 6.4 show an estimate of vertical ground settlement that may occur due to liquefaction-induced settlement. These estimates are based on the measured SPT N-values and CPT tip resistances, factors of safety against liquefaction calculated using the NCEER (1997) procedure, and the methods presented in Ishihara and Yoshimine (1992). Using the Ishihara and Yoshimine (1992) method, volumetric strains were estimated that could occur within submerged layers due to dissipation of seismically-induced pore pressures. The estimated volumetric strains associated with liquefaction are shown by the purple shading to the left of the line representing the boring and CPT locations on the liquefaction analyses cross sections.

The estimated volumetric strains were then used in conjunction with the corresponding layer thicknesses to evaluate the magnitude of seismically-induced settlements at the boring locations. The settlements below any elevation are shown by the thick black line to the left of the line representing the boring and CPT locations on the liquefaction analyses cross sections.

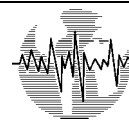
As shown on Plates 6.1 through 6.4, this analysis suggests that the liquefaction-induced ground settlement on the existing Mole will be on the order of 0.1 to 0.15 meter and may occur over wide areas. Large differential settlements should be expected. Differential settlement also may be as much as total settlement.

It should be noted and emphasized that the estimated liquefaction settlements are based on empirical procedures for level ground. Those estimates, therefore, do not consider the possible effects created by the adjacent Mole slope nor the possibility of lateral spreading, which would increase the amount of settlement in the graben area behind the slope. For those reasons, the estimated settlements shown on Plates 6.1 through 6.4 and discussed above are probably lower bound estimates of the settlements that will be realized during seismic shaking at the site.

6.4.2 Seismically-Induced Settlement of Dry Fill

Earthquake shaking also can result in seismically-induced settlement of relatively loose, dry, granular materials. However, the upper fill is generally dense, and therefore settlement of the dry fill is expected to occur primarily in the areas where voids exist in the dry, upper Mole fill. Except in those areas underlain by local voids or loose zones, the settlement of the dry fill





should be significantly less than the settlement due to liquefaction of the underlying submerged fill.

6.5 SEISMICALLY-INDUCED STRENGTH DEGRADATION OF YOUNG BAY MUD

The design earthquake is expected to generate multiple cycles of strong ground shaking. Young Bay Mud is a moderately sensitive clay (sensitivity ranges from about 2 to 5). The in situ remote vane test data show that shear strains of 20 to 30 percent are required to degrade the strength to a residual value. At large strains where soil remolding could occur, the strength of Young Bay Mud could be two to five times lower than its peak undrained static shear strength. If the Young Bay Mud layer is on a slope, such a loss of strength could contribute to lateral (downslope) movements.

The potential for cyclical strains produced by earthquake shaking to reduce the undrained strength of Young Bay Mud was evaluated by conducting a series of static and cyclic simple shear tests at the University of California at Berkeley. Those tests, whose results are provided in Volume 4 (UC Berkeley, 1999), included monotonically loaded static strength measurements after cyclic loading (25 cycles at a single amplitude shear strain of between 1 and 3 percent). The results indicate that although the shear modulus is reduced, the strength degradation due to seismic loading is about 10 to 15 percent.

Thus, it appears likely that the potential for significant strength degradation of Young Bay Mud during earthquake shaking is relatively low unless the seismic shaking produces a large strain slope-type failure. Since the test results indicate that degraded shear strength due to cyclic shear strains will be only slightly smaller than the undisturbed shear strength, the evaluation of slope-type failure mechanisms can be made based on static undrained shear strengths rather than remolded shear strengths.

6.6 LATERAL SPREADING

Lateral spreading is a phenomenon where large lateral soil movements (up to several meters) can occur if soils liquefy or otherwise lose strength, and there is sufficient degree of ground slope such that the slope becomes unstable. Slopes over much of the Oakland Mole range from about 0 to 2 degrees but can be steeper locally, particularly at the water's edge where they are about 15 to 20 degrees.

Lateral ground spreading induced by soil liquefaction or soil strength loss can result in an unstable slope and large lateral ground movement. This phenomenon can cause reduction and loss of soil support for foundations and roadways. Lateral spreading also can result in both loss of support for and large lateral loads and forces on abutments, piles, pile caps, and other buried structures (e.g., pipelines, utility conduits). The amount of relative movement required to induce





large forces is usually small (less than 0.5 meter). Forces are usually applied in one direction and are not cyclic in nature.

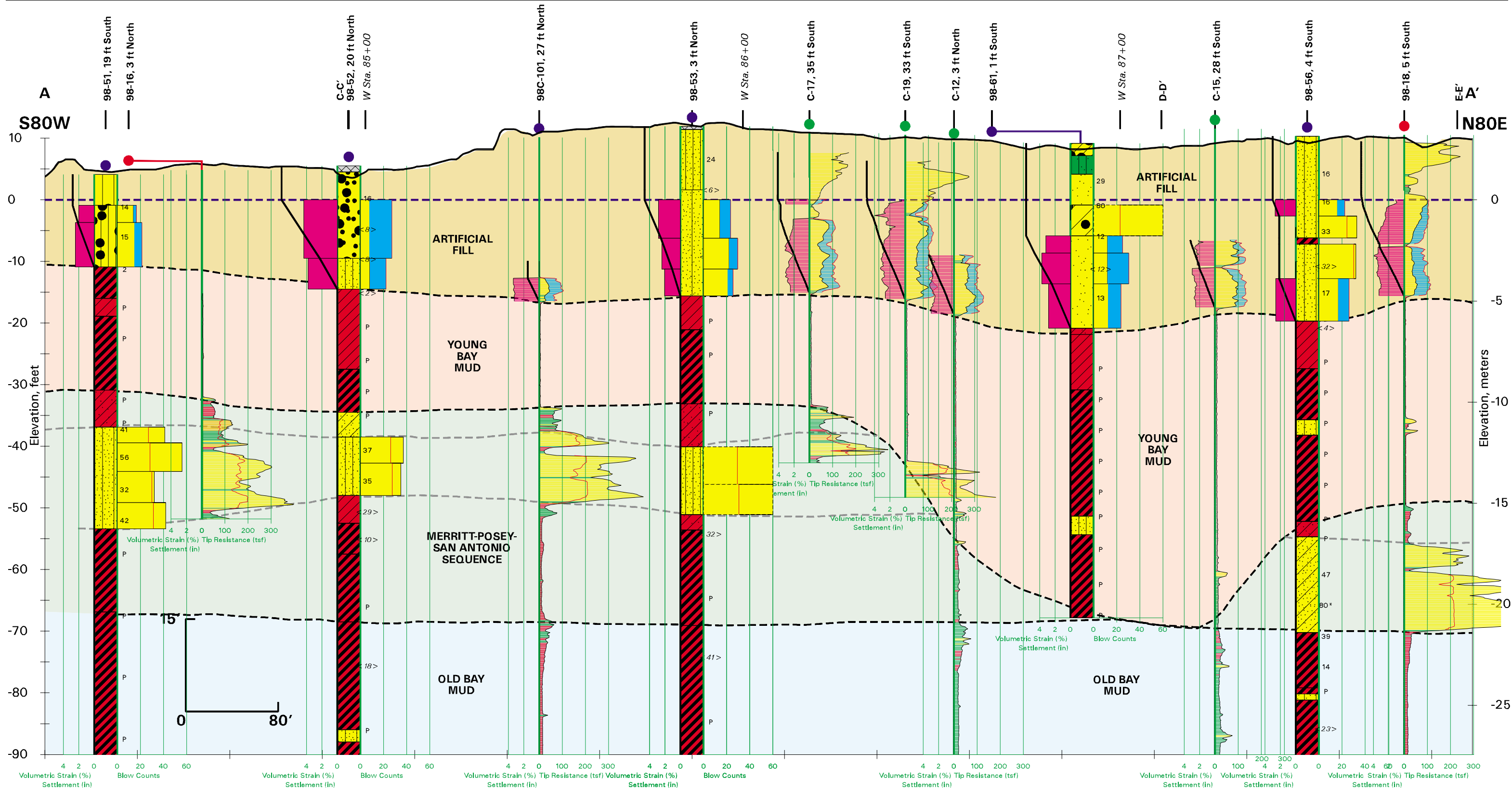
Mitigation against the effects of lateral spreading is usually accomplished in one of three ways:

1. Improve the ground to strengthen the soil, or provide better drainage and minimize the potential for lateral spreading. Ground improvement may include: a) soil replacement, soil densification by vibroflotation, compaction, or similar methods; or b) soil stabilization by the introduction of grout, soil-cement mixing, stone columns, or similar methods.
2. Design the foundation system to resist the applied loads at acceptable displacements.
3. Design new fills for acceptable displacements.

Ground improvement methods usually require that the area extent and depth of the soil mass involved be relatively well defined, and that an evaluation be made of the area of influence to be improved. The design of a foundation system to resist applied forces also requires knowledge of the extent and depth, but a uniform design could be used throughout an area prone to lateral spreading without the need to pinpoint the boundaries of spreading. For example, a single pile type and size (diameter, wall thickness, yield strength) could be specified for all the foundations in an area where lateral spreading may occur, as well as beyond the expected boundaries of lateral spreading.

The issues related to lateral spreading have been evaluated by Fugro-EM, Caltrans, and the Seismic Peer Review Panel. A summary description of the methods and assumptions used in the analyses as well as the analyses results are presented in a report in Volume 4 and in the Oakland Shore Approach Foundation Report (Fugro-EM, 2000). The purpose of the studies was to ascertain the effects of lateral spreading on proposed pile foundations and approach fill alternatives.





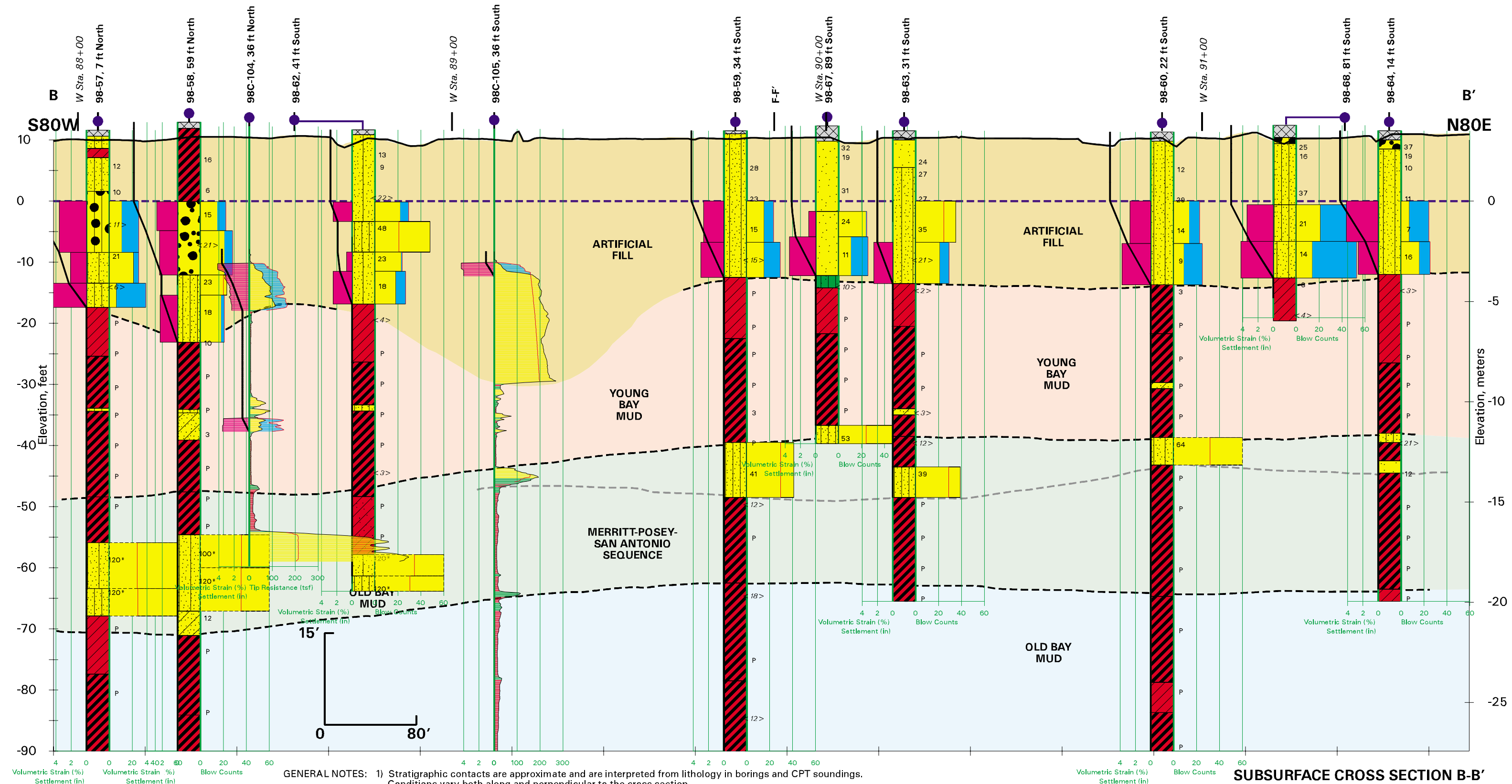
SUBSURFACE CROSS SECTION A-A'

With Liquefaction Evaluation

Magnitude = 7.5, Acceleration = 0.52

SFOBB East Span Seismic Safety Project

PLATE 6.1a

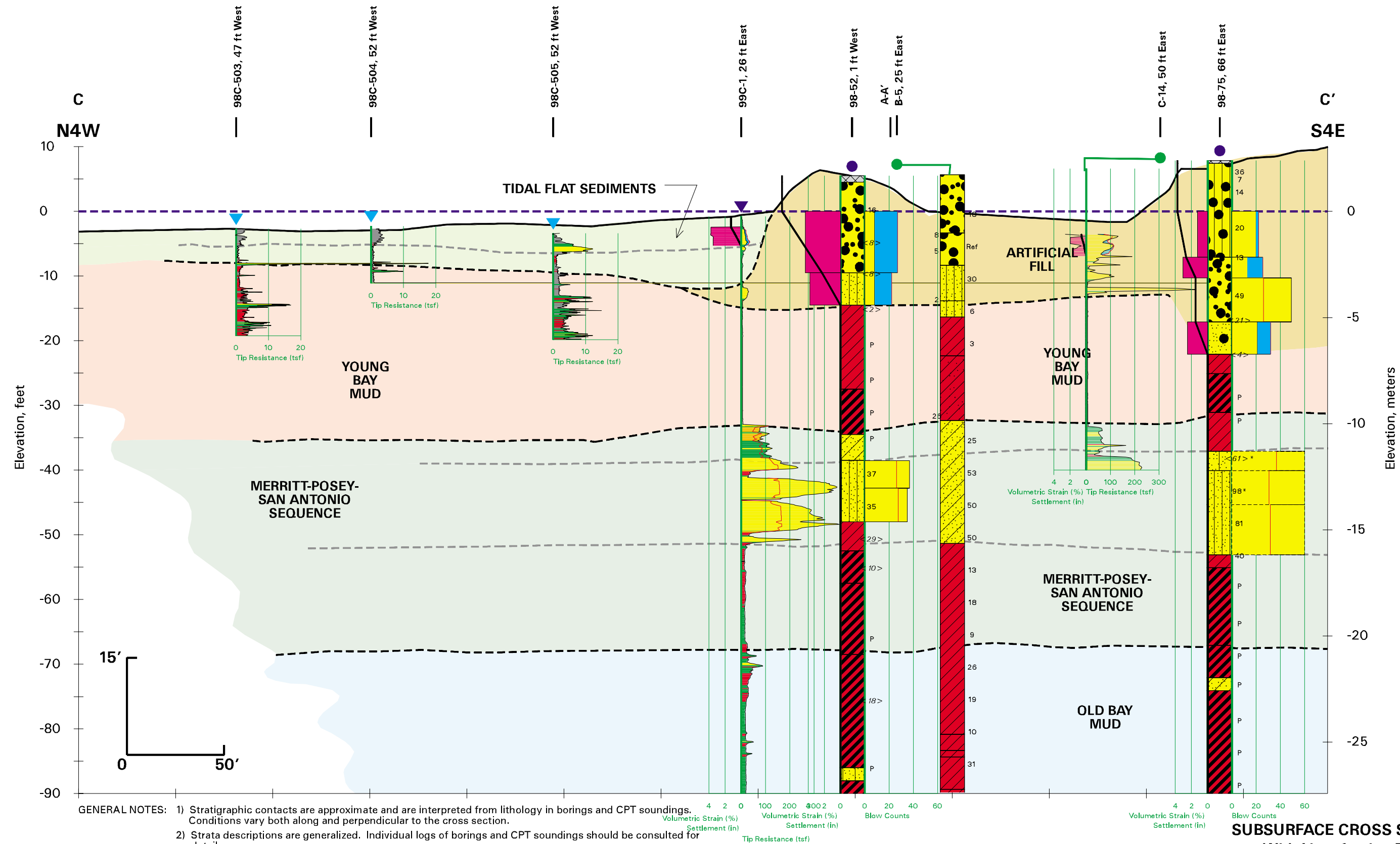


SUBSURFACE CROSS SECTION B-B'
With Liquefaction Evaluation

Magnitude = 7.5, Acceleration = 0.52
SFOBB East Span Seismic Safety Project

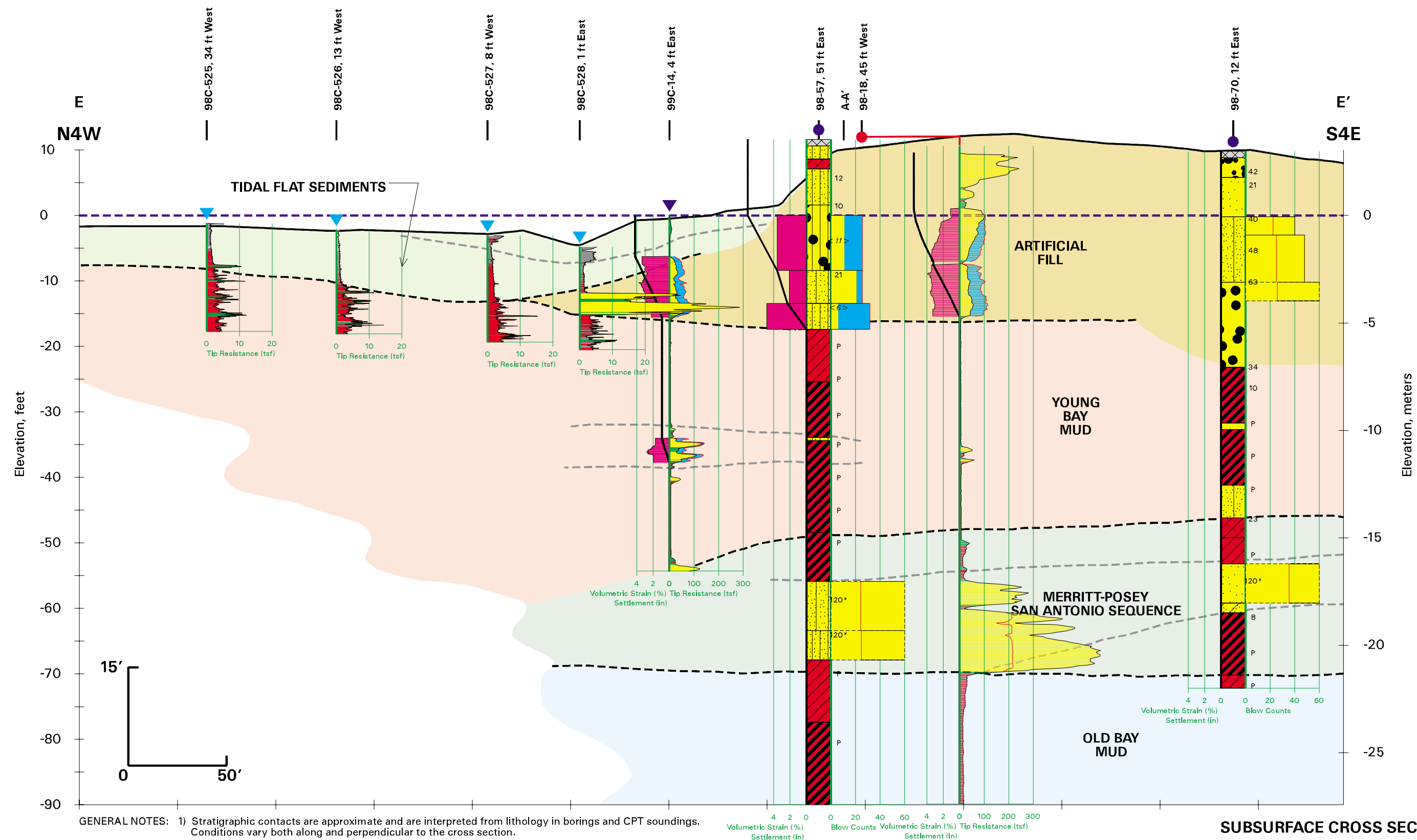
PLATE 6.1b





SUBSURFACE CROSS SECTION C-C'
With Liquefaction Evaluation

Magnitude = 7.5, Acceleration = 0.52
SFOBB East Span Seismic Safety Project



SUBSURFACE CROSS SECTION E-E'

With Liquefaction Evaluation

Magnitude = 7.5, Acceleration = 0.52

SFOBB East Span Seismic Safety Project

PLATE 6.3



SECTION 7.0 REFERENCES

SECTION 7.0



7.0 REFERENCES

- American Petroleum Institute (1993), Recommended Practice for Planning, Designing, and Constructing Fixed Offshore Platform-Load and Resistance Factor Design, API Recommended Practice 2A-LRFD (RP 2A-LRFD), 1st Ed., API, Washington, DC.
- American Society of Testing Materials (ASTM) (1998), "Standard Test Method for Performing Electronic Friction Cone and Piezocone Penetration Testing of Soil", ASTM D5778-95, Vol. 04.09, Soil and Rock (II): D4943-latest; Geosynthetics.
- Baldi, G., Bellotti, R., Ghionna, V., Jamiolkowsky, M., and Pasqualini, E. (1986), "Interpretation of CPT's and CPTU's, 2nd Part: Drained Penetration in Sands," Fourth International Geotechnical Seminar Field Instrumentation and In-Situ Measurements, Nanyang Technological Institute, Singapore, Nov., pp. 143-156.
- Becker, D.E., Crooks, J.H.A., Been, K., and Jefferies, M.G. (1987), "Work as a criterion for determining in situ and yield stresses in clays," Canadian Geotechnical Journal, Vol. 24, pp. 549-564.
- California Department of Transportation (Caltrans) (1932), *Final Report - Foundation Investigations, San Francisco-Oakland Bay Bridge (Boring Contracts Nos. 1, 1a and 1b)*, prepared by A.J. Stocks, Resident Engineer, May 25.
- _____ (1933), Special Provisions Proposal and Contract for Constructing a Dredger Fill in Alameda County Between the Westerly End of the Key Mole Fill and the Foot of Folger Avenue, Berkeley, District IV, East Bay Approach, San Francisco-Oakland Bay Bridge, prepared by the Department of Public Works, Division of Highways.
- _____ (1934), "First Annual Progress Report, San Francisco Oakland Bay Bridge," Designed and Constructed by the Department of Public Works of the State of California for the California Toll Bridge Authority, July.
- _____ (1994), Log of Test Borings, Existing East Approach to San Francisco-Oakland Bay Bridge.
- _____ (1997), Internal Caltrans Memorandum dated December 17 from SFOBB Investigations Section to Office of Structure Design, Subject: Addendum - Vertical Datum, Caltrans File Nos. 04-SF-80, 04-0434A1, C1, E1, F1, G1, Project Nos. 3, 4, 5, 6, 8, 21, Bridge No. 33-0025.





Casagrande, A. (1936), "Determination of the Preconsolidation Load and Its Practical Significance," Proceedings, First International Conference on Soil Mechanics and Foundation Engineering, Cambridge, Mass., Vol. 3, pp. 60-64.

Fugro-Earth Mechanics (Fugro-EM) (1998), *Subcontractor Reports, Preliminary Geotechnical Site Characterization, San Francisco-Oakland Bay Bridge East Span Seismic Safety Project, Volumes 1 through 4*, FWI Job No. 98-42-0035, prepared for California Department of Transportation, June 1998.

_____ (2000), *Oakland Shore Approach Foundation Report, San Francisco-Oakland Bay Bridge East Span Seismic Safety Project*, FWI Job No. 98-42-0058, prepared for California Department of Transportation, July 31 (date).

_____ (2001a), *Analysis and Design Procedures for Pile Foundations Supporting Temporary Towers, Skyway Structures, San Francisco-Oakland Bay Bridge East Span Seismic Safety Project*, FWI Job No. 98-42-0054, prepared for California Department of Transportation, March 5.

_____ (2001b), *Axial Pile Design and Drivability, Main Span-East Pier & Skyway Structures, San Francisco-Oakland Bay Bridge East Span Seismic Safety Project*, FWI Job No. 98-42-0054, prepared for California Department of Transportation, March 5.

_____ (2001c), *Final Marine Geophysical Survey, San Francisco-Oakland Bay Bridge East Span Seismic Safety Project*, FWI Job No. 98-42-0054, prepared for California Department of Transportation, March 5.

_____ (2001d), *Final Marine Geotechnical Site Characterization, San Francisco-Oakland Bay Bridge East Span Seismic Safety Project, Volumes 1 and 2A through 2H*, FWI Job No. 98-42-0054, prepared for California Department of Transportation, March 5.

_____ (2001e), *Lateral Pile Design for Main Span-Pier E2 and Skyway Structure, San Francisco-Oakland Bay Bridge East Span Seismic Safety Project*, EMI Job No. 98-145, prepared for California Department of Transportation, February 28.

_____ (2001f), *Pile Installation Demonstration Project (PIDP) Geotechnical Report, San Francisco-Oakland Bay Bridge East Span Seismic Safety Project*, FWI Job No. 98-42-0061, prepared for California Department of Transportation, March 5.

_____ (2001g), *Seismic Ground Motion Report, San Francisco-Oakland Bay Bridge East Span Seismic Safety Project*, EMI Job No. 97-146, prepared for California Department of Transportation, February 28.





- _____. (2001h), *Subcontractor Reports, Final Geotechnical Site Characterization, San Francisco-Oakland Bay Bridge East Span Seismic Safety Project, Volumes 1 through 3*, FWI Job No. 98-42-0054, prepared for California Department of Transportation, March 5.
- Fugro South, Inc. (1998), *Data Summary Report: Results of Resonant Column and Strain-Controlled Cyclic Direct Simple Shear Tests, San Francisco-Oakland Bay Bridge East Span Seismic Safety Project*, prepared for Fugro-Earth Mechanics, June.
- Idriss, I.M. (1991), "Earthquake Ground Motion at Soft Soil Sites," Proceedings, Second International Conference on Recent Advances in Geotechnical Earthquake Engineering and Soil Dynamics, St. Louis, Missouri, March 11-15.
- Ishihara, K., and Yoshimine, M. (1992), "Evaluation of Settlements in Sand Deposits Following Liquefaction During Earthquakes", Soils and Foundations, Japanese Society of Soil Mechanics and Foundation Engineers, Vol. 32, No. 1, p. 173-188.
- ISSMFE (1989), "Report on the ISSMFE Technical Committee on Penetration Testing of Soils - TC16 With Reference Test Procedures CPT - SPT - DP - WST", Appendix A, International Reference Test Procedure for Cone Penetration Test (CPT), pp. 6 - 23.
- Kulhawy, F.H., and Mayne, P.W. (1990), *Manual on Estimating Soil Properties for Foundation Design*, EL-6800, Research Project 1493-6, Final Report, prepared for Electric Power Research Institute, August.
- National Center for Earthquake Engineering Research (NCEER) (1997), Proceedings of the NCEER Workshop on Evaluation of Liquefaction Resistance of Soils, edited by T.L. Youd and I.M. Idriss, Technical Report NCEER-97-0022, December 31.
- Robertson, P.K. and Campanella, R.G. (1989), *Guidelines for Geotechnical Design Using PCPT and PCPTU*, The University of British Columbia, Soil Mechanics Series No. 120, Vancouver, B.C., Canada V6T 1W5.
- Schmertmann, J.H. (1976), "Predicting the q_c/N Ratio," Final Report D-636, Engineering and Industrial Experiment Station, Department of Civil Engineering, University of Florida, Gainesville.
- Terzaghi, K. and Peck, R.B. (1967), *Soil Mechanics in Engineering Practice*, 2nd Ed., John Wiley and Sons, New York, 729 p.
- Trask, P.D. and Rolston, J.W. (1961), "Engineering Geology of San Francisco Bay, California," in Bulletin of the Geological Society of America, Vol. 62, p. 1079-1110, September.





TY Lin/Moffatt & Nichol (TY Lin/M&N) (2001) E-Mail Transmittal of Microstation File “n6_r8.dgn”, by Mr. Tom Ho of TY Lin International, received January 26, 2001.

University of California at Berkeley (1999), *UC Berkeley Geotechnical Testing for the East Bay Crossing of the San Francisco-Oakland Bay Bridge*, prepared for Earth Mechanics, Inc., February.

University of Texas at Austin (1998), *Laboratory Evaluation of the Dynamic Properties of Intact Soil Specimens: San Francisco-Oakland Bay Bridge East Span Seismic Safety Project, Phase I – Site Characterization*, Geotechnical Engineering Report GR98-8, Civil Engineering Department, University of Texas at Austin, July 1.

